DEVELOPMENT OF ELECTROACTIVATED HETEROGENEOUS TRANSITION METAL-BASED SYSTEMS TO SYNTHESIZE DEUTERATED COMPOUNDS AND ALKYLAMINES

By

Souful Bhatia

A DISSERTATION

Submitted to
Michigan State University
in partial fulfillment of the requirements
for the degree of

Chemistry – Doctor of Philosophy

2016

ABSTRACT

DEVELOPMENT OF ELECTROACTIVATED CATALYTIC HETEROGENOUS-BASED SYSTEM TO SYNTHESIZE DEUTERATED COMPOUNDS AND ALKYLAMINES

By

Souful Bhatia

The work explained here introduces heterogeneous transition-metal catalyzed carbon-hydrogen (C-H) activation performed in an electrochemical environment. This method is mild, inexpensive and regioselective and is conducted in an aqueous environment compared to conventional methods that involve homogeneous catalysis or high-pressure high-temperature batch reactor conditions. The synthesis of carbon-deuterium (C-D) and carbon-nitrogen (C-N) bond is significant as deuterated and nitrogenous compounds have wide arrays of applications in chemical and pharmaceutical industry. The post-synthetic replacement of metabolically labile C-H bond to a relatively stable C-D bond has attracted lot of attention in the pharmaceutical industry as deuterated drugs tend to have altered metabolic profile.

Herein, we describe the development and optimization of an aqueous-based electrocatalytic and electrochemical systems with the ability to activate C-H bonds. The ruthenium on activated carbon cloth (Ru/ACC) showed the ability to transform C-H to C-D bonds in amines, alcohols and amino acids regio- and stereoselectively in minutes to hours at 2.2 mA/cm^2, 60 °C and ambient pressure. We expanded this electrocatalytic method using palladium on activated carbon cloth (Pd/ACC) to deuterate benzylic and *ortho*-C-H sites on the substituted benzene.

The alkylation of amines is conventionally carried out using alkyl halides as alkylating agents or carbonyl-based compounds in the presence of strong reducing agents. We have developed a 1-compartment (1-C) and 2-compartment (2-C) electrochemical systems to alkylate amines using alcohols as alkylating agents in an aqueous-based environment. The optimized conditions for alkylation of amines with alcohols are 60 °C, 2.2 mA/cm^2 and 5% v/v of alcohol.

ACKNOWLEDGEMENTS

I would like to sincerely thank Dr. James (Ned) E. Jackson for his mentorship, personal, and professional support throughout my stay at Michigan State University. Any success I have had at MSU during the past five years is due in large part to Ned. He was and remains my best role model for a scientist, teacher, and mentor. He has allowed me to grow scientifically and has provided me with the intellectual freedom to carve my own path in research. In addition to being an amazing advisor in the lab, he has always encouraged me to pursue new experiences and programs outside of the lab and I am a more well-rounded thinker because of his understanding and support. I cannot imagine a better advisor than Ned and I am a stronger scientist, teacher, mentor and all around a better person because of him. Ned, thank you for all your guidance, all your support, and mostly for all the second chances.

Over these past five years, I have had the pleasure to work with many undergraduate and high school students who have been instrumental in my research endeavors. Nehal Boukhamsin and Troy Dolmetsch performed significant preliminary work to develop proof of concept for my H/D exchange and alkylation projects. Catherine Zeng, a high school student from California was instrumental in establishing benzylic H/D exchange project in a span of 8 weeks. I would also like to thank Alexis Faber, Eric Foster, Justin Wang, and Jawahir Mohammed for their contribution to my research projects.

A good workgroup is key in grad school and in Ned's lab, I had the opportunity to work with a truly impressive cohort of scientists. My colleagues helped me every step of the way intellectually and personally during the past 5 years. They were my research time, my

sounding board, my test audience, and my friends. I would like to specifically thank Dr. Greg Spahlinger, Mahlet Garedew, GracieLou Klinger, Aseel Bala, Dr. Chun Ho Lam, Benjamin Appiagyei, Tayeb Kakeshpour, Pengchao Hao, Andrew Henika, Darya Howell, Dr. Zhenglong Li and Fatmata Jalloh for company, memories, and occasionally taking samples for me.

I would like to thank Annalisa Grunwald for believing in me and the love during the past couple years. Thank you too to the entire Grunwald family, especially Kris and Dave, for their care, hospitality, and good wishes. You have made me feel like part of the family. Finally, I would like to thank my family back home: my mom, dad and sister. My hard-working parents, Ashok and Kiran Bhatia, have worked their entire lives to give my sister and myself every opportunity. They have always provided us with unconditional love and support, as well as the thirst for knowledge that lead me to MSU in the first place. I am so proud to be your son. My sister Purva too has also been my friend all my life and has been a constant source of advice and encouragement. Though they have been far away geographically, they are the underpinning of everything I do.

Table of Contents

LIST OF TABLES

LIST OF FIGURES

LIST OF SCHEMES

Chapter 1. Introduction: H/D Exchange

1.1 Kinetic Isotope Effect

The kinetic isotope effect (KIE) refers to the change in the rate of a reaction when an atom is replaced by its isotope. The rate of reaction can be affected by: (a) primary (1°) KIE or (b) secondary (2°) KIE. A 1° KIE may be observed when an isotope bearing bond is made or broken in a reaction's rate determining step (RDS), whereas a 2° KIE occurs when the isotopic substitution is on a bond that is neither made nor broken during the RDS. The 1° and 2° KIE's are described as normal (KIE >1) or inverse relationship (KIE <1). In a normal relationship, the rate of reaction decreases with the heavier isotopic replacement whereas, it increases in the inverse relationship (**Eqn. 1**).

$$\boxed{KIE = \frac{k_L}{k_H}} \qquad \textbf{Eqn. 1}$$

where k_L and k_H represent the rate constants of reactions with the lighter and heavier atom.

The KIE arises due to differences in the zero-point vibrational energy of bonds bearing isotopes of different masses. The energy levels associated with the vibration of a bond are approximated by **Eqn. 2**. Due to the uncertainty principle, even at 0 K, a bond has a minimum vibrational energy in its ground vibrational state (i.e. n = 0), called zero-point energy (ZPE). Since the force constant (k_F) is defined by the electronic bonding structure, it is the same for a bond, regardless of isotopic mass. The vibrational levels, including the ZPE, depend also on the reduced mass (μ) (**Eqn. 3**). The reduced mass, calculated using the masses of the atoms

involved in the diatomic species dictates its ZPE and hence forms the basis of the KIE (**Eqn. 4**).

$$E_n = (n + 1/2)h\nu \qquad \textbf{Eqn. 2}$$

$$\nu = \frac{1}{2\pi}\sqrt{\frac{k_F}{\mu}} \qquad \textbf{Eqn. 3}$$

$$\mu = \frac{m_1.m_2}{m_1 + m_2} \qquad \textbf{Eqn. 4}$$

where h = Planck constant, ν = vibrational frequency, n = vibrational level, μ = reduced mass, and m_1 and m_2 are the masses of atoms in the diatomic molecule.

The significance of reduced mass can be explained by considering deuterium (^{2}H or D), which is a heavier isotope of hydrogen (^{1}H). **Figure 1** indicates the μ values of ^{12}C-H and ^{12}C-D bonds, calculated using **Eqn. 4**. The calculations indicate the ZPE for C-H and C-D bonds to be 4.15 kcal/mol and 3.0 kcal/mol respectively, providing the C-D bond a relative stability of 1.15 kcal/mol. At 300 K, this corresponds to a factor of 7 in the relative rate of homolyis of C-H *vs*. C-D bond (*Note: The effective mass of carbon in a molecule is different than its atomic mass (12) but for mathematical convenience, its atomic mass is used as approximation*) .[1]

$$\text{C-H, } \mu = 12x1/(12 + 1) = 12/13 = 0.923$$
$$\text{C-D, } \mu = 12x2/(12 + 2) = 24/14 = 1.714$$

$$\frac{\nu_{C\text{-}H}}{\nu_{C\text{-}D}} = \frac{\frac{1}{2\pi}\sqrt{\frac{k_F}{\mu_{C\text{-}H}}}}{\frac{1}{2\pi}\sqrt{\frac{k_F}{\mu_{C\text{-}D}}}} = \frac{\sqrt{\frac{k_F}{\mu_{C\text{-}H}}}}{\sqrt{\frac{k_F}{\mu_{C\text{-}D}}}} = \sqrt{\frac{\mu_{C\text{-}H}}{\mu_{C\text{-}D}}} = \sqrt{\frac{1.714}{0.923}} = 1.363$$

$$\nu_{C\text{-}D} = \frac{\nu_{C\text{-}H}\,(3000\ cm^{-1})}{1.363},\ \nu_{C\text{-}D} = 2201\ cm^{-1}$$

using Eqn. 2

$(E_n)_{C\text{-}H} = (n + 1/2)h\nu_{C\text{-}H} = (n + 1/2)hc\bar{\nu}_{C\text{-}H}$

for ZPE (n = 0) per mole; $(E_0)_{C\text{-}H} = 1/2hc\bar{\nu}_{C\text{-}H}N$;(N = # moles)

$(E_0)_{C\text{-}D} = 1/2hc\bar{\nu}_{C\text{-}D}N$

$$(E_0)_{C\text{-}H} - (E_0)_{C\text{-}D} = \Delta E_0 = \frac{1}{2}(6.626 \times 10^{-34}(J.s) \times 2.997 \times 10^{10}\ (cm.s^{-1}) \times 799\ (cm^{-1}) \times 6.023 \times 10^{23}\ (mol^{-1}))$$

$$= 4783(J.mol^{-1})$$

$$\approx 1.15(kcal.mol^{-1})$$

Figure 1. Difference in Bond Dissociation Energy of C-H *vs*. C-D

The pictorial representation of the relative stability of C-D bond can be represented by the Morse potential curve (**Figure 2**). The transition state demonstrates the homolytic cleavage of C-H and C-D (**Figure 1**) bonds and the relative difference of 1.15 kcal/mol is responsible for the observed KIE. This concept and deuterium-labeled compounds are commonly used in studying chemical and biological reaction mechanisms (deuterium tracer studies), protein and peptide structures, manufacture of optical fibers, and as internal standards for forensic analysis and their application as therapeutic agents. Two of the most prevalent applications with direct impact in the field of organic and medicinal chemistry are deuterium tracer studies and use of deuterium-labeled compounds as therapeutic agents. Both these topics will be addressed here in detail, with latter forming the driving force for the work described in the following chapters.

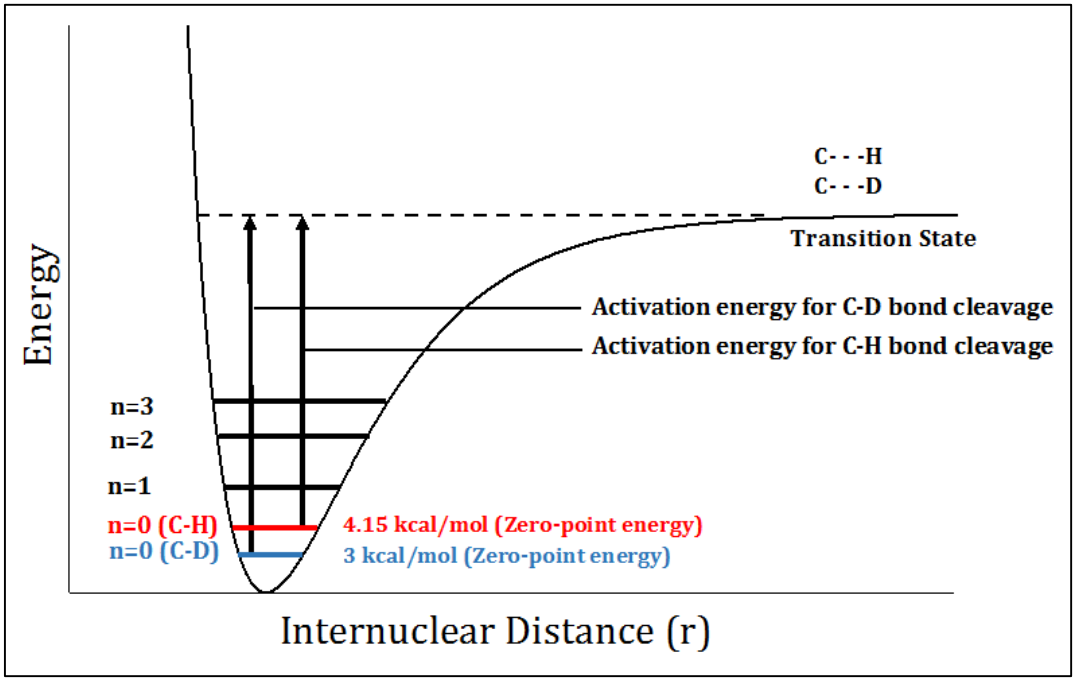

Figure 2. Morse Potential Curve of C-H *vs*. C-D

1.2 Deuterium Tracer Studies

The introduction of deuterium in an organic structure and its presence across subsequent reactions have been extensively used to perform mechanistic analysis since the discovery of deuterium in 1931. This practice has been used to understand many reaction mechanisms and a few of those studies are discussed here to demonstrate the significance of deuterium-labeled compounds and KIE.

1.2.1 Jones Oxidation

Jones oxidation of 2° alcohols in the presence of chromium (Cr(VI)) produce ketones in high yield.[2,3] To understand the mechanism of this reaction, Westheimer and Nicolaides[4] performed kinetic analysis, using protiated and deuterated isopropyl alcohol. The principle behind the analysis is to determine if the 2° C-H is involved in the RDS. If so, its replacement by deuterium should slow down the reaction as revealed by an observable KIE, but if the 2°

C-H site is not involved, deuterated isopropyl alcohol should undergo oxidation at the same rate as the protiated version. It was observed that the deuterated isopropyl alcohol oxidized at about 1/6.7th the rate of the protiated form, confirming that the 2° C-H cleavage during RDS (**Scheme 1**).

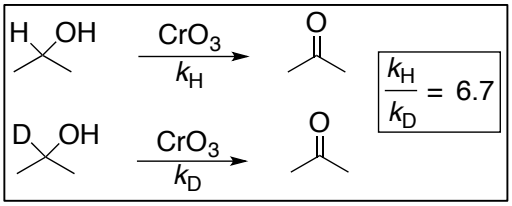

Scheme 1. A Primary Kinetic Isotope Effect: Jones Oxidation

1.2.2 E2 Elimination

The mechanism of E2 elimination was investigated by Shiner *et al.*[5] using protiated and deuterated isopropyl bromide (**Scheme 2**). Their rates of elimination would demonstrate a significant difference if β-hydrogen abstraction were involved in the RDS. The kinetic data showed a revealed a primary KIE of 6.7, confirming the involvement of β-hydrogens in the RDS during E2 elimination.

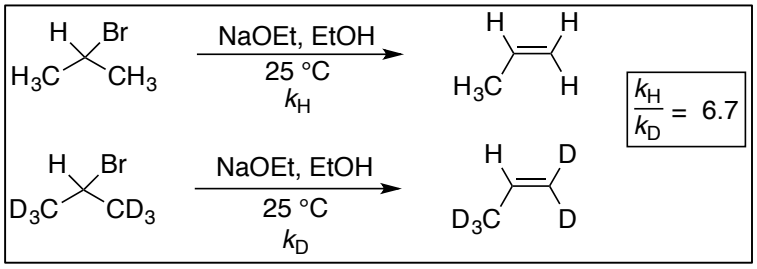

Scheme 2. A Primary Kinetic Isotope Effect: E2 Elimination

1.2.3 Hofmann-Löffler Reaction

The Hofmann-Löffler reaction involves the formation of cyclic amines using *N*-bromo or *N*-chloroamines.[6] Syntheses of pyrrolidine-based species like nicotine[7] and L-proline,[8] using these reaction conditions have been reported (**Scheme 3**).

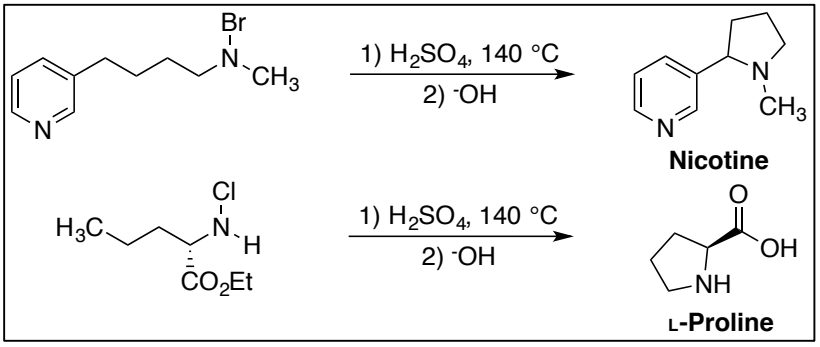

Scheme 3. Examples of Hofmann-Löffler Reaction

The synthesis of pyrrolidines, being mechanistically unusual, was studied by Corey *et al.*[9] using deuterated *N*-chloroamines. They synthesized the desired *N*-chloroamine (**1**) and used Hofmann-Löffler reaction conditions to make 1,2-dimethylpyrrolidines (**2a/2b**). Combustion analysis of **2** showed the presence of 0.78 D per molecule, which translated into a KIE of 3.54. This demonstrated the cleavage of the C-H/C-D site during the reaction. In addition to this mechanistic detail, they also learnt that the pyrrolidine was optically inactive, indicating a trigonal C4 (**Scheme 4**).

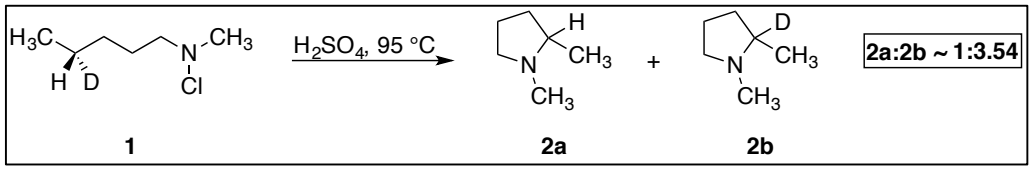

Scheme 4. Kinetic Isotope Effect: Hofmann-Löffler Reaction

1.2.4 Diels-Alder Reaction

The Diels-Alder reaction is a cycloaddition involving a conjugated diene (1,3-diene) and an alkene (dienophile). It is commonly used to develop 6-membered ring systems with specific regio- and stereoselectivity. Houk and coworkers[10] in 1986 traced deuterium to determine the mechanism of the Diels-Alder reaction using 1,3-butadiene and ethylene. The reaction was conducted using d_4-1,3-butadiene (**3**) and d_2-ethylene (**4a**: *cis* & **4b**: *trans*) at

185 °C and 1800 psi pressure to synthesize cyclohexene (**5(a** & **b)**). It was followed by epoxidation using *m*-chloroperbenzoic acid (*m*-CPBA) and the structures were analyzed using ^{1}H NMR. The ^{1}H NMR indicated less than 1% of the *trans*-adduct in the *cis*-products and vice versa (**Scheme 5**). These observations contradicted the presence of diradical intermediate proposed by some, and confirmed that the mechanism follows a concerted pathway.

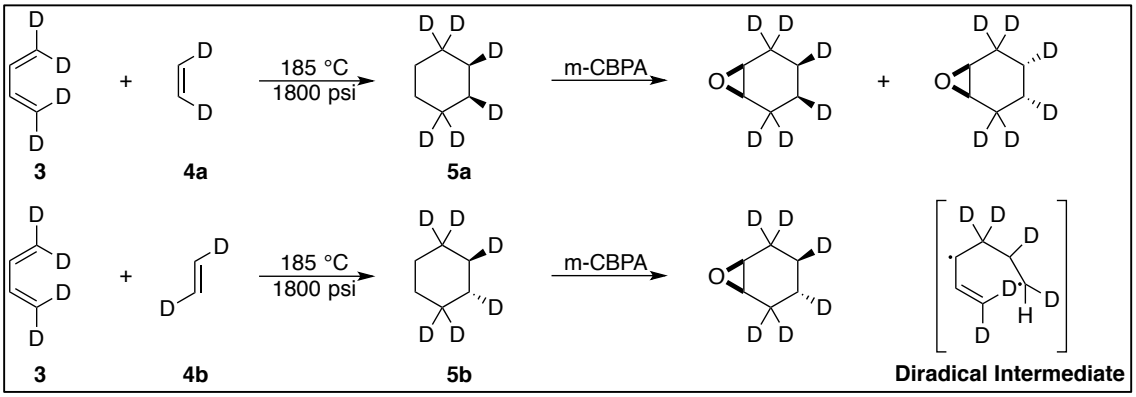

Scheme 5. Deuterium Tracer Studies: Diels-Alder Reaction

1.2.5 Palladium (Pd)-Catalyzed C-H Activation of Allylic Arenes

The mechanism of the coupling reaction between phenylglycine azlactone (**6**) and toluene in a recent communication by Curto and Kozlowski[11] was studied using KIE. The chemoselectivity of the reaction showed that the mechanism involved Pd-catalyzed C-H activation at the benzylic position. To explore this hypothesis, protiated and deuterated toluene was used in the reaction and a KIE of 3.5 was observed, confirming the hypothesis (**Scheme 6**).

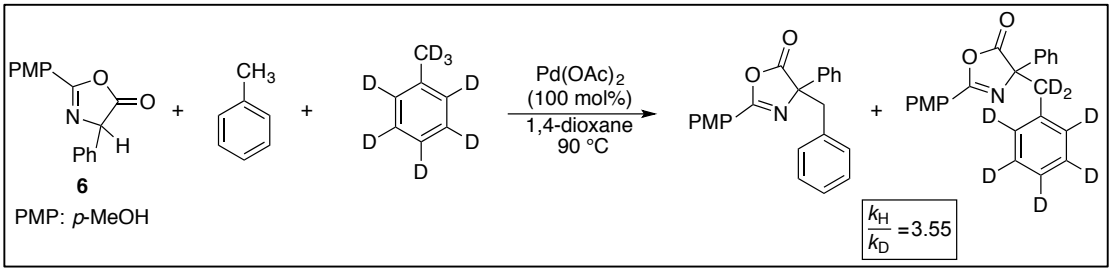

Scheme 6. Kinetic Isotope Effect: Pd-Catalyzed C-H Activation

1.2.6 Mechanistic Analysis: European Honeybee Trehalose Catalyzed Hydrolysis

Trehalase, an anomer-inverting glycosidase, hydrolyzes *α*,*α*-trehalose to an equimolar amount of *β*-glucose and *α*-glucose. Trehalases are widely distributed in micro-organisms,[12,13] plants,[14,15] invertibrates,[16–18] and vertibrates[19,20] and it has been noted that trehalases in flying insects are responsible for providing a rapid supply of glucose by hydrolyzing trehalose. The mechanism of this hydrolysis was investigated by means of a KIE study using trehalase obtained from the European honeybee. The two common mechanisms proposed for the hydrolysis were nucleophilic double displacement or stepwise cleavage via an oxocarbenium ion intermediate. The α-secondary KIE (α-SKIE) for the hydrolysis of trehalose by European honeybee trehalase was calculated using protiated and deuterated trehaloses. The α-SKIE of 1.53 confirmed an oxocarbenium ion intermediate reaction over the nucleophilic double displacement as shown below (**Scheme 7**).[21]

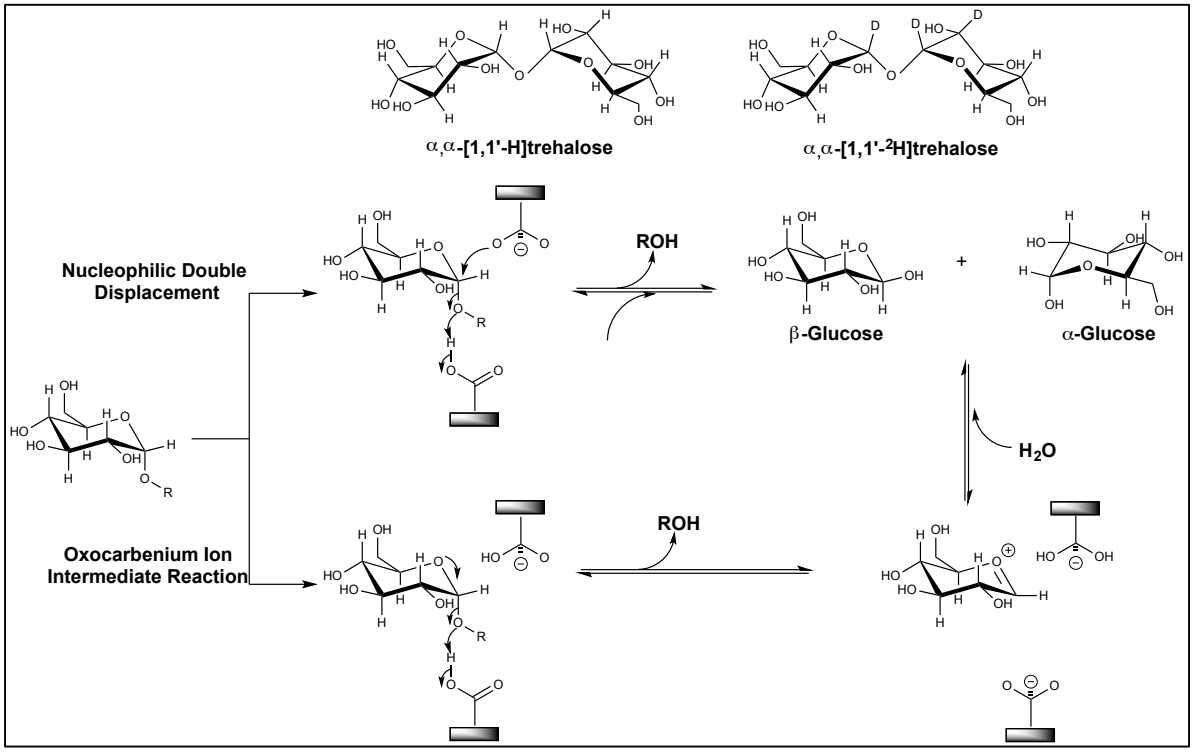

Scheme 7. Kinetic Isotope Effect: European Honeybee Trehalose Catalyzed Hydrolysis[21]

1.2.7 Mechanistic Analysis: Formose Reaction

The Formose reaction, which describes the formation of sugars from formaldehyde has been proposed to explain the origins of life. Since its discovery in 1861 by Aleksandr Butlerov,[22] extensive research has been done to understand its mechanism and in 1959, Breslow[23] proposed a mechanism for this process that involved formation of enediols during the conversion of **7** to **8** and of **3** to **4** (**Scheme 8**).

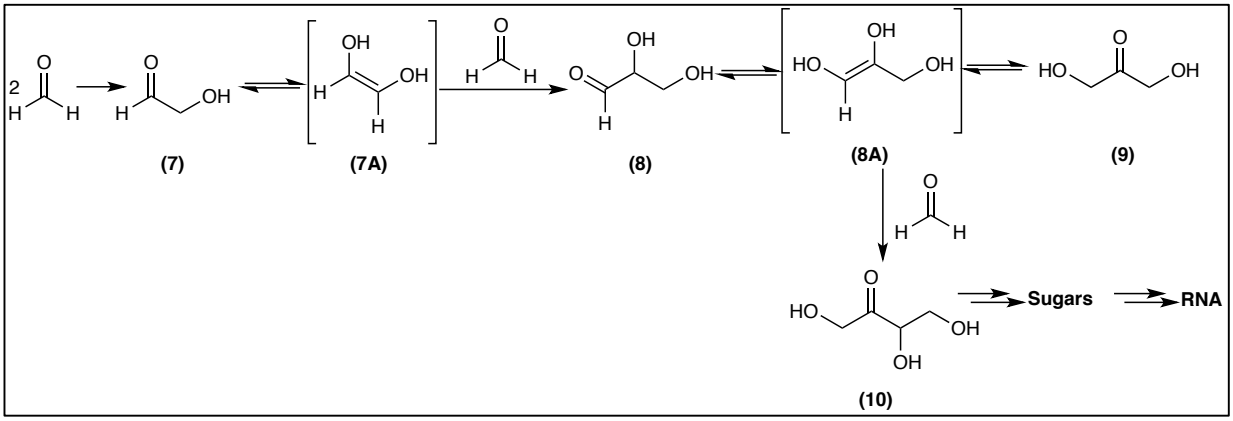

Scheme 8. Formose Reaction: Breslow's Hypothesis

Benner[24] studied these reactions in D_2O and did not observe deuterium in the products, contradicting Breslow's hypothesis that involved enolization. Breslow revised his mechanism and proposed hydride shift instead of enolization.[25] To confirm this hypothesis, he used 2-deuteroglyceraldehyde (**11**) and observed the formation of 1-deuterodihydroxyacetone (**12**) with 74% of the deuterium still retained (**Scheme 9**). This reaction explained the absence of deuterium in products under Benner's conditions.

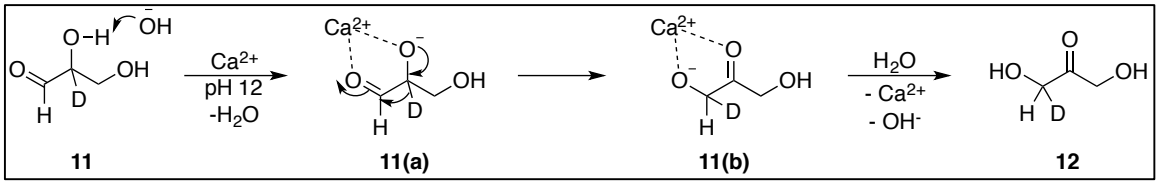

Scheme 9. Revised Mechanism: Formose Reaction

In addition to the mechanisms mentioned above, KIE and deuterium tracer studies have been employed in wide array of conditions to achieve mechanistic insight and further optimization of the reactions. Introduction of deuterium into molecules has proved to be an essential tool in understanding chemical and biological transformations and in the following section, we will discuss how it alters the interaction of deuterium-labeled molecules in a biological environment, leading to their application as medicinal agents.

1.3 Deuterium Labeled Molecules as Medicinal Agents

Deuterium-labeled compounds have recently found its way their clinical applications, wherein pharmaceutical companies replace metabolically labile C-H bonds with C-D bonds. Depending on their mechanism of metabolism and elimination, medicinal agents may show significant KIE's especially if one of the C-H bonds is cleaved during the metabolism of the drug. By replacing the metabolically labile C-H bond with a relatively stable C-D bond, the metabolism of a drug may be slowed resulting in a longer duration of action. In many cases, this modification has demonstrated a positive effect on safety, efficacy and/or tolerability of the drug. By starting from compounds with well-defined human pharmacological effects, especially FDA-approved drugs, this approach can create significantly differentiable, patentable new medicines that can address important unmet medical needs. Here, we will discuss few of the deuterium-labeled drugs currently under investigation or in clinical trials.

1.3.1 Kinetic Isotope Effect: Morphine

The protiated (**13**) and deuterated (**14**) morphine were tested for their pharmacological effects using swiss albino mice.[26,27] The study showed the LD_{50} of protiated morphine to be 256 mg/kg and deuterated morphine to be 400 mg/kg., giving protiated morphine a potency advantage of 1.56. Considering that *N*-demethylation of morphine is necessary to produce the active species (**15** (normorphine)), the data supports the decrease in the rate of metabolism of morphine with the presence of deuterium (**Scheme 10**).

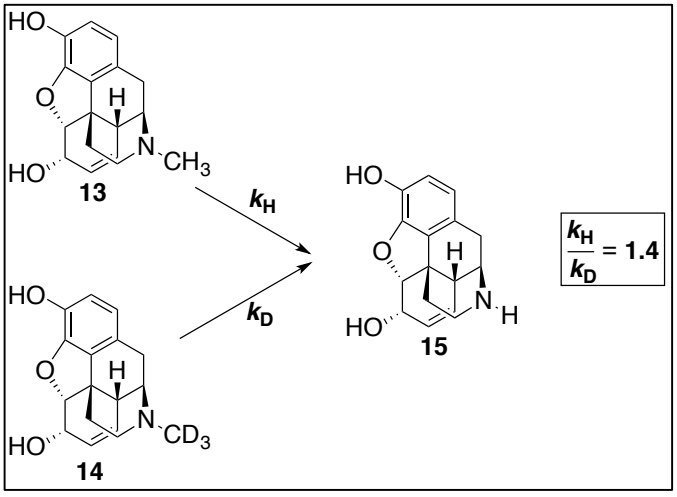

Scheme 10. Kinetic Isotope Effect: Morphine

1.3.2 Kinetic Isotope Effect: Butethal

Butethal is a commonly used sedative and to enhance its half-life ($t_{1/2}$), deuterated butethal was synthesized and tested.[28] The sleeping time in mice was used to study deuterated (**18**) and protiated butethal (**16**) and it was determined that the biological $t_{1/2}$ of deuterated butethal was approximately 2.5 times longer. This difference in $t_{1/2}$ can be explained by the metabolism of butethal that involves hydroxylation of the C-H bond. The in vitro hydroxylation of deuterated and protiated butethal gave a KIE of 1.59, suggesting that the slower cleavage of the C-D bond is responsible for the longer $t_{1/2}$ (**Scheme 11**).

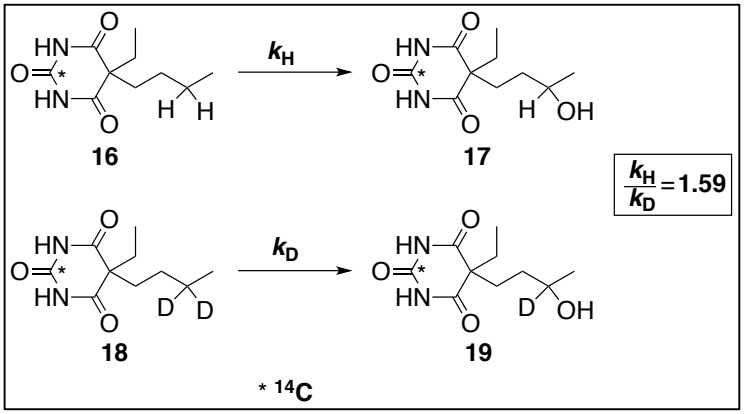

Scheme 11. Kinetic Isotope Effect: Butethal

1.3.3 Kinetic Isotope Effect: Sevoflurane

Sevoflurane, a volatile anesthetic drug, is commonly used for general anesthesia. This drug, metabolized by the cytochrome P450 2E1 enzyme, generates hexafluoroisopropanol, carbon dioxide (CO_2) and fluoride anion (F^-).[29] To investigate the effect of deuteration on its pharmacokinetic profile, a labile C-H site was deuterated. The metabolism study performed on the protiated and deuterated sevoflurane showed a KIE of 17, opening a possibility of using deuteriosevoflurane as a potential candidate with a longer $t_{1/2}$ (**Scheme 12**).[30]

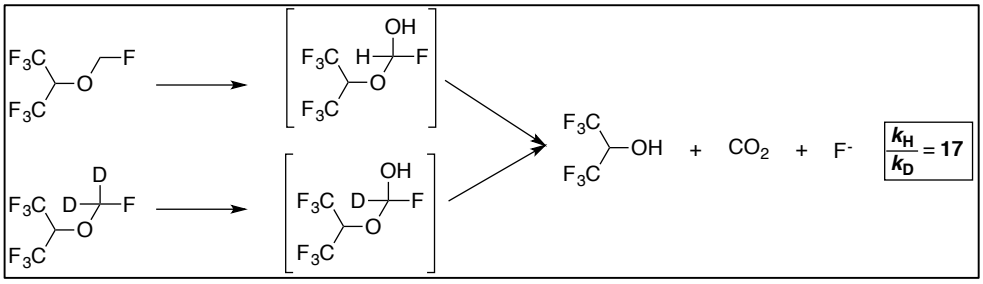

Scheme 12. Kinetic Isotope Effect: Sevoflurane

1.3.4 Kinetic Isotope Effect: Paroxetine

Paroxetine, an anti-depressant drug is used to treat major depressive disorders as well as hot flashes and night sweats. Due to the metabolic profile of paroxetine that includes CYP2D6-induced metabolism of the methylenedioxy ring to produce a carbene species that can irreversibly covalently bind to the P450 enzyme (**Scheme 13**), it is not recommended to patients taking additional drugs. It can slow down the metabolism (detoxification) of other drugs as P450 enzyme is responsible for the metabolism of almost 50% of medications.

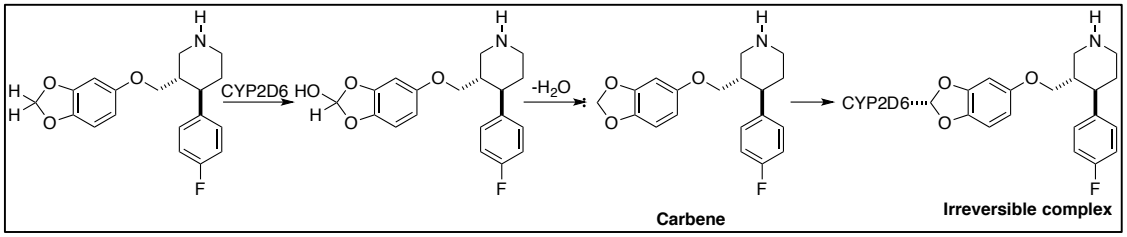

Scheme 13. Metabolic Profile: Paroxetine

Concert Pharmaceuticals, a major player in deuterium-labeled drugs, has applied the concept of KIE to paroxetine and developed CTP-347 (**Scheme 14**) in an attempt to reduce the formation of carbene species.[31] The pharmacological effect of CTP-347 (deuterated) was found to be similar to paroxetine (protiated) and in order to determine its effect on CYP2D6 metabolized drugs, it was administered with tamoxifen, a drug metabolized by CYP2D6. The deuterated species made no alteration to the rate of metabolism of tamoxifen whereas paroxetine, when administered with tamoxifen decreased its metabolism.

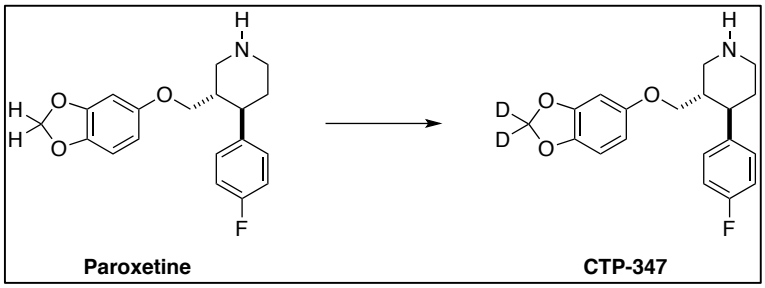

Scheme 14. Deuterium Switching: Paroxetine

1.3.5 Kinetic Isotope Effect: Venlafaxine

Venlafaxine, a dual serotonin/norepinephrine reuptake inhibitor approved for the treatment of depression, undergoes *O*-demethylation and *N*-demethylation as major metabolic pathways by enzymes CYP2D6 and 2C19.[32] In order to slow down its metabolism, Auspex Pharmaceuticals (acquired by Teva Pharmaceuticals) developed a deuterated analogue (SD-254) of venlafaxine.[33] In vitro studies of SD-254 showed a decrease in its rate

of metabolism by 50%, as compared to the protiated form, leading to a higher bioavailability in early clinical studies (**Scheme 15**).

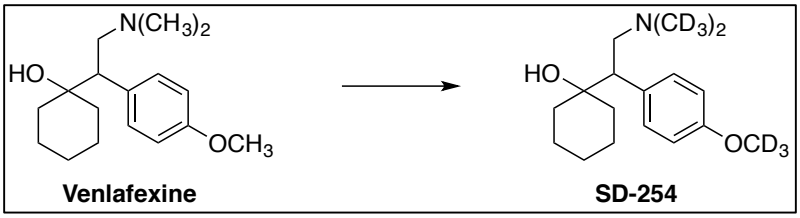

Scheme 15. Deuterium Switching: Venlafexine

1.3.6 Kinetic Isotope Effect: Efavirenz

Efavirenz (**20**), a non-nucleoside reverse transcriptase inhibitor used in the treatment of HIV-1 metabolizes to **21**, which is responsible for the nephrotoxicity associated with this drug. Applying the concept of KIE, the labile propargylic C-H site was deuterated to develop **22**. In vivo studies showed a decrease in the formation of **21** in the case of deuterated analogue (**Scheme 16**).[34]

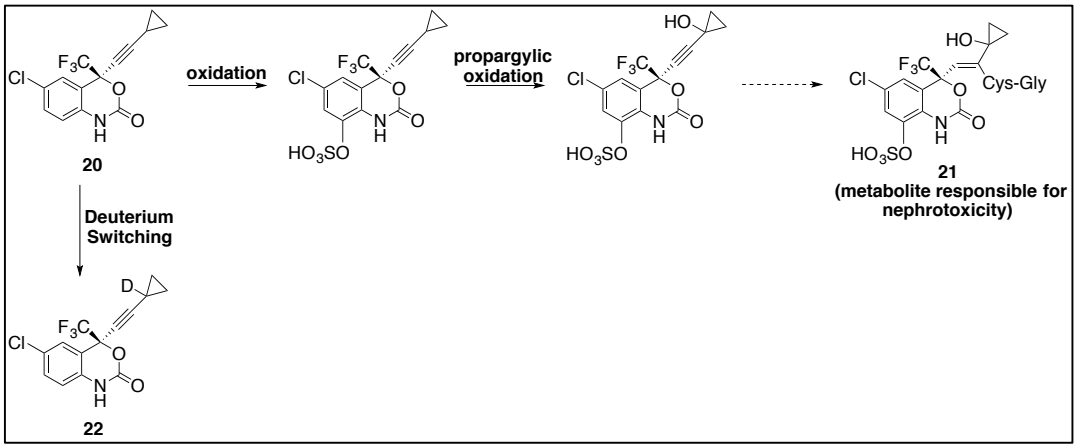

Scheme 16. Metabolic Profile: Efavirenz

1.3.7 Kinetic Isotope Effect: Telaprevir

Telaprevir, co-developed by Vertex Pharmaceuticals and Johnson & Johnson, is approved for the treatment of hepatitis C.[35] At higher pH, the (*S*)-α-ketoamide (**23**) racemizes to a less

active (*R*)-diastereomer (**24**), that accounts for 40% of the drug concentration after oral dosing. To develop a more stable species, deuterated analogue (**25**) was investigated and it showed increased stability to racemization compared to the protiated telaprevir. The deuterated telaprevir only produced 10% of the diastereomer after 1 h, compared to 35% for the protiated form (**Scheme 17**).

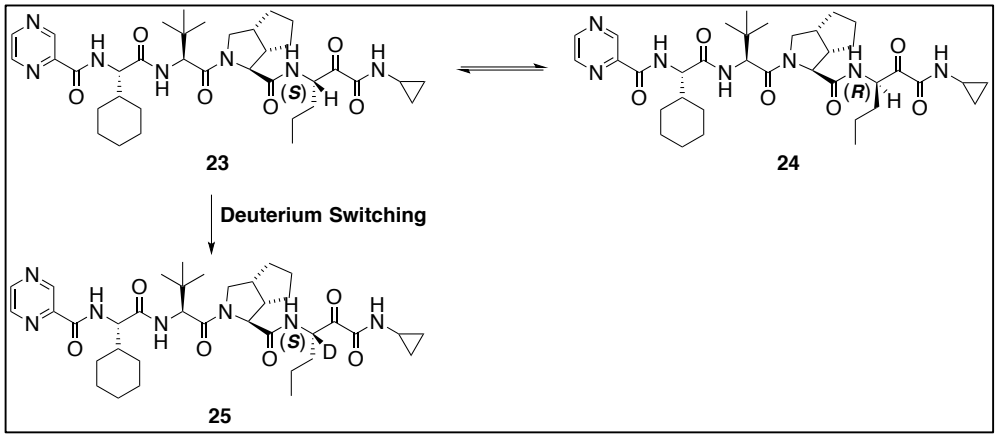

Scheme 17. Kinetic Isotope Effect: Telaprevir

1.3.8 Kinetic Isotope Effect: Tamoxifen

Tamoxifen (**26**) is used to treat breast cancer and can undergo metabolic activation to produce electrophilic species capable of making DNA adducts (**27**) that can lead to liver cancer. Phillips and coworkers[36] determined that deuteration at the labile C-H sites (**28**) can reduce the adduct formation and lower genotoxicity. In their metabolic studies, they noticed that the adduct formation went down two-fold in the case of deuterated tamoxifen (**Scheme 18**).

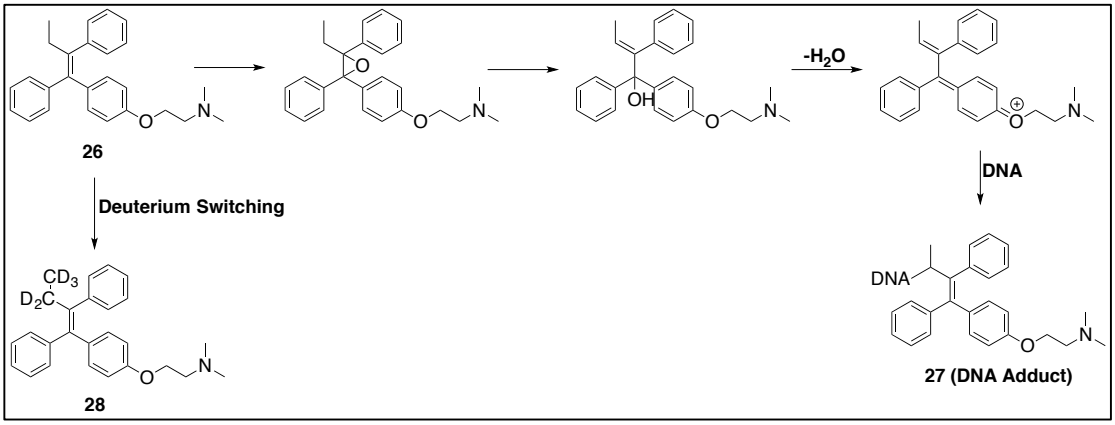

Scheme 18. Kinetic Isotope Effect: Tamoxifen

1.3.9 Kinetic Isotope Effect: Tetrabenazine

Tetrabenazine (**29**), approved in 2008 for the treatment of chorea associated with Huntington disease, has a $t_{1/2}$ of 10 h. Due to a shorter $t_{1/2}$, it has to be administered 2 to 3 times a day to prevent withdrawal symptoms.[37] To resolve this issue, Auspex Pharmaceuticals developed SD-809 (**30**) by deuterating the metabolically labile methoxy sites in tetrabenazine. The deuterated tetrabenazine substantially slowed down the formation of inactive metabolites. SD-809 is currently in phase III clinical trials (**Scheme 19**).

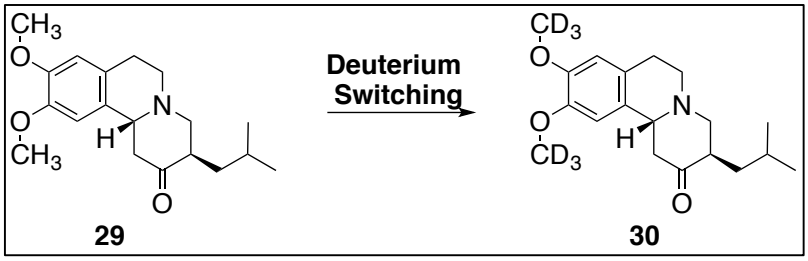

Scheme 19. Kinetic Isotope Effect: Tetrabenazine

1.3.10 Kinetic Isotope Effect: Dextromethorphan

Dextromethorphan (**31**), a non-competitive N-methyl-D-aspartate (NMDA) antagonist, is a widely-used cough suppressant. In addition to acting as an NMDA antagonist, it acts on numerous receptors in the brain. The limited benefit seen with dextromethorphan in clinical

studies is attributed to its hepatic metabolism that involves *O*-demethylation and *N*-demethylation. Avanir Pharmaceuticals in 2010 gained FDA-approval to market Nuedexta, a combination dose of dextromethorphan and quinidine to treat pseudobulbar effect, an emotional condition prevalent in patients with brain disorders. The presence of quinidine slows down the metabolism of dextromethorphan but it often leads to adverse cardiac side effects.[38] To counter this problem, Concert Pharmaceuticals designed a deuterated dextromethorphan (AVP-786, **32**) that cut the amount of quinidine required by half, and is currently in phase III clinical trials (**Scheme 20**).

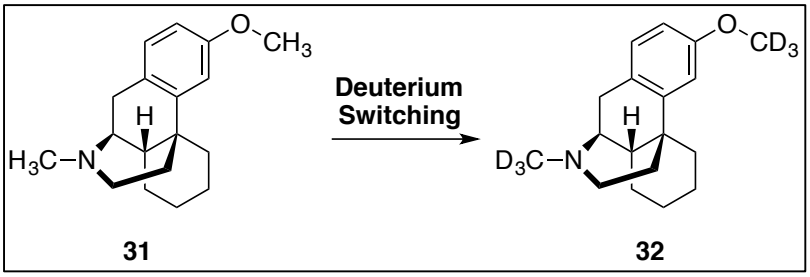

Scheme 20. Kinetic Isotope Effect: Dextromethorphan

In addition to deuterated medicinal agents mentioned above, many more have shown promising results and are currently being investigated. Though, none of the deuterium-labeled compounds have entered the market, the current trend suggests an entry in 2 to 3 years. Another promising candidate is CTP-656 (**33**), a deuterated analogue of Ivacaftor approved for the treatment of cystic fibrosis. The deuterated analogue has a $t_{1/2}$ of 15 h, compared to protiated with the $t_{1/2}$ of 12 h. Recently, Vertex Pharmaceuticals launched a deuterated agent for the treatment of cancer (VX-984) and contrary to the common practice of developing deuterated versions of FDA-approved drugs. Some of the other candidates currently under investigation are shown in **Figure 3**.[39–44]

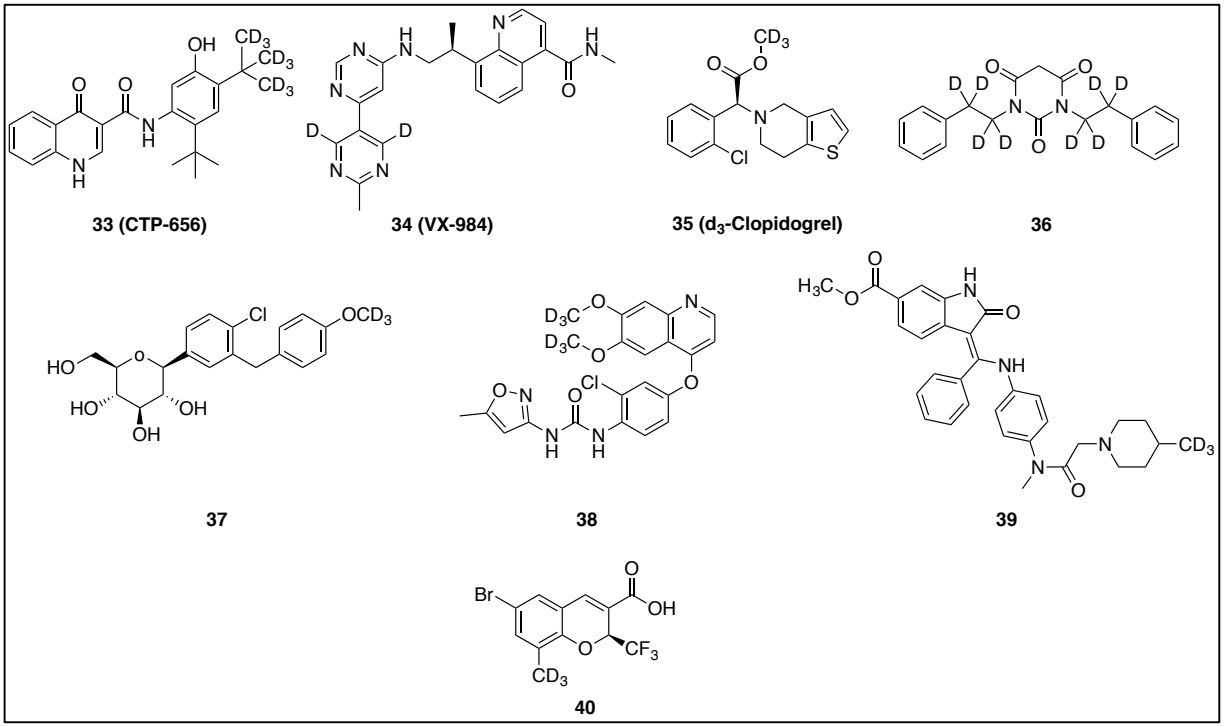

Figure 3. Deuterium-Labeled Medicinal Agents

1.4 Methods of H/D Exchange

There are two contrasting strategies for the synthesis of deuterium-labeled compounds, one of which is a total synthetic approach using commercially available deuterated precursors as starting materials. This approach generally involves multistep synthetic routes and expensive reagents, compared to the second strategy that is based on post-synthetic H/D exchange, which is more cost and time effective if it can be accomplished with minimal losses. Depending on where in the synthesis the deuterated component is incorporated, costly losses of isotope may occur en route to final product. Traditional post-synthetic H/D exchange strategies involve: (a) *pH*-dependent H/D exchange, (b) H/D exchange under hydrothermal or supercritical conditions and (c) transition metal-catalyzed H/D exchange.

1.4.1 *pH*-Dependent H/D Exchange

Application of high temperature and dilute acid (HTDA) has been widely used to introduce deuterium into aromatic compounds. Kadai *et al*.[45–47] and Gaston *et al*.[48] extensively studied deuteration and tritiation of aromatic compounds and observed exchange between aromatic hydrogens and deuterium in the presence of HCl at 250 ˚C to 280 ˚C with D_2O as a primary source of deuterium. The aromatic systems investigated under these conditions were substituted benzene, heterocycles, and polycyclic compounds.[49,50] Martins *et al*.[51] also demonstrated regioselective H/D exchange at *ortho* and/or *para* positions to nitrogen in substituted anilines using HCl and D_2O at 180 °C. Microwave mediated H/D exchange of aromatic compounds has also been reported by Vaidyanathan *et al*.[52] using DCl and D_2O with higher deuteration achieved at 175 °C.

Introduction of deuterium under basic conditions at benzylic sites[53–57] or aromatic sites[58] in D_2O and at sites adjacent to heteroatoms like nitrogen or sulfur[53] in deuterated dimethylsulfoxide (DMSO-d_6)[37,59–61] has also been explored (**Scheme 21**). In addition to the sites described, various site-selective H/D exchange methods performed under basic conditions[62,63] have been published however, these conditions are not compatible with acid or base sensitive molecules, which limits the application of these strategies.

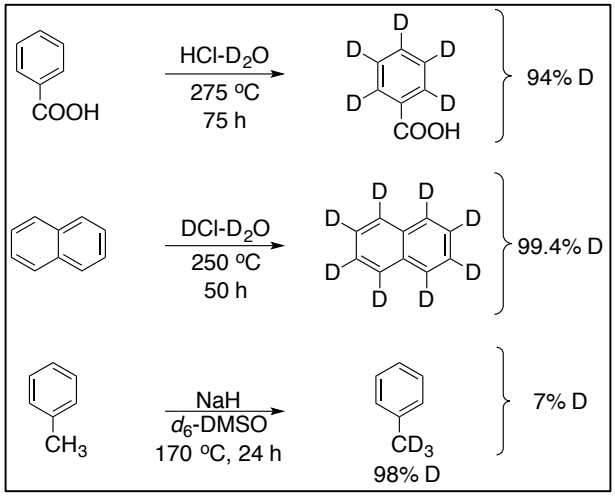

Scheme 21. *pH*-Dependent H/D Exchange

Giles *et al.*[64] recently published deuterotrifluoroacetic acid (CF_3COOD)-catalyzed H/D exchange of ketones,[65] aromatic amines and amides, with CF_3COOD serving as solvent and the source of deuterium. The reaction, conducted at 110 °C in the absence of metal salts or co-catalyst, showed deuterium incorporation in pharmaceutically relevant moieties like acetaminophen (**Scheme 22**) and diclofenac.

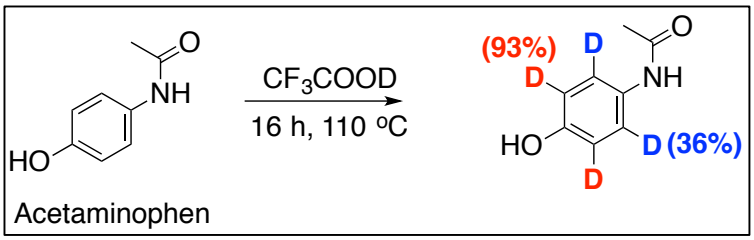

Scheme 22. CF_3COOD-Catalyzed H/D Exchange

Moozeh *et al.*[66] used an pyridoxal analogue (2%) and a chiral base (4%) to deuterate L-alanine with stereochemical inversion to make deuterated D-alanine (**Scheme 23**). The reaction conducted at pH 7 and 25 °C in the absence of a protected group, showed 99% deuteration in 72 h with 67% *ee*.

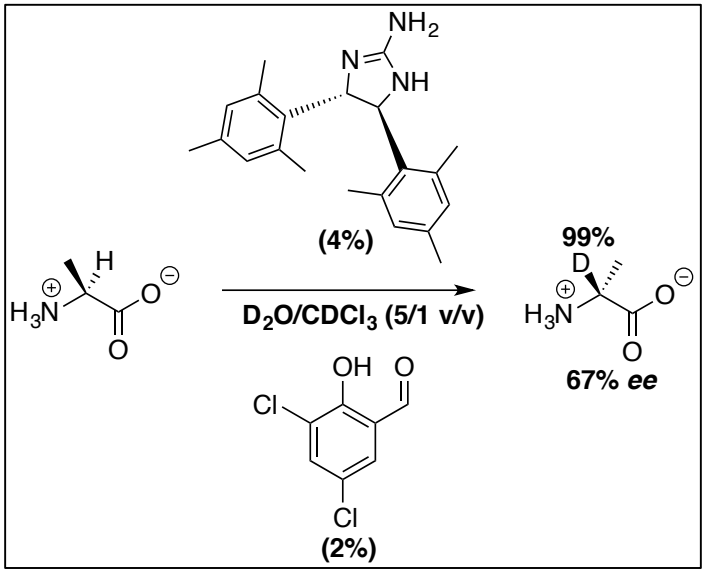

Scheme 23. Stereoselective Deuteration of L-alanine

1.4.2 H/D Exchange under Hydrothermal or Supercritical Conditions

The use of supercritical conditions in D_2O has been investigated extensively to perform deuteration of organic molecules. The key factors proposed to explain the effectiveness of this method are the dramatic changes in the properties of D_2O as it reaches and exceeds its critical point. These changes result in large increases in the equilibrium constants for the reactions of weak organic acids with deuteroxide ($^-$OD) anions. This property has been demonstrated in deuteration of arenes and heteroarenes[67] with excellent deuterium incorporation efficiencies (**Scheme 24**).

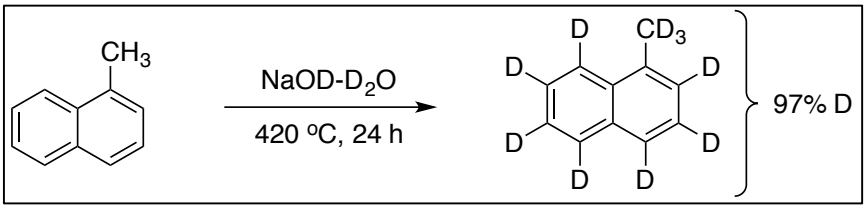

Scheme 24. H/D Exchange Reaction in Supercritical or Hydrothermal Water

1.4.3 Transition Metal-Catalyzed H/D Exchange

Transition metal catalysis has evolved into the most desirable strategy for H/D exchange

owing to its efficiency, regio- and stereoselectively, and high tolerance towards functional groups; it thus avoids undesirable side reactions. Transition metal-catalyzed H/D exchange has been widely exercised in homogeneous and heterogeneous environments. For practical large-scale applications, heterogeneous processes are favored due to their ease of product separation, usually via simple filtration.

Though a wide variety of transition metals, such as Ir,[68–106] Rh,[80,81,107–116] Co,[117,118] Pt,[119–125] Ru,[112,126–145] Pd,[146–151] Ni,[152,153] Os,[154] Sn,[155] Mn,[156] or group 5 and 6 metals[157] have been applied as homogeneous catalysts to introduce deuterium into substrates, we will limit our discussion to those metals used in heterogeneous catalysis in order to keep the discussion pertinent to our research goal.

1.4.3.1 Ru-Catalyzed H/D Exchange

Heterogeneous Ru has been effective in activating C-H bonds in substrates containing heteroatoms like nitrogen or oxygen. Evain *et al*.[158] and Alexakis *et al*.[159] reported selective deuteration of pyridine derivatives at the *ortho* positions using 5% Ru/C (ruthenium on carbon) in the presence of D_2 (**Scheme 25**). This reaction, performed at ambient temperature without any catalyst pretreatment showed >90% deuterium exchange. On the other hand, substrates like 4-dimethylaminopyridine, 2-picoline, 2-fluoropyridine, 2,2'-bipyridyl and phthalazine failed to exchange under these reaction conditions; this inactivity was explained by the inability of the ring to develop the requisite alpha-pyridyl complex.

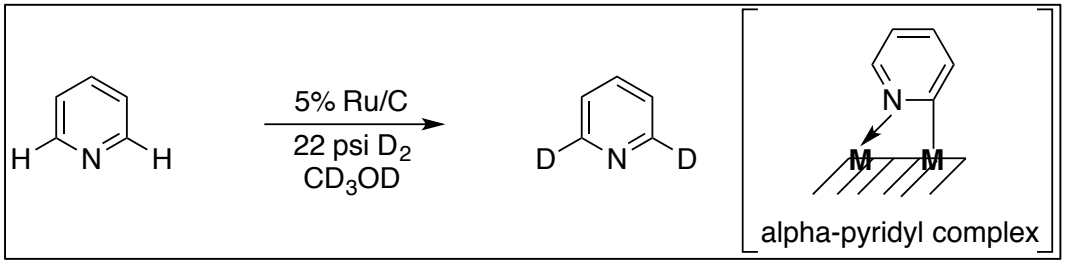

Scheme 25. Ru/C-Catalyzed Ortho-H/D Exchange in Pyridine Derivatives

During the study of hydrogenation of L-alanine to L-alaninol, Jere *et al.*[160] observed stereoretentive deuterium exchange at sites α to the amine group in the presence of Ru/C, D_2O at 1000 psi D_2 and 100 ˚C. Deuterium incorporation occurred over 6 h without any loss of optical purity in both L-alanine and its hydrogenated product L-alaninol. Increasing the temperature resulted in the completion of the reaction in 1 h but also resulted in partial racemization of the substrates (**Scheme 26**).

Jacobs[161] further expanded the substrate scope by exploring the Ru/C-catalyzed H/D exchange process in nitrogen-based substrates like glycine, *N*-methylglycine (sarcosine), *N,N*-dimethylglycine and betaine. The reaction, run in D_2O in the presence of 5% Ru/C at 100 ˚C and 1000 psi H_2 showed deuteration at the methylene (85.5%) position of glycine in 5 h. Under the similar conditions, *N*-methylglycine showed deuterium incorporation of 85.5% at the methylene and 90% at the methyl site. Similar observations were made in the case of *N, N*-dimethylglycine that showed 85% deuterium incorporation at methylene and 92% at the methyl sites in 6 h. Betaine, studied at 130 ˚C, 1000 psi H_2 and with 5% Ru/C, showed 95% deuterium incorporation at the methylene site in 6 h with no activation at the methyls; however, in this case, H/D exchange was also observed in the absence of catalyst.

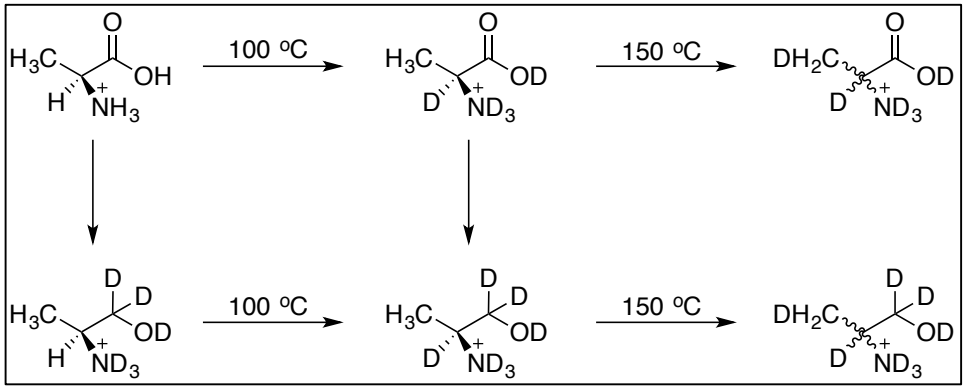

Scheme 26. Ru/C-Catalyzed H/D Exchange in L-alanine

Sajiki *et al.*[162] developed a Ru/C-catalyzed regioselective method to induce H/D exchange at sites α to hydroxy groups. The reaction was operated at 80 ˚C in the presence of 5% Ru/C, and H_2 with D_2O serving as a deuterium source. 1° and 2° alcohols showed excellent reactivity under these reaction conditions and deuterations of *di*- and *triols* were performed in a regioselective manner with H/D exchange occurring at sites α to hydroxyl groups. Deuteration of chiral alcohols under these conditions led to a racemized product and the proposed pathway for this behavior is the formation of an intermediate keto or aldehyde species.

Sajiki *et al.*[163,164] expanded the substrate scope by targeting sites α to hydroxyl groups in sugars. In the presence of 10% Ru/C by weight, 80 ˚C, H_2 and D_2O, they observed deuteration of sugars in a completely regio-, chemo-, and stereoselective manner. The deuteration proceeded with high deuterium efficiency in all but the sites adjacent to ethereal oxygens, where no activity was found (**Scheme 27**).

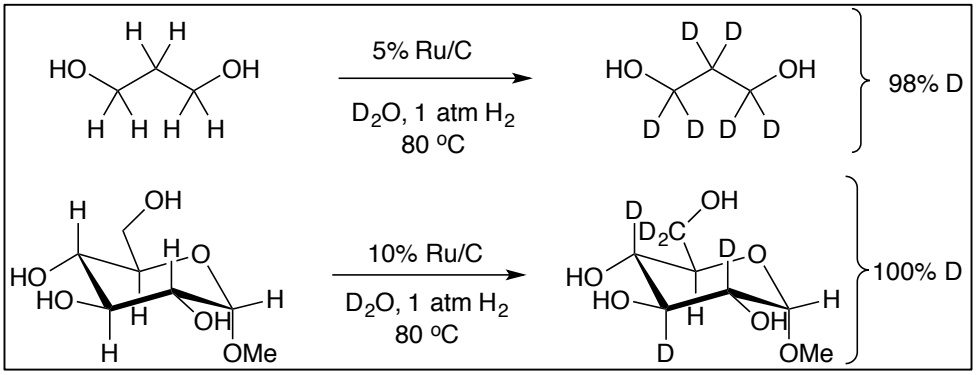

Scheme 27. Ru/C-Catalyzed H/D Exchange in Alcohols

The H/D exchange reaction described by Bresó-Femenia *et al.*[165] allowed selective deuteration at the ortho position of phenylalkylphosphines including diphosphines. The reaction conducted in the presence of Ru/PVP nanoparticles and D_2 showed deuterium incorporation in phosphines, phosphine oxides and phosphites.

Recently, Pietrs *et al.*[166] reported an H/D exchange method to deuterate pyridines, quinolones, indoles and alkylamines using D_2 and Ru/PVP nanoparticles. The reaction was operated at 20-55 °C and 14.5 psi - 29 psi pressure. The results suggested that the C-H bond α to nitrogen atom is broken and reformed on the Ru surface. They followed this work with stereoretentive H/D exchange using similar conditions and expanded the substrate scope to amino acids.[167]

1.4.3.2 Pd-Catalyzed H/D Exchange

Heterogeneous Pd systems have been extensively studied with a wide range of substrates and have shown great affinity for C-H bonds in heterocycles and at benzylic positions. Burwell *et al.*[168] reported H/D exchange in cyclopentane in the presence of 5% Pd on alumina at 40 ˚C, 2 psi of cyclopentane vapor and 12.6 psi of D_2. This was followed by a study from Stuart *et al.*[169] in which they demonstrated deuteration of hydrocarbons with 10 to 36

carbon atoms. This system permitted the use of unsaturated and saturated, cyclic and acyclic substrates and resulted in the perdeuterated form. This exchange was performed between hydrocarbon liquid and D_2 over Pd/C at 190–200 °C. No cracking or structural isomerization was reported under these conditions, but epimerization of asymmetric carbon did occur. The hydrocarbons targeted were *n*-decane, *n*-docecane, *n*-hexadecane, *n*-octadecane, *n*-tetracosane, *n*-octacosane, *n*-hexatriacontane, pristine, squalane, cyclododecane, 1,2-dicyclohexylethane and decalin.

Application of hydrothermal conditions (250 °C, 580-725 psi) in the presence of a transition metal, such as Pd, also shown high deuterium incorporation in aromatics[170,171] as well as aliphatic[171,172] substrates. Although quantitative deuterium incorporations are generally accomplished under these conditions, special equipment is required to tolerate the high-pressure and high-temperature conditions to avoid corrosion by the strongly oxidative nature of supercritical D_2O.

Buchman *et al*.[173] studied isotopic exchange reactions of bibenzyl and benzylic derivatives with D_2 and tritium gas in the presence of 10% Pd/C by weight. They observed that the reactions performed in aprotic solvents such as dioxane, ethyl acetate and cyclohexane resulted in the exchange of 3.1 to 3.5 D atoms in 1 h whereas in benzene, exchange in this same period was 1 D atom. They also observed that oxygen or nitrogen atoms in the substrate enhanced the rate of exchange, while sulfur atoms inhibited the catalytic activity (**Scheme 28**). Sajiki *et al*.[174–176] expanded the scope of this strategy by developing a mild, one-pot method for the chemoselective H/D exchange reaction at the benzylic position with excellent deuterium incorporation efficiencies.

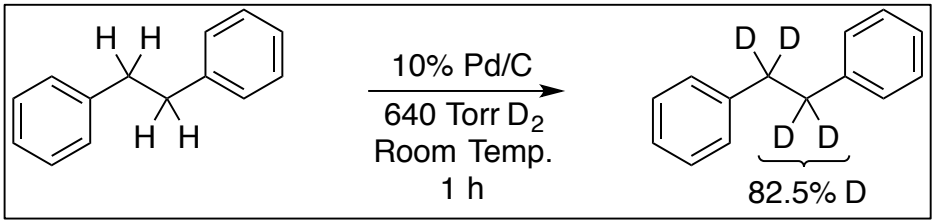

Scheme 28. Pd/C-Catalyzed H/D exchange in Bibenzyl

The experiments were conducted in the presence of 10% Pd/C and H_2 at ambient pressure and room temperature for 72 h. The methoxy and the hydroxy substituents in the substrates showed no influence on the course of H/D exchange reaction. Benzylic substrates with carboxylic acid or ester groups showed only moderate deuterium incorporation, which can be rationalized by invoking coordination of Pd with the carboxylic acid or ester oxygen, leading to a less reactive catalyst (**Scheme 29**).

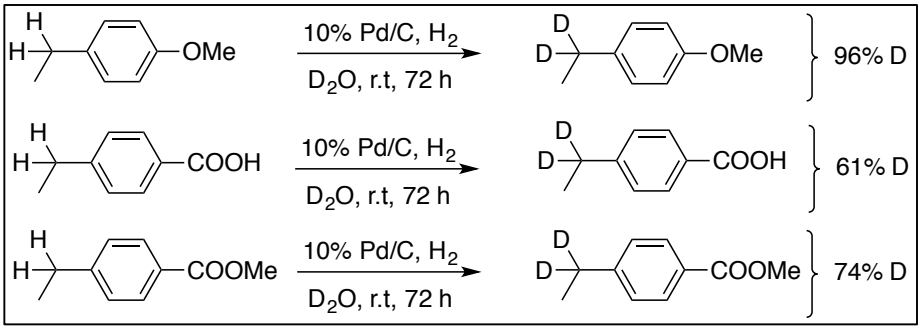

Scheme 29. Pd/C-Catalyzed H/D Exchange in Substituted Benzylic Sites of Arenes

Expanding on this methodology, Sajiki *et al.*[175] reported deuteration of benzyl ethers, which are generally unstable under Pd/C-catalyzed hydrogenation conditions, with a high deuterium efficiency using Pd/C-ethylenediamine complex [Pd/C(*en*)]. Using a mixture of THF and D_2O (7:3) as a solvent, they successfully suppressed the hydrogenolysis of the corresponding benzyl ether (**Scheme 30**).

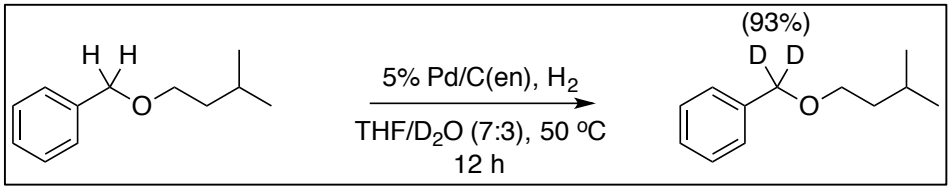

Scheme 30. Pd/C(*en*)-Catalyzed H/D Exchange

Pd-catalyzed deuteration of substituted imidazoles and 1,3-dialkylimidazolium salts, using D_2O as a source of deuterium over a heterogeneous Pd catalyst has been reported by McMath *et al*.[177] They demonstrated the deuteration of 1,3-dimethylimidazolium chloride at H{2} (99%) and H{4/5} (90%) positions using 10% Pd/C in D_2O pre-reduced under H_2 gas for 1 h, at ambient pressure and temperature. The deuteration of imidazolium chlorides demonstrated the general applicability of this system, with 90-96% deuterium incorporation at the ring (**Scheme 31**).

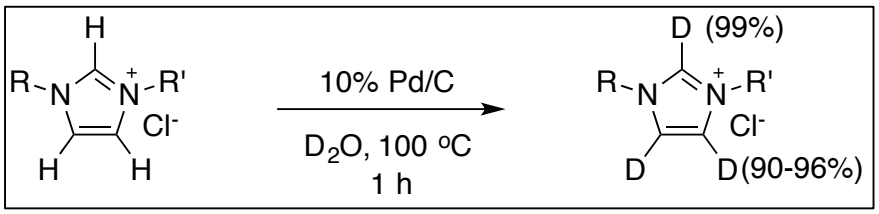

Scheme 31. Pd-Catalyzed H/D Exchange in Imidazoles

Sajiki *et al*.[178] also investigated the scope of the Pd-catalyzed aromatic H/D exchange in the base moiety of nucleosides. They could demonstrate Pd/C-catalyzed deuteration in adenine, uracil, cytosine and thymine derivatives. These reactions were conducted in the presence of 10% Pd/C, H_2 and D_2O in a temperature range of 110-160 ˚C and showed deuterium incorporation efficiency of >90% in most of the cases (**Scheme 32**).

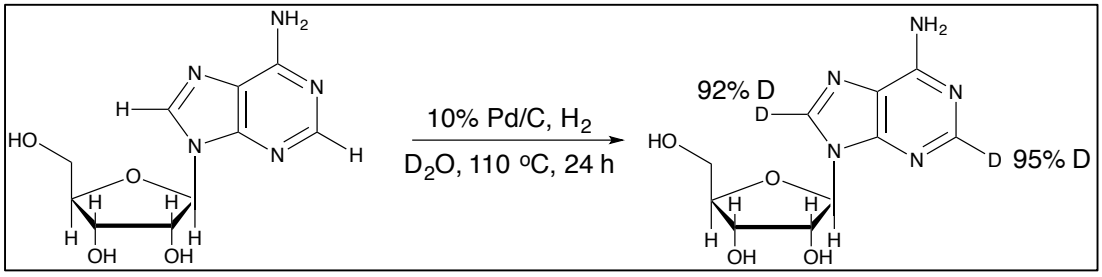

Scheme 32. Pd/C-Catalyzed H/D Exchange in Nucleosides

The technique mentioned above was also used to introduce deuterium into derivatives of pyridine, indole, and pyrimidine. The effect of Pd in activating aromatic hydrogens paved the way for incorporating deuterium into various bioactive molecules, like sulfamethazine, nalidixic acid and antipyrine (**Figure 4**).[179]

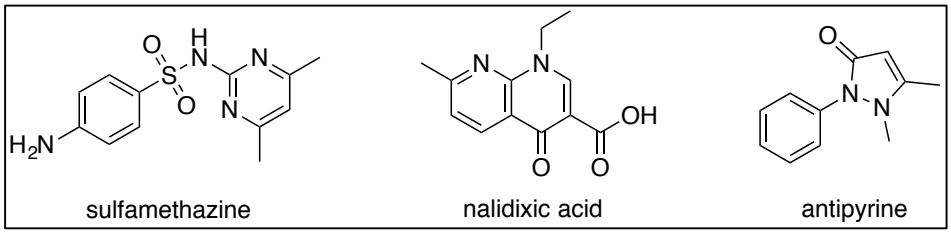

Figure 4. Bioactive Molecules

Sajiki *et al.*[180] combined the abilities of heterogeneous Pd to activate aromatic and benzylic C-H bonds and attempted to introduce deuterium at both sites simultaneously in benzyladenine. When the reaction was carried out at 110 ˚C in the presence of 10% Pd/C, debenzylation was observed, whereas replacing the catalyst with 5% Pd/C(en) at 180 ˚C remarkably promoted the H/D exchange reaction (**Scheme 33**).

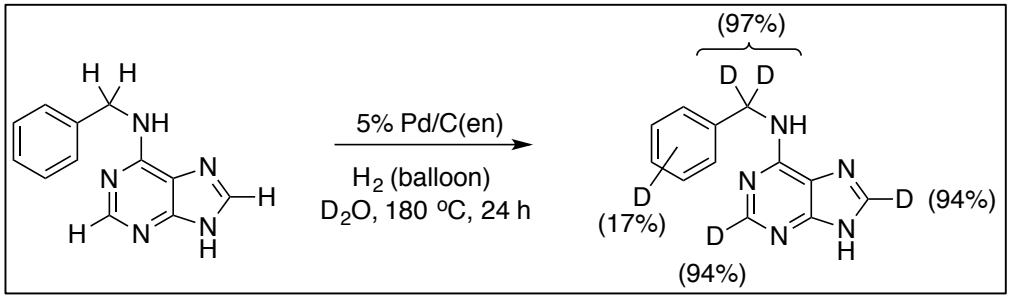

Scheme 33. Pd/C-Catalyzed H/D Exchange in Benzyladenine

Pd/C-H_2-D_2O-catalyzed multideuterium incorporation into unactivated linear or branched alkyl chains that bear a carboxyl, hydroxyl, ether, ester, or amide moiety and are connected with the benzene ring has been reported.[181,182] Apart from the benzylic activation shown by heterogeneous Pd, heating the reaction to a temperature as high as 160 ˚C demonstrated deuterium incorporation at otherwise non-labile carbons (**Scheme 34**).

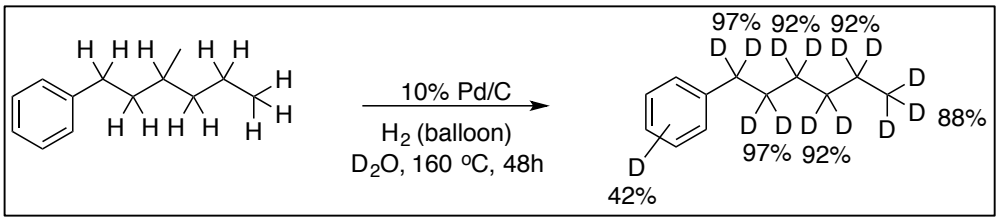

Scheme 34. Pd/C-Catalyzed H/D Exchange in Alkyl Chains of Aromatic Compounds

This effect has also been mimicked by Atzrodt *et al.*[183] employing Pd/C in the presence of sodium borodeuteride ($NaBD_4$) as a reducing agent to activate the catalyst. The reaction was conducted using D_2O as a primary source of deuterium and, at 130 ˚C, they achieved moderate deuterations at unactivated carbons (**Scheme 35**).

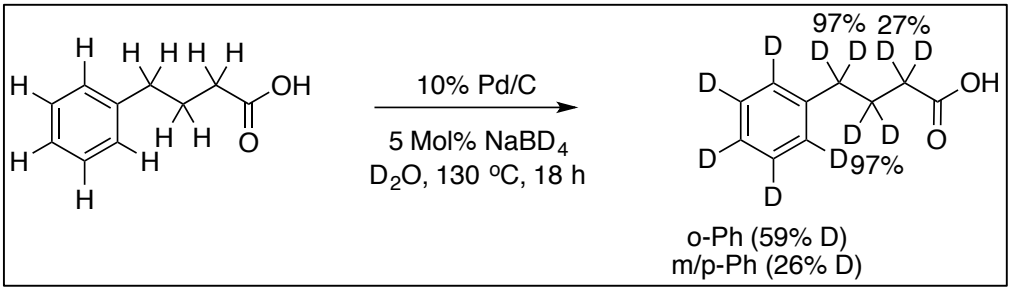

Scheme 35. Pd-Catalyzed H/D Exchange in Alkyl Chains

Sajiki *et al*. developed an effective catalytic isotope exchange reaction between H_2 and D_2O in the presence of Pd/C to generate D_2. The D_2 was generated in the system using 10% Pd/C in the presence of H_2 at room temperature, with D_2O serving as the deuterium source. The D_2 generated was eventually used for Pd/C-catalyzed one-pot catalytic reduction of functionalized aromatic halides, epoxide, nitrile and unsaturated hydrocarbons with quantitative deuterium incorporation efficiencies.[181,184]

Sajiki *et al*.[185] also demonstrated a liquid-phase redox system between 2° alcohols and ketones, in the presence of the Pd/C-H_2-D_2O system, that produced a mixture of deuterium-labeled 2° alcohols and ketones. They hypothesized that the 2° alcohol was oxidized to the corresponding ketone under the hydrogenation conditions and the hydrogenation of the aliphatic ketone to the corresponding 2° alcohol with deuterium is responsible for the deuterium incorporation (**Scheme 36**).

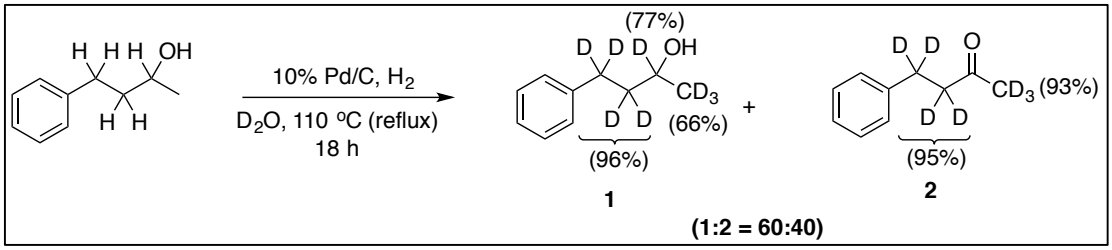

Scheme 36. Pd/C-Catalyzed H/D Exchange in Alcohols

Utilizing the concept of *in situ* D_2 generation, Sajiki *et al.*[186] developed a Et_3N-mediated H/D exchange reaction of alkynes to produce deuterated alkynes in a mixture of D_2O and THF at room temperature. They also developed a method of Pd/BN (palladium/boron nitride) catalyzed regioselective reduction of alkynes to give deuterated alkenes with excellent deuterium content. A variety of reducible functionalities, such as nitro groups, benzyl ethers, TBS ethers, and silanes were well tolerated under these reaction conditions (**Scheme 37**).

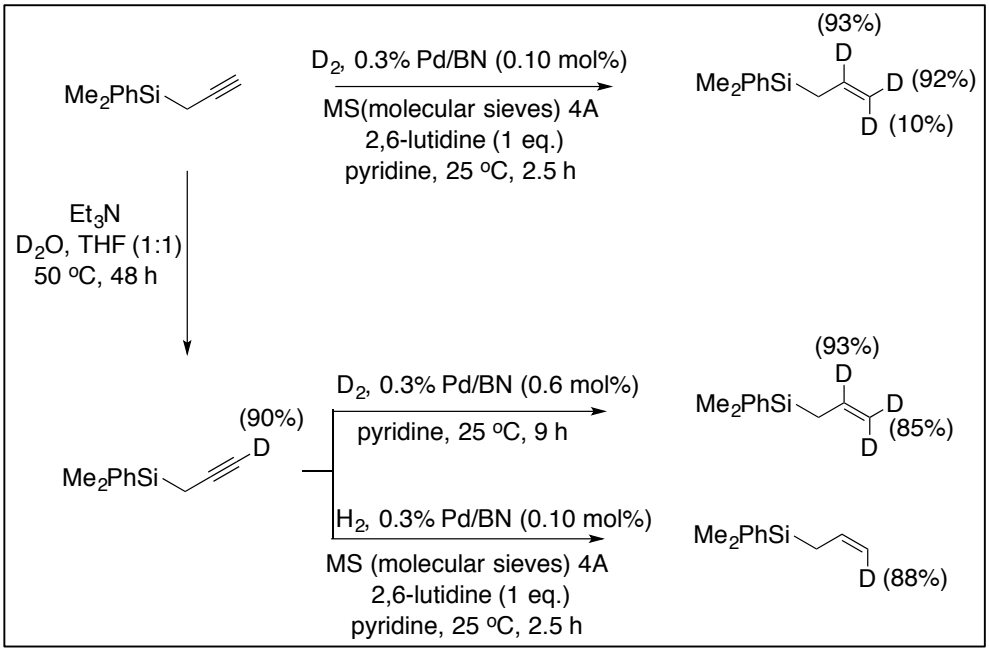

Scheme 37. Pd/BN-Catalyzed Deuterogenation of Alkynes

Oshima *et al.*[172] have also reported a Pd-catalyzed decarboxylative deuteration process under hydrothermal conditions. They hypothesized that Pd under hydrothermal conditions in D_2O leads to the formation of palladium deuteride that serves as a reagent for the decarboxylation of free carboxylic acids and decarbonylation of aldehydes, and concurrently deuterate the substrates (**Scheme 38**).

Scheme 38. Pd-Catalyzed Decarboxylative Deuteration

1.4.3.3 Pt-Catalyzed H/D Exchange

Compared to Pd/C-H_2-D_2O, Pt has better reactivity towards aromatic hydrogens. Garnett *et al*.[187,188] reported a Pt-catalyzed (pre-reduced platinum oxide with D_2) H/D exchange reaction using D_2O for the deuteration of benzoic acid and its sodium salt, bromobenzene, isopropyl benzoate, aniline, nitrobenzene, p-nitrobenzoic acid, phenol, pyridine, and trimesic acid.

Sajiki *et al*.[189,190] also introduced a deuteration method for aromatic rings, using the Pt/C-D_2O-H_2 system. The reaction was operated in the temperature range of 25–180 ˚C. This method was used to investigate deuteration of aromatic rings possessing an electron-donating group like phenol, which showed excellent deuterium incorporation at the aromatic ring. Deuteration of aromatic rings possessing an electron-withdrawing group like in benzoic acid showed lower reactivity; this was compensated by an increase in the temperature. Introduction of an electron-withdrawing group, such as nitro, strongly diminished the reactivity of substrates even at high temperatures.

Sajiki *et al*.[191] investigated Pt-catalyzed reactions in a H_2 free environment employing Pt/C in a mixture of isopropyl alcohol, cyclohexane and D_2O in which zero valent Pt metal was self-activated by the *in situ* generated H_2 derived from isopropyl alcohol. The presence of acetone in the reaction resulted in this mechanistic interpretation.

1.4.3.4 Pd/Pt Hybrid Catalyzed H/D Exchange

The simultaneous use of multiple catalysts enables the reduction of reaction steps for perdeuteration and is cost saving in comparison to stepwise reactions with the individual use of a catalyst. Moreover, composite catalysts have been shown to possess novel and unique activities such as the Ziegler–Natta catalyst composed of titanium (Ti) and aluminum (Al) or the Pd/Pt supported dendrimer catalyst for polymerization.[192] The use of mixed Pd/C and Pt/C[193–195] or the novel bimetallic Pd/Pt on a carbon catalyst[196] were found to be more efficient in the H/D exchange reaction than the independent use of Pd/C or Pt/C (**Scheme 39**). Modutlwa *et al.*[197] expanded on this work and applied the synergistic effect in developing deuterated medicinal agents. The transformations were conducted using Pd/C, Pt/C and Rh/C in the presence of H_2 and D_2O at 160 °C to deuterate valpromide, phenytoin and trimethoprim.

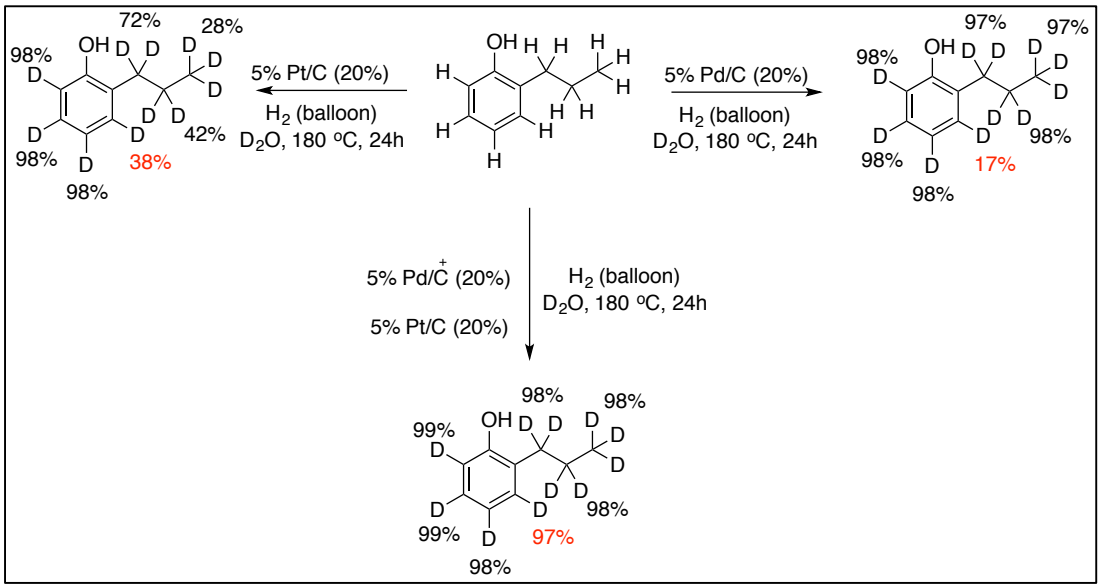

Scheme 39. Pd/Pt Hybrid Catalyzed H/D Exchange

The synergistic effects of Pd-Pt/C were further investigated by Derdau *et al*.[198] in which they applied microwave conditions to $NaBD_4$-activated metal catalysts. A variety of aromatic and heterocyclic compounds were investigated and they demonstrated significant deuterium incorporation in the presence of Pd-Pt mixtures (**Scheme 40**).

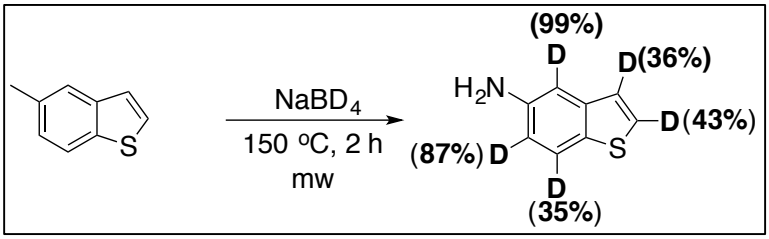

Scheme 40. Pd/Pt-Catalyzed Deuteration under Microwave Conditions

1.4.3.5 Rhodium Catalyzed H/D Exchange

Simple alkanes, which are inactive substrates by most definitions showed efficient deuteration under Rh/C-catalyzed conditions at 160 °C in a H_2 filled sealed tube using D_2O as a solvent and the source of deuterium. Not only linear alkanes but also the cyclic and branched alkanes underwent deuteration to afford the corresponding fully deuterated products with high deuterium efficiencies (**Figure 5**).[199]

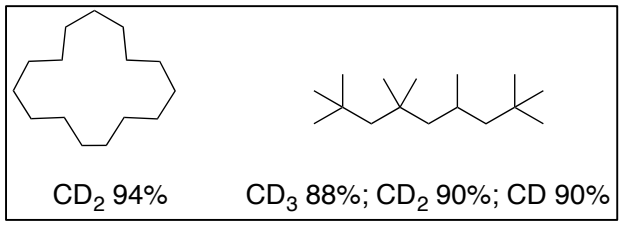

Figure 5. Rh/C-Catalyzed H/D Exchange in Saturated Hydrocarbons

1.4.3.6 Miscellaneous

Deuterated Raney-nickel demonstrated aromatic H/D exchange at 70 ˚C in D_2O. Substrates investigated using these reaction conditions were sodium cinnamate and sodium benzoate.[200] Raney-Ni has also effected H/D exchange in the presence of D_2O to give

deuterated aromatics,[201] glucose,[202] glycosides,[203] 1,6-anhydrohexoses[204] and various other carbohydrates.[202,205,206]

Mukumoto *et al*.[207] reported H/D exchange in optically active benzylic compounds like (*R*)-2-phenylpropnoic acid, (*R*)-2-hydroxy-2-phenylacetic acid and (*R*)-2-amino-2-phenylacetic acid without any racemization using Cobalt-Aluminum Alloy. The reaction, conducted in D_2O using sodium carbonate (Na_2CO_3), gave 70-89% deuteration with *ee* values ranging from 46-99%.

A solid-phase Ir-based catalyst has been developed to label aromatic compounds containing suitable directing groups. The reactions carried out at ambient temperature with D_2 have been explored with substituted acetophenones, 2-phenylpyridine, benzanilide, *N,N*-dimethylbenzamide and 7,8-benzoquinoline.[208]

Deuteration of carbonyl compounds using pyrrolidine as an organocatalyst in the presence of D_2O has been described by Zhan *et al*.[209] Deuterium incorporations up to 99% and functional group tolerability against $-NO_2$, $-OCH_3$, $-N(CH_3)_2$, -Br, -COOH, $-NH_2$ was observed with this methodology.

Ito *et al*.[210] reported deuterative cyclization reactions of sulfanyl 1,6-diynes to form *N*- and *O*-containing heterocycles (furans and pyrroles) using $NaBD_4$ and ethanol. A range of substituted furans and pyrroles were deuterated using this method with 100% deuterium incorporation in certain cases (**Scheme 41**).

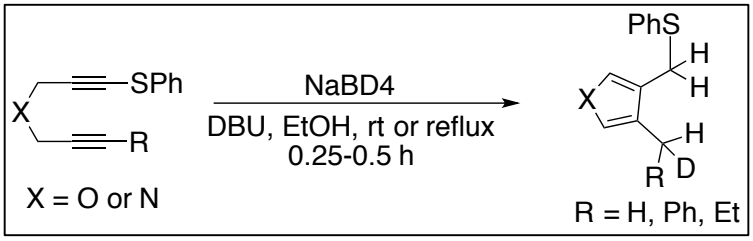

Scheme 41. Deuterative Cyclization to Develop Deuterated Heterocycles

1.5 Summary

This chapter outlines various uses of deuterium-labeled compounds as probes to understand reaction mechanisms, as tracers in metabolism studies, and as medicinal agents. The ability of deuterium to alter the metabolic and pharmacokinetic profile of a drug is used extensively nowadays to develop new therapeutic agents or test the deuterated analogues of drugs in the pipeline to protect patents. This application represents an significant need for post-synthetic H/D exchange methods applicable on a large scale. The three traditional methods of introducing deuterium have been discussed in this chapter: (1) *pH*-dependent H/D exchange; (2) H/D exchange under hydrothermal or supercritical conditions; and (3) transition-metal catalyzed H/D exchange. The H/D exchange under acidic or basic conditions can achieve high deuterium incorporation but is not appropriate for acid or base-labile substrates; hydrothermal or supercritical methods, in turn, can be effective, but only for thermally stable substrates that can withstand such aggressive conditions. The generally milder transition-metal catalyzed H/D exchange is most commonly used but the available include a few drawbacks. Heterogeneous catalysis is preferred at the industrial level due to the ease of catalyst removal and product isolation but currently available heterogeneous transition-metal catalyzed H/D exchange requires the use of H_2 or D_2 gas and often significant pressures to dissolve these gases.

1.6 Goal of this Research Project

Most of the current H/D exchange methods that are selective, robust and efficient are homogeneous or heterogeneous transition-metal based systems. The heterogeneous transition-metal based systems are preferred over homogenous due to the ease of separation but the current heterogeneous methods for H/D exchange operate in the presence of H_2 or D_2 gas that is not considered ideal on a large scale. The inability of these systems to be scaled up to an industrial setting creates an opportunity for us to develop a method that satisfies five basic goals: (1) mild (temperature & pressure); (2) inexpensive; (3) aqueous-based; (4) selective and (5) No H_2 or D_2 gas.

With the goal of incorporating these principles, we present in this dissertation a heterogeneous transition-metal based electrocatalytic system with the ability to activate C-H sites in organic molecules and introduce deuterium in a regioselective and stereoretentive manner. In the following chapters, we will discuss the development of our electrocatalytic system that addresses all these goals while giving high deuterium incorporations.

Chapter 2. Stereoretentive H/D Exchange via an Electroactivated Heterogeneous Catalyst at sp^3 C-H Sites Bearing Amines or Alcohols

2.1 Introduction

Our research group has focused on the development of strategies to convert inexpensive substrates to valuable products. One of the primary targets has been conversion of lactic acid. Over the last two decades, our research group has examined ways to convert lactic acid to acrylic acid, and later to 2,3-butanedione over phosphate,[211] sodium,[212,213] or ammonium salts.[214]

In keeping with the ongoing focus on development of paths to valuable products, Zhang *et al.*[215,216] studied the Ru/C-catalyzed system of hydrogenating lactic acid to produce propylene glycol, a commodity chemical. This reaction, conducted at 150 ˚C and 2100 psi H_2, produced propylene glycol with 87% conversion (90% yield) in 5 h. This observation was followed by the work of Jere *et al.*[160,217] who demonstrated the hydrogenation of L-alanine to L-alaninol with 93% conversion (91% yield) at 100 °C and 1000 psi H_2 in 6 h (**Scheme 42**).

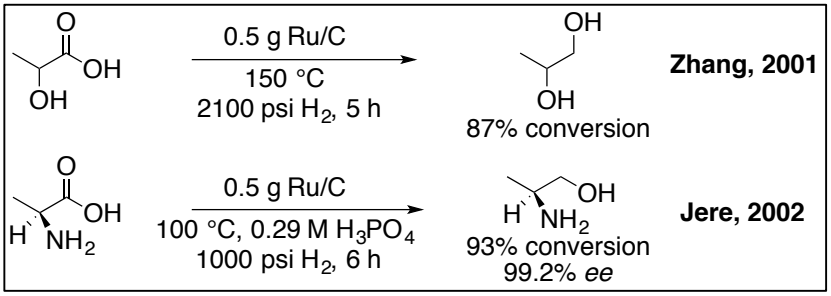

Scheme 42. Hydrogenation of Carboxylic Acid Derivatives

To probe the mechanism of hydrogenation of L-alanine and the retention of stereochemistry in L-alaninol, Jere *et al.*[160] performed H/D exchange studies. At 150 °C and

1000 psi H_2, they observed H/D exchange at the α site in L-alanine and L-alaninol without any loss in optical purity (**Scheme 43**).

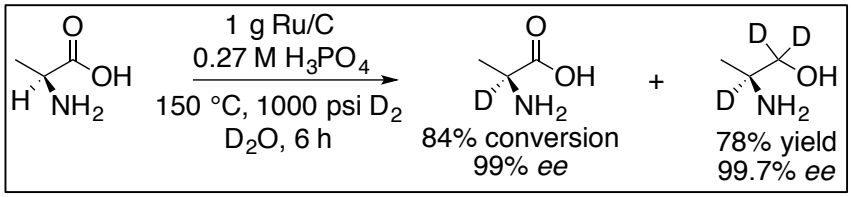

Scheme 43. Stereoretentive H/D Exchange in L-alanine and L-alaninol

Due to the low solubility of H_2 in water, higher pressure was required its concentration in the liquid. To avoid the use of H_2 and high pressure to dissolve it, Dalavoy *et al.*[218] developed electrocatalytic hydrogenation (ECH) of lactic acid to propylene glycol as a mild alternative to the traditional transition metal-catalyzed high-pressure batch reactor hydrogenation method. In this method, the carboxylic acid moiety is reduced by Ru/C using atomic hydrogen formed at the catalytic cathode via reduction of protons (H^+) generated at anode. The ECH experiment was conducted at ambient pressure using lactic acid and an RVC (reticulated vitreous carbon) electrode suffused with 5% wt. Ru/C powder catalyst serving as the cathode, while Pt wire was the anode. Using a two-compartment (2-C) cell, anode and cathode compartments were separated by a glass frit preventing the diffusion of gaseous species. At 70 ˚C and 100 mA, using 0.01 M HCl as an electrolyte, 80.3% lactaldehyde and 2.9% propylene glycol were formed in 21 h (**Scheme 44**).

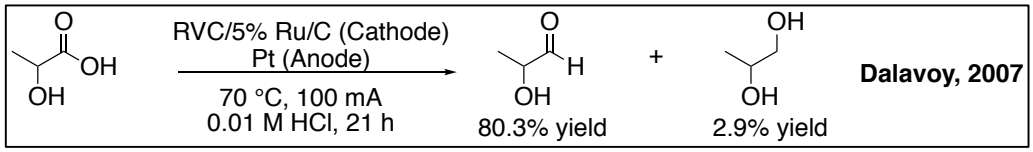

Scheme 44. ECH Reduction of Lactic Acid

A new research hypothesis, that transition-metal catalyzed reaction in high-pressure batch reactor can be replicated in an electrochemical setting, emerged from the findings of the studies mentioned above. Most important were the following three: a) hydrogenation of lactic acid to propylene glycol, catalyzed by Ru/C powder catalyst as demonstrated by Zhang *et al*. in high-pressure high-temperature batch and continuous reactors; b) stereoretentive H/D exchange at the amine-bearing sp^3 C-H site in L-alanine by Jere *et al*.; and c) electrocatalytic hydrogenation of lactic acid by Dalavoy *et al.* in a benchtop electrochemical cell obviating the need for pressure or external supply of H_2. Taken together, these results suggested that the electrocatalytic context should be capable of effecting H/D exchange at sites like those activated in Jere's studies. We therefore developed a heterogeneous approach that was mild, green, inexpensive, regioselective and stereoretentive in C-H to C-D conversion. The transformation was carried out in a 2-C cell separated by a Nafion® membrane where replacement of a hydrogen atom with a deuterium atom on the organic substrate was effected by ruthenium on activated carbon cloth (Ru/ACC), a support optimized by Li *et al*.[219] to deposit ruthenium. A Pt wire served as a counter electrode and the electrolyte used in the system was 0.01 M phosphate buffer (pH 7) prepared in D_2O that provided the ions for the conduction of current and served the source of deuterium.

The results described here reveal the capability of heterogeneous Ru/ACC to activate C-H bonds α to heteroatom (N or O) with only a modest current density. The present study used D_2O, and bypassed the high-pressure conditions and equipment needed to dissolve the poorly soluble D_2 (or H_2) in an aqueous environment at concentrations effective for mass transport and dissociation on the catalyst surface.

2.2 Experimental

2.2.1 Reagents and Materials

All reagents were purchased from commercial vendors and were used without further purification. D_2O (99.9%) was purchased from Cambridge Isotope Laboratories, Inc. The Pt (0.404 mm) wire used as a counter electrode was purchased from Alfa Aesar. Omegaette Model HHM33 multimeter and Lambda (Model: LPD 422A FM) galvanostats were used to maintain a constant current density in the system. HPLC grade purity methyl alcohol (MACRON Fine Chemicals) and water (Sigma-Aldrich) were used for HPLC analysis. Zorflex® ACC FM110 was obtained from the Calgon Carbon Co. Hexammineruthenium (III) chloride ($Ru(NH_3)_6Cl_3$), 99% was purchased from Strem Chemicals and ultra-high purity H_2 (AGA Gas 99.999%) was used for the preparation of the catalyst. Phosphate buffer (0.01 M) at pH 7 was prepared using potassium phosphate (monobasic and dibasic purchased from Jade Scientific) in D_2O.

2.2.2 Reaction Procedure

The experiment was carried out in a 2-C glass cell (volume of each cell: 30 mL) separated with a Dupont® Nafion-117 membrane (**Figure 6**). Ru/ACC was used as a working electrode (cathode) and a 0.404 mm Pt wire served as the counter electrode (anode). 20 mL of 0.01 M phosphate buffer (pH 7) prepared in D_2O was placed in each compartment to serve as electrolyte. The cell was placed in an oil bath for temperature control. The reaction was carried out under galvanostatic control, typically with a 30-minute pre-electrolysis phase at 2.2 mA/cm^2 to activate the Ru catalyst (*Note: Current density is calculated using the 4.5 cm^2* projected area of the ACC electrode). Substrate was then added to the catholyte to reach 20

mM concentration and subjected to electroactivated label exchange. The reaction was monitored via ^{1}H NMR.

The experiment for the scale-up reaction was carried out in a procedure like the one mentioned above except that 1 g (500 mM in 20 mL) of cyclopentanol was added to the catholyte. After the completion of the reaction, the cloth, catholyte and anolyte were extracted with 20 mL of methylene chloride (three times) and dried with $MgSO_4$ followed by filtration. Methylene chloride was evaporated under vacuum and the product was weighed.

The experiments to investigate the efficacy of electrodeposited Ru/ACC were carried out with a pre-electrolysis phase of 1 h at 33.3 mA/cm^2. Next, cyclopentanol (20 mM in 20 mL) was added to the catholyte (*Note: After pre-electrolysis phase, the pH of the solution is approximately 12*) and the current density was decreased to 2.2 mA/cm^2 for the remainder of the reaction. After the completion of the first run, the Ru/ACC was dried under a stream of N_2 overnight followed by vacuum drying for 12 h and the during the second run with the same cloth, no pre-electrolysis at 33.3 mA/cm^2 was performed.

The experiments to optimize for isolated yield were carried out via a procedure like that above but without any pre-electrolysis. After the completion of the reaction, the Ru/ACC was washed with the respective organic solvent (5 mL) and then dried under a stream of N_2 overnight. The same cloth was then used for the second run to test for deactivation.

To quantify the migration of cyclopentanol to the anodic chamber, we sat up a 2-C cell with a Nafion® membrane separating the chambers. 20 mL of 0.01 M phosphate buffer pH 7 was added to each chamber and the reaction was stirred without cathode or anode. Anolyte was analyzed via ^{1}H NMR to determine the concentration of cyclopentanol. To determine the

loss of cyclopentanol to the adsorption in ACC or Ru/ACC, reaction was run per the above procedure and the concentration of cyclopentanol was monitored in the catholyte.

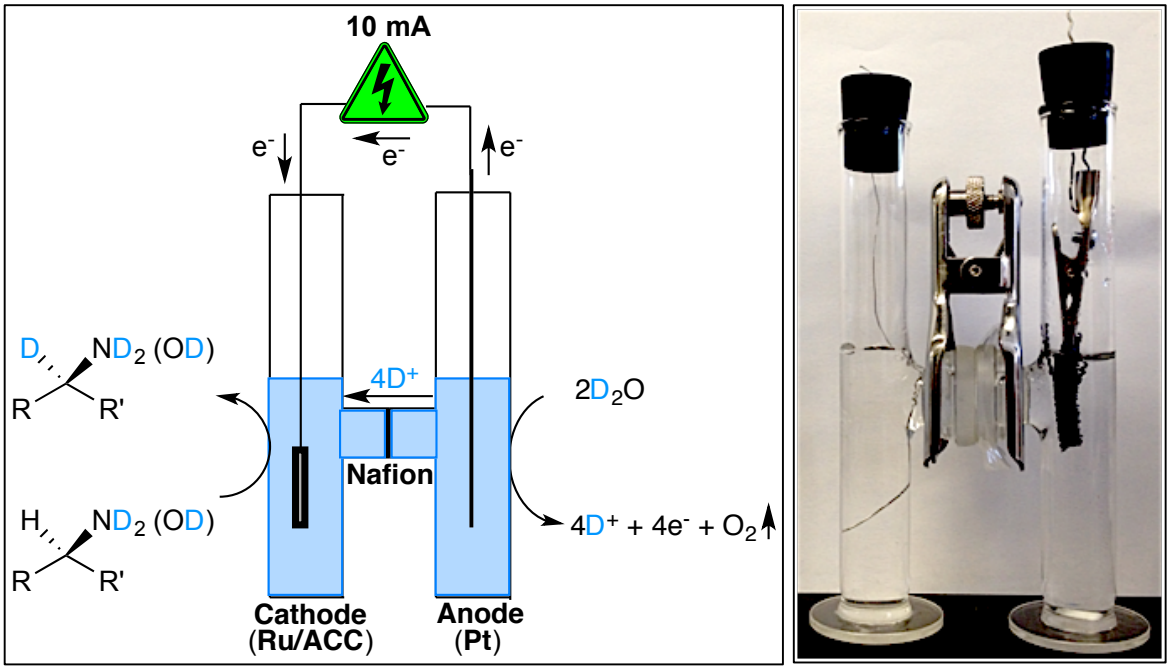

Figure 6. 2-C Cell

2.2.3 Product Analysis

2.2.3.1 ^{1}H NMR

Liquid samples were analyzed using an Agilent 500 MHz superconducting NMR spectrometer at 298 K. NMR tubes with an external diameter of 5 mm were used (Wilmad-LabGlass, Buena, NJ). A non-labile C-H site was used as an internal standard to determine the relative hydrogen content at the reactive site. Spectra were referenced using dimethyl sulfoxide (DMSO). The yield of the substrates was determined using the qEstimate tool of Agilent VnmrJ 4 employing 0.0485 M solution of triphenyl phosphate in $CDCl_3$. Chemical shift differences between initial and final spectra reflect the electrochemically induced pH shift to more basic conditions due to formation of $^{-}$OD.

2.2.3.2 HPLC

A Waters 600 liquid chromatograph instrument with Hitachi UV detector model L-4000H was employed for the HPLC analysis. An Astec CHIROBIOTIC™ T (25 cm x 4.6 mm, 5 µm) chiral column was used to determine the enantiopurity for amino acid analysis. Water:Methanol:Formic Acid (30:70:0.02) was used as a mobile phase and the UV wavelength was set at 205 nm. Analyses was run for durations of 20 or 30 minutes based on the retention time of the stereoisomers. The flow rate of the mobile phase was maintained at 0.5 mL/min for L-valine and L-threonine and 1 mL/min for L-alanine.

2.2.4 Development of the Catalyst

2.2.4.1 High Pressure/High Temperature H_2 Based Reduction

Following the earlier report of Li *et al.*,[219] Zorflex® ACC FM100 was chosen as the support for Ru due to its high conductivity and large surface area. ACC (3 cm x 1.5 cm) was initially washed in de-ionized (DI) water and then allowed to dry in an oven overnight at 105 ˚C. It was then soaked in a solution of $Ru(NH_3)_6Cl_3$ (1.0089 g) dissolved in ammonium hydroxide (1.98 ml) and water (13.02 ml). The damp ACC was then dried on the laboratory bench for 24 h, followed by vacuum drying at room temperature. The Ru impregnated in ACC was then chemically reduced with H_2 in a Parr reactor (model 452HC) at 500 psi and 310 ˚C for 12 h.

2.2.4.2 Electrochemical Based Reduction (Electrodeposition)

Electrodeposited Ru/ACC catalyst was developed using Zorflex® ACC FM100 as well. The ACC was heated overnight in the oven at 150 °C followed by drying under vacuum for 48 h. The dried ACC was then soaked in $Ru(NH_3)_6Cl_3$ (1.01 g), dissolved in ammonium hydroxide

(1.96 ml) and water (13.02 ml). The ACC sat overnight in the Ru salt solution and the solution was then evaporated under a stream of N_2 with the immersed ACC. The ACC impregnated with Ru salt solution was then dried under vacuum for 48 h.

2.2.5 Characterization of the Catalyst

2.2.5.1 Brunauer-Emmett-Teller (BET) Analysis

Brunauer-Emmett-Teller (BET) surface area,[220] micropore area and micropore volume of the samples were measured on a Micromeritics® ASAP 2010 system using a static volumetric adsorption and desorption method. At 77 K, the nitrogen adsorption gas pressure was increased until 99% of the saturation pressure was reached. The total surface area of the sample was calculated using the BET method from the adsorption isotherm from 0.06 to 0.20 relative pressures. The micropore volume was calculated from the desorption isotherm using the Barrett, Joyner and Halenda (BJH) method.[221]

2.2.5.2 Scanning Electron Microscopy (SEM) Analysis

SEM studies on JEOL JSM-7500F and JEOL 6400V instruments were used to image the catalyst support and morphology of Ru particles on the support. The catalysts were mounted onto aluminum stubs with carbon paste and then dried under vacuum overnight. Secondary electron imaging was used to obtain the images. Energy-Dispersive X-Ray (EDX) coupled with the JEOL 6400V SEM was used to characterize surface chemical composition.

2.2.5.3 Inductively Coupled Plasma Optical Emission Spectrometry (ICP-OES) Analysis

The Ru content of the catalyst was measured on a Varian 710-ES inductively plasma optical emission spectrometer (ICP-OES). The catalyst was digested using aqua regia in a

boiling water bath for 4 h, filtered and diluted with deionized water. The Ru was measured at 240.272 nm using standards of ruthenium (III) chloride (500 ppm, 50 ppm, 10 ppm, 2 ppm, 0.4 ppm and 0.08 ppm).

To investigate leaching of Ru from the ACC support, the catholyte solution, after the reaction, was evaporated under nitrogen followed by digestion with 4% aqua regia. The solution was then analyzed using ICP-OES for the presence of Ru.

2.2.6 Computational Method

The neutral closed shell species of each molecule and its corresponding anion, cation and radical were first optimized in GAMESS[222] at the HF/3-21G level of theory (UHF wavefunctions were used for radicals) and visualized in MacMolPlt[223] in order to determine symmetry. Species were then run using the G3 calculation of Pople *et al*.[224] in the gas phase using symmetry where applicable. All G3 calculations were run using Gaussian 2003.[225] The G3 calculation is a high quality composite method which has been extensively benchmarked for thermochemical accuracy when applied to ground state species (including radicals).[224] G3 calculations rely on two geometry optimizations, at the HF/6-31G(d) and MP2(full)/6-31G(d) levels of theory. Generally when used in this context, G3 calculations can be counted on to give "chemical accuracy" meaning the result will fall within ±1 kcal/mol of the true value.[223] The values reported include thermal corrections and represent the bond dissociation) ΔH_{diss} values at 298 K.

2.3 Results and Discussion

2.3.1 Characterization of the Catalyst

The cathode's BET surface area, micropore area and micropore volume reported here were measured by Li *et al.*[219] The reported surface area of blank ACC was 1,010 m^2/g. The volume of the pores reported was 0.30 cm^3/g and were microporous. The data suggested a decrease in the micropore volume after incipient wetness loading with $Ru(NH_3)_6Cl_3$ solution and reduction to 0.26 cm^3/g indicating the blockage of those pores by Ru (**Table 1**).

Sample	BET surface area (m^2g^{-1})	Micropore area (m^2g^{-1})	Micropore volume (cm^3g^{-1})
ACC	1010	685	0.30
Ru/ACC	800	551	0.26

Table 1. Brunauer-Emmett-Teller (BET) Analysis

Figure 7 shows an SEM image of blank ACC and the fibers knitted together are responsible for its high conductivity.[226] Its high conductivity, flexibility to cut conveniently into any shape and monolithic property obviate the need for filtration or decantation, making it a good electrocatalytic support for the metal. **Figure 8** shows the SEM image of the unused Ru/ACC and **Figure 9** shows the SEM image of used catalyst. Both these images indicate the retention of Ru on the surface of ACC responsible for the efficacy of catalyst during consecutive use. **Figure 10** and **Figure 11** indicates the distribution of Ru in spots with size larger than 100 nm with white spots formed by the accumulation of Ru particles. In addition to SEM images, EDX dot map confirms the white spots as ruthenium on the surface of ACC (**Figure 12**). ICP-

OES analysis performed to calculate the amount of Ru impregnated per ACC demonstrated a loading of 4 wt.% i.e. 0.001 g Ru per 0.0247g of ACC (**Table 2** & **Table 3**).

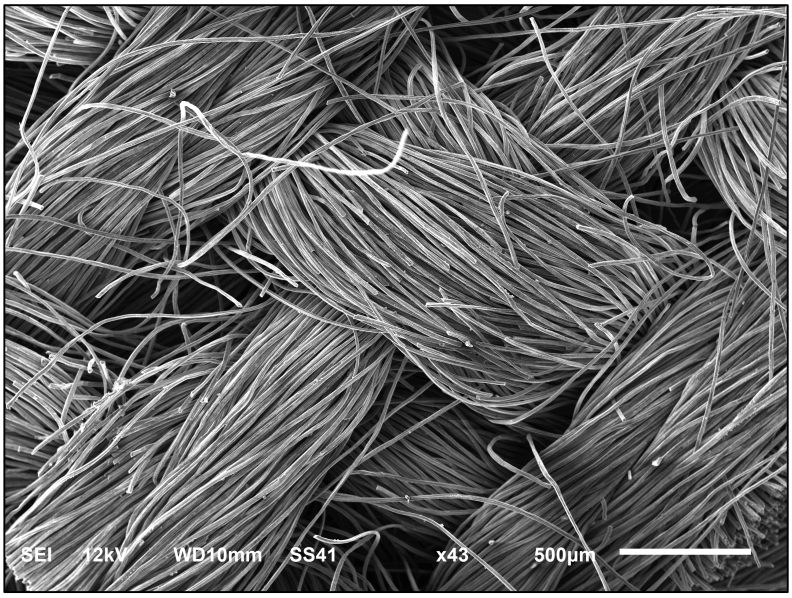

Figure 7. ACC

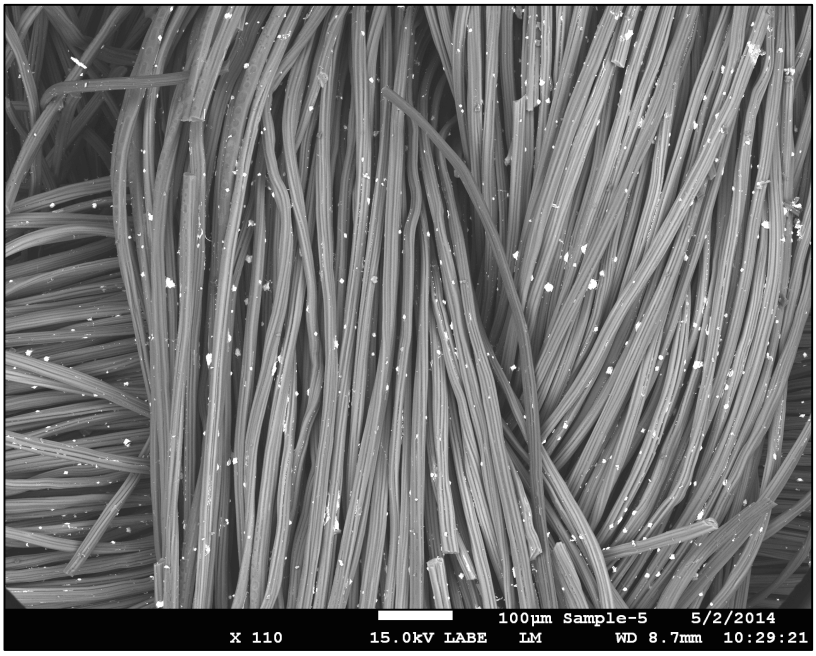

Figure 8. Ru/ACC (Unused)

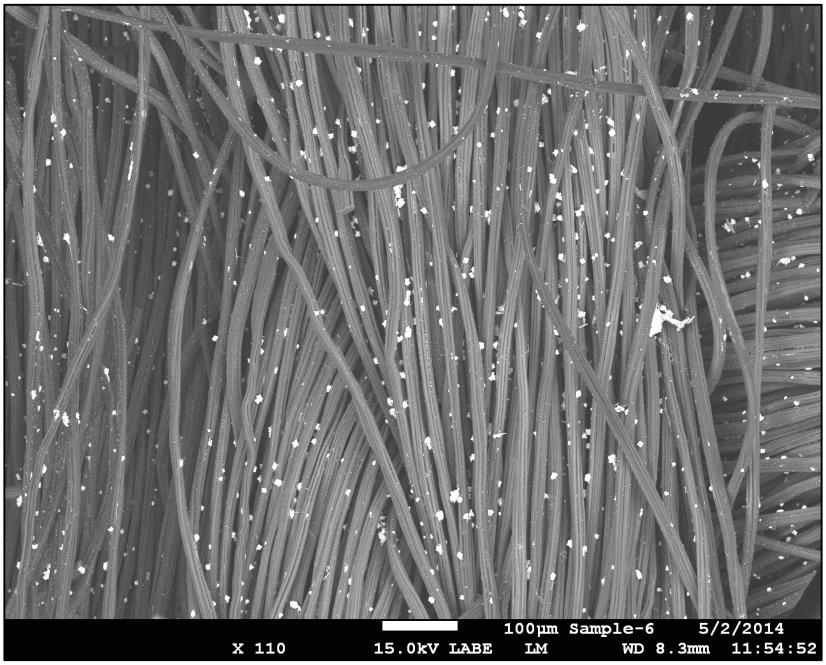

Figure 9. Ru/ACC (Used)

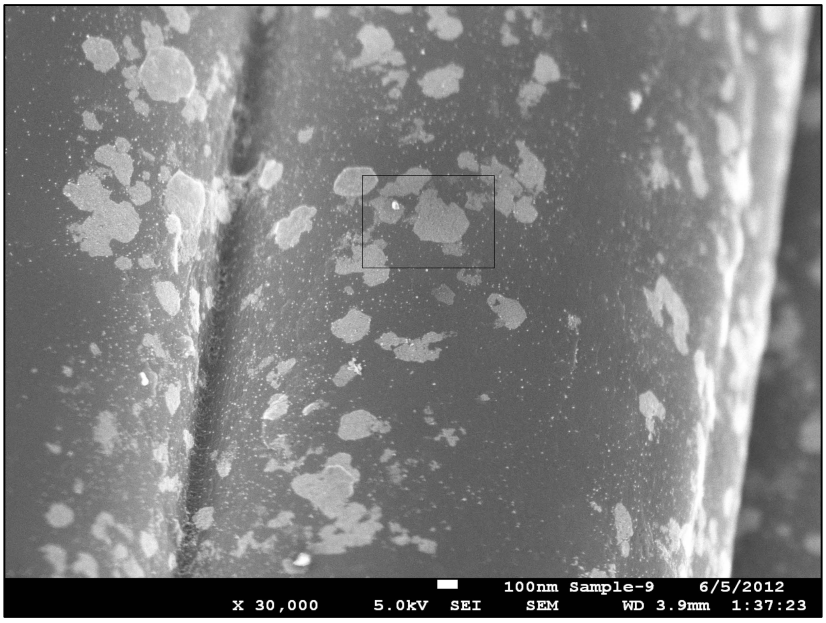

Figure 10. Ru/ACC (100 nm, x 30,000)[219]

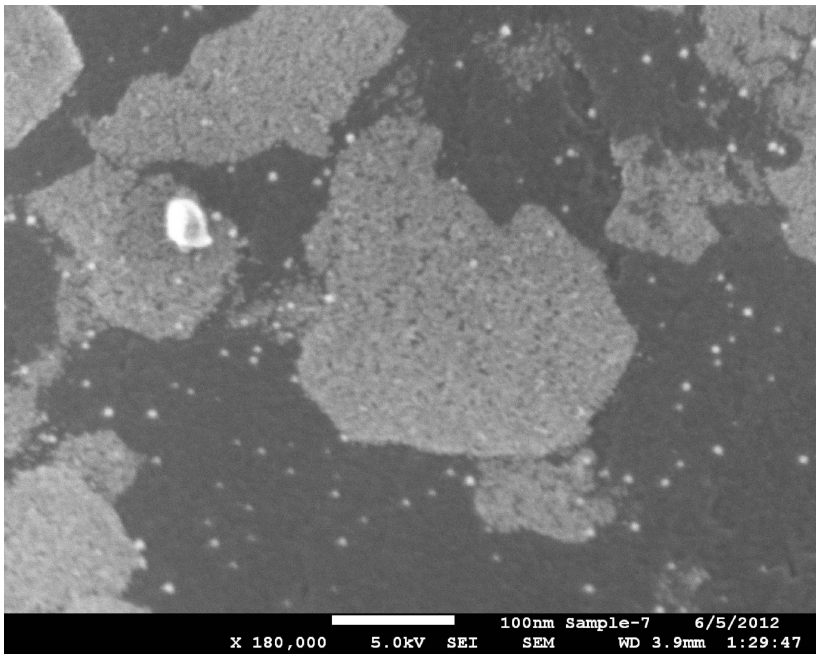

Figure 11. Ru/ACC (100 nm, 180,000)[219]

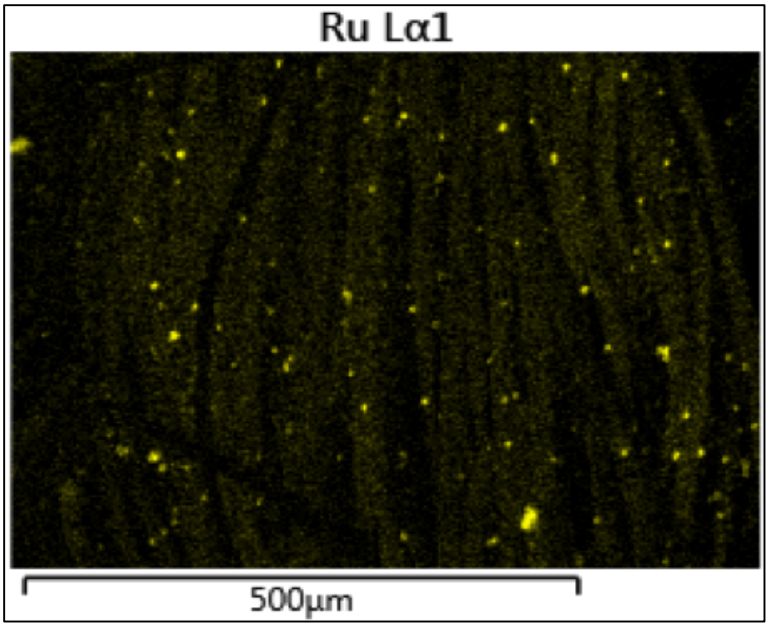

Figure 12. EDX Dot Map (yellow: Ru)

Element	Apparent Concentration	Wt%	Standard Label
C	33.64	85.54	C Vit
O	1.58	5.91	SiO_2
Na	0.21	0.27	Albite
Al	2.26	3.08	Al_2O_3
Cl	0.84	1.10	NaCl
Ca	0.04	0.05	Wollastonite
Zn	2.39	4.05	Zn
Total:		100.00	

Table 2. EDX Analysis: ACC

Element	Apparent Concentration	Wt%	Standard Label
C	28.74	69.46	C Vit
O	3.26	10.78	SiO_2
Na	0.16	0.19	Albite
Mg	0.04	0.06	MgO
Al	1.85	2.40	Al_2O_3
Si	0.05	0.06	SiO_2
P	1.77	1.46	GaP
S	0.10	0.11	FeS_2
K	5.91	6.88	KBr
Ca	0.16	0.20	Wollastonite
Fe	0.05	0.07	Fe
Zn	2.79	4.25	Zn
Ru	2.90	4.06	Ru (v)
Total:		100.00	

Table 3. EDX Analysis of Ru/ACC

2.3.2 Preliminary Experiments

The reaction of 2-aminobutane (racemic) was explored at 2.2 mA/cm^2 and room temperature, commonly achieving 45% deuteration in 8 h. Heating to 60 ˚C accelerated the reaction to 90% deuteration in 9 h. The Ru/ACC was effective even when the concentration of 2-aminobutane was increased to 500 mM, delivering 66% deuteration at 70 °C in 21 h.

To confirm the significance of the catalyst and current, two control reactions were performed. The first experiment using blank ACC and 2-aminobutane was electrolyzed at 60 ˚C at 2.2 mA/cm^2 and resulted in no H/D exchange. Likewise, use of a Ru/ACC cathode (no pre-electrolysis) at 60 ˚C in the absence of current showed no H/D exchange either. The absence of H/D exchange in the absence of current or of Ru confirmed that Ru and steady state current are essential for the system to perform H/D exchange.

2.3.3 Substrate Scope

With the above promising preliminary results in hand, we extended our studies to a wider array of amines. Isopropylamines **42-44** showed 93-97% deuteration in 5 h with similar reaction rate constants for the 2˚ carbon sites ($k_{\mathbf{42}}$ = 9.9x10^{-3} s^{-1} *vs*. $K_{\mathbf{43}}$ = 9.0x10^{-3} s^{-1} *vs*. $K_{\mathbf{44}}$ = 8.1x10^{-3} s^{-1}) regardless of the *N*-methylation level. These results suggest that steric crowding around the nitrogen center, or competition from an increased number of labile C-H sites on the surrounding alkyl groups had little effect on the rate of H/D exchange at the 2˚ carbon site. The 1° hydrogens of the *N*-methyl groups in **43** and **44** exchanged at rates competitive with those for the 2˚ carbon site (**Figure 13**).

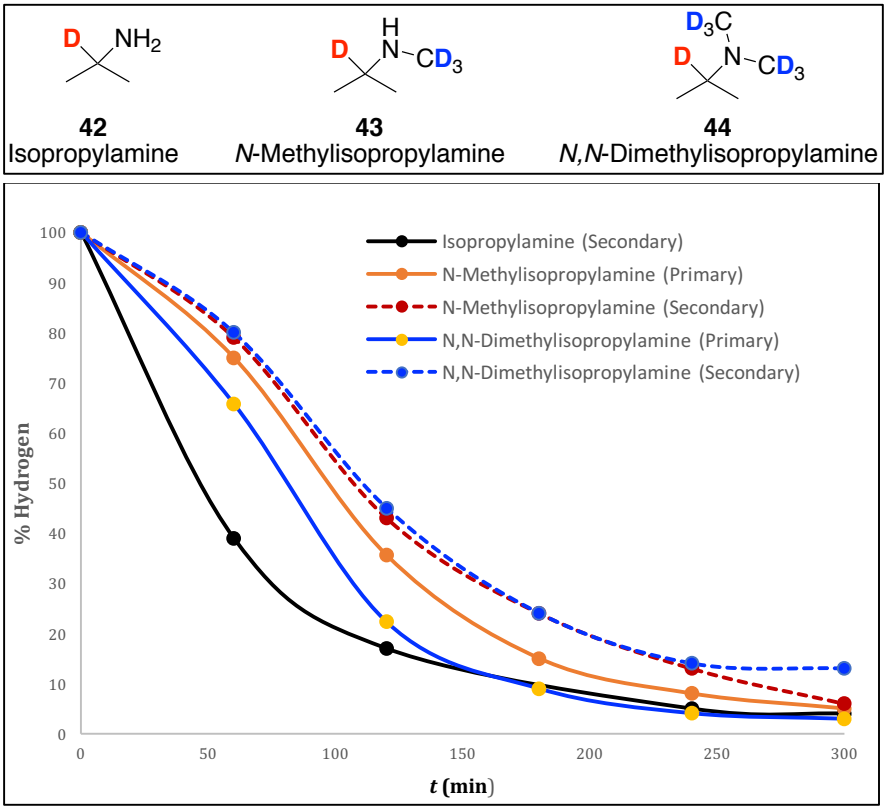

Figure 13. Amine Substitution. Conditions: Substrate (20 mM in 20 mL), 2.2 mA/cm^2 & 60 °C. Primary and secondary are referred to as the C-H sites. The β-CH_3's are non-labile hydrogens and % hydrogen at the α C-H site(s) is calculated relative to them.

Likewise, in *N,N*-diisopropylethylamine **45** (**Figure 15**), comparable deuteration at 1˚ carbon (74%) and 2˚ carbon (68%) sites was observed. Like other 2˚ carbon systems, cyclohexylamine **46** (**Figure 15**) underwent 92% deuterium incorporation in 8 h.

Alcohol substrates show reactivity like that seen in the amines described above. With 3-pentanol **47** (**Figure 15**) at 60 ˚C, 87% deuterium incorporation was seen in 8 h. Similarly, cyclopentanol **48** (**Figure 15**) showed 93% deuteration. Substituted cyclohexanols **49-52** (**Figure 15**) revealed functional group tolerance and rate effects; compared to 4-methylcyclohexanol **49** (k_{49} = 16.7x10^{-3} s^{-1}), the presence of a methoxy substituent in **50** had a negligible effect on the rate of deuteration (k_{50} = 13.1x10^{-3} s^{-1}); evidently, the ethereal oxygen introduces neither competition nor activation. However, the slower deuterium

incorporation seen in 4-carboxycyclohexanol **51** ($k_{\mathbf{51}}$ = 0.5x10^{-3} s^{-1}) suggests inhibition by competitive binding of the carboxylate group to the catalytic sites, and/or tethering of substrate in a way that limits access to its labile C-H sites. We prefer the former interpretation as it echoes observations from earlier studies of lactic acid reduction to propylene glycol in water with pressurized hydrogen over a Ru/C powder catalyst. In those instances, the presence of lactic acid slowed H/D exchange in initially added propylene glycol.[227] As a probe for a similar phenomenon in the electroactivated system, an equimolar amount of 4-methylcyclohexanol and acetic acid were added to catholyte. The presence of the acetic acid decreased the H/D exchange rate constant to 1.2x10^{-3} s^{-1} as compared to 4-methylcyclohexanol **49** ($k_{\mathbf{49}}$ = 16.7x10^{-3} s^{-1}). Polyhydroxylations however, posed no problem; 1,3,5-cyclohexanetriol **52** underwent 70% deuteration in 24 h.

To probe the relative reactivity of alcohol *vs*. amine sites, compound **53** was studied. Sites α to hydroxy groups underwent deuterium incorporation more rapidly than those α to amine (**Figure 14**).

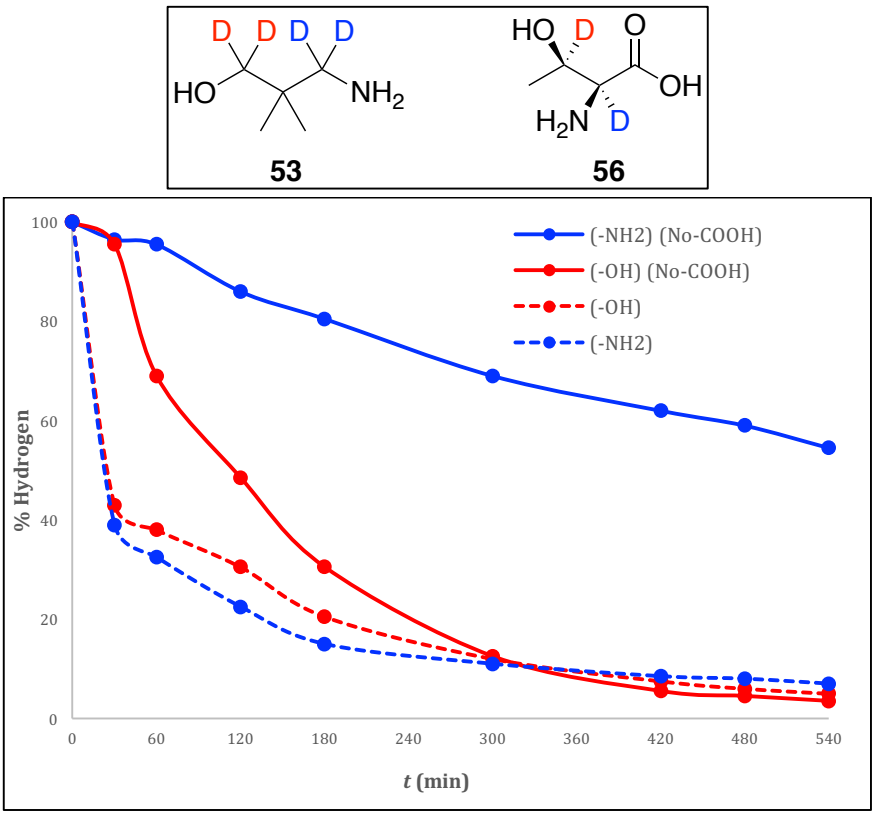

Figure 14. Reactivity of -OH *vs*. -NH_2. Conditions: Substrate (20 mM in 20 mL), 2.2 mA/cm^2 & 70 °C (**53**)/75 °C (**56**). In 53, γ-CH_3's are non-labile hydrogens and % hydrogen at the α C-H site(s) is calculated relative to them. In 56, β-CH_3 are non-labile hydrogens and % hydrogen at the α C-H site(s) is calculated relative to them.

The chemoselectivity in favor of alcohols, and the inability of ethereal groups to enable H/D exchange was further explored by analyzing bond strengths using *ab initio* methods. To this end, quantum chemical calculations using the G3 method[224] were run on isopropyl alcohol, isopropyl ether, isopropyl amine, isopropyl methyl amine, and isopropyl dimethyl amine. To consider a range of behaviors, all the uncatalyzed bond cleavages were modeled, including hydride, hydrogen atom, and proton abstraction at the secondary C-H sites α to the N- or O-heteroatom. In the cases of deprotonation and homolytic C-H cleavage, the values were weakly sensitive to heteroatom identity (O or N) and to the alkyl substituents on the heteroatom. The energies for hydrogen atom removal varied over a range of ±2.5 kcal/mol,

and deprotonation energies were within ±3.5 kcal/mol. As expected for these gas-phase values, the hydride abstraction energies showed selectivity based on the ability of the substituents to stabilize the resulting positive charge. The hydride abstraction energies were significantly lower in the amines than the alcohol and ether, and the presence of methyl groups on oxygen or nitrogen also lowered the energy (**Table 4**).

Compound	Deprotonation	Hydrogen abstraction	Hydride abstraction
Isopropyl alcohol	409.4	94.5	226.5
Isopropyl methyl ether	408.0	95.2	218.1
Isopropyl amine	412.6	91.2	202.1
Isopropyl methyl amine	405.9	91.0	194.5
Isopropyl dimethyl amine	406.6	94.4	192.3

Table 4. Homo- and Heterolytic C-H Bond Dissociation Energies (kcal/mol) at the G3 Level of Theory

Considering these results, it seems unlikely that the C-H activation chemoselectivity against ethers can be explained in terms of substrate electronics, as the only obvious trend would predict favorable H/D exchange in the case of ethers. Amines are generally good ligands, and should be capable of coordinating to ruthenium, but alcohols and ethers are much weaker. If an alkoxide anion were required for adequate interaction with the surface, then the inactivity of ethers **(50)** could be explained. The stability of the Ru coordinated –OH in the alkaline environment *vs.* $-NH_2$ might be understood to enhance the reactivity of sites alpha to -OH while this phenomenon is not so obvious in the case of **56** (**Figure 15**) where –COOH also contributes to the coordination **(Figure 14**).

In our previously reported high-pressure/high temperature hydrogenation studies of L-alanine, Jere *et al.*[160] had uncovered stereoretentive H/D exchange on the C-H site α to amine.

In the electrochemical apparatus, L-alanine **54** (**Figure 15**) at 75 ˚C showed 98% deuterium incorporation in 5 h with no observable racemization. Though slower, L-valine **55** (**Figure 15**) achieved 93% deuterium incorporation in 9 h, and 99% after 21 h, again with complete stereochemical retention. We attribute the slower rate of L-valine *vs.* L-alanine deuteration to steric crowding at the reactive site, consistent with our earlier studies of amino acid hydrogenations to amino alcohols[228] but in apparent contrast to the above results with simple amines **42-44**.

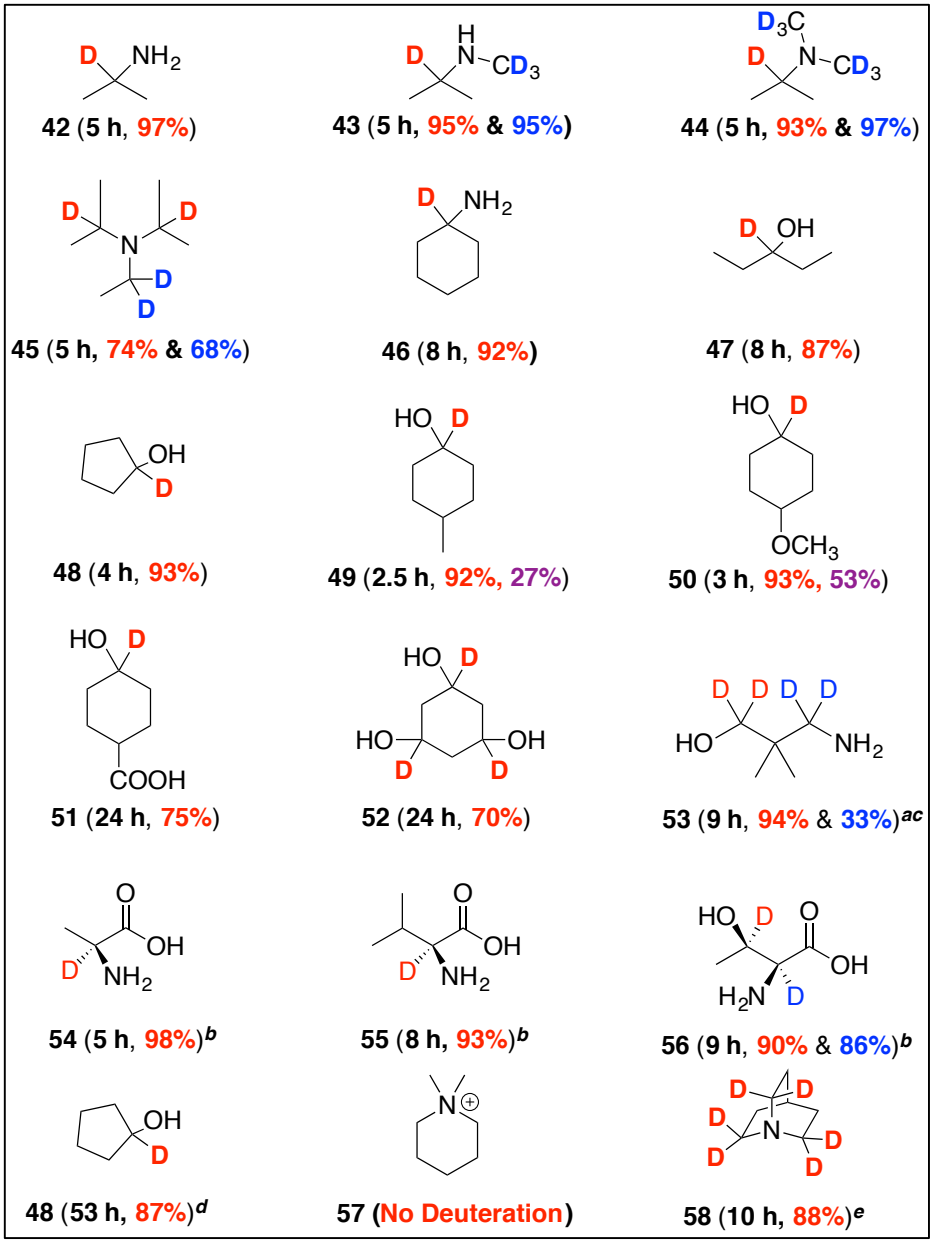

Figure 15. Substrate Scope ([a]70 °C, [b]75°C, [c]pH 12, [d]1 g substrate, [e]80°C). Conditions: Substrate (20 mM in 20 mL) & 2.2 mA/cm^2.

With both amine and alcohol–bearing stereocenters, L-threonine **56** was of particular interest. After 9 h, >85% deuteration was observed at both sites, and >99% in 21 h with stereochemical retention at both stereocenters. Interestingly, the rate of activation of sites α to hydroxy (k_{OH} = 3.9x10^{-3} s^{-1} *vs.* k_{NH2} = 3.0x10^{-3} s^{-1}) was not observed to be significantly

faster as it was in the case of **53**; we attribute this to possible guidance by the carboxylate group in L-threonine (**Figure 14**).

2.3.4 Catalyst Deactivation Studies

Effective catalyst lifetime is a key factor determining the practical value of any catalytic system. To probe the extent of deactivation, we reused the Ru/ACC cathode for five consecutive runs with alanine (racemic) as the substrate. After the first cycle, used Ru/ACC cathode was washed with 5 mL of D_2O and dried overnight under N_2. Levels of deuterium incorporation were comparable throughout all the runs, demonstrating the stability of the Ru/ACC catalyst. The catalyst was subsequently used for the sixth time with valine (racemic) to test for cross-contamination and for changes in efficacy with another substrate. The reaction showed 93% deuterium incorporation in 8 h, comparable to the results observed with the fresh Ru/ACC (93% in 9 h).

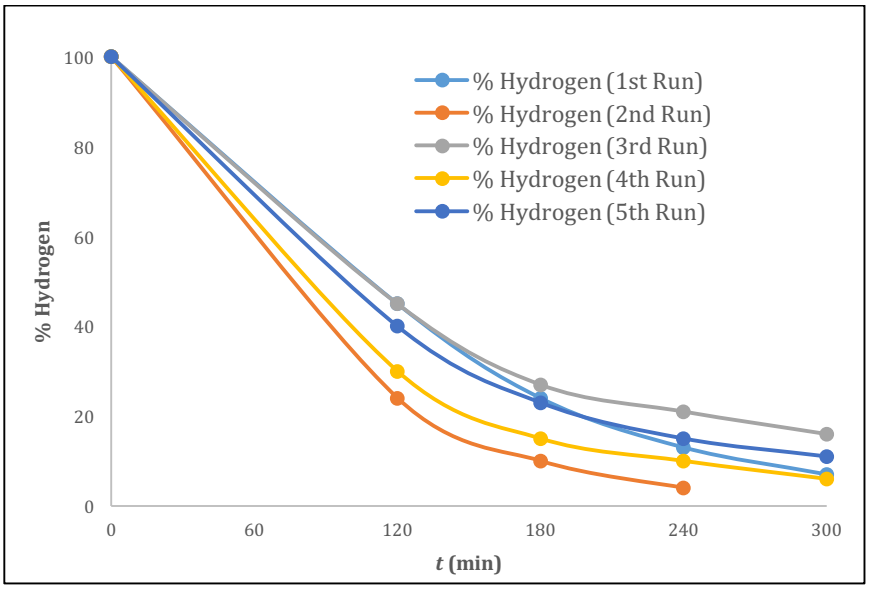

Figure 16. Catalyst Deactivation Studies. Conditions: Cyclopentanol (20 mM in 20 mL), 2.2 mA/cm^2 & 60 °C. The CH_2's are non-labile hydrogens and % hydrogen at the α C-H site is calculated relative to them.

2.3.5 Effect of Current Density

The effect of current density on the extent and rate of the deuterium incorporation was also studied using L-valine as substrate with current densities ranging from 1.1 mA/cm^2 to 11.1 mA/cm^2. The projected macroscopic cloth area of 4.5x10^{-4} m^2 was used to calculate current densities, as it was difficult to measure the actual effective electrode surface area. The goal was to find an optimum current density that could oxidize D_2O to generate deuterium cations on Pt, and reduce them on the Ru surface (**Scheme 45**, **Eqns. 8** & **5**) but to avoid saturation of the catalytic sites leading to the D_2 formation (**Scheme 45**, Eqns. **6** & **7**). In these H/D exchange reactions, application of current is necessary for two reasons: (a) reduction of ruthenium to the active state and (b) reduction of D^+ or D_2O on the ruthenium surface to generate Ru (D) while the C-H activation step of organic substrates to effect H/D exchange did not need any electrons. This aspect of our chemistry would render our reactions high current efficiency as limited charge is required to drive these reactions.

Theoretically, electrons supplied in the H/D exchange reactions were only responsible for the generation of D_2 and would provide relatively higher current efficiencies.

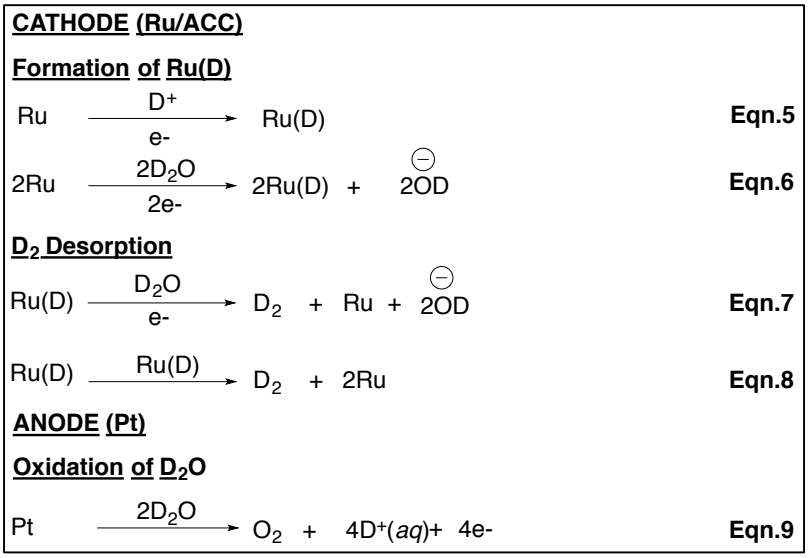

Scheme 45. Electrochemical Reactions at Cathode and Anode

Based on preliminary analysis, 2.2 mA/cm^2 was an effective current density for the pre-electrolysis activation phase of 30 minutes. After pre-electrolysis, reactions were run at 0.4 mA/cm^2, 1.1 mA/cm^2, 2.2 mA/cm^2 and 11.1 mA/cm^2; 1.1 mA/cm^2 turned out to be the most effective in maintaining a balance between the favorable (oxidation and reduction) and unfavorable (D_2 desorption) steps. Interestingly, the slower H/D exchange rates found at higher current density suggest that D_2 desorption processes or deuteroxide anions may tie up active sites via surface saturation, partially inhibiting reaction. Notably, in all these experiments, the stereochemistry of L-valine was completely retained.

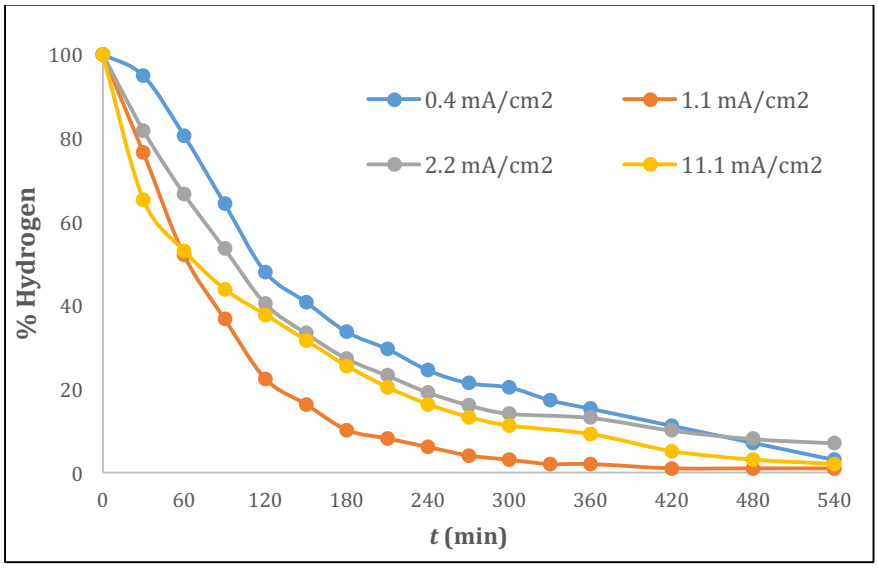

Figure 17. Effect of Current Density. Conditions: L-valine (20 mM in 20 mL) & 75 °C. The β CH_3's are non-labile hydrogens and % hydrogen at the α C-H site is calculated relative to them. A pre-electrolysis phase of 30 minutes at 2.2 mA/cm^2 was applied in all the cases.

2.3.6 Factors Effecting Isolated Yield

Despite clean deuterium incorporation with little to no observable product degradation, the initial studies found full recovery of labeled substrates to be difficult. The yields showed direct correlation with the organic character of the molecules and, as expected,[229] amino acids were obtained in higher yields as compared to other substrates. Two easily checked hypotheses were considered to explain these losses: (a) substrate migration to the anodic cell compartment through the Nafion® membrane, and (b) substrate adsorption by ACC. The net migration to the anodic chamber was calculated to be less than 2% using cyclopentanol (20 mM, 20 ml) as a model substrate. However, the adsorption of cyclopentanol into ACC was calculated to be 40% irrespective of the presence of Ru. To extract the organic substrate from the cloth, various organic solvents were employed (**Figure 18**). In all the cases, product was recovered without any loss in activity of Ru/ACC during a consecutive run. To demonstrate the scalability of this methodology, a 1 g reaction (588 mM, 20 mL solution) of cyclopentanol

was conducted at 60 ˚C and 2.2 mA/cm^2. In 53 h, 51% yield of 87% deuterated cyclopentanol was obtained, with no byproduct impurities observable by ^{1}H NMR.

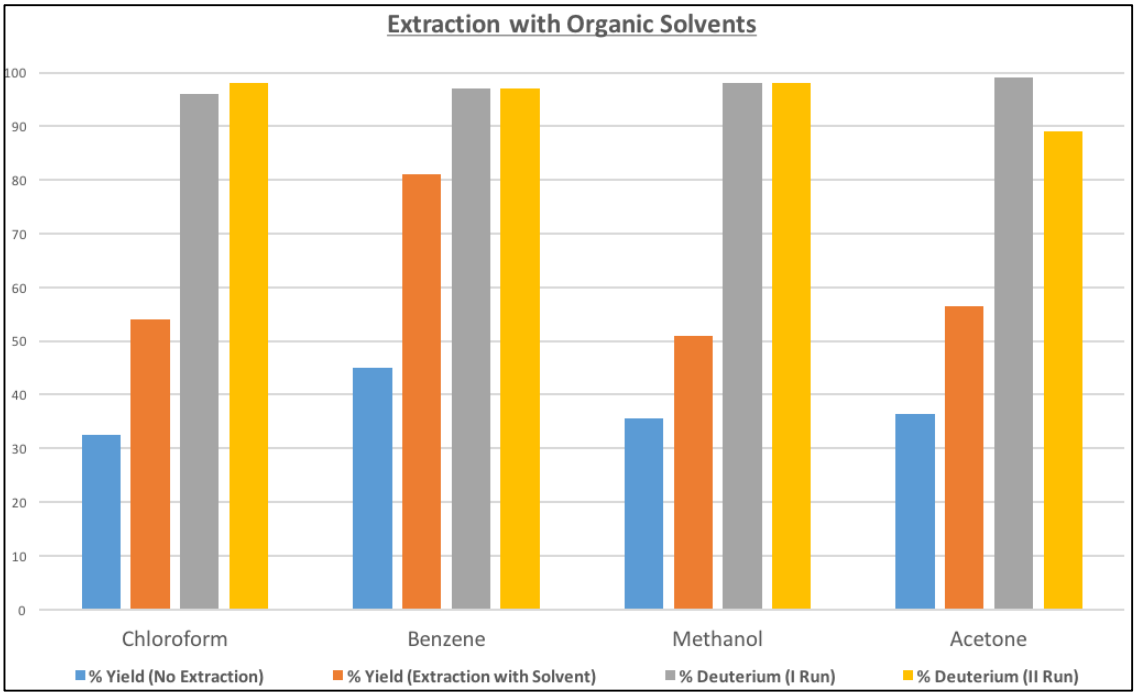

Figure 18. Extraction with Organic Solvents. Conditions: Cyclopentanol (20 mM in 20 mL), 2.2 mA/cm^2 & 60 °C.

2.3.7 Mechanistic Analysis

Mechanistic insight into this method is complemented by the work recently published by Pieters *et al.*[167] describing "*Enantiospecific C-H Activation using Ruthenium Nanocatalysts*." We hypothesized the coordination of the heteroatom (*N* or *O*) to the catalyst to be essential for the reaction to proceed (**Scheme 46**, **[1A]**). This is validated by an experiment demonstrating the inability of dimethylpiperidinium chloride **57** (**Figure 15**) to undergo deuteration, presumably owing to the absence of a lone pair on nitrogen. Following the coordination, the C-H bond α to the heteroatom undergoes oxidative addition to generate a 4-membered dimetallacycle (**Scheme 46**, **[1B]**). We considered two possibilities following this step: (a) generation surface bound imine or carbonyl species **(Scheme 46**, **[1C]**)

followed by deuterogenation, or (b) H/D exchange with surface deuterium followed by reductive elimination. (**Scheme 46**, **[1D]**)

Our experimental observations of stereoretention in the case of amino acids **54-56** and the H/D exchange in quinuclidine **58** (**Figure 15**), which is unable to form imine-type species, indicated that the former pathway is unlikely. Based on SEM images, we noticed that the clusters of Ru particles (>100 nm) are distributed throughout ACC. These clusters are varied in size but are much larger overall than the catalytic nanoparticles studied by Pieters *et al*. Thus, although the authors characterize the H/D exchange as nanocatalysis, it is not clear that this type of C-H activation reflects special nanocatalytic reactivity.

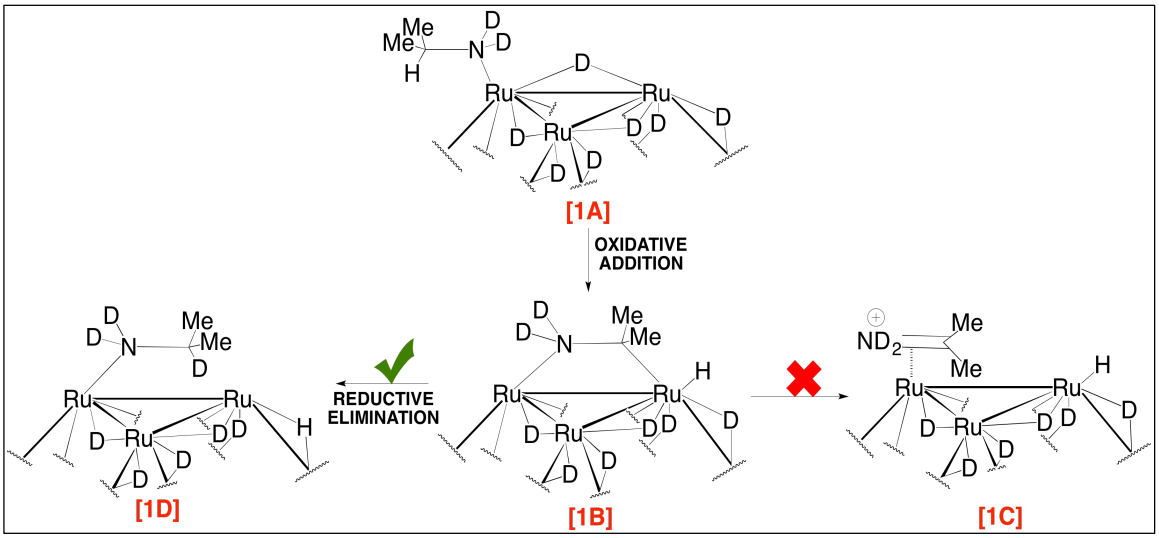

Scheme 46. Mechanistic Analysis

2.3.8 Electrochemical Activation of Ru/ACC (Electrodeposition)

One of the necessary steps in the development of Ru/ACC is the reduction of Ru in a high-pressure batch reactor under H_2 at 500 psi and 310 °C for 12 h. To obviate the use of H_2 gas, it is essential to replace this step with a greener method of comparable efficacy and kinetics. To do that, we sought to electrodeposit Ru on ACC. After synthesizing Ru/ACC catalyst via

incipient wetness (*see section 2.3.4.2*), we conducted pre-electrolysis for 1 h at 33.3 mA/cm^2. Though there was observable leaching initially, following the addition of the catalyst to the catholyte, after an hour, the solution became colorless. We used cyclopentanol to understand the efficacy of this catalyst and observed 89% deuterium incorporation in 4 h, which is comparable to the rate of H/D exchange using traditionally synthesized Ru/ACC. To evaluate catalyst deactivation, we used the same catalyst for another consecutive run with cyclopentanol without any pre-electrolysis phase. In this case, we observed 92% deuterium incorporation in 3 h confirming our proof of concept (**Figure 19**).

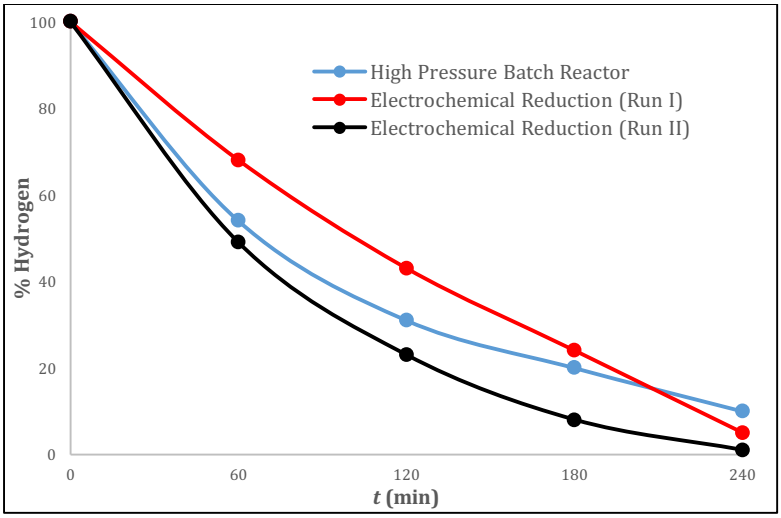

Figure 19. H/D Exchange by Ru/ACC Developed by High Pressure Batch Reactor *vs.* Electrochemical. Conditions: Cyclopentanol (20 mM in 20 mL), 2.2 mA/cm^2 & 60 °C. No pre-electrolysis phase for high-pressure batch reactor or Run II of electrochemical reduction. 1 h of pre-electrolysis at 33.3 mA/cm2 in Run 1 of electrochemical reduction. The CH_2's are non-labile hydrogens and % hydrogen at the α C-H site is calculated relative to them.

The distribution of Ru and its morphology on ACC, prepared via electrodeposition, was analyzed using SEM and EDX. The SEM and EDX analysis of Ru/ACC before electrodeposition, after electrodeposition, and after running two cycles with the prepared catalyst gave important insight into the prepared catalyst. The impregnation of ACC with the Ru salt solution resulted in a non-uniform deposition of the salt consisting or Ru (33.32 wt%) and

Cl (28.19 wt%) confirmed by SEM (**Figure 20**) and EDX analysis (**Figure 21**). After electrodeposition of Ru at 33.3 mA/cm^2 for 1 h, Ru particles underwent a relatively homogenous deposition (**Figure 22** & **Figure 23**) with concentration of Cl getting down to 0.16 wt% and Ru at 32.56 wt%. After two consecutive runs, the distribution and morphology of Ru did not alter, indicating its robustness, which was further demonstrated by comparable deuteration of cyclopentanol in both the runs (**Figure 24** & **Figure 25**).

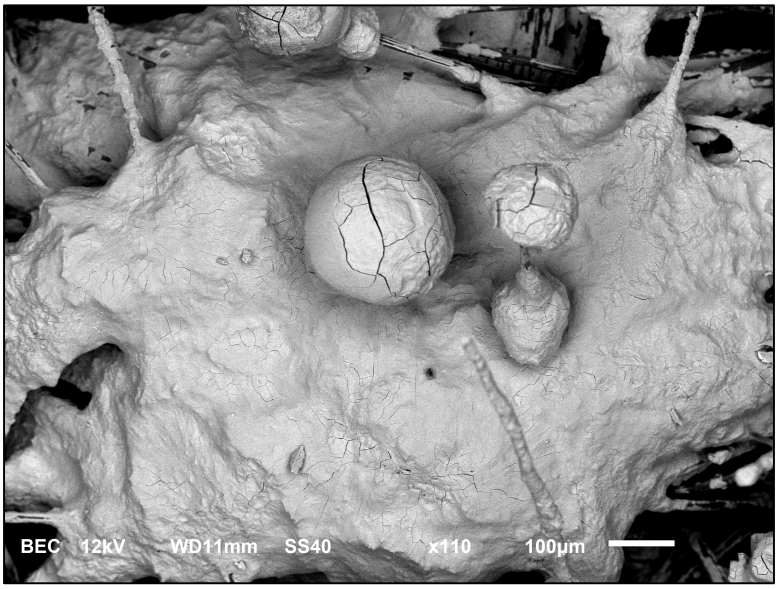

Figure 20. SEM Analysis: $Ru(NH_3)Cl_3$/ACC

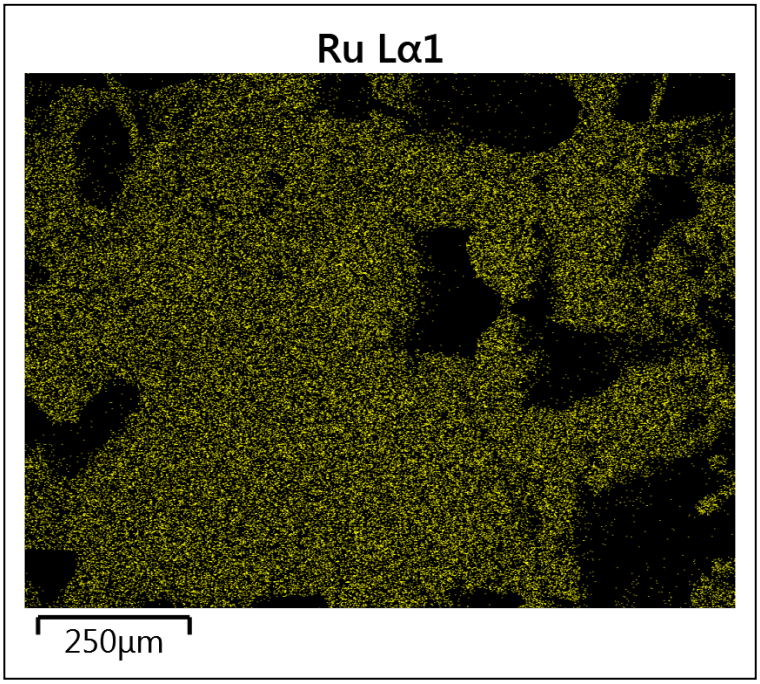

Figure 21. EDX Analysis: Ru $(NH_3)Cl_3$/ACC

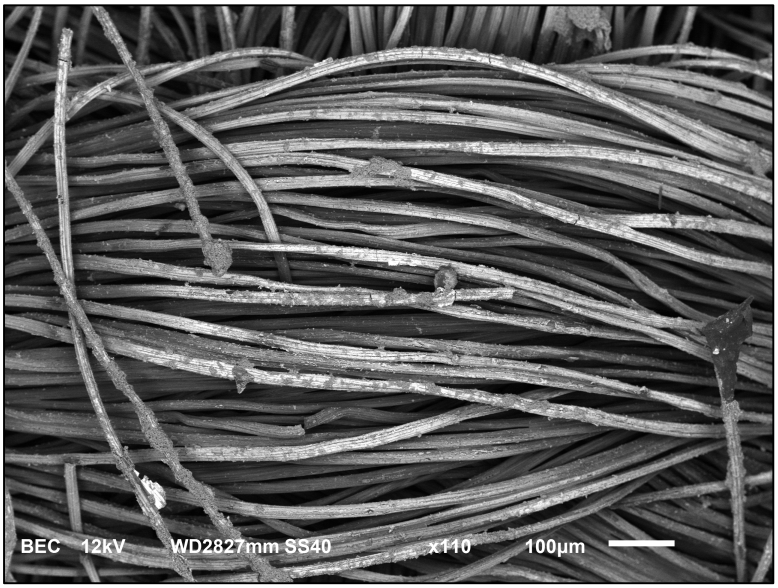

Figure 22. SEM Analysis: Ru/ACC (After 1 h at 150 mA)

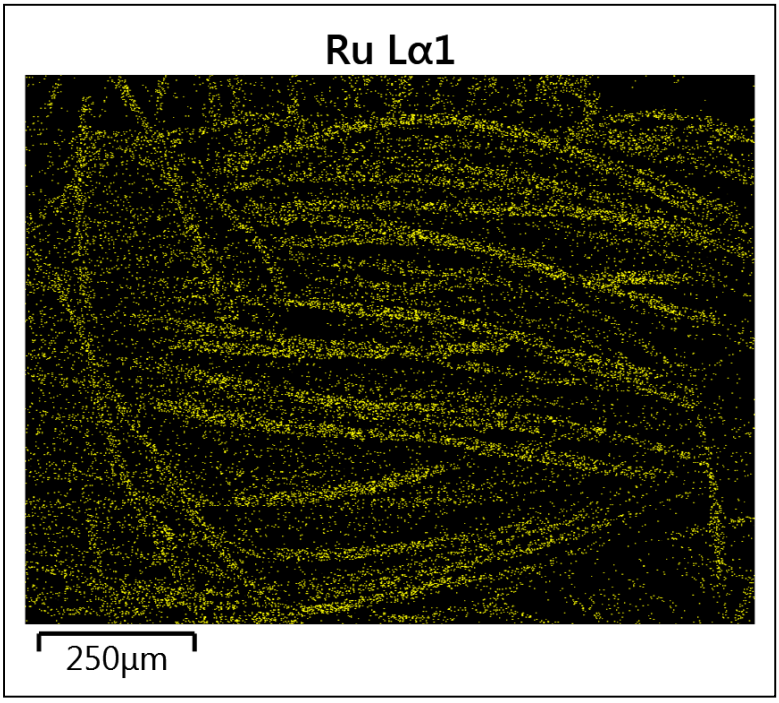

Figure 23. EDX: Ru/ACC (After 1 h)

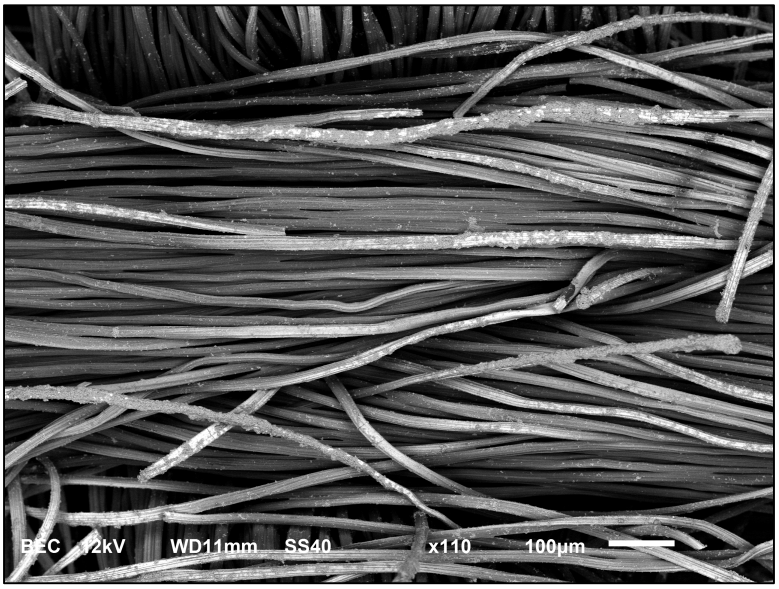

Figure 24. SEM: Ru/ACC (After Reaction)

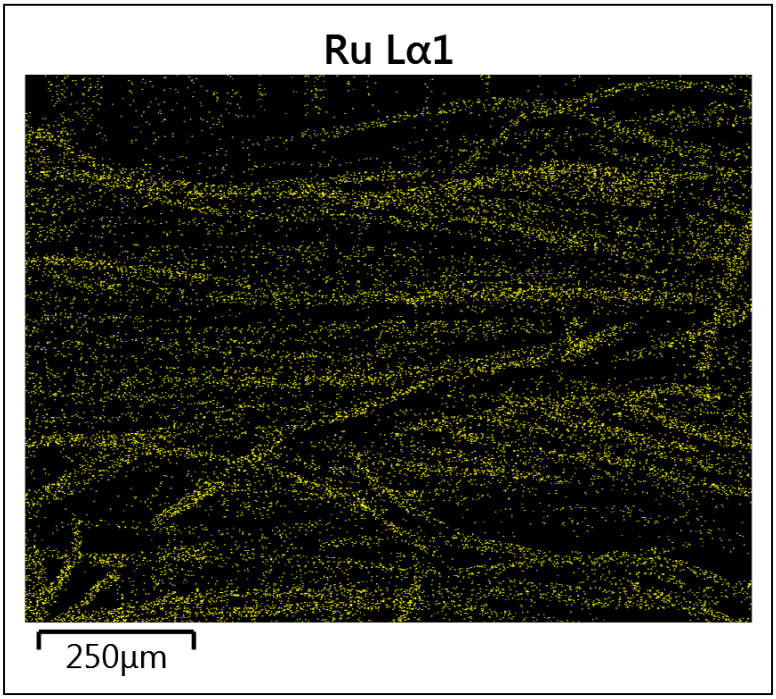

Figure 25. EDX: Ru/ACC (After Reaction)

2.3.9 Anode Replacement

To expand our methodology to an industrial setting, it is essential to utilize cheaper material in the reaction set-up. Besides Ru, Pt is another expensive metal that is currently being used in our system as a counter electrode. Encouraged by the precedent[230] that demonstrates the ability of carbon-based materials to electrolyze water, we investigated the use of our support material ACC as an anode. We proposed that it would electrolyze D_2O to generate the required deuterons (D^+). To explore this, we ran a reaction at our optimal conditions (2.2 mA/cm^2 and 60 °C) and could incorporate 99% deuterium in 4.5 h, which is comparable to deuteration of cyclopentanol using Pt as a counter electrode (93% in 4 h). Although a major concern of using carbon as an anode is its erosion due to the formation of CO_2, no visual disintegration was observed.

2.4 Summary

This chapter described a mild, aqueous-phase strategy for stereoretentive C-H activation at sp^3 C-H sites bearing amine or alcohol groups. The transformation utilized D_2O to replace the hydrogen with deuterium while retaining stereochemistry. The deuterium cations, generated on the Pt via oxidation of D_2O migrated to the surface of Ru where they were reduced. Electroactivated Ru particles, supported on activated carbon cloth, introduced that deuterium into the organic substrate on a timescale of minutes to hours. This method yielded optimal results at low current density of 2.2 mA/cm^2, mild temperature (60–75 °C) and at ambient pressure. Various amines, alcohols and amino acids were studied using this method and they all showed high deuteration levels at the optimized conditions. The primary concern of losing the organics to ACC was dealt with by extracting the substrates using organic solvents. The use of organic solvents didn't impact the ability of Ru/ACC to catalyze H/D exchane in subsequent reactions. A method to impregante Ru on ACC via electrodeposition was also developed and the resulting electrocatalysts showed comparable deuterium incorporporation to Ru/ACC synthesized via incipient wetness and high-pressure reduction. The use of ACC instead of Pt wire as the anode also proved successful

2.5 Characterization

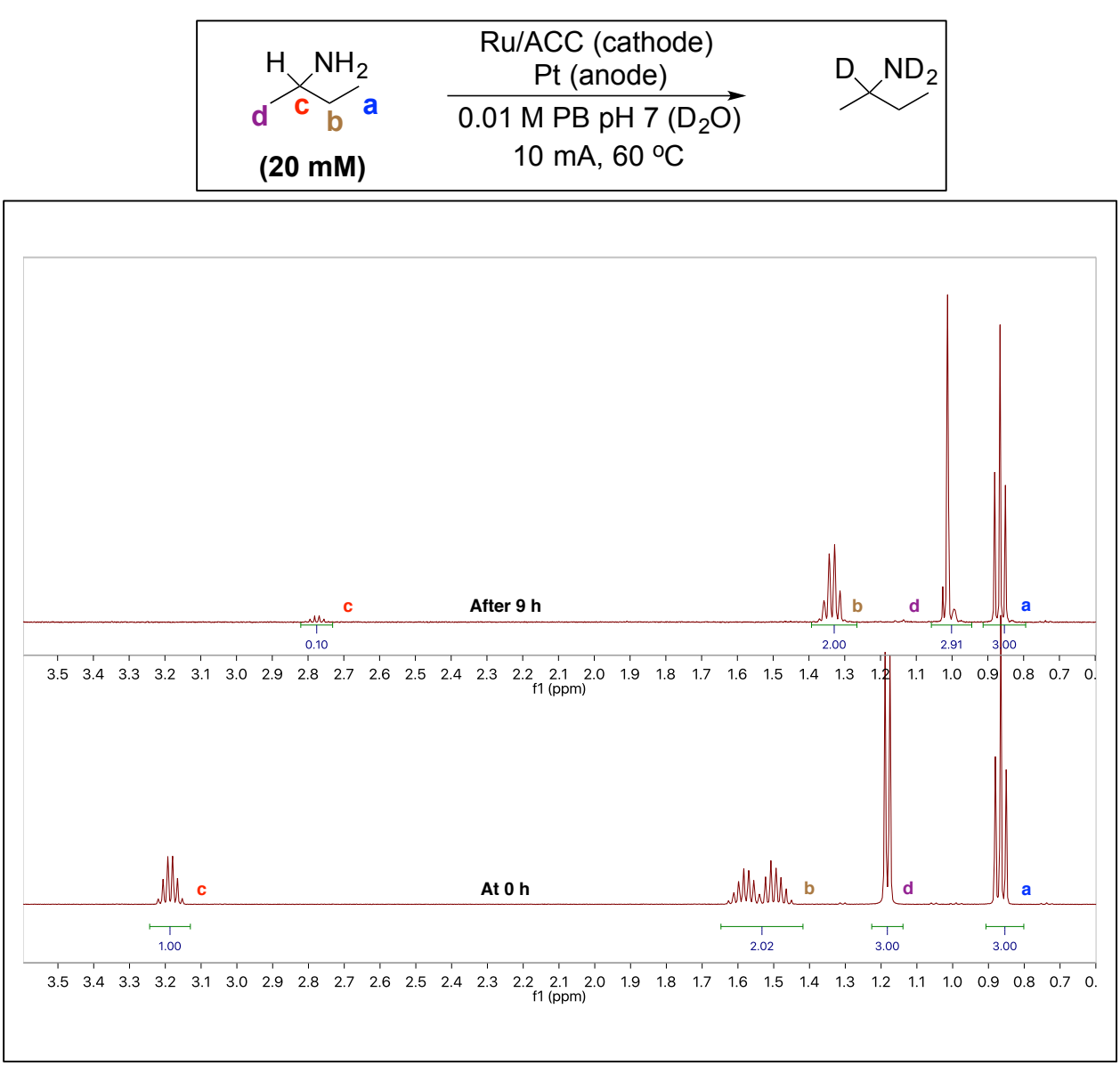

Figure 26. ^{1}H NMR spectrum of 2-aminobutane, 41 (Yield (28%)). Changes in chemical shifts are due to the change in pH resulting from electrochemical consumption of D^{+} ions. The γ-CH_3 sites are the non-labile hydrogens and % hydrogen remaining at the α C-H site is calculated relative to them.

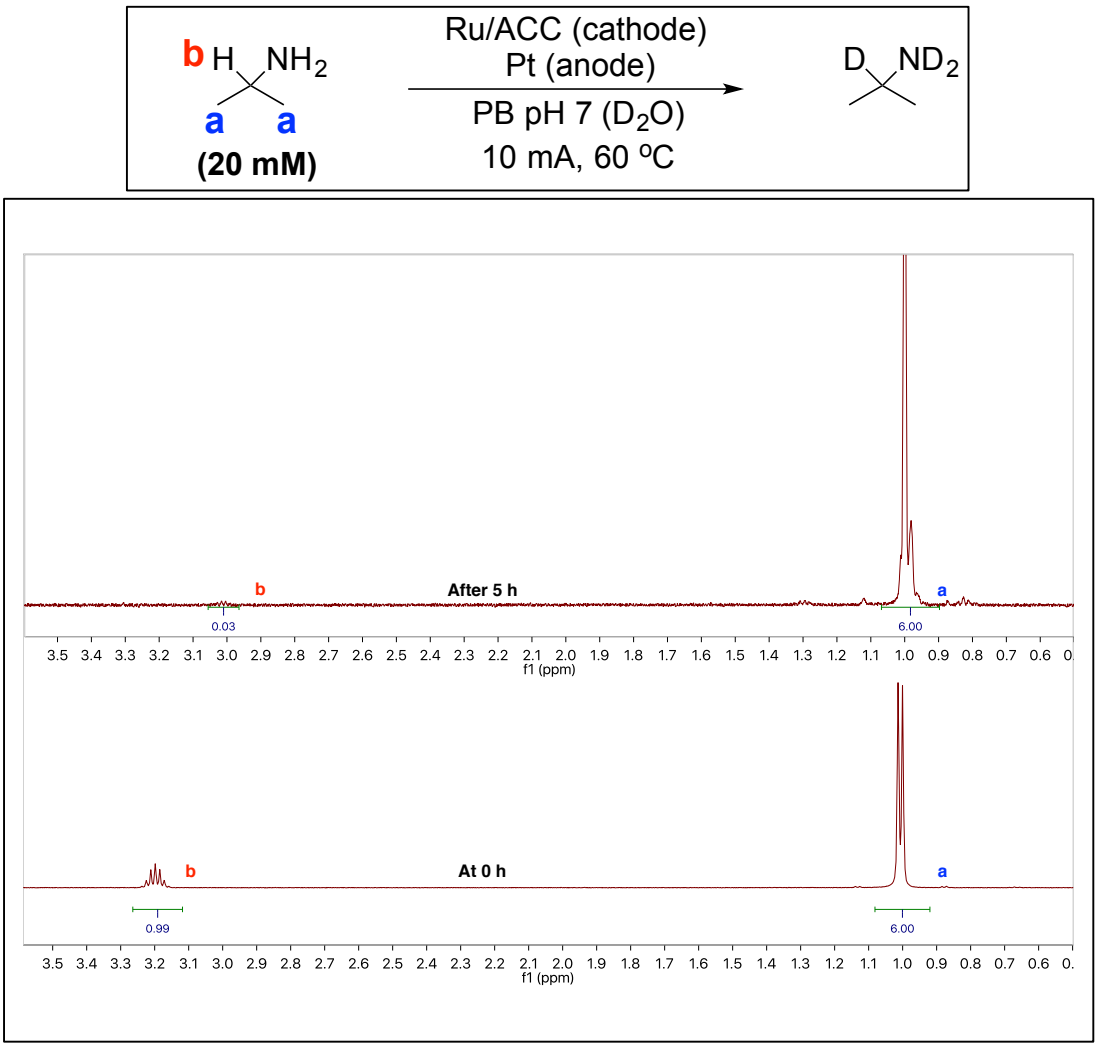

Figure 27. ^{1}H NMR spectrum of Isopropylamine, 42 (Yield (35%)). Changes in chemical shifts are due to the change in pH resulting from electrochemical consumption of D^{+} ions. The β-CH_3's are the non-labile hydrogens and % hydrogen at the α C-H site is calculated relative to them.

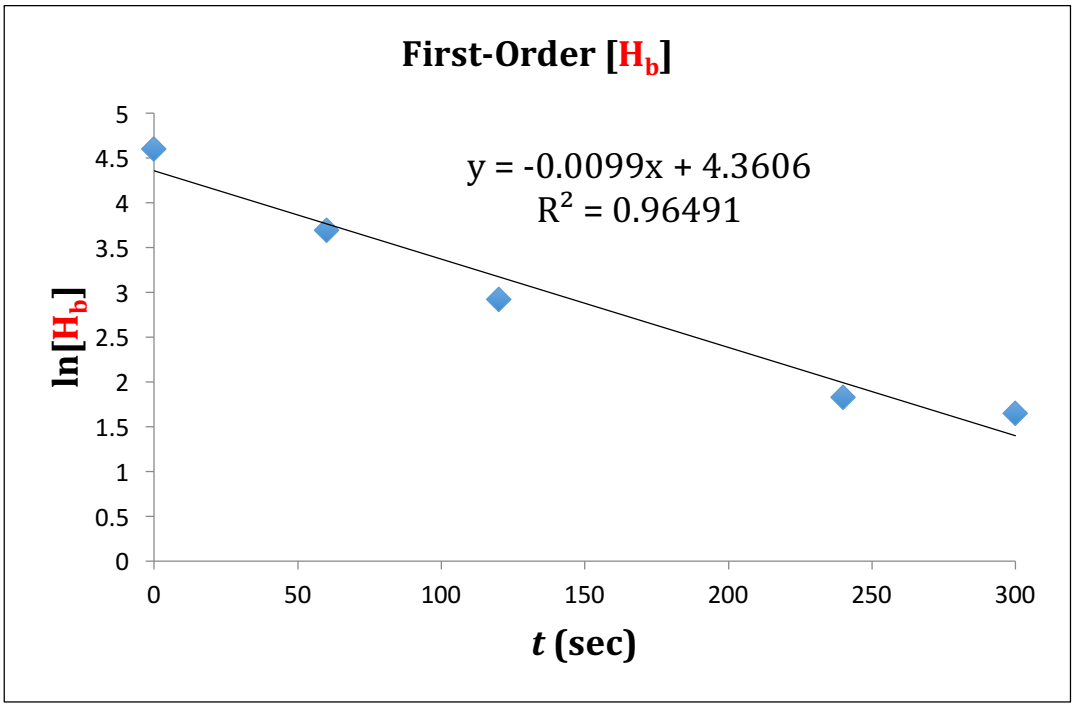

Figure 28. Kinetic Analysis: Isopropylamine

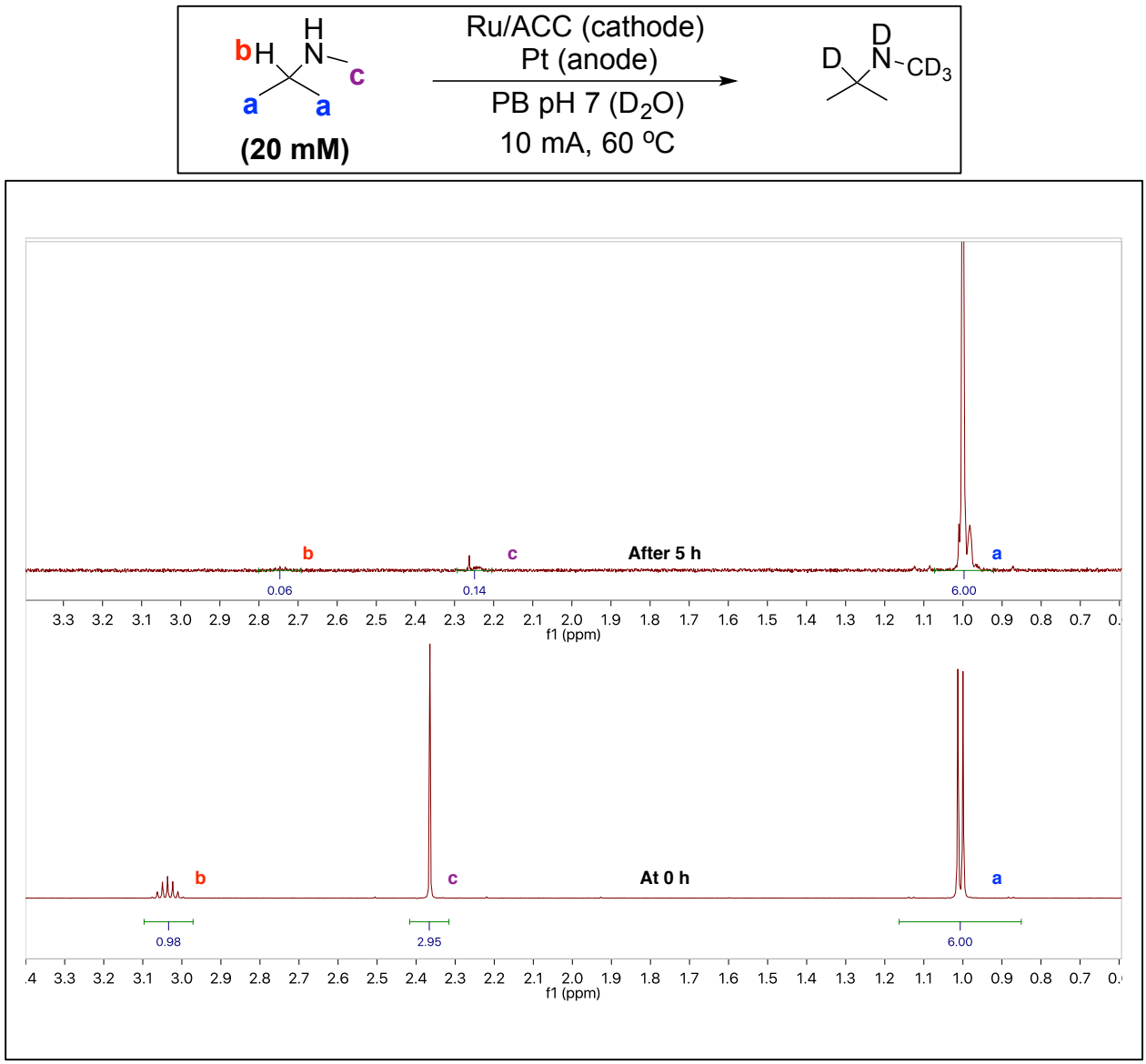

Figure 29. ^{1}H NMR spectrum of *N*-methylisopropylamine, 43 (Yield (28%)). Changes in chemical shifts are due to the change in pH resulting from electrochemical consumption of D^{+} ions. The β-CH_3's are the non-labile hydrogens and % hydrogen at the α C-H site is calculated relative to them.

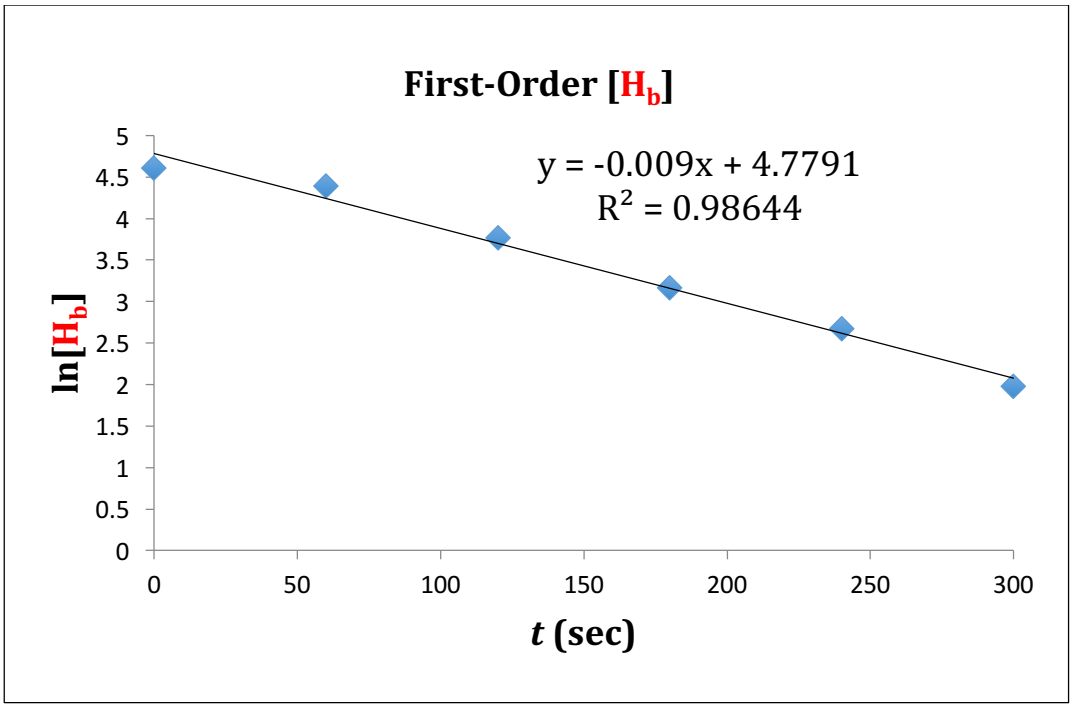

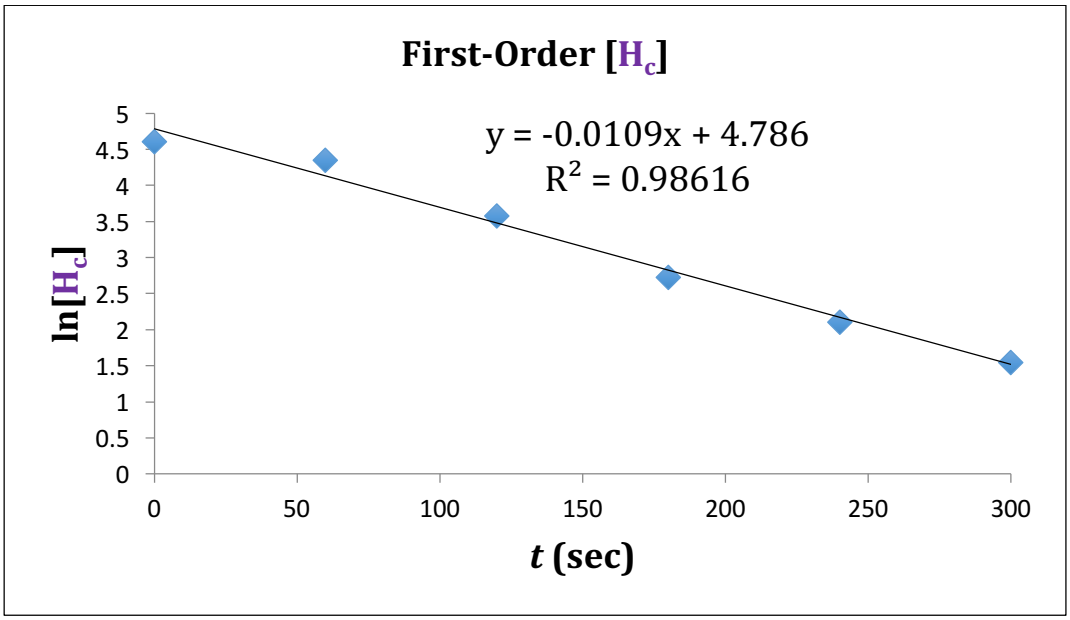

Figure 30. Kinetic Analysis: *N*-methylisopropylamine

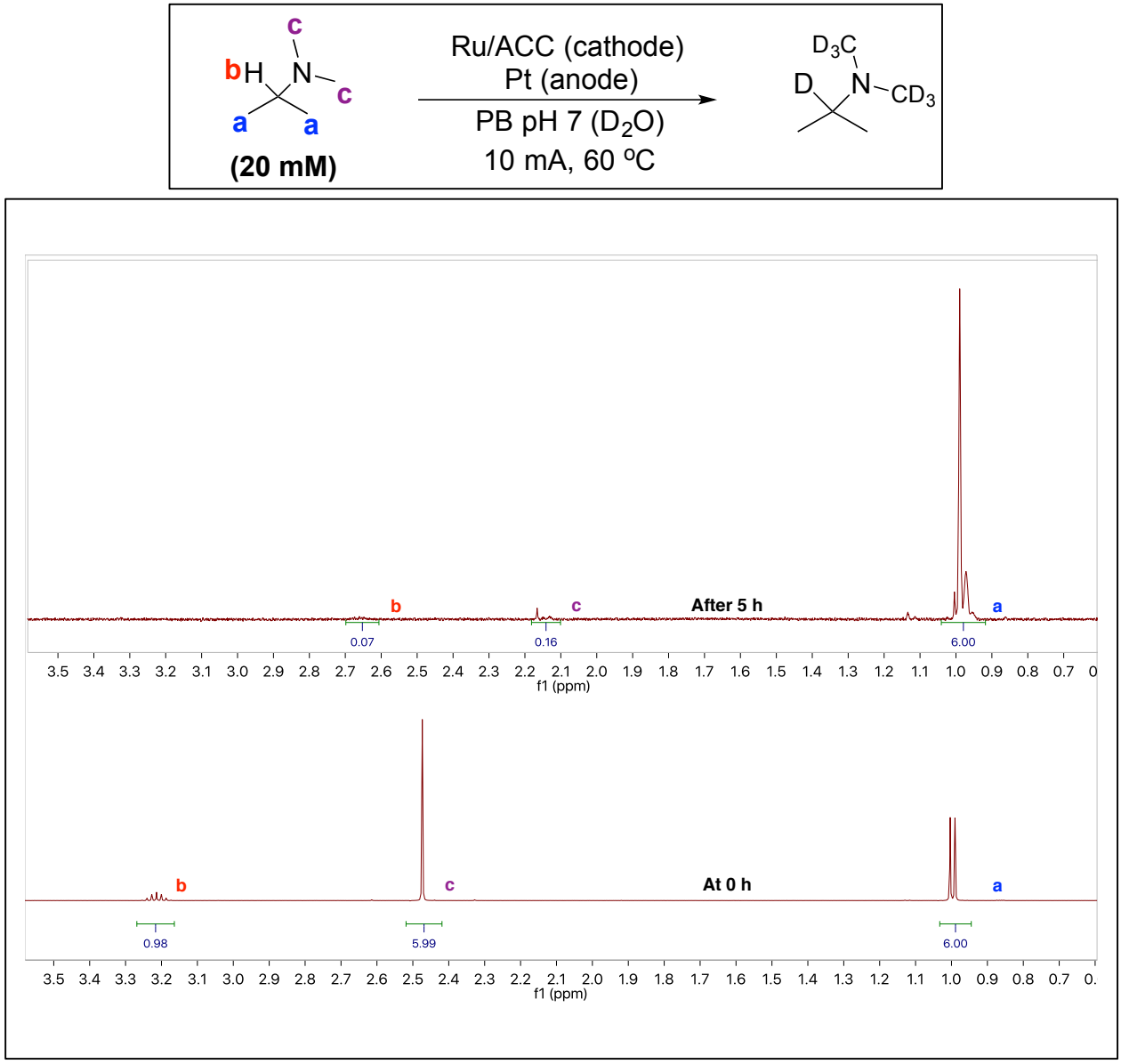

Figure 31. ^{1}H NMR spectrum of *N,N*-dimethylisopropylamine, 44 (Yield (16%)). Changes in chemical shifts are due to the change in pH resulting from electrochemical consumption of D^{+} ions. The β-CH_3's are the non-labile hydrogens and % hydrogen at the α C-H site is calculated relative to them.

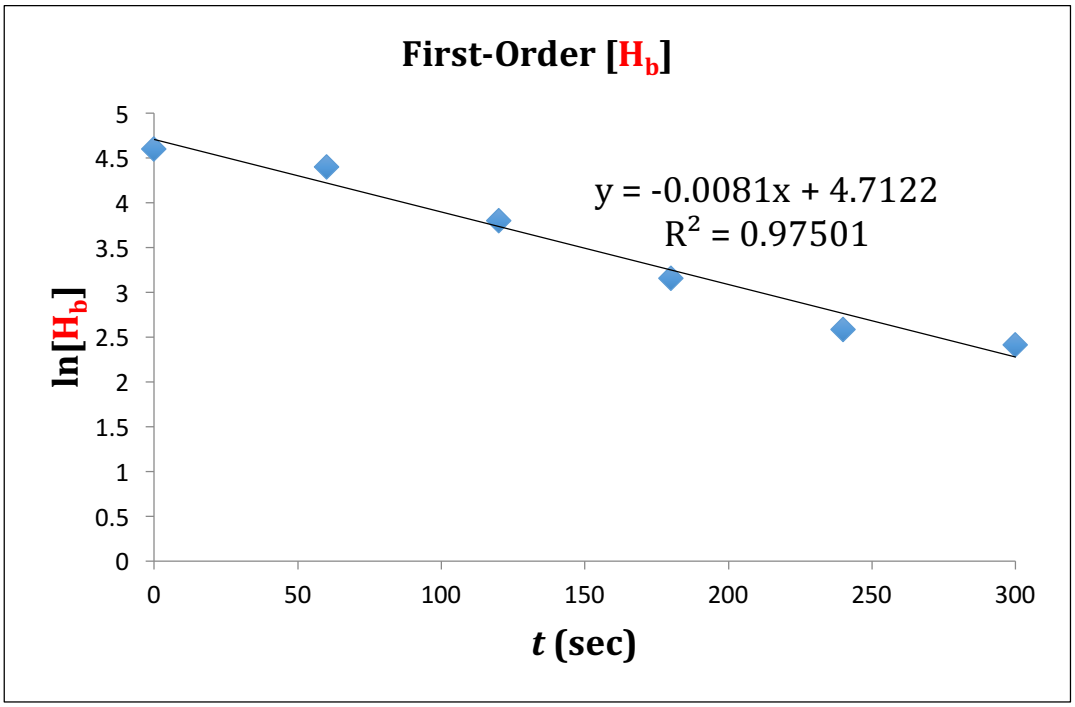

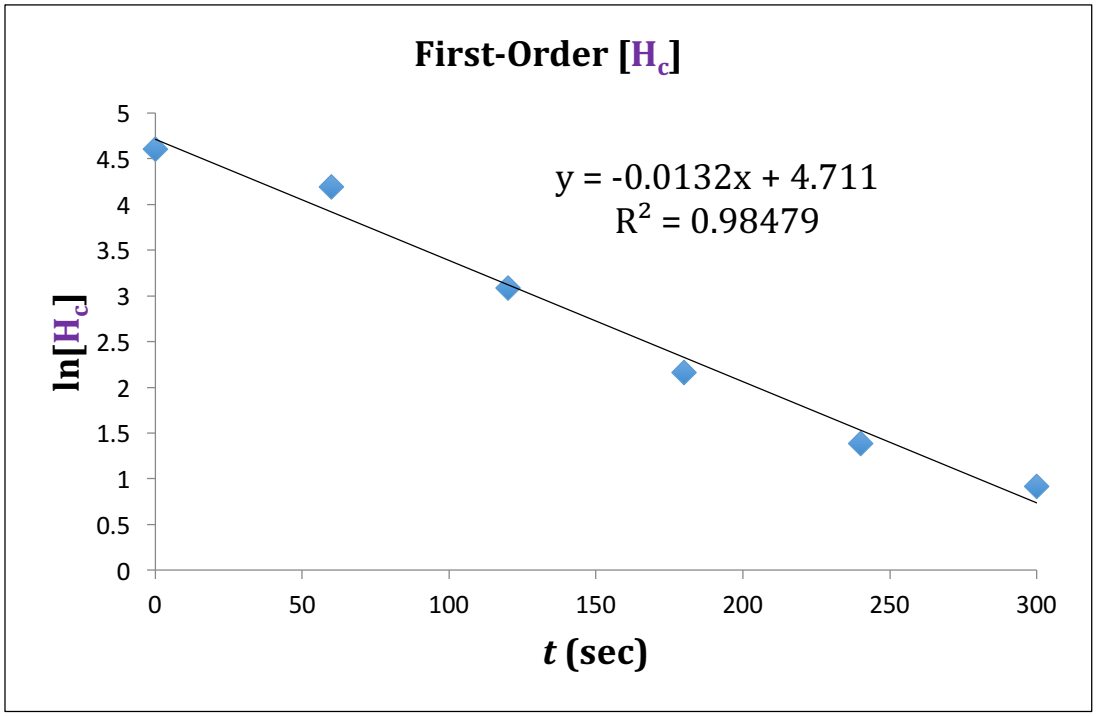

Figure 32. Kinetic Analysis: *N,N*-dimethylisopropylamine

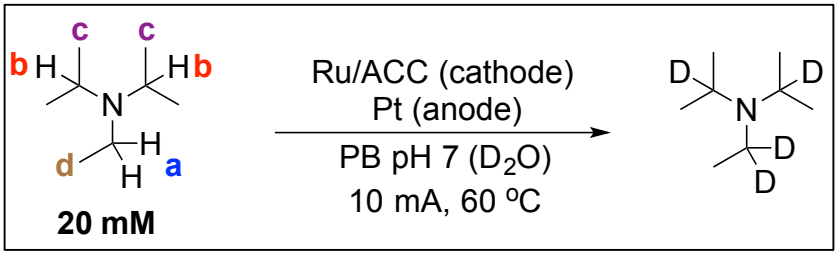

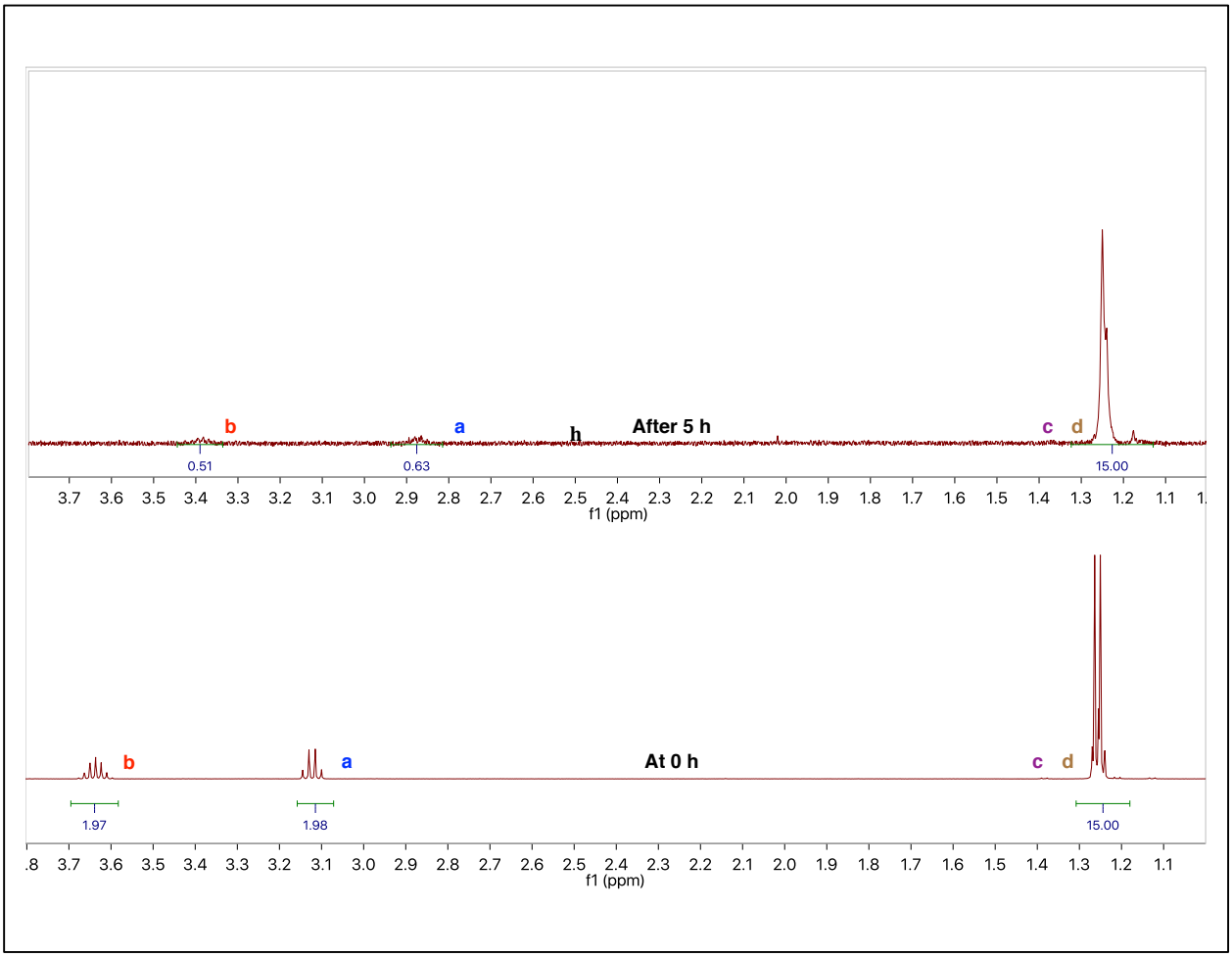

Figure 33. ^{1}H NMR spectrum of *N,N*-diisopropylethylamine, 45 (Yield (41%)). Changes in chemical shifts are due to the change in pH resulting from electrochemical consumption of D^{+} ions. The β-CH_3's are the non-labile hydrogens and % hydrogen at the α C-H site is calculated relative to them.

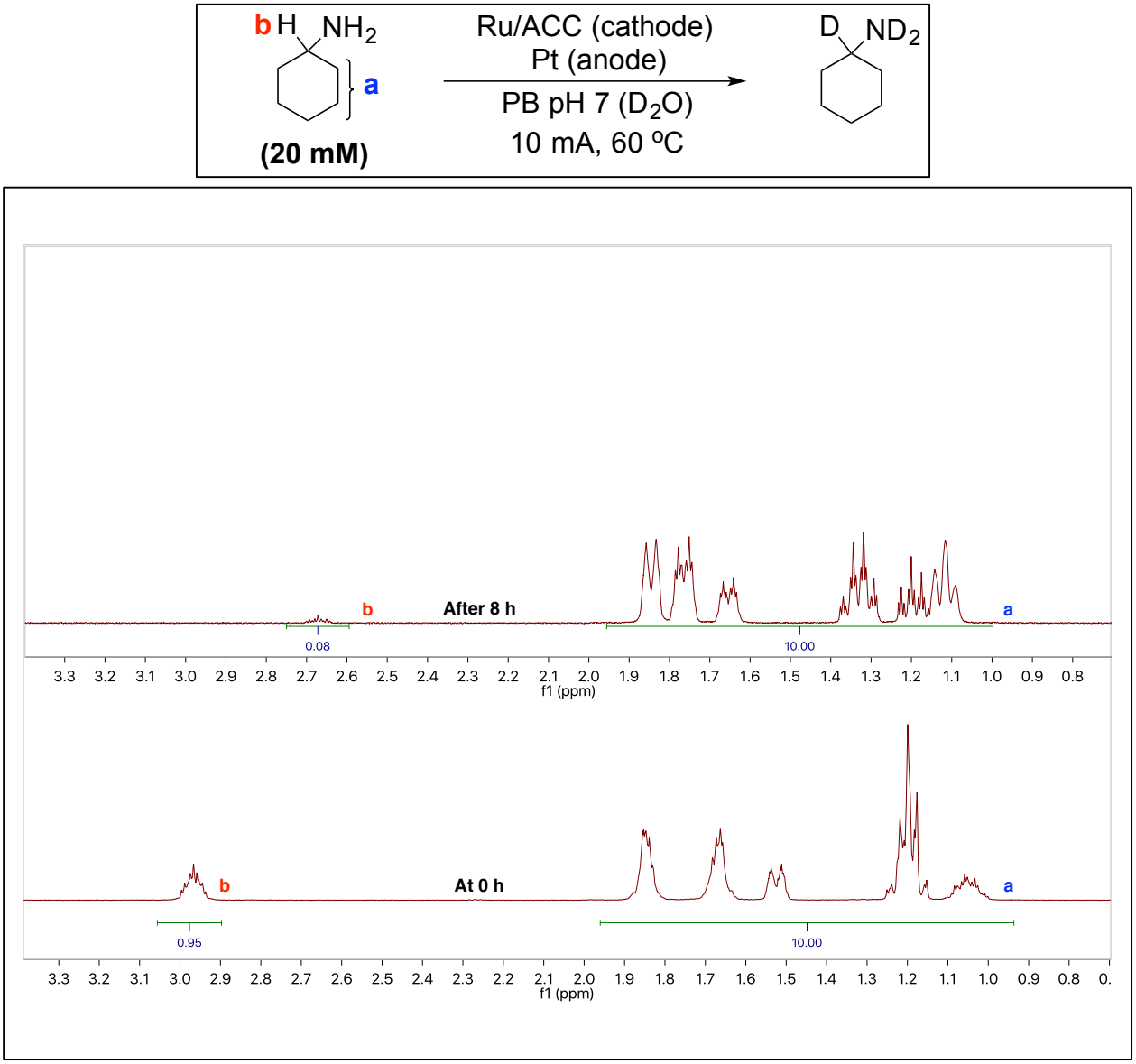

Figure 34. ^{1}H NMR spectrum of Cyclohexylamine, 46 (Yield (41%)). Changes in chemical shifts are due to the change in pH resulting from electrochemical consumption of D^{+} ions. The CH_2's are the non-labile hydrogens and % hydrogen at the α C-H site is calculated relative to them.

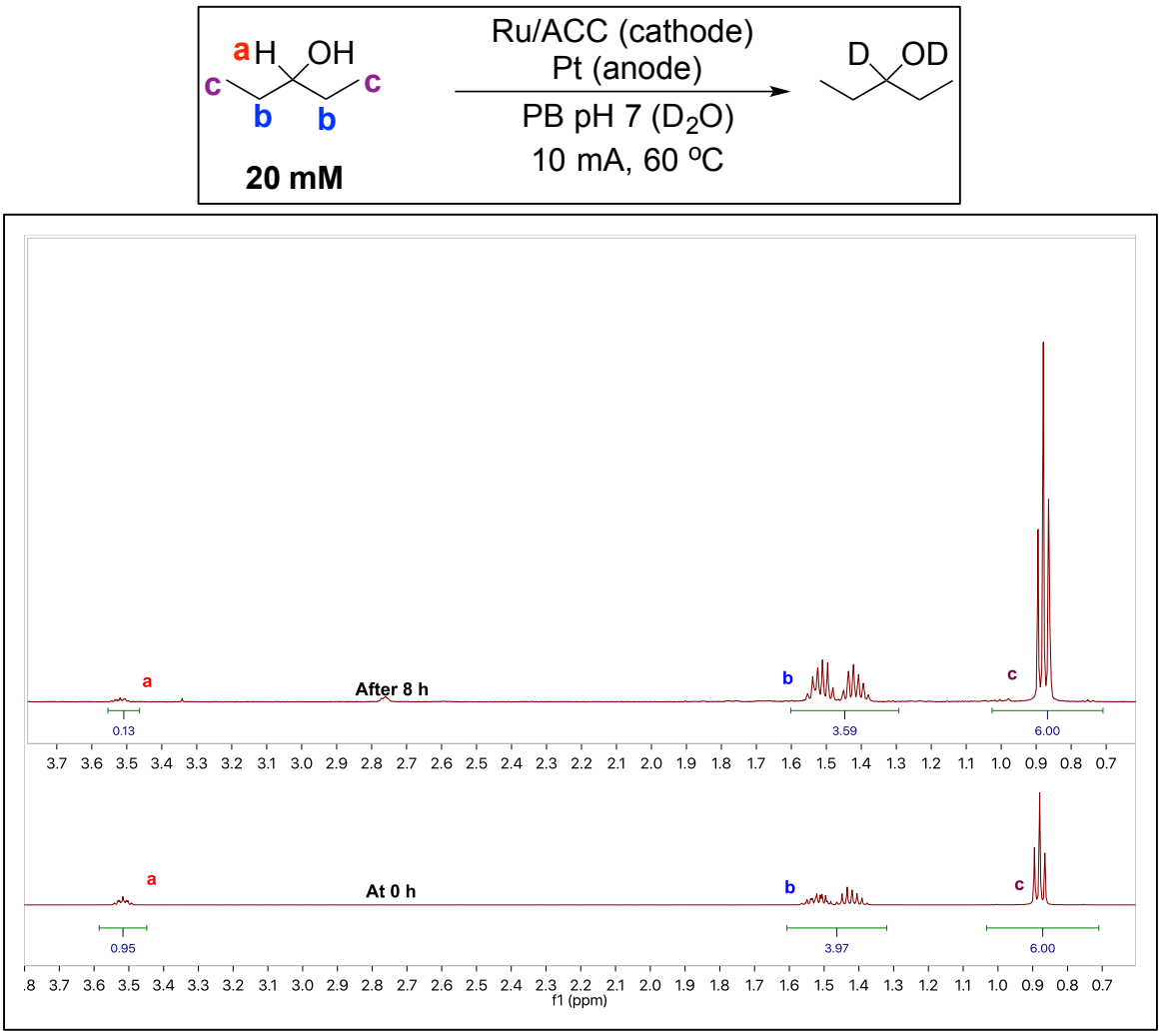

Figure 35. ^{1}H NMR spectrum of 3-pentanol, 47 (Yield (16%)). Changes in chemical shifts are due to the change in pH resulting from electrochemical consumption of D^{+} ions. The β-CH_2's and γ-CH_3's are the non-labile hydrogens and % hydrogen at the α C-H site is calculated relative to them.

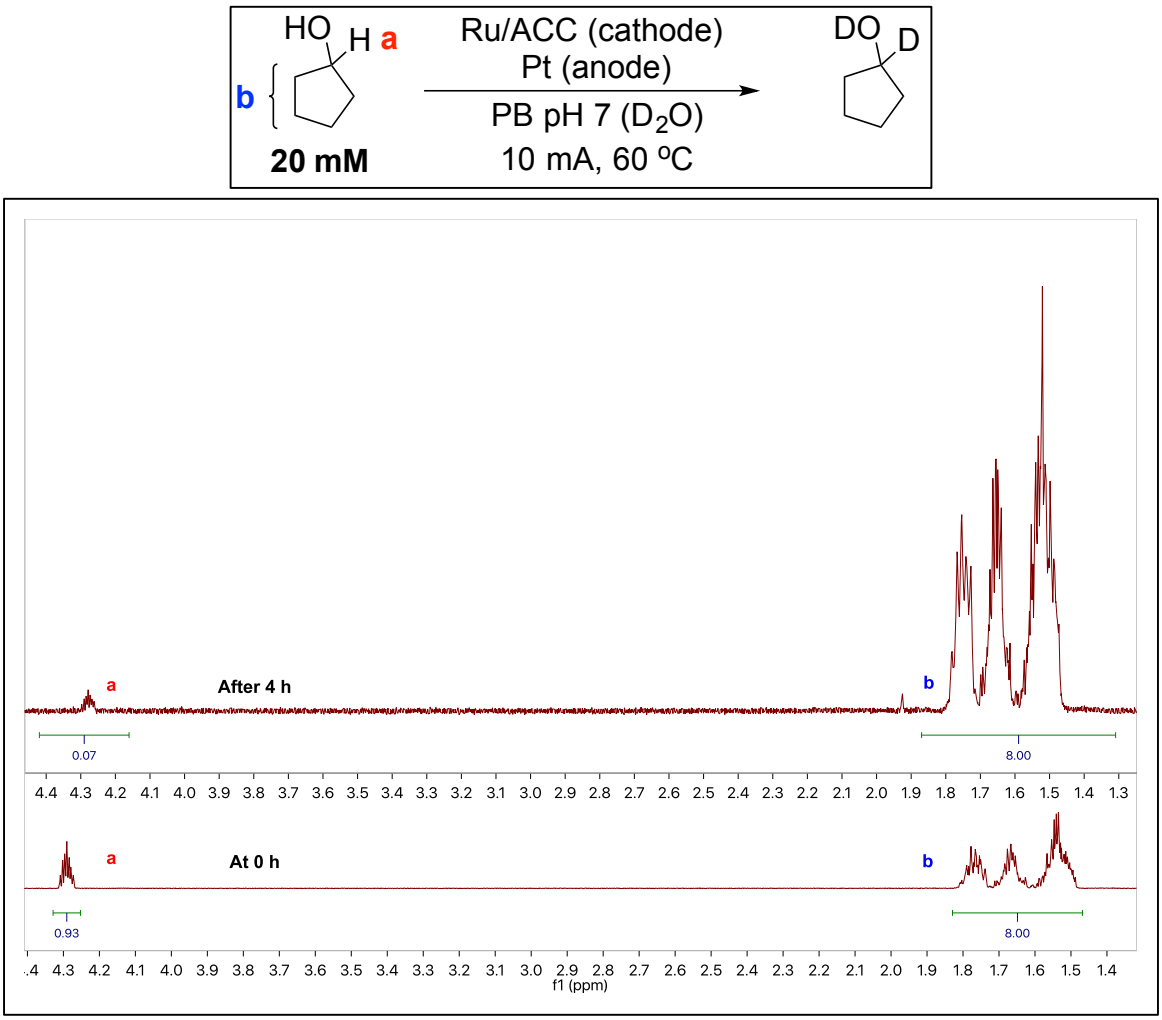

Figure 36. ^{1}H NMR spectrum of Cyclopentanol, 48 (Yield (44%)). Changes in chemical shifts are due to the change in pH resulting from electrochemical consumption of D^{+} ions. The CH_2's are the non-labile hydrogens and % hydrogen at the α C-H site is calculated relative to them.

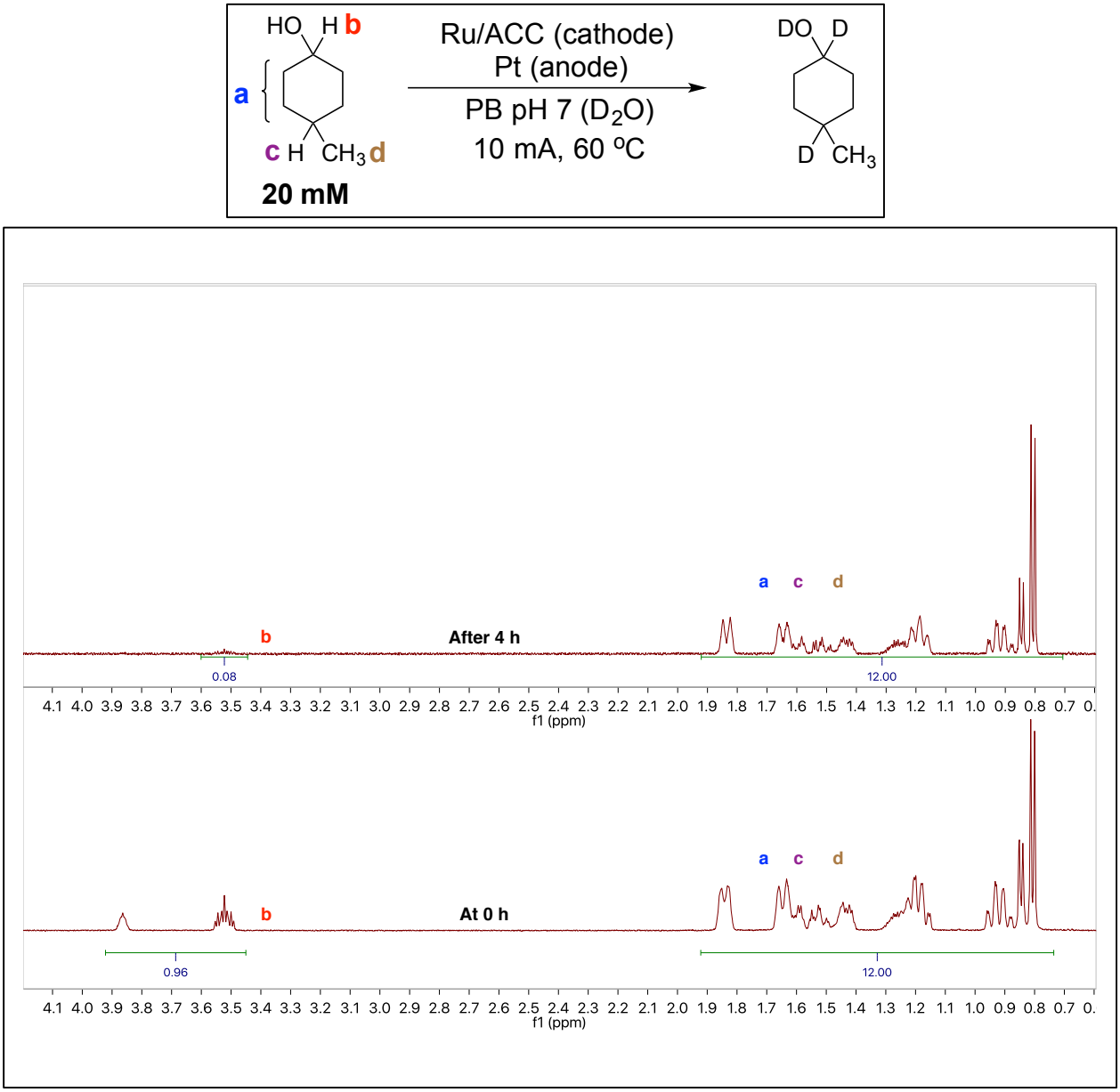

Figure 37. ^{1}H NMR spectrum of 4-methylcyclohexan-1-ol (*cis* + *trans*), 49 (Yield (27%)). Changes in chemical shifts are due to the change in pH resulting from electrochemical consumption of D^{+} ions. The CH_2's are the non-labile hydrogens and % hydrogen at the α C-H site is calculated relative to them.

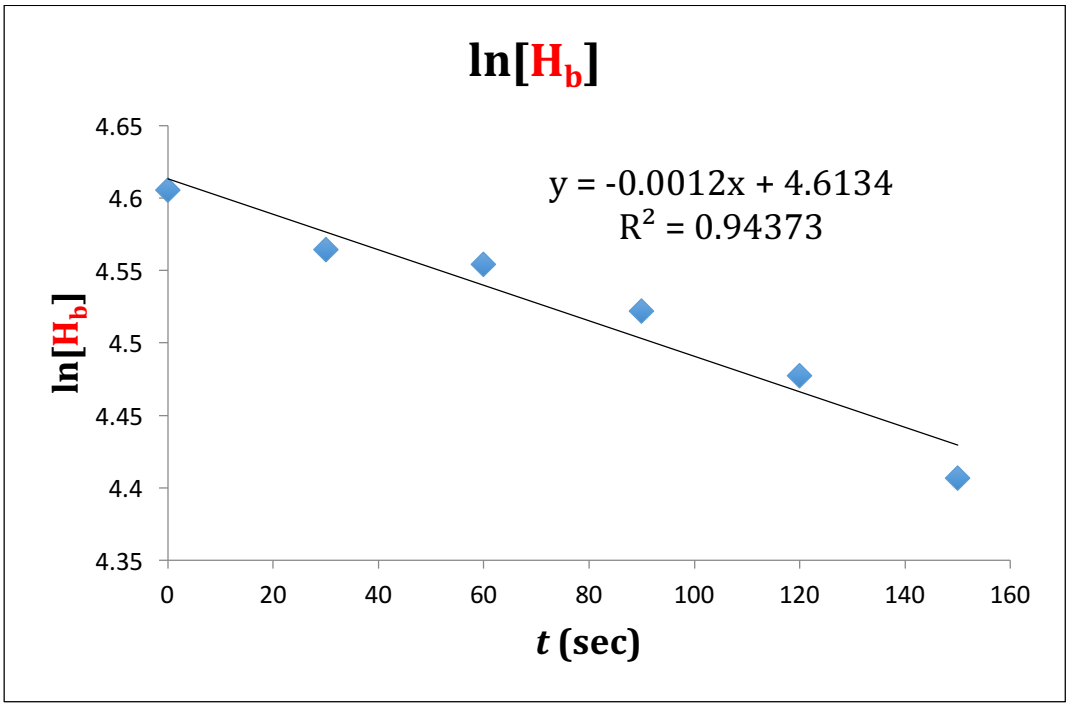

Figure 38. Kinetic Analysis: 4-methylcycloxan-1-ol and Acetic Acid

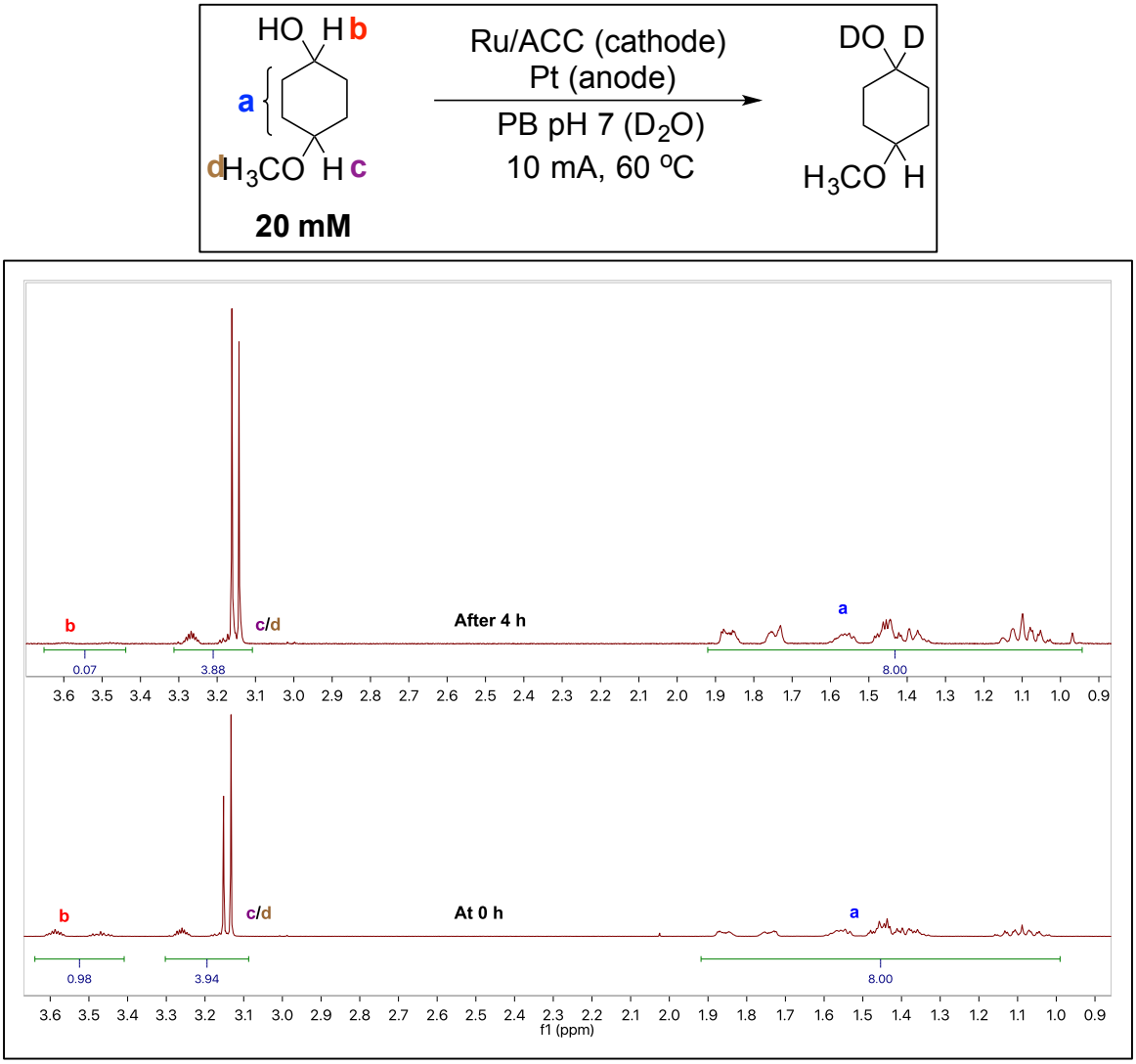

Figure 39. ^{1}H NMR spectrum of 4-methoxycyclohexan-1-ol, 50 (Yield (53%)). Changes in chemical shifts are due to the change in pH resulting from electrochemical consumption of D^{+} ions. T's are the non-labile hydrogens and % hydrogen at the α C-H site is calculated relative to them.

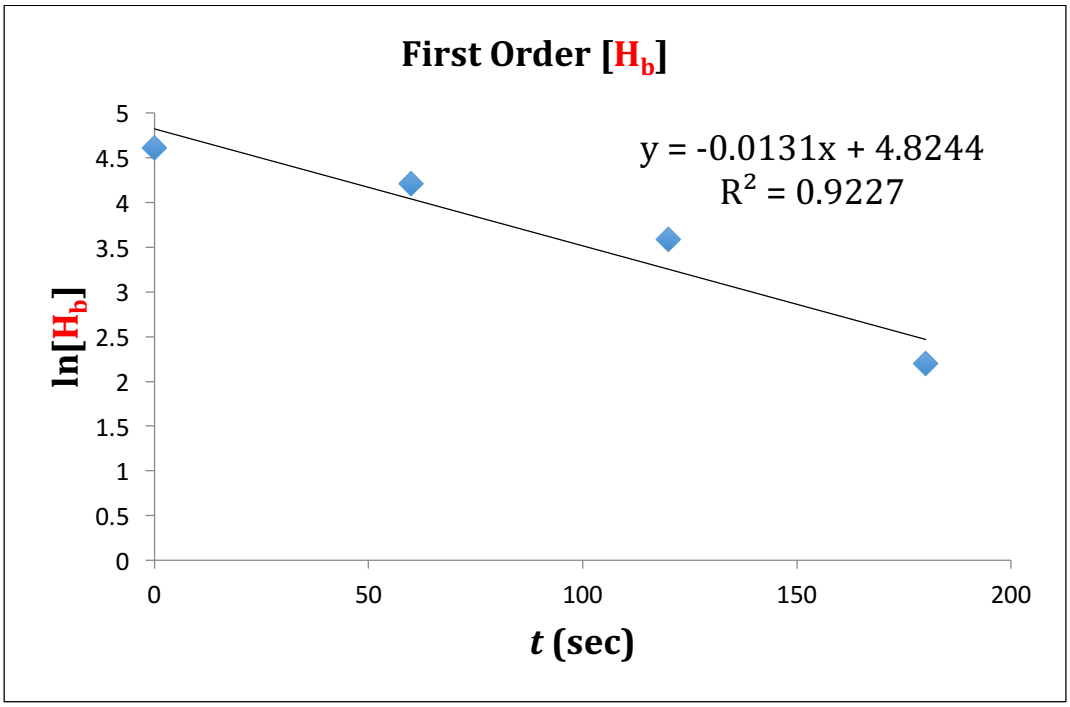

Figure 40. Kinetic Analysis: 4-methoxycyclohexan-1-ol

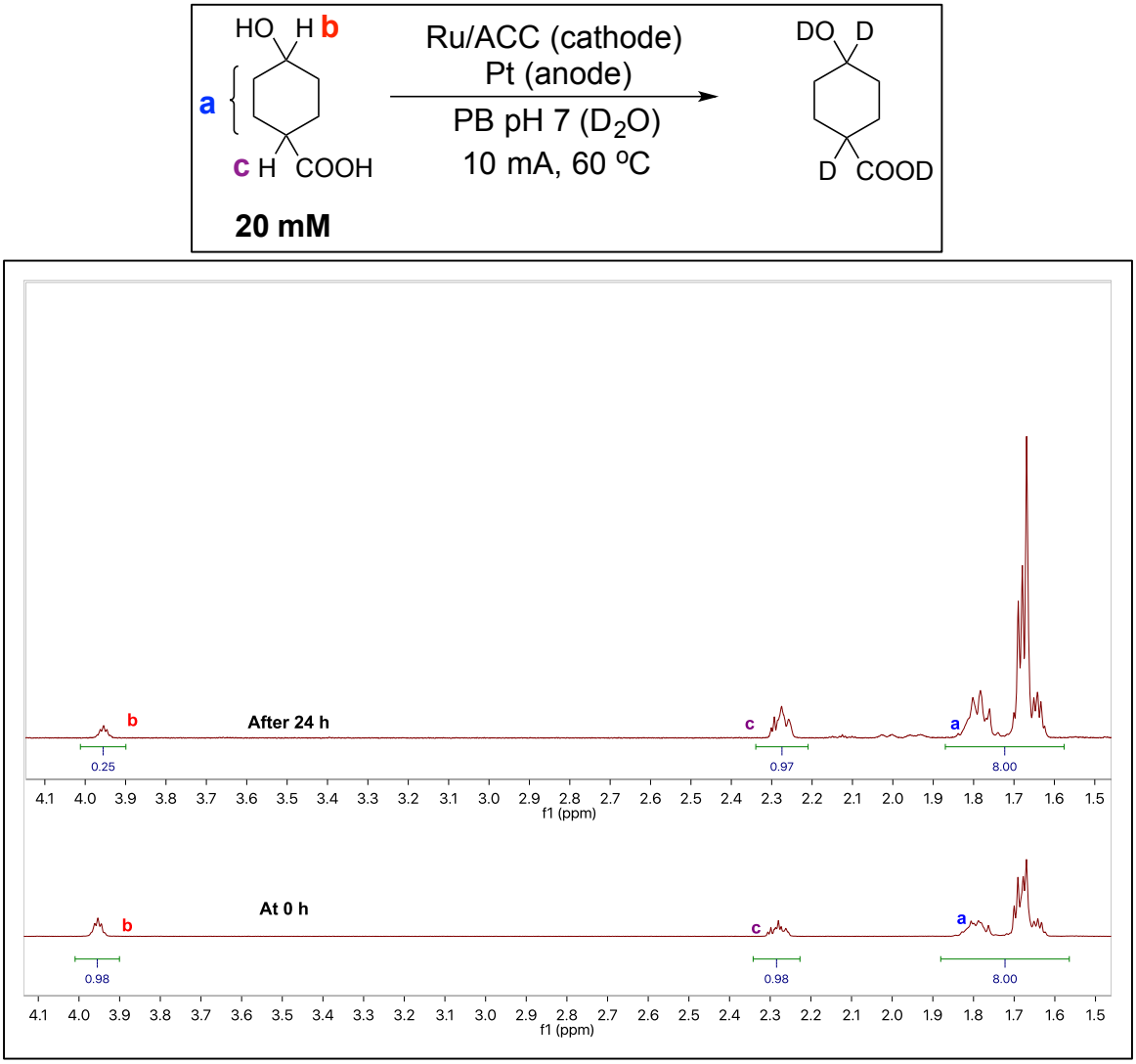

Figure 41. ^{1}H NMR spectrum of 4-hydroxycyclohexane carboxylic acid (*cis*), 51 (Yield (70%)). Changes in chemical shifts are due to the change in pH resulting from electrochemical consumption of D^+ ions. The CH_2's are the non-labile hydrogens and % hydrogen at the α C-H site is calculated relative to them.

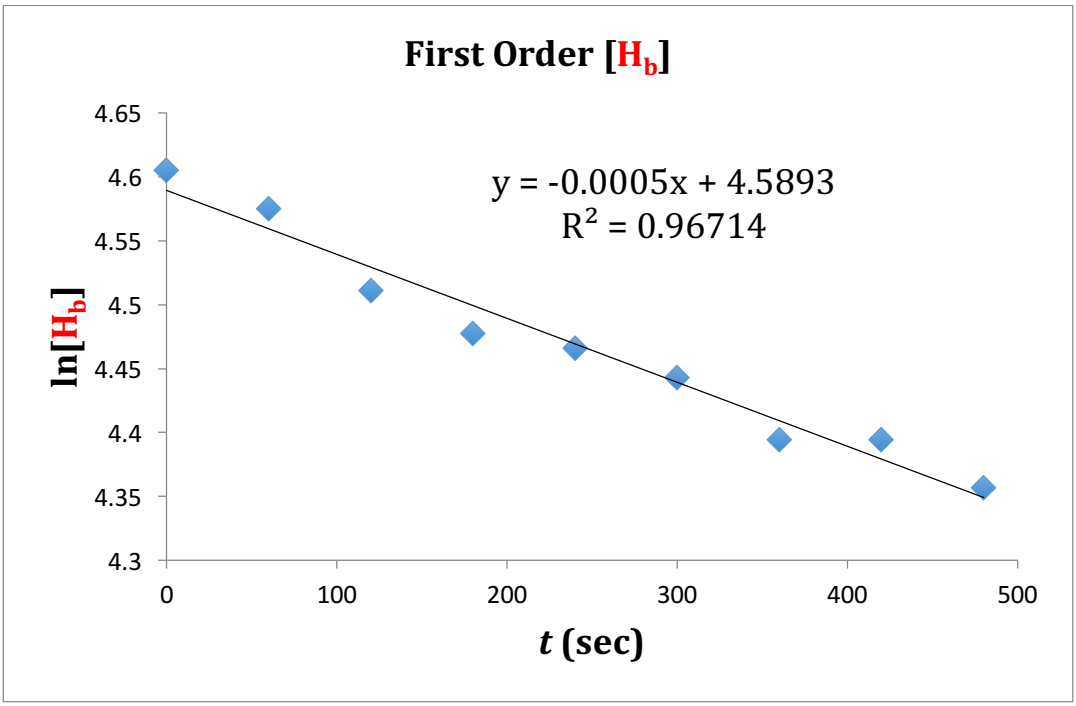

Figure 42. Kinetic Analysis: 4-hydroxycyclohexane carboxylic acid

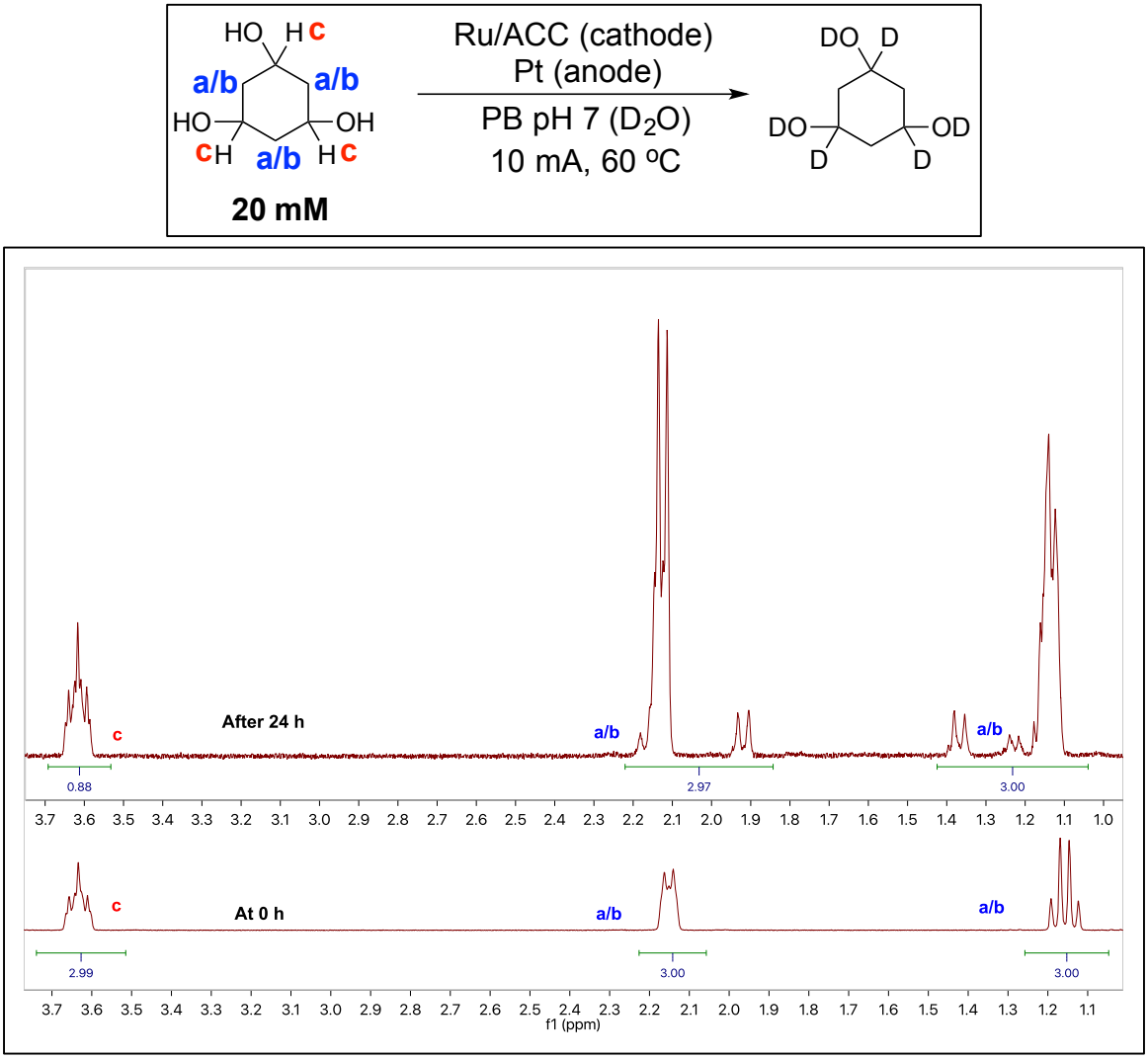

Figure 43. ^{1}H NMR spectrum of 1,3,5-cyclohexanetriol, 52 (Yield (69%)). Changes in chemical shifts are due to the change in pH resulting from electrochemical consumption of D^{+} ions. The β-CH_2's are the non-labile hydrogens and % hydrogen at the α C-H site is calculated relative to them.

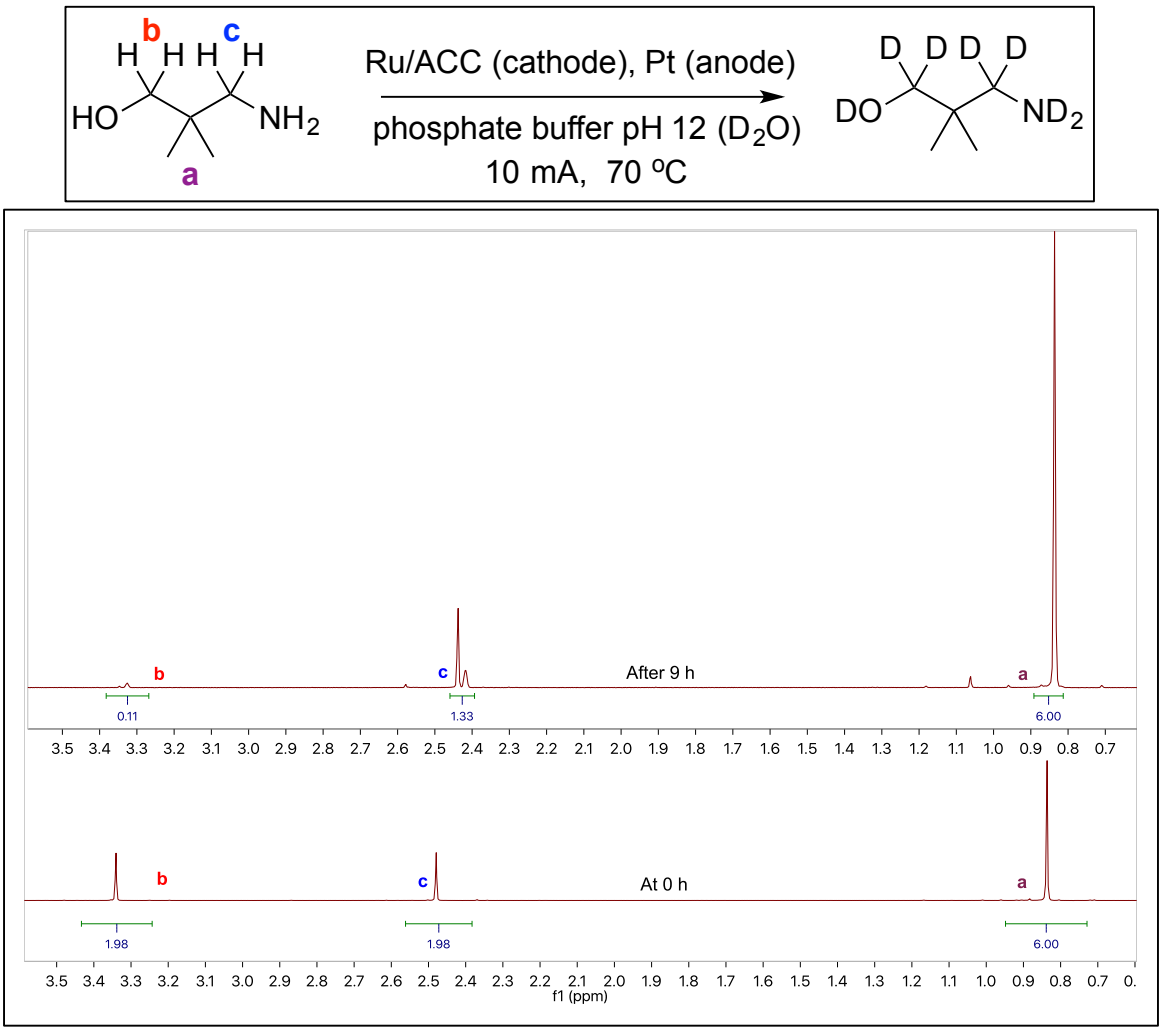

Figure 44. ^{1}H NMR spectrum of 2,2-dimethyl-3-aminopropan-1-ol, 53 (Yield (47%)). Changes in chemical shifts are due to the change in pH resulting from electrochemical consumption of D^{+} ions. The γ-CH_3's are the non-labile hydrogens and % hydrogen at the α C-H site is calculated relative to them.

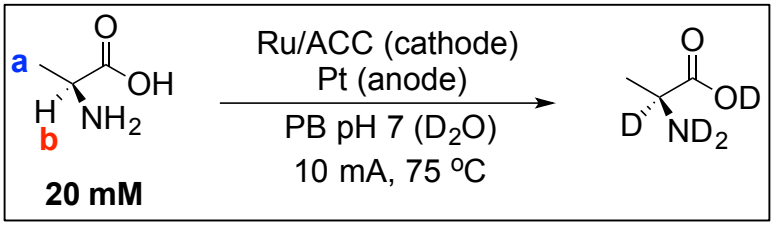

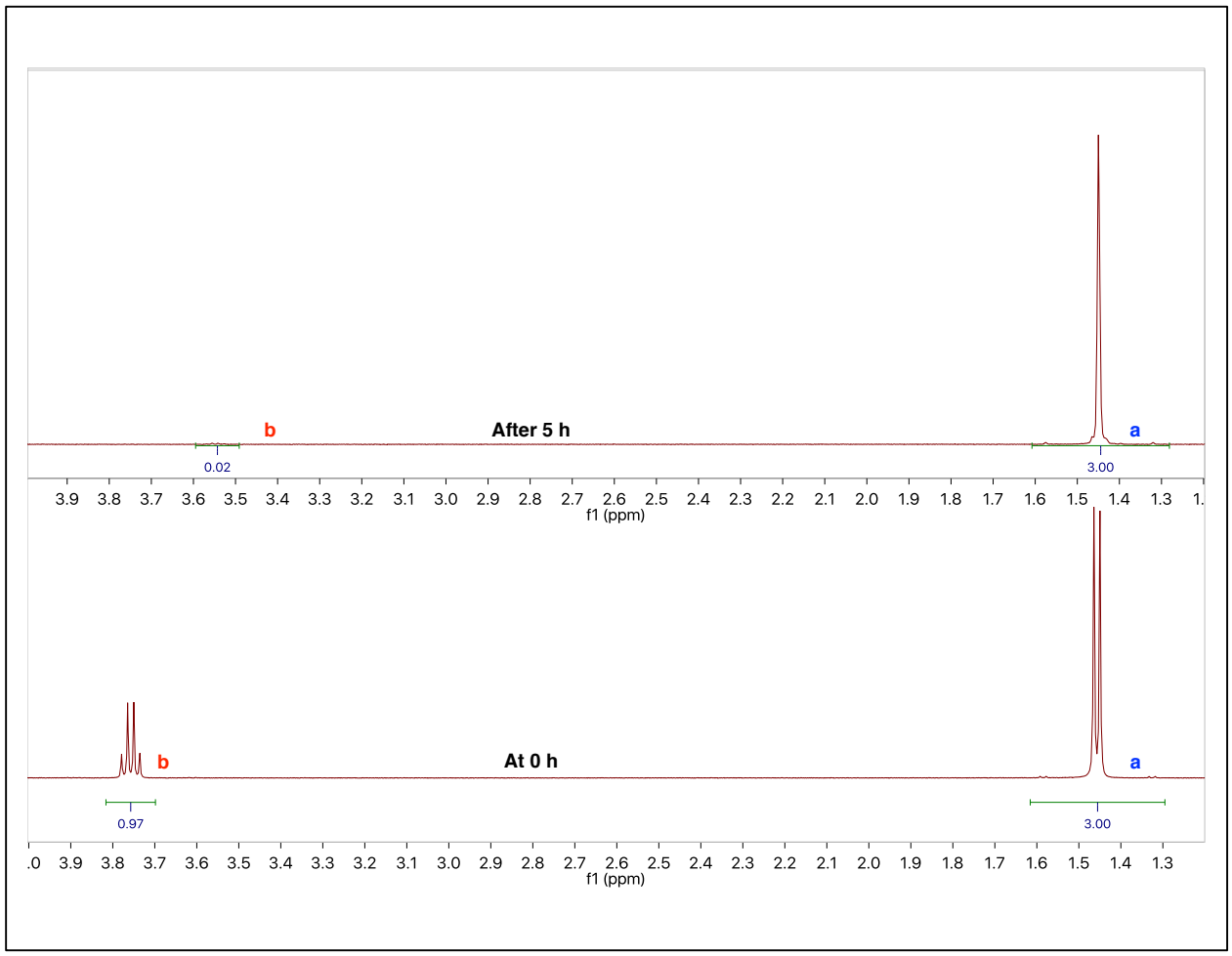

Figure 45. ^{1}H NMR spectrum of L-alanine, 54 (Yield (87%)). Changes in chemical shifts are due to the change in pH resulting from electrochemical consumption of D^{+} ions. The β-CH_3's are the non-labile hydrogens and % hydrogen at the α C-H site is calculated relative to them.

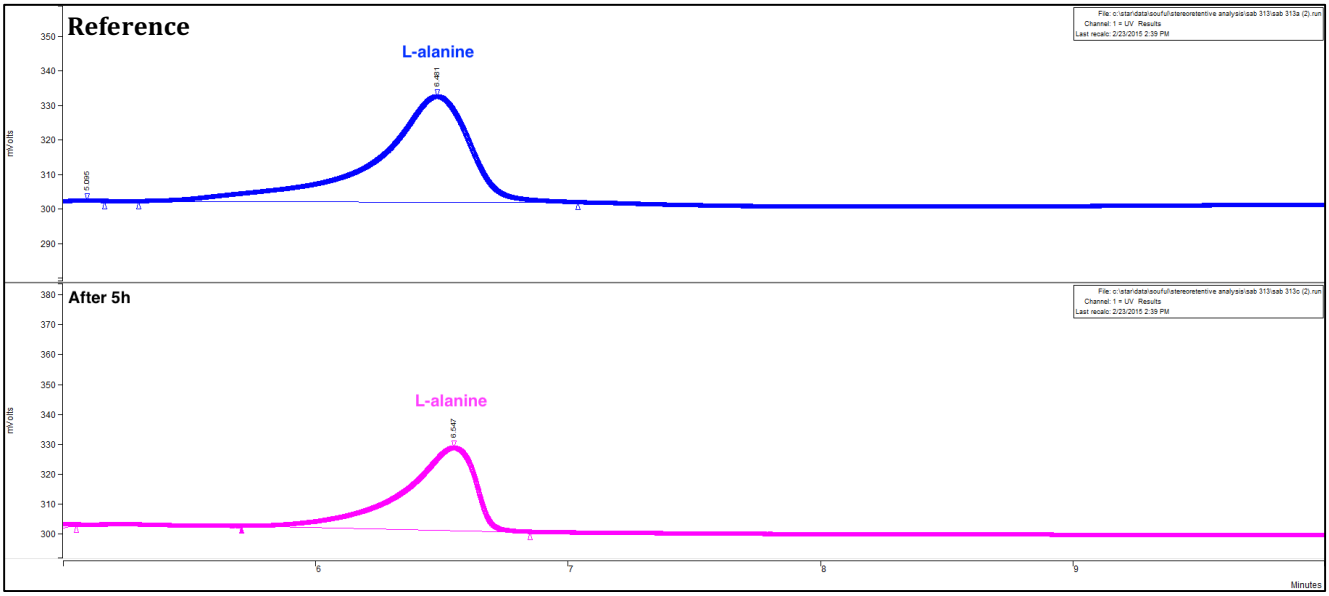

Figure 46. HPLC of L-alanine. Column: Astec CHIROBIOTIC™ T (25 cm x 4.6 mm, 5 µm). Mobile phase: Water:Methanol:Formic Acid (30:70:0.02). UV wavelength: 205 nm. Flow time: 20 minutes. Flow rate: 1 mL/min.

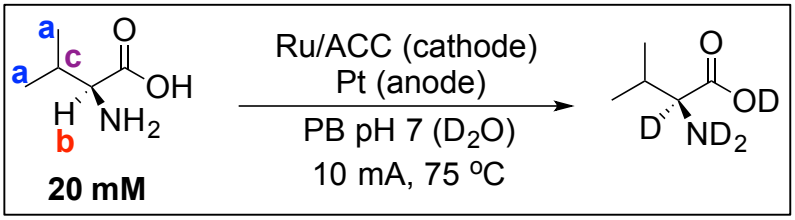

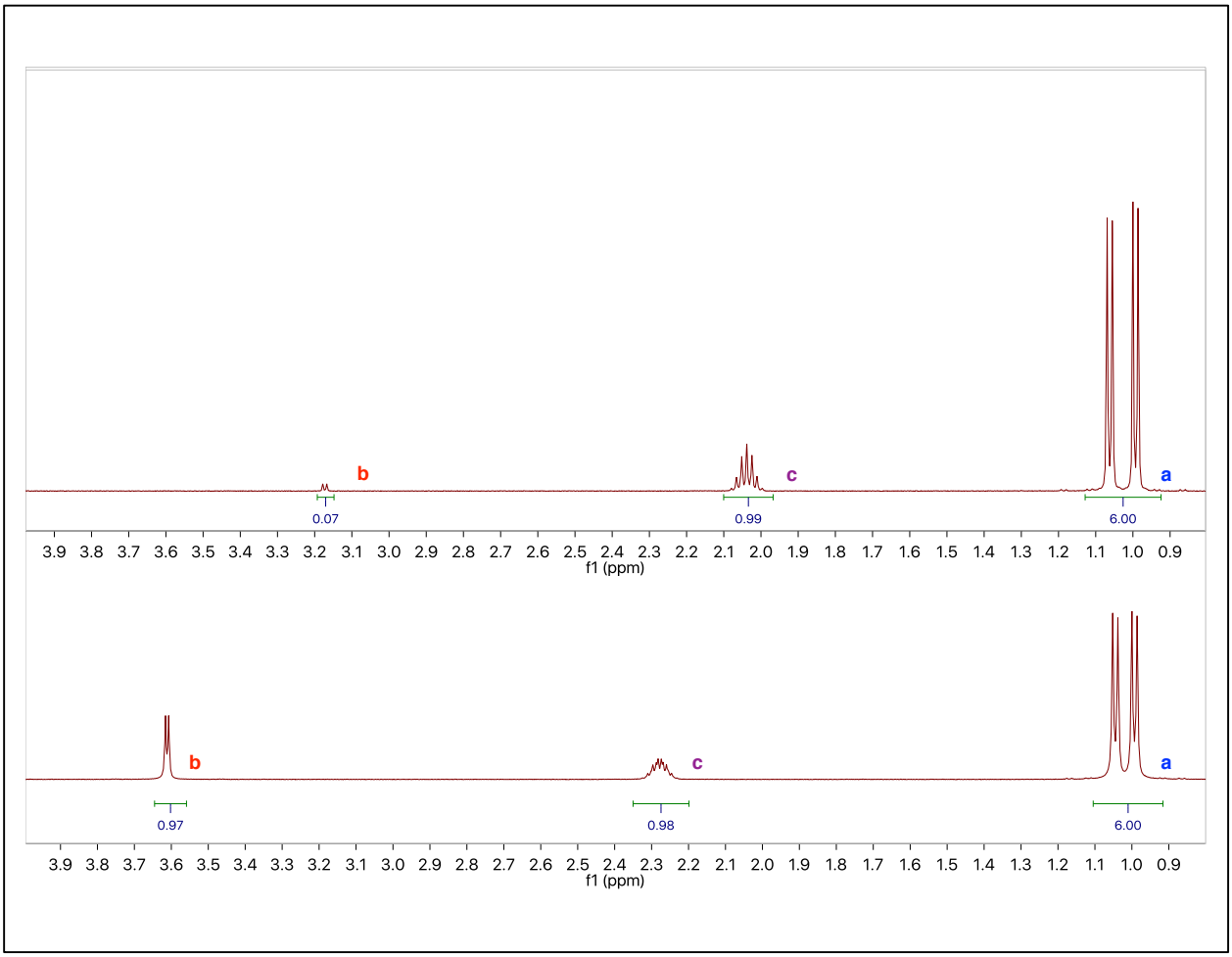

Figure 47. ^{1}H NMR spectrum of L-valine, 55 (Yield (76%)). Changes in chemical shifts are due to the change in pH resulting from electrochemical consumption of D^{+} ions. The γ-CH_3's are the non-labile hydrogens and % hydrogen at the α C-H site is calculated relative to them.

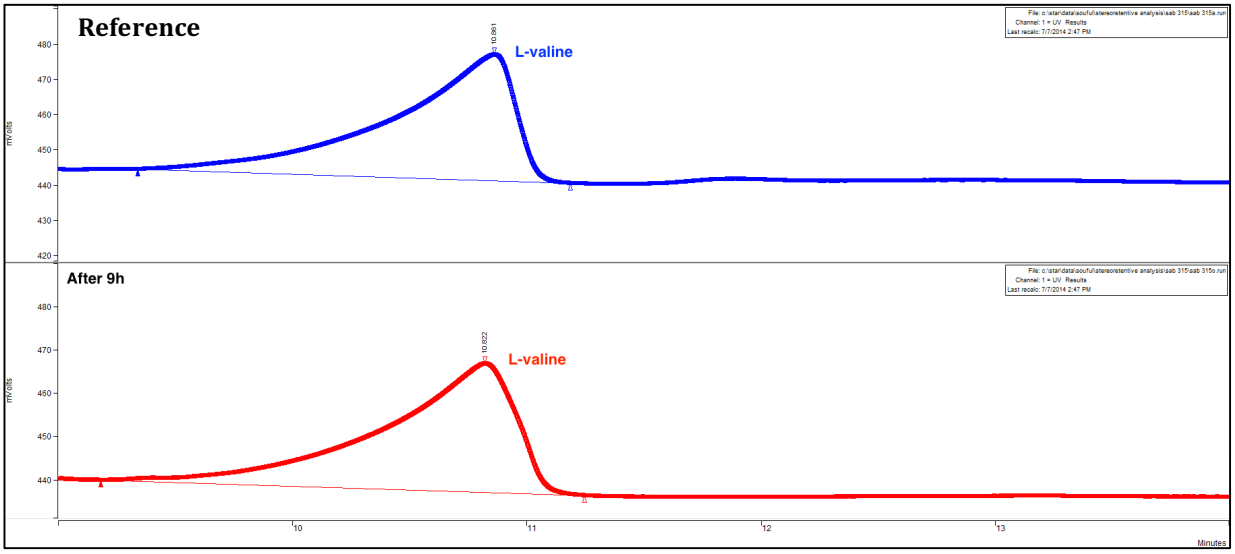

Figure 48. HPLC of L-valine. Column: Astec CHIROBIOTIC™ T (25 cm x 4.6 mm, 5 µm). Mobile phase: Water:Methanol:Formic Acid (30:70:0.02). UV wavelength: 205 nm. Flow time: 20 minutes. Flow rate: 0.5 mL/min.

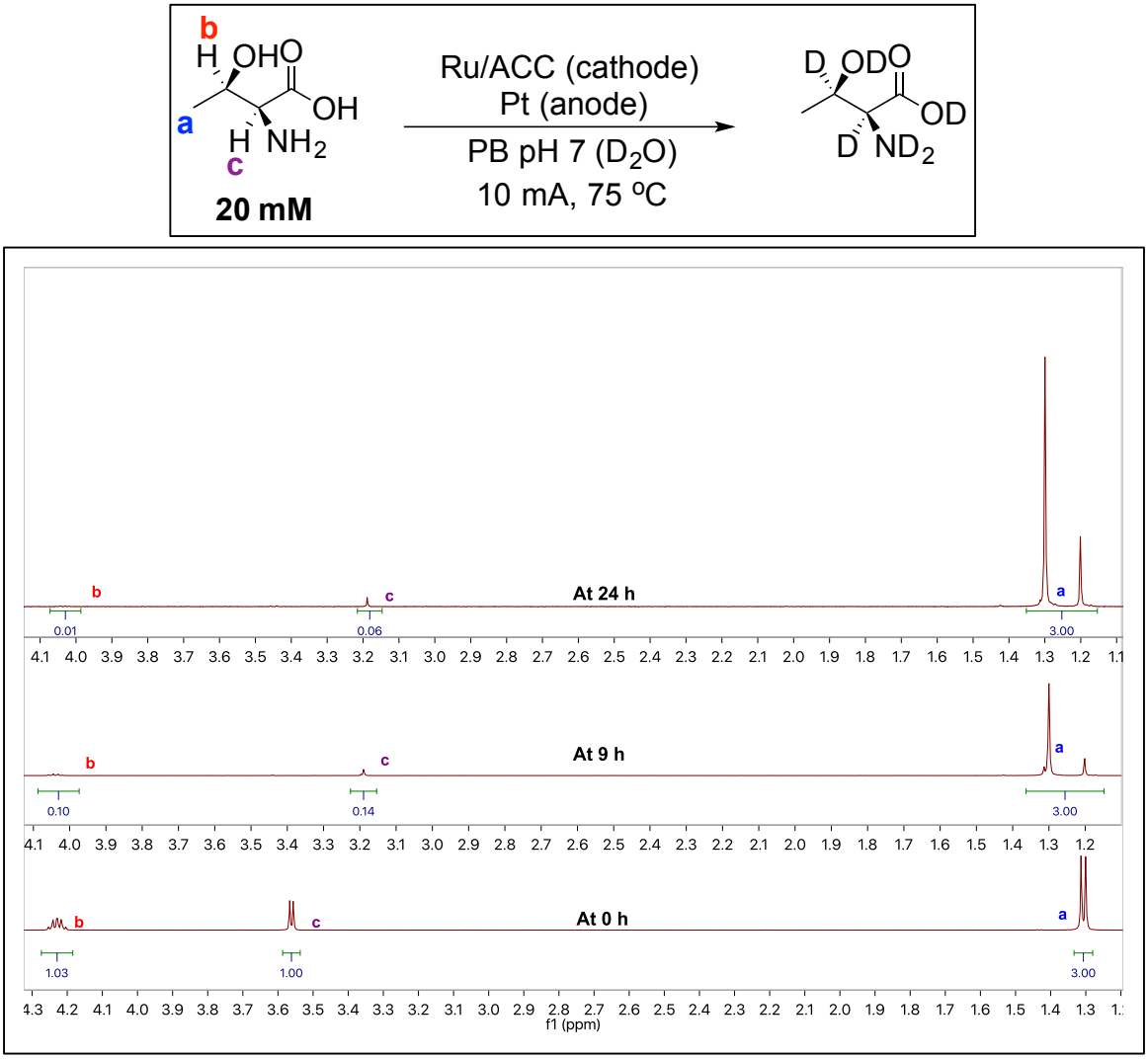

Figure 49. ^{1}H NMR spectrum of L-threonine, 56 (Yield (66%)). Changes in chemical shifts are due to the change in pH resulting from electrochemical consumption of D^{+} ions. The β-CH_3's are the non-labile hydrogens and % hydrogen at the α C-H site is calculated relative to them.

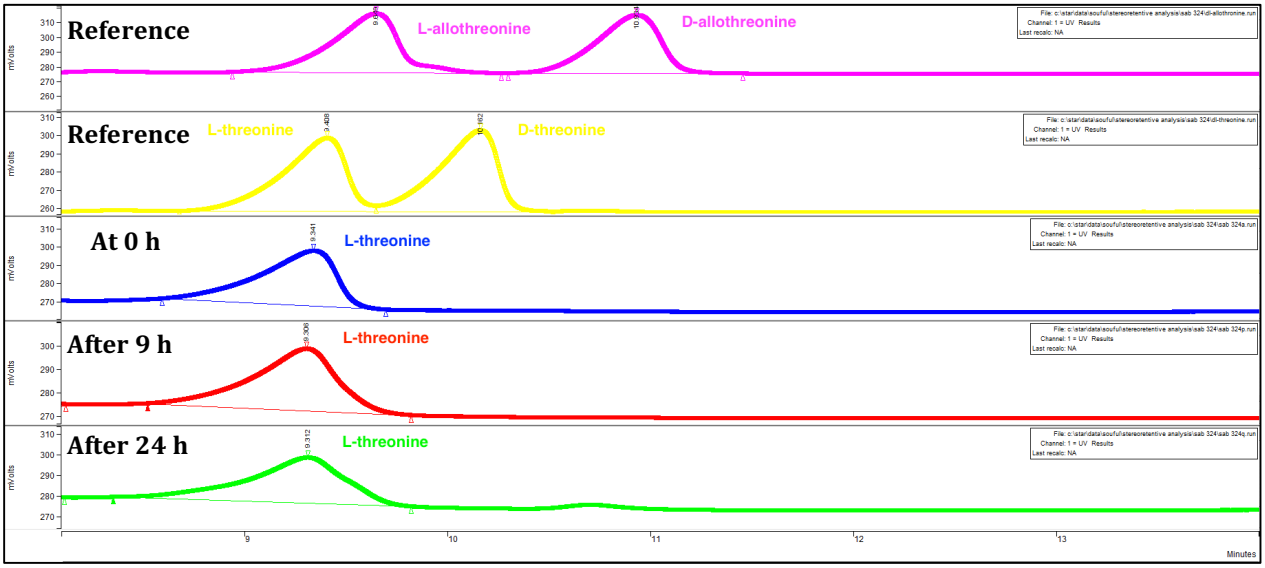

Figure 50. HPLC of L-threonine. Column: Astec CHIROBIOTIC™ T (25 cm x 4.6 mm, 5 µm). Mobile phase: Water:Methanol:Formic Acid (30:70:0.02). UV wavelength: 205 nm. Flow time: 30 minutes. Flow rate: 0.5 mL/min.

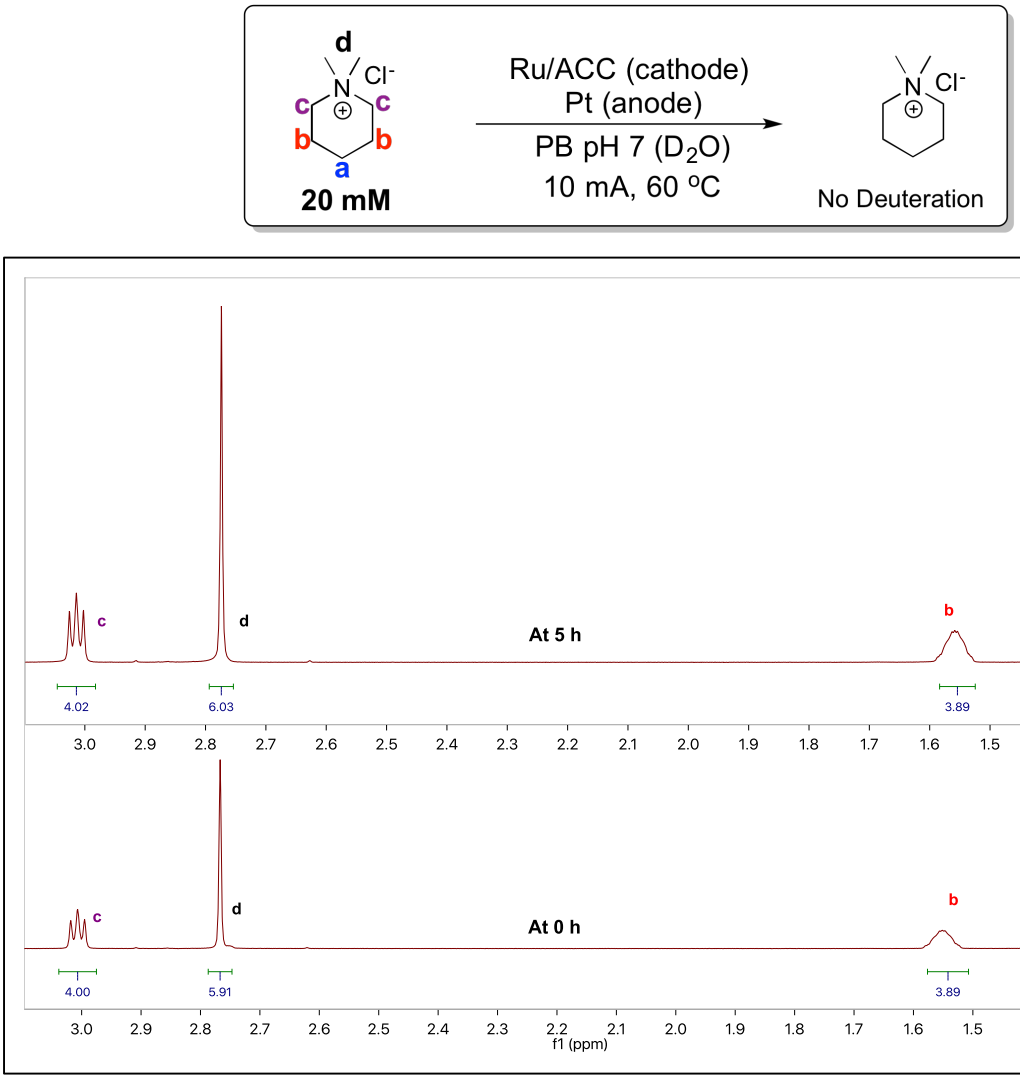

Figure 51. ^{1}H NMR spectrum of Dimethylpiperidinium, 57.

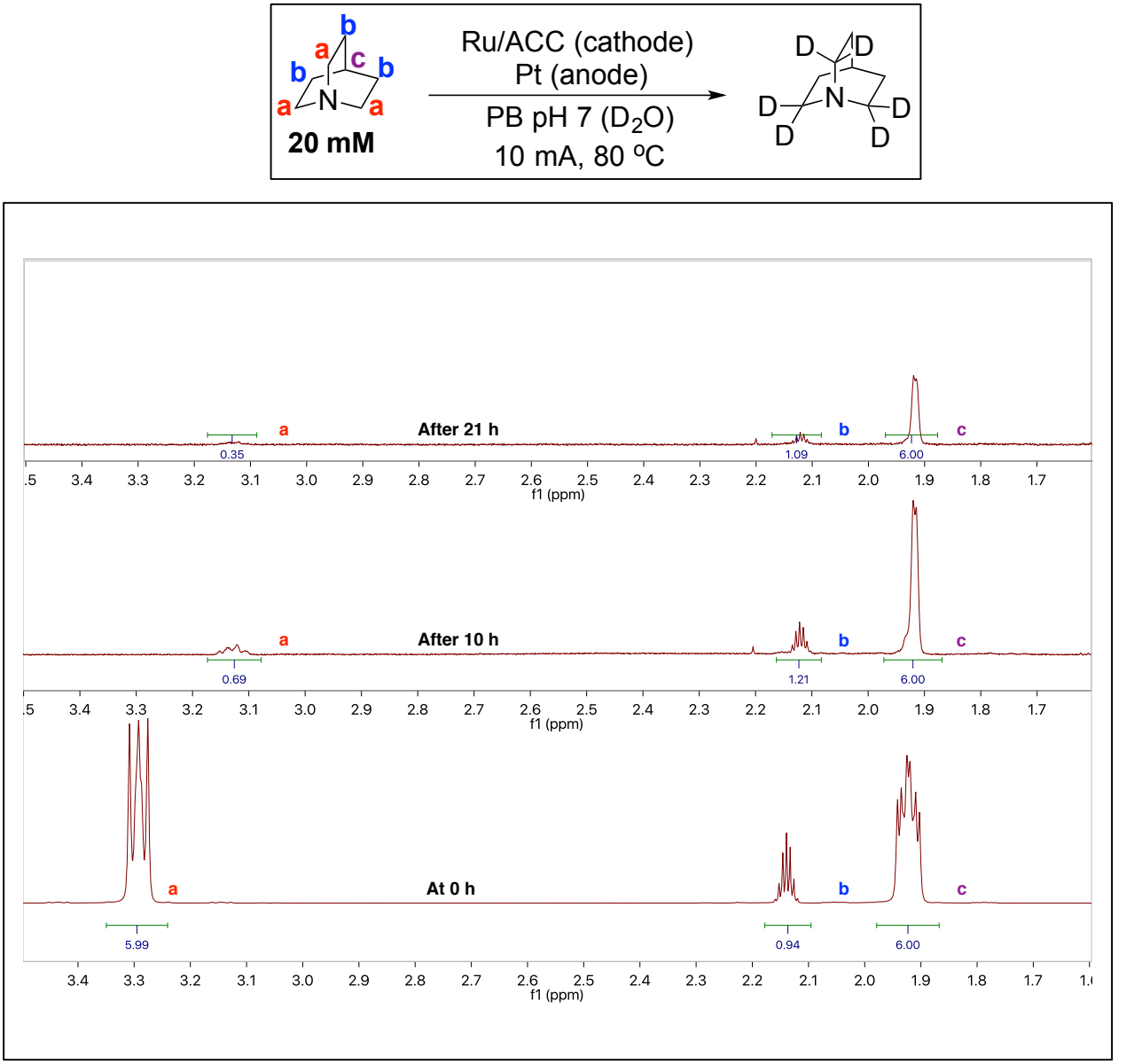

Figure 52. ^{1}H NMR spectrum of Quinuclidine, **58** (Yield (5% (10 h)). Changes in chemical shifts are due to the change in pH resulting from electrochemical consumption of D^+ ions. The β-CH_2's are the non-labile hydrogens and % hydrogen at the α C-H site is calculated relative to them.

Chapter 3. Electroactivated Palladium-Catalyzed Benzylic H/D Exchange in Aromatic Compounds

3.1 Introduction

In chapter 2, after establishing Ru/ACC–catalyzed H/D exchange in aliphatic amines, alcohols and amino acids, I and coworkers wanted to expand the scope of our methodology to aromatic substrates as they are present in most medicinal agents. The application of Ru/ACC catalyst was unsuccessful with the aromatic substrates as it resulted in the reduction of benzene rings. Seeking an alternative to Ru for selective H/D exchange in aromatic compounds, we came across the work by Sajiki *et al*.[174] who reported Pd/C-catalyzed benzylic H/D exchange in substituted aromatics (**Scheme 47**).

Taking our cue from Sajiki's work, we developed an electroactivated Pd/ACC catalyst with the ability to regioselectively activate C-H bonds in aromatic compounds in mild, aqueous conditions. The use of H_2 was not warranted in our set-up as palladium is activated by current rather than H_2 as in the case of Sajiki's work. The work described here using electroactivated Pd/ACC (palladium on activated carbon cloth) showed the ability to effect H/D exchange selectively at the benzylic site at a cuurent density of 33.3 mA/cm^2, 60 °C and at ambient pressure. In addition to benzylic H/D exchange, we also observed substituent-directed *ortho*-H/D exchange in substituted aromatic compounds.

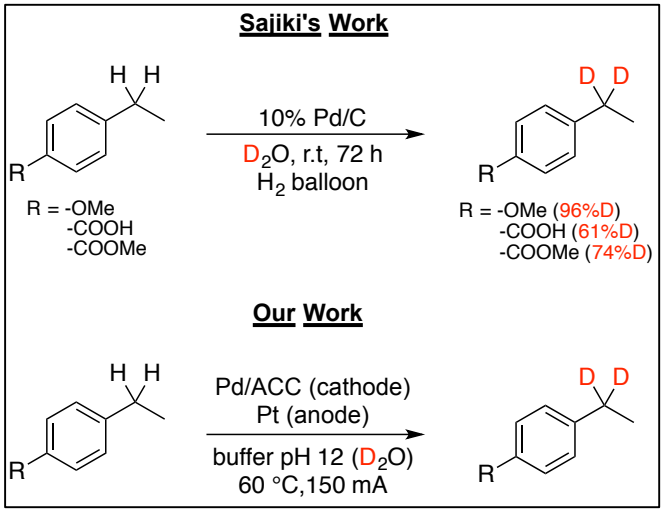

Scheme 47. Pd/C-Catalyzed Benzylic H/D Exchange

3.2 Experimental

3.2.1 Reagents and Materials

All reagents were purchased from commercial vendors and were used without further purification. Deuterium oxide (99.9%) was purchased from Cambridge isotope Laboratories, Inc. The Pt (0.404 mm) wire used as a counter electrode was purchased from Alfa Aesar, Omegaette Model HHM33 multimeter and Lambda (Model: LPD 422A FM) galvanostat were used to maintain a constant current density in the system. Zorflex® ACC FM110 was obtained from the Calgon Carbon Co. Palladium (II) chloride, 98% was purchased from Oakwood Chemical and was used for the preparation of the catalyst. Phosphate buffer (0.01M) at pH 7 was prepared using potassium phosphate (monobasic and dibasic, purchased from Jade Scientific) in D_2O.

3.2.2 Reaction Procedure

The experiment was carried out in a 2-C cell separated with a Dupont® Nafion-117 membrane. Pd/ACC was used as a working electrode (cathode) and Pt wire was used as a

counter electrode (anode). 20 mL of 0.01 M phosphate buffer (pH 7) prepared in D_2O was placed in each compartment to serve as the electrolyte (catholyte & anolyte) for the experiment. The cell was placed in an oil bath to operate at the desired temperature and the reaction was carried out under galvanostatic control. Substrate was added to the catholyte and was stirred for 30 minutes at 60 °C to dissolve, and then subjected to electroactivated H/D exchange. No pre-electrolysis phase was applied.

3.2.3 Analysis

Liquid samples were analyzed using an Agilent 500 MHz superconducting NMR spectrometer at 298 K. NMR tubes with an external diameter of 5 mm were used (Wilmad-LabGlass, Buena, NJ). A non-labile C-H site was used as an internal standard to determine the relative hydrogen content at the reactive site. Spectra were referenced using dimethyl sulfoxide (DMSO). The yield of the substrates was determined using the qEstimate tool of Agilent VnmrJ 4 employing 0.0485 M solution of triphenyl phosphate in $CDCl_3$. Chemical shift differences between initial and final spectra reflect electrochemically induced pH shift to more basic conditions due to H^+ consumption.

3.2.4 Development of the Catalyst

Zorflex® ACC FM100 was chosen as the support for the Pd due to its high conductivity and large surface area. ACC (3 cm x 1.5 cm) was initially washed in de-ionized (DI) water and allowed to dry in an oven overnight at 150 ˚C. The palladium salt was deposited via incipient wetness via diffusion by soaking ACC in a solution of tetrachloropalladate (II) $[PdCl_4]^{2-}$ prepared by adding $PdCl_2$ to 5 ml of 1 M HCl. $PdCl_2$ is converted to $[PdCl_4]^{2-}$ to enhance its solubility in water and the liquid was evaporated under a stream of N_2 gas overnight and was

then placed under vacuum for 48 h before its use. This process resulted in $[PdCl_4]^{2-}$ deposited on ACC ($[PdCl_4]^{2-}$/ACC) that is electroreduced in the reaction. The amount of catalyst used in the discussion is represented as μmoles of $PdCl_2$ per gram of ACC. *(Note: No prereduction was performed and $[PdCl_4]^{2-}$/ACC was used directly with the substrate and the reaction was monitored)*.

3.3 Results and Discussion

3.3.1 Characterization of the Catalyst

To understand the distribution of $[PdCl_4]^{2-}$ prepared with incipient wetness and investigate any change in its distribution and morphology after electrocatalytic reduction during the H/D exchange reaction, we performed SEM and EDX analysis of the used and unused catalyst. The SEM image of the $[PdCl_4]^{2-}$/ACC (unused, **Figure 53** & **Figure 55**) showed a uniform distribution of Pd across the ACC fibers confirmed by the EDX analysis (**Figure 54** & **Figure 56**). The distribution is not altered during its use in the H/D exchange reaction as shown in the SEM images (**Figure 57** & **Figure 59**) of the Pd/ACC catalyst after three consecutive runs and confirmed by EDX analysis (**Figure 58** & **Figure 60**). This is consistent with the results obtained during catalyst deactivation studies with *p*-toluic acid.

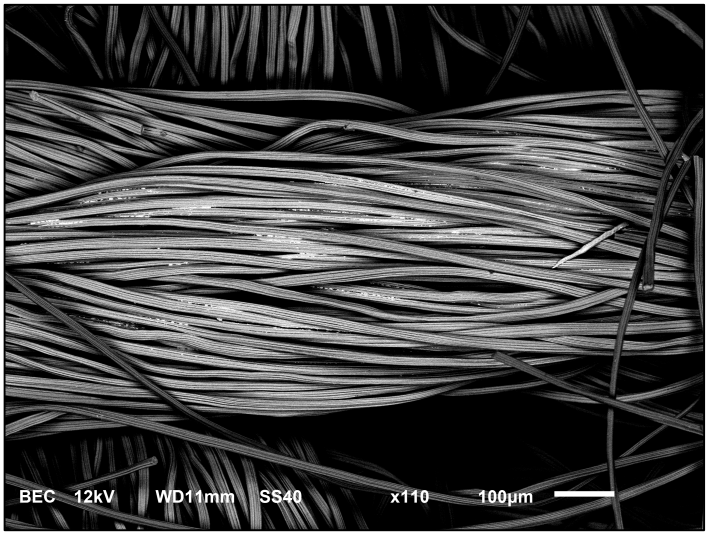

Figure 53. SEM: $[PdCl_4]^{2-}$/ACC (Unused)

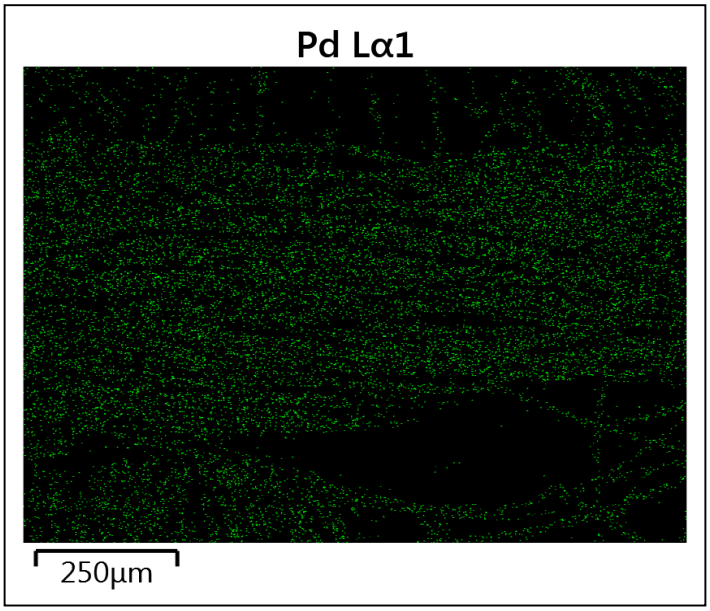

Figure 54. EDX: $[PdCl_4]^{2-}$/ACC (Unused)

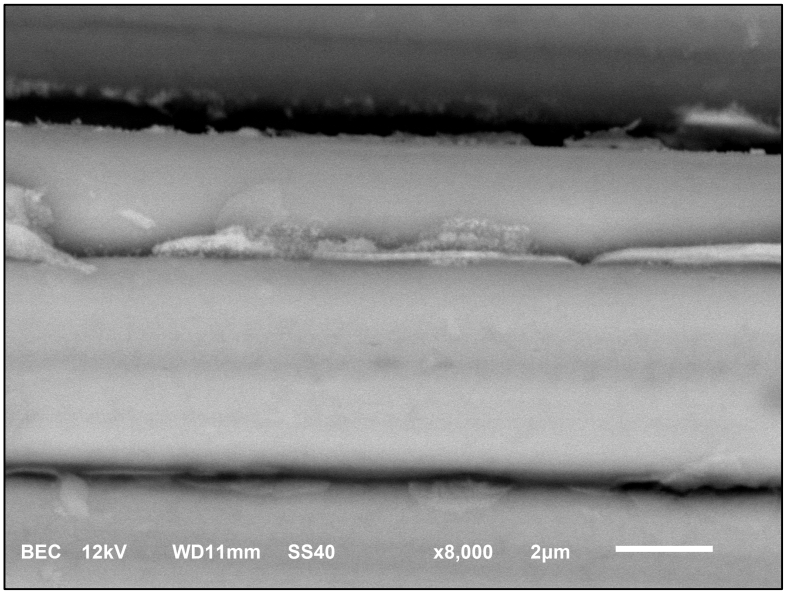

Figure 55. SEM: $[PdCl_4]^{2-}$/ACC (Unused)

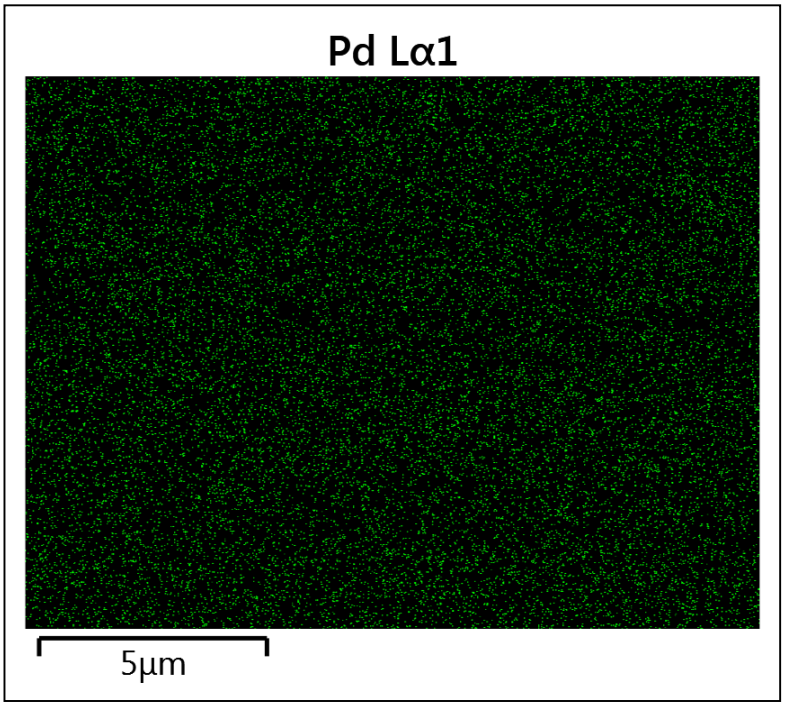

Figure 56. EDX Analysis: $[PdCl_4]^{2-}$/ACC (Unused)

Figure 57. SEM: $[PdCl_4]^{2-}$/ACC (Used)

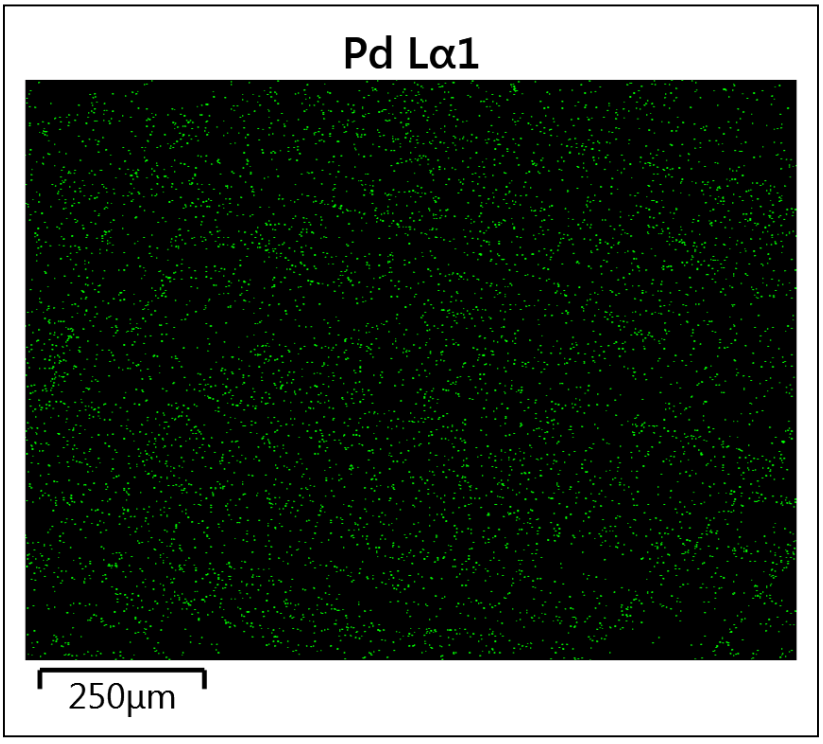

Figure 58. EDX: $[PdCl_4]^{2-}$/ACC (Used)

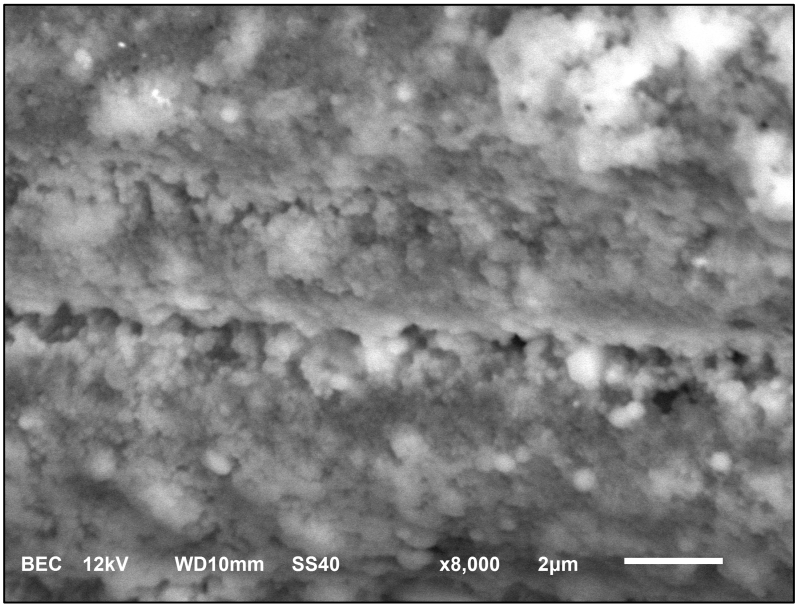

Figure 59. SEM: $[PdCl_4]^{2-}$/ACC (Used)

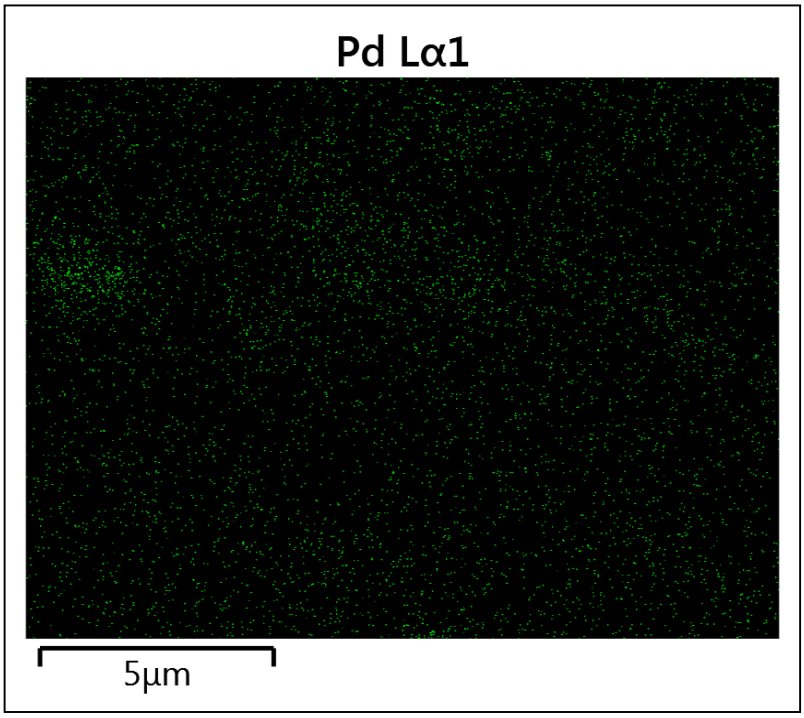

Figure 60. EDX: $[PdCl_4]^{2-}$/ACC (Used)

3.3.2 Preliminary Experiments & Optimization

We used 2-phenylethylamine (**59**) as a model compound to investigate and optimize the Pd/ACC-catalyzed reaction. We ran 2-phenylethylamine at 60 °C and 2.2 mA/cm^2 using $[PdCl_4]^{2-}$/ACC (200 μmol/g). After 21 h, 29.5% deuteration was observed demonstrating the ability of Pd/ACC catalyst to activate benzylic C-H bonds selectively. Increasing the concentration to 400 μmol/g of $[PdCl_4]^{2-}$/ACC at 2.2 mA/cm^2 produced deuterium incorporation of 33.5% in 21 h selectively at the benzylic site. The increase in deuterium incorporation in response to the increase in Pd concentration indicated that the increase in Pd loading could enhance the rate of H/D exchange. With an increase in Pd loading to 2000 μmol/g, we observed 88.5% deuteration in 21 h and a further increase to 4000 μmol/g yielded 91% deuterium incorporation selectively at the benzylic site in 8 h. Like Ru-catalyzed H/D exchange, the application of current is necessary for the Pd-catalyzed reactions as determined from our control reaction. The current is applied to reduce D^+ on the Pd surface and for the reduction of Pd^{2+} to Pd^0 to drive the reaction. We investigated the relationship between current density and the rate of H/D exchange using 2-phenylethylamine as a model compound. Using 4000 μmol/g $[PdCl_4]^{2-}$/ACC, we conducted reactions at current densities of 2.2 mA/cm^2, 11.1 mA/cm^2, 22.2 mA/cm^2, 33.3 mA/cm^2 and 44.4 mA/cm^2 and noticed a direct relationship between the reaction rate and current density.

With the increases in Pd loading on ACC and current density enhancing the rate of H/D exchange, we explored to find the optimum combination of both to drive the reaction to completion in a practically viable time (**Figure 61**). The results showed 2000 μmol/g at 33.3 mA/cm^2 and 4000 μmol/g at 44.4 mA/cm^2 to be the most optimal conditions and we decided to use the former for further investigation. We noticed that the relatively higher current

density of 33.3 mA/cm^2 is required to complete this reaction in a practical time, as compared to the Ru-catalyzed reaction that needed only 2.2 mA/cm^2 to activate the catalyst. Both these methodologies are electrocatalytic rather than electrochemical as there is no net transfer of electrons in the replacement of hydrogen with deuterium. We therefore attributed the need for higher current density to activate palladium from Pd^{2+} to Pd^0. In the case of Ru/ACC, we had reduced ruthenium in a high-pressure batch reactor under H_2 before the electroactivation phase so presumably, the high current density was not warranted. In the case of Ru/ACC that did not go through high pressure batch reactor conditions, we had to apply current density of 33.3 mA/cm^2 for 1 h to elecroactivate Ru/ACC prior to its use as an electrocatalyst.

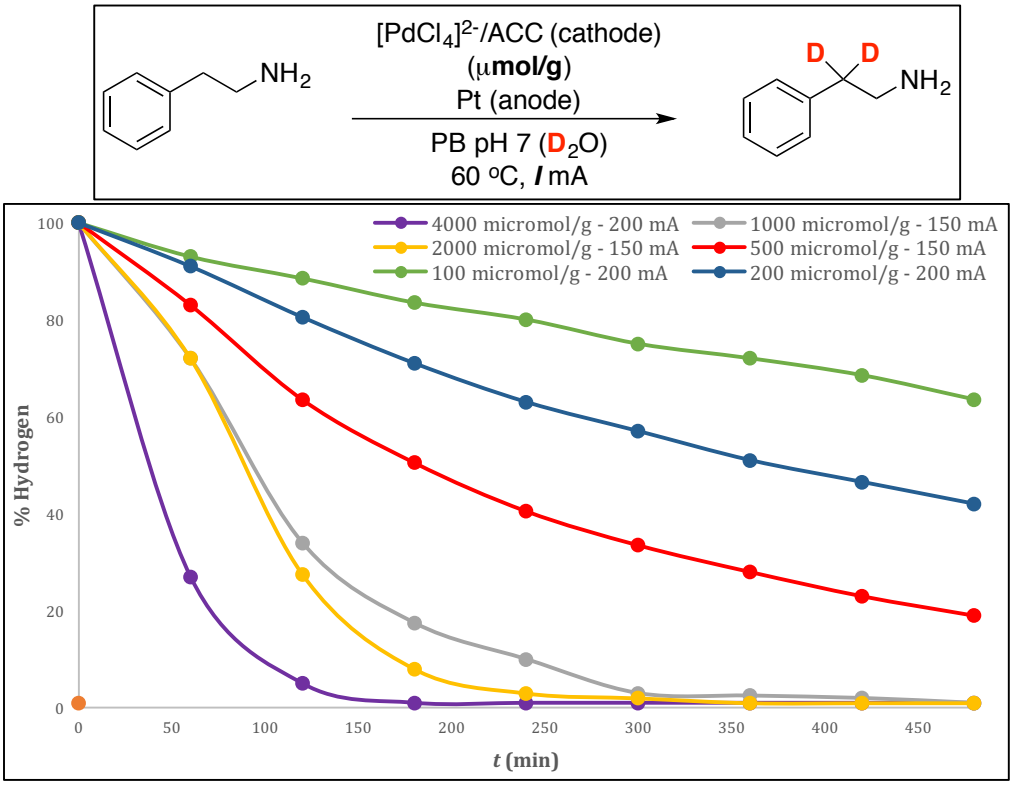

Figure 61. Optimization of Pd/ACC using 2-phenylethylamine as a Model Compound.

3.3.3 Substrate Scope

After establishing optimal conditions for Pd-catalyzed benzylic H/D exchange, we attempted to expand the scope and determine the functional group tolerance of this methodology. We investigated *p*-toluidine (**60**) at 33.3 mA/cm^2 and 60 °C using 2000 μmol/g Pd/ACC and observed 99% deuteration at the benzylic site in 210 min (3.5 h). Although we use 0.01 M phosphate buffer pH 7 in our reaction, the solution turns alkaline in the first 30 min due to the formation of deuteroxide anions in the reaction. In addition to the benzylic hydrogens in *p*-toluidine, we observed H/D exchange at the C-H ortho to sites to the amino group (72.5% in 11.5 h) (**Figure 62**). We proposed that this activation may be due to two reasons, (a) coordination of nitrogen to Pd and (b) reactivity of *ortho* C-H sites due to directing group effect of amino (electron donating).

To confirm if coordination of nitrogen is necessary for the activation at the *ortho* C-H sites, we ran a reaction at pH ~1, where amine is protonated to the quaternary level and cannot coordinate to the Pd. Under these conditions, we inhibited the exchange at the *ortho* position completely while selectively deuterating the benzylic sites (**Figure 62**)

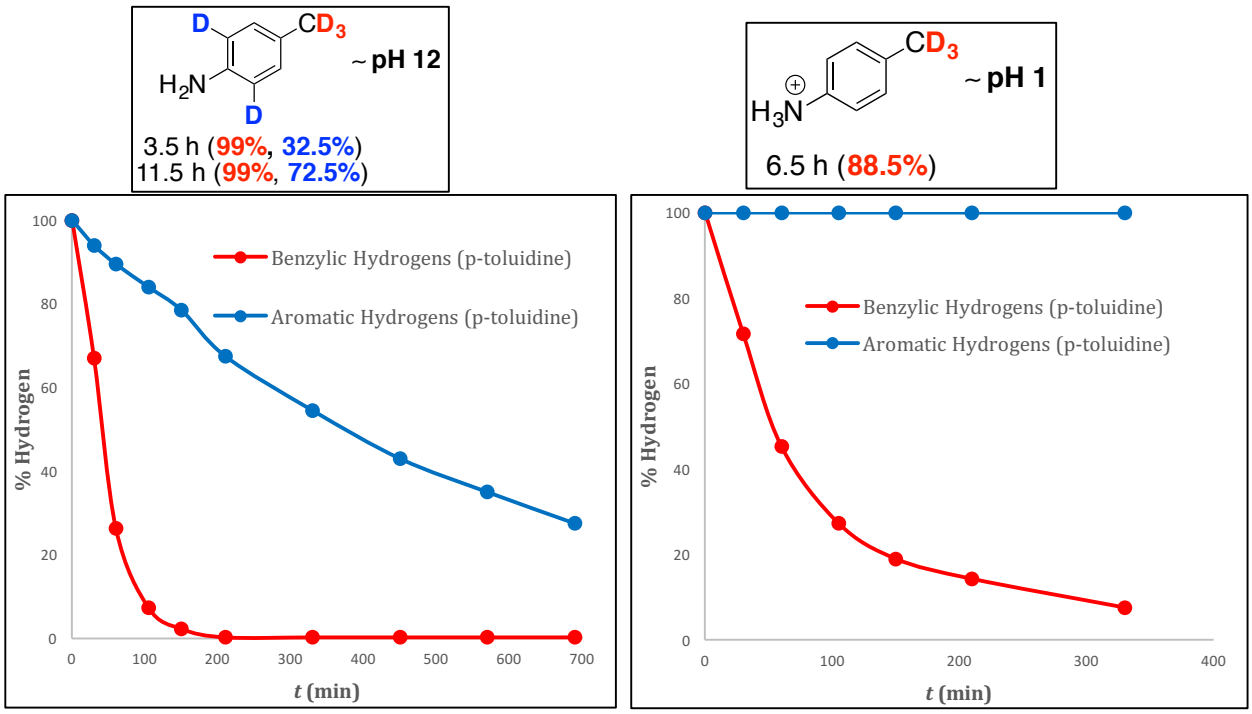

Figure 62. Pd-Catalyzed H/D Exchange of *p*-toluidine at pH 12 and 1

To determine if coordination to heteroatom is only required for H/D exchange or electronics play a role in the *ortho*-H/D exchange, we studied 4-(2-aminoethyl) aniline (**61**) in the presence of electroactivated Pd/ACC. The aliphatic C-H sites α to the amino did not get exchanged whereas we observed 22% deuterium incorporation at the *ortho*-C-H sites in addition to 93.5% deuteration at the benzylic site in 9 h.

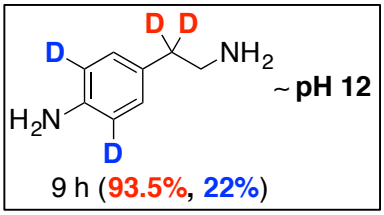

Figure 63. Pd/ACC-Catalyzed H/D Exchange: 4-(2-aminoethyl) aniline (61)

We presumed that benzylic H/D exchange is effected by electroactivated Pd but we also considered acid/base mediated *ortho*-H/D exchange as a possible mechanism in D_2O. To investigate if this in fact is happening in our system, we ran a control reaction in the absence

of Pd at 33.3 mA/cm^2 at pH 12 and observed no H/D exchange. The absence of *ortho*-H/D exchange confirmed that Pd is necessary to introduce deuterium and that electronics play a role in the activation of those sites.

We also studied *p*-cresol (**62**) to test for benzylic H/D exchange and directing group ability of the hydroxyl group to perform *ortho*-H/D exchange. In addition to 98.6% deuteration at the benzylic position in 3.5 h, we observed 22% *ortho*-H/D exchange. Under acidic pH, Pd/ACC showed selective H/D exchange at the benzylic position like *p*-toluidine. We believe that this behavior is due to the inability of oxygen to coordinate to Pd in the neutral state whereas at pH 12, substituted phenol (i.e. phenoxide anion) can coordinate to Pd due to increased electron density.

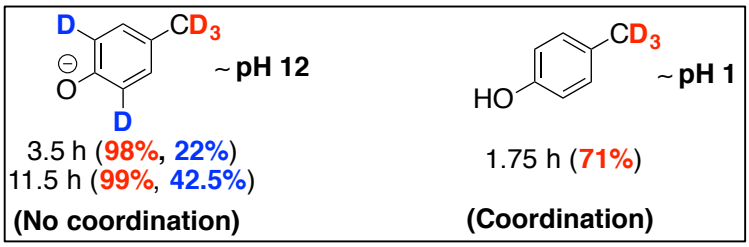

Figure 64. Pd/ACC-Catalyzed H/D Exchange: *p*-Cresol (62)

We investigated *p*-toluic acid (**63**) to understand the tolerability of the carboxylate moiety. We observed 93.5% deuterium incorporation in 8 h at the benzylic site selectively without any *ortho*-H/D exchange. One interpretation is that the carboxylate (electron withdrawing) group does not activate the aromatic sites in the same manner as –NH_2 and –OH, explaining the absence of aromatic H/D in *p*-toluic acid. Another explanation could be the way the carboxylate anion coordinates to Pd, preventing its access to aromatic sites. We have also studied benzylic H/D exchange in benzyl alcohol (**64**) and observed 99% deuterium incorporation in 3 h.

Catalyst deactivation studies were done to evaluate the ability of Pd/ACC to withstand reaction conditions and reusability. We did three consecutive with *p*-toluic acid with previously used Pd/ACC catalyst and observed a decrease in the rate of reaction between runs I and II, while run III was consistent with the second. This behavior could be due to leaching of the Pd into the solution in the first run. Then, once it's reduced, it doesn't leave the surface. However, no visual evidence for leaching was observed; ICP-OES analysis remains to be performed to confirm or refute the presence of Pd in the solution.

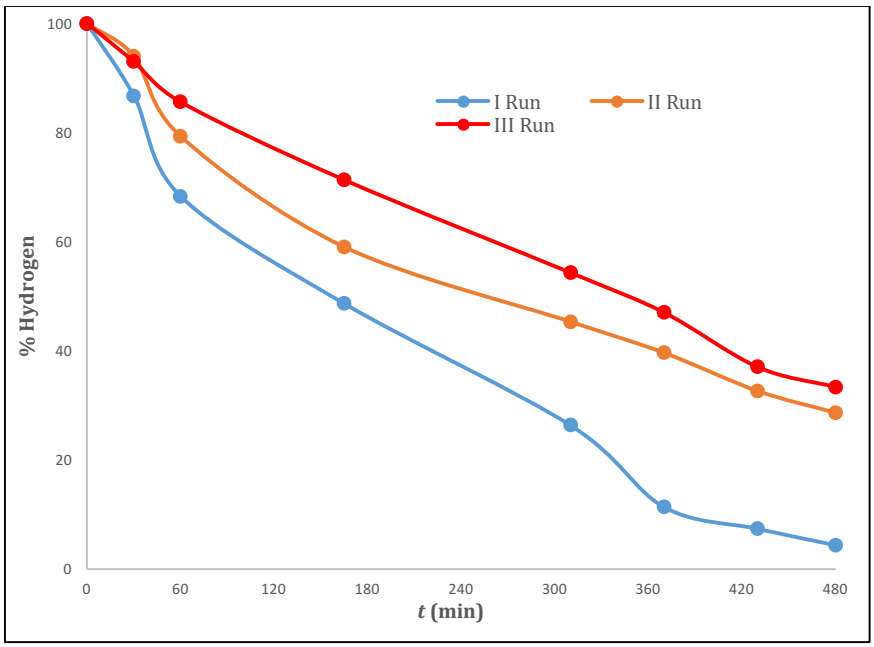

Figure 65. Pd-Catalyzed H/D Exchange: Catalyst Deactivation Studies. Conditions: *p*-toluic acid (20 mM in 20 mL), 33.3 mA/cm^2 & 60 °C.

3.4 Summary

We have complemented our original discovery of electroactivated Ru-catalyzed H/D exchange in amines, alcohols and amino acids with Pd-catalyzed H/D exchange in aromatic substrates. In addition to the benzylic C-H activation, this system showed the ability to effect aromatic H/D exchange in the presence of electron donating directing group on the benzene

ring. This effect could also be inhibited by means of acidic conditions as shown with the substrates *p*-toluidine and *p*-cresol. A broader substrate scope and mechanistic understanding is warranted in this methodology and combining the features of Ru and Pd by developing an alloy could be used to deuterate benzylic and α sites C-H sites concurrent.

3.5 Characterization

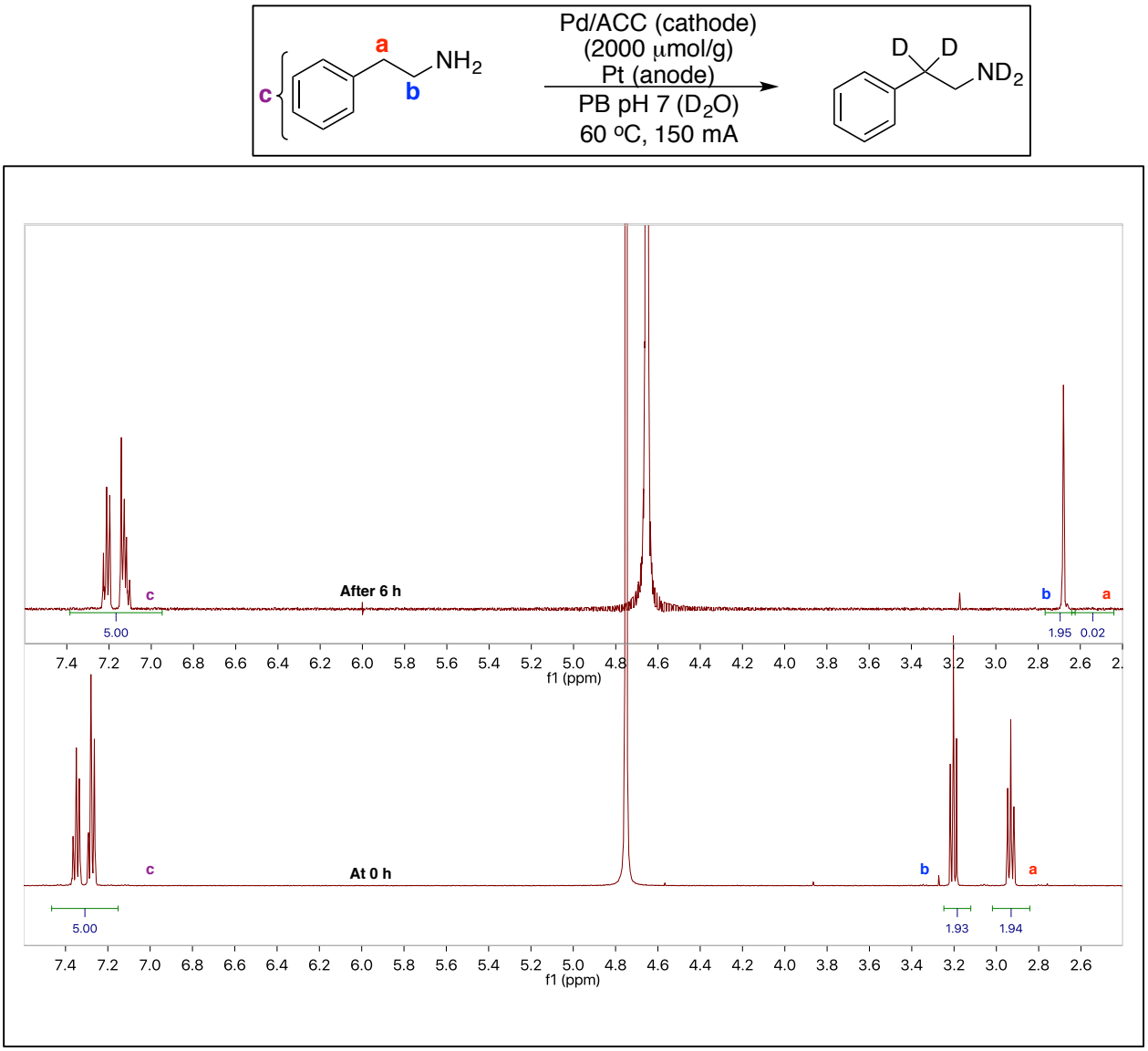

Figure 66. ^{1}H NMR spectrum of 2-phenylethylamine, 59 (pH 12, Yield (24%)). Changes in chemical shifts are due to the change in pH resulting from electrochemical consumption of D^{+} ions. The aromatic protons are the non-labile hydrogens and % hydrogen at the α C-H site is calculated relative to them.

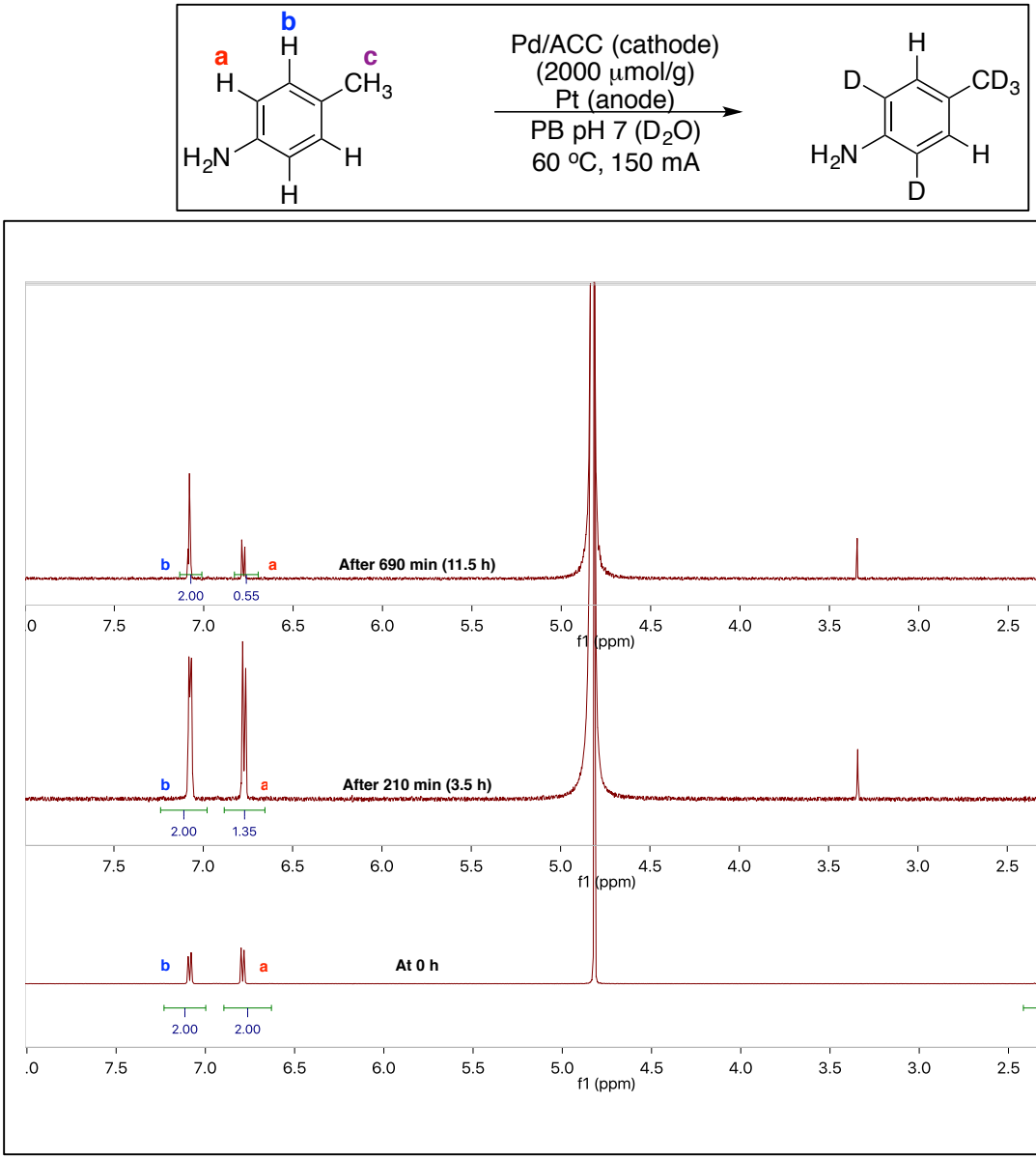

Figure 67. ^{1}H NMR spectrum of *p*-toluidine, 60 (pH 12, Yield (27%)). Changes in chemical shifts are due to the change in pH resulting from electrochemical consumption of D^{+} ions. The aromatic protons (meta to $-NH_2$) are the non-labile hydrogens and % hydrogen at the α C-H site is calculated relative to them.

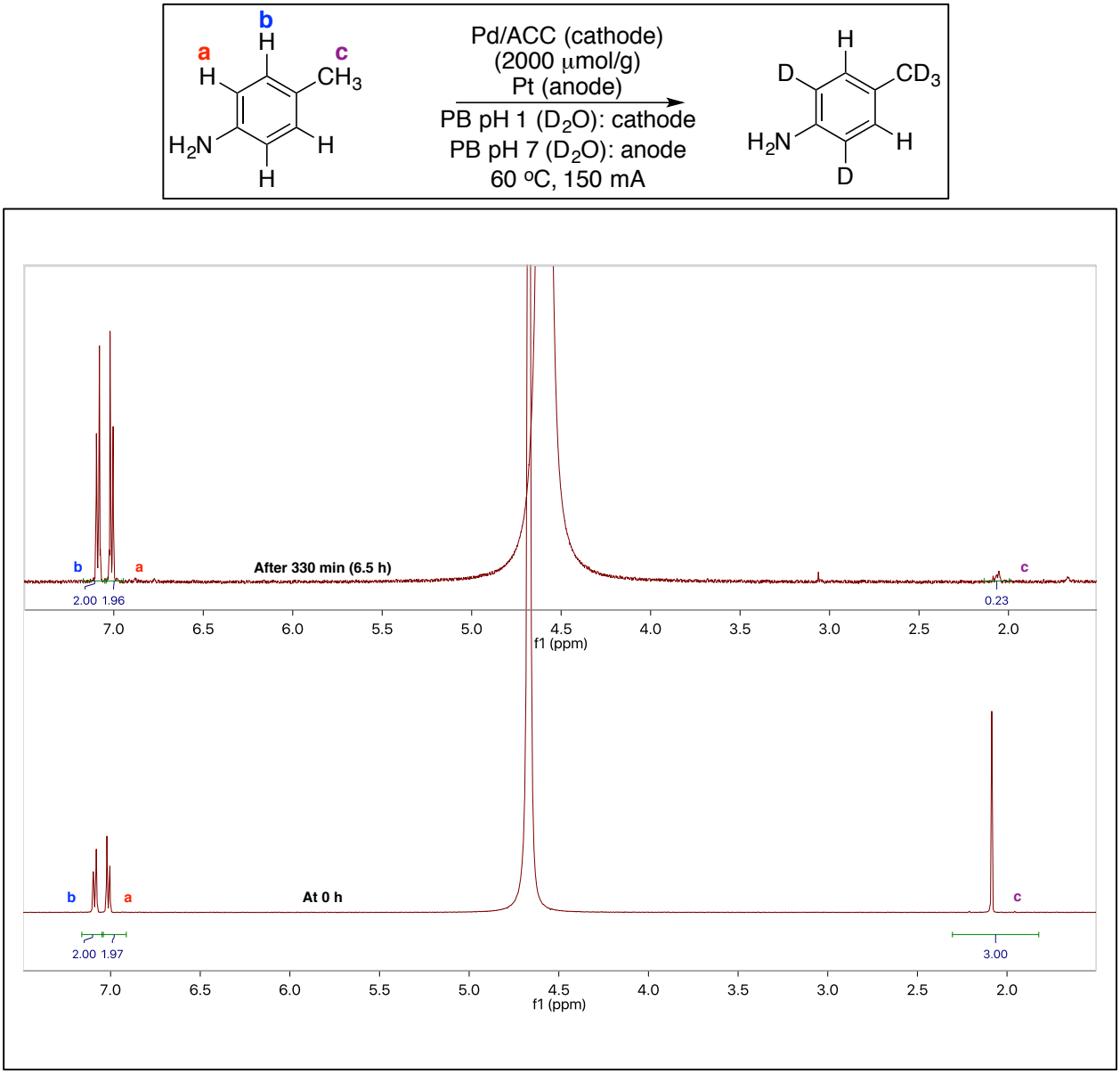

Figure 68. ^{1}H NMR spectrum of *p*-toluidine, 60 (pH 1, Yield (50%)). Changes in chemical shifts are due to the change in pH resulting from electrochemical consumption of D^{+} ions. The aromatic protons (meta to $-NH_2$) are the non-labile hydrogens and % hydrogen at the α C-H site is calculated relative to them.

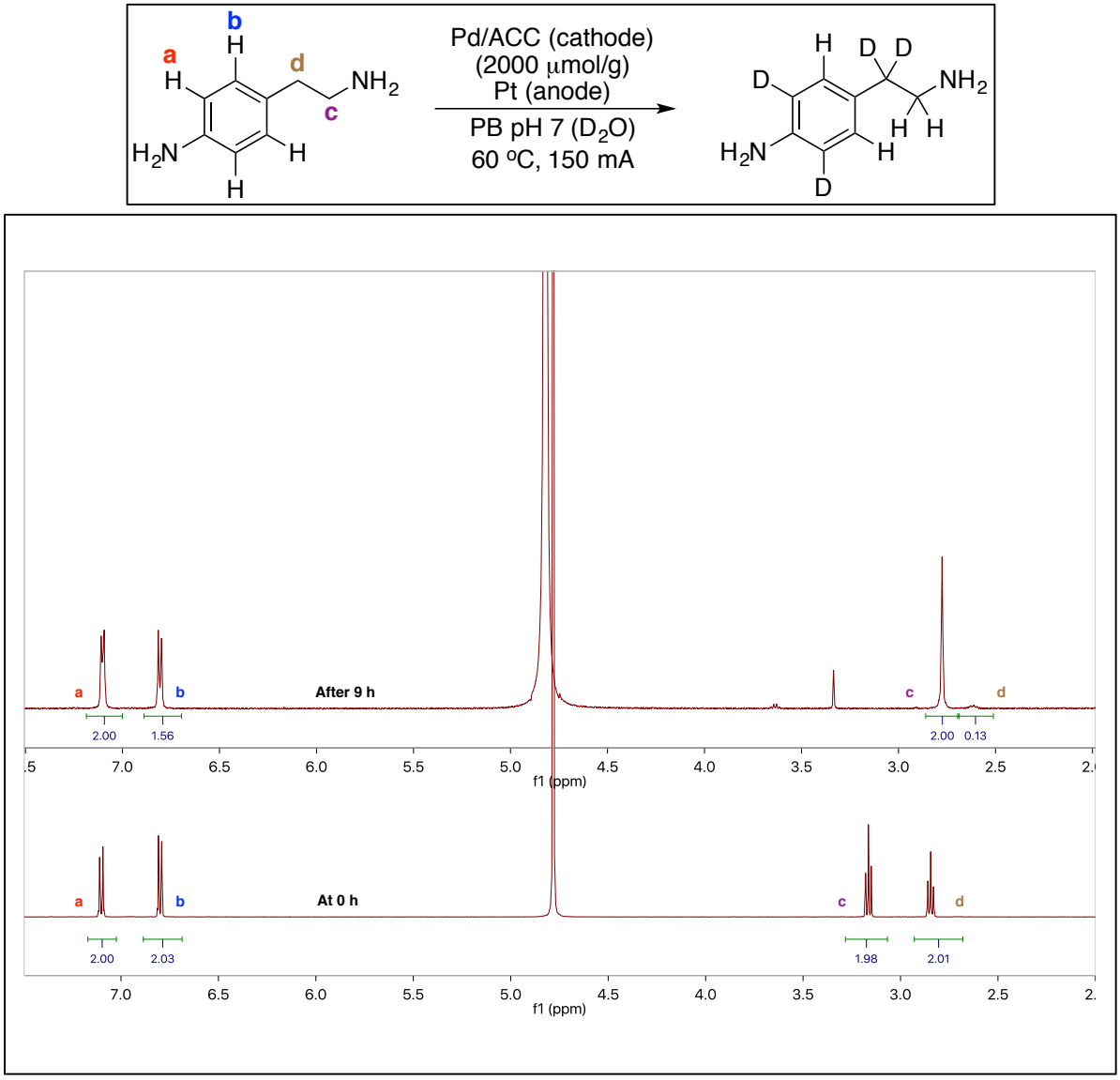

Figure 69. ^1H NMR spectrum of 4-(2-aminoethyl) aniline, 61 (pH 12, Yield (69.5%)). Changes in chemical shifts are due to the change in pH resulting from electrochemical consumption of D^+ ions. The aromatic protons (meta to $-NH_2$) are the non-labile hydrogens and % hydrogen at the α C-H site is calculated relative to them.

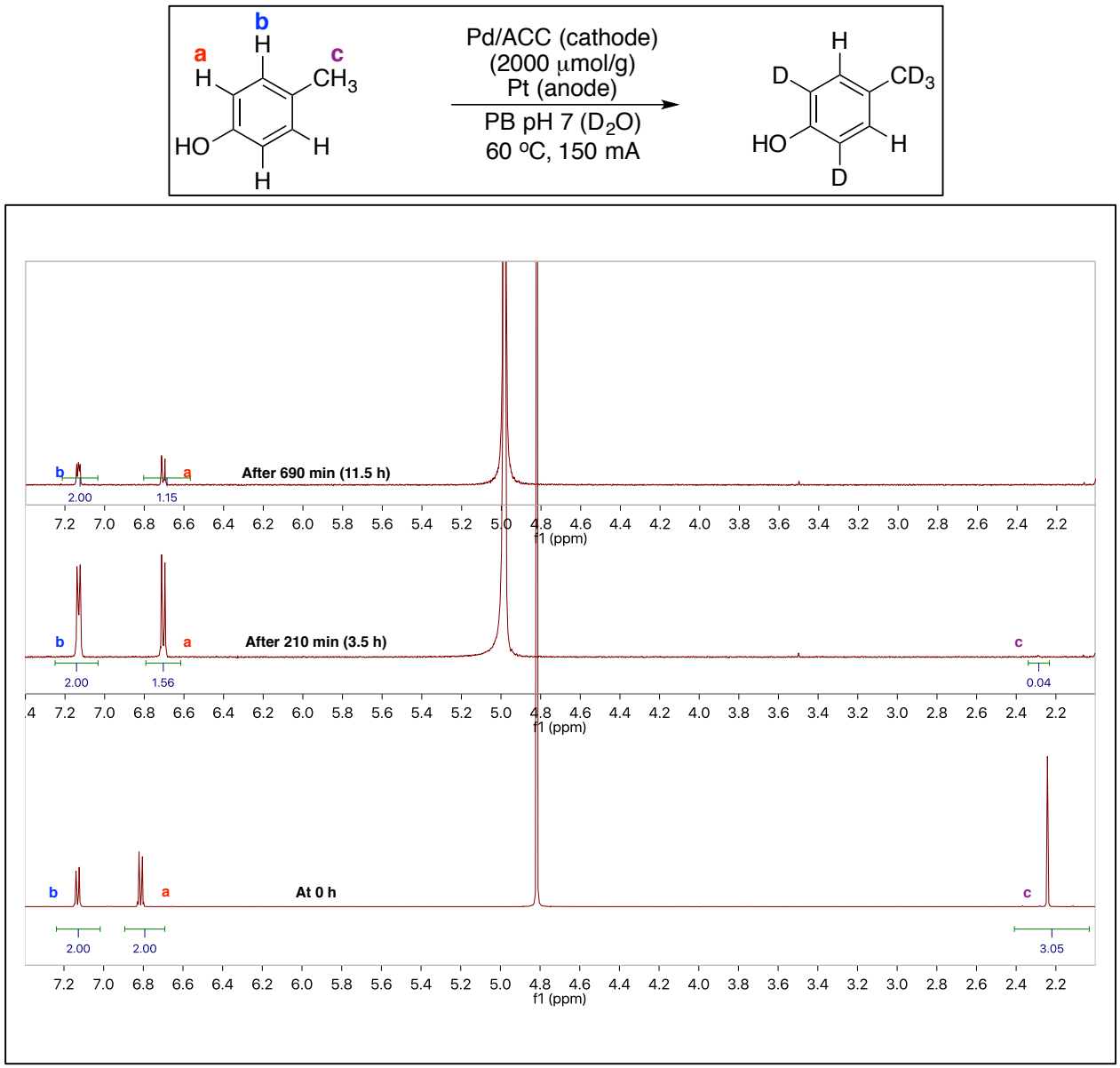

Figure 70. ^{1}H NMR spectrum of *p*-cresol, 62 (pH 12, Yield (37.4%)). Changes in chemical shifts are due to the change in pH resulting from electrochemical consumption of D^{+} ions. The aromatic protons (meta to –OH) are the non-labile hydrogens and % hydrogen at the α C-H site is calculated relative to them.

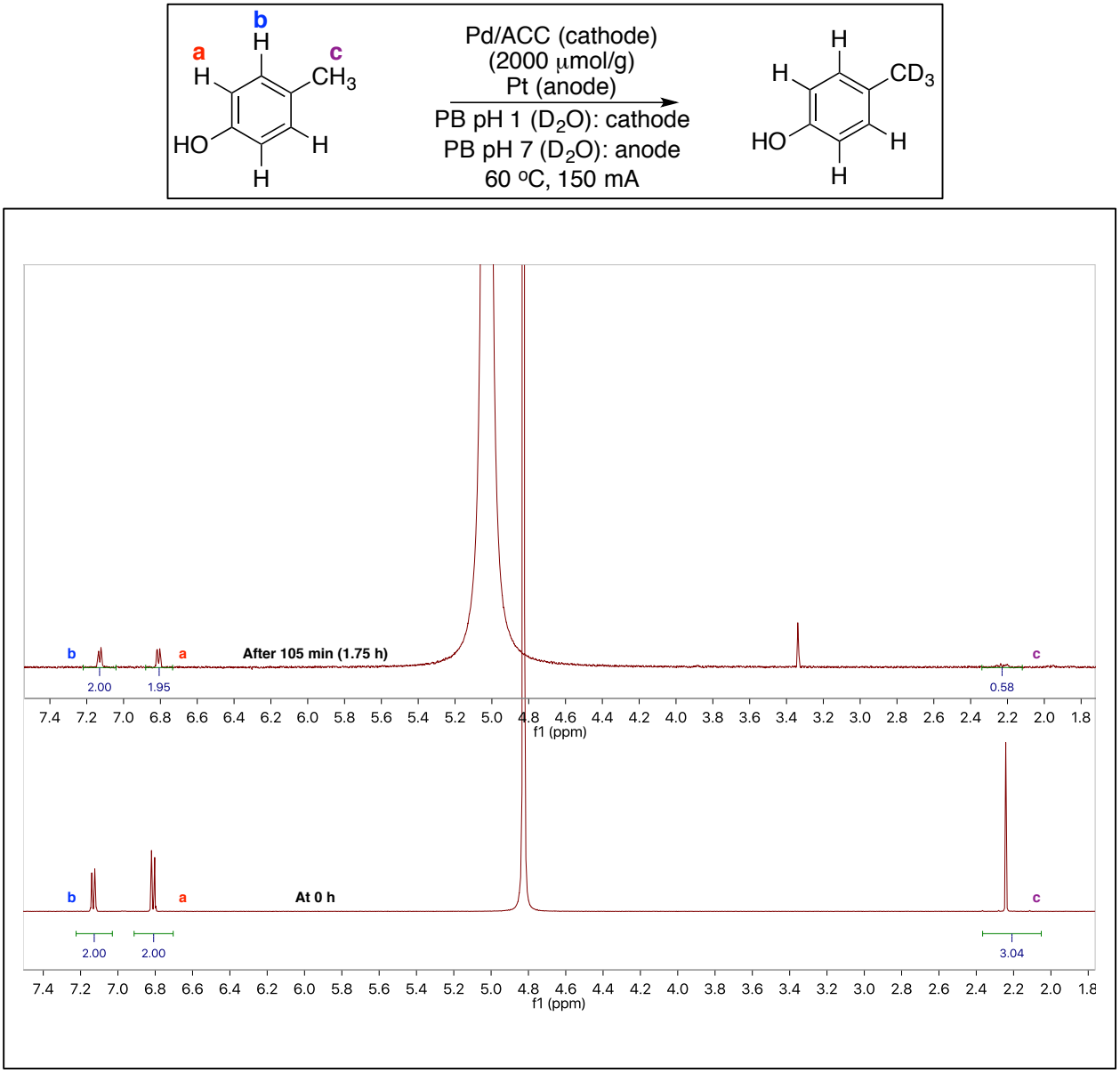

Figure 71. ^{1}H NMR spectrum of *p*-cresol, 62 (pH 1, Yield (7.1%)). Changes in chemical shifts are due to the change in pH resulting from electrochemical consumption of D^{+} ions. The aromatic protons (meta to –OH) are the non-labile hydrogens and % hydrogen at the α C-H site is calculated relative to them.

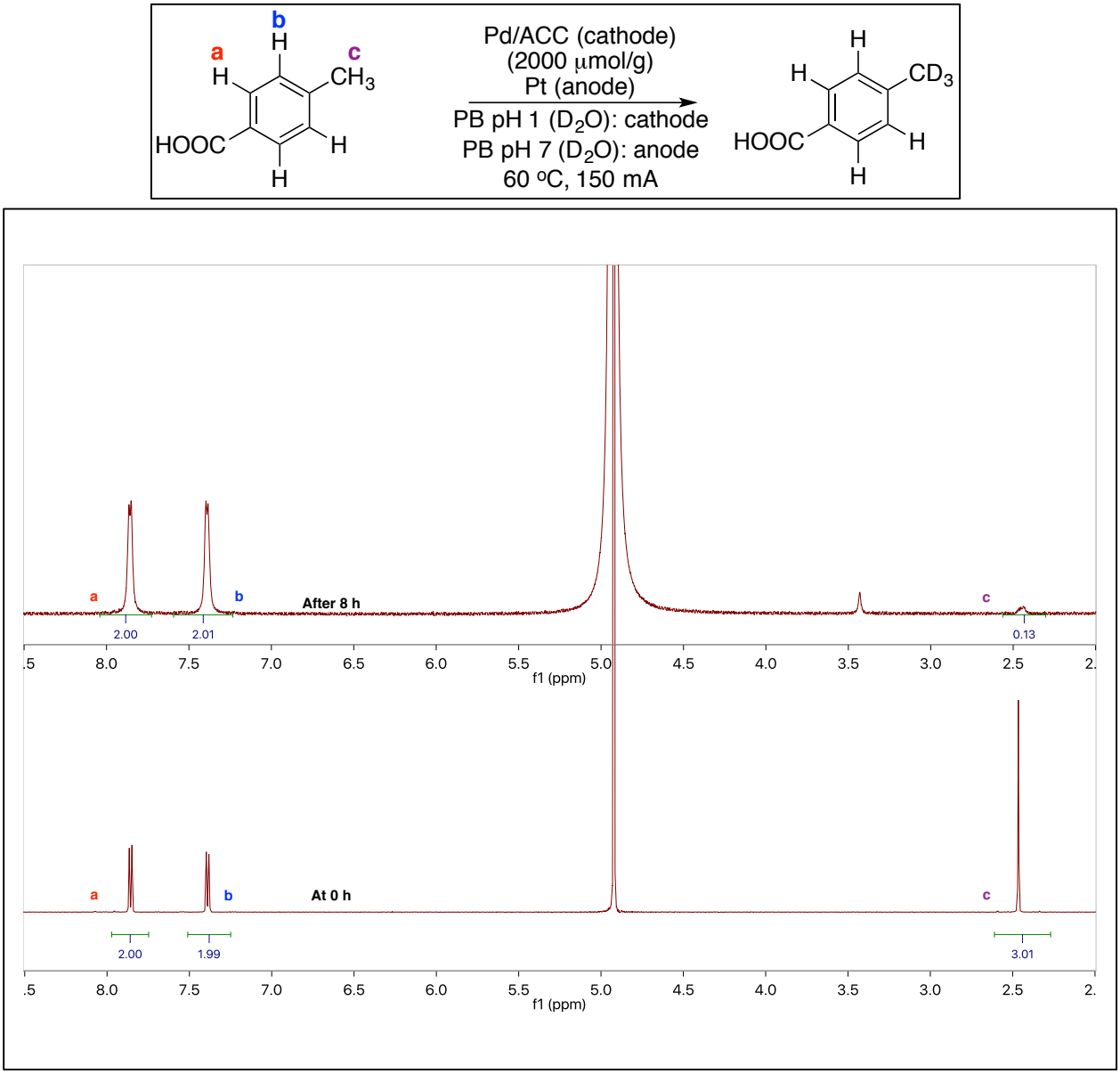

Figure 72. ^{1}H NMR spectrum of *p*-toluic acid, 63 (pH 12, Yield (48.7%)). Changes in chemical shifts are due to the change in pH resulting from electrochemical consumption of D^{+} ions. The aromatic protons (meta to –COOH) are the non-labile hydrogens and % hydrogen at the α C-H site is calculated relative to them.

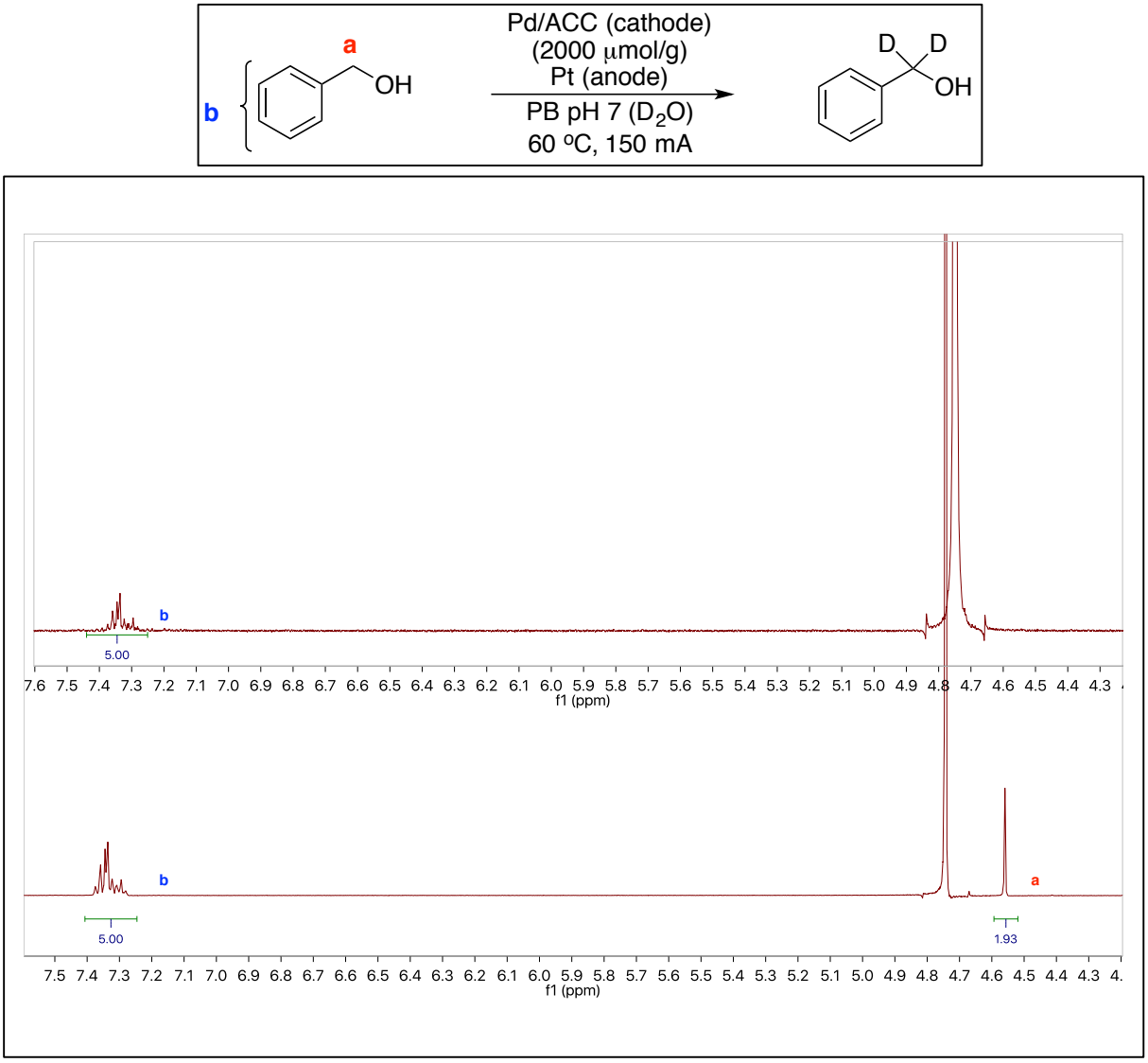

Figure 73. ^{1}H NMR spectrum of benzyl alcohol, 64 (pH 12, Yield (7.5%)). Changes in chemical shifts are due to the change in pH resulting from electrochemical consumption of D^{+} ions. The aromatic protons are the non-labile hydrogens and % hydrogen at the α C-H site is calculated relative to them.

Chapter 4. Electroactivated Reductive Alkylation of Amines using Alcohols

4.1 Introduction

Nitrogen containing compounds have a great significance in the chemical, pharmaceutical, agrochemical and petroleum industries. Amongst the functional groups derived from nitrogen, amines are the most studied. Synthesis of amines is commonly achieved using reductive alkylation and electrophilic alkylation.[11,231–235] These methods and their variants have been studied and perfected over the years. However, the conventional reactions suffer from several disadvantages: (a) the use of alkyl halides or strong reducing reagents that are undesirable from an environmental point of view; (b) the fact that these reactions generate equimolar amounts of wasteful salts as byproducts; and (c) undesired overalkylation to form quaternized ammonium ions.

To understand the environmental issues, a key issue is the atom efficiency of the amine synthesis techniques. Atom efficiency describes the percentage of the starting material that is incorporated into the product *vs*. that discarded as waste. Due to low incorporation of stoichiometric amounts of reagents used and the presence of high molecular weight leaving groups, conventional methods like reductive alkylation and electrophilic alkylation have very low atom efficiency.

4.2 Atom Efficient Alkylation of Amines

Considering atom efficiency as an important factor, two distinct methodologies have been developed for the synthesis of alkylated amines: (a) hydroamination of olefins and

alkynes[236–240] and (b) hydrogen autotransfer processes.[241,242] Though hydroamination has shown promising results, as it is utilized by P&G Chemicals, Albermarle and Huntsman in their industrial preparation, this process is limited due to the electrophilic character of the nitrogen species, the need for the corresponding unsaturated reagents (alkene or alkynes), and the inability to perform methylation or benzylation using this method.

4.2.1 Hydrogen Autotransfer Process

Hydrogen autotransfer or hydrogen borrowing is an atom efficient process that is widely used in industries for synthesizing amines. It is exemplified by its incorporation by Lonza (U.S.), Clariant (Germany), Kao (Japan) and Feixiang Chem. (China). The general pathway of this reaction involves abstraction of the hydrogen atom by the catalyst to give the oxidized species (I) followed by the nucleophilic attack of amine to generate the imine species (II). This imine species is then reduced using the abstracted hydrogen to give the alkylated amine product (**Scheme 48**).

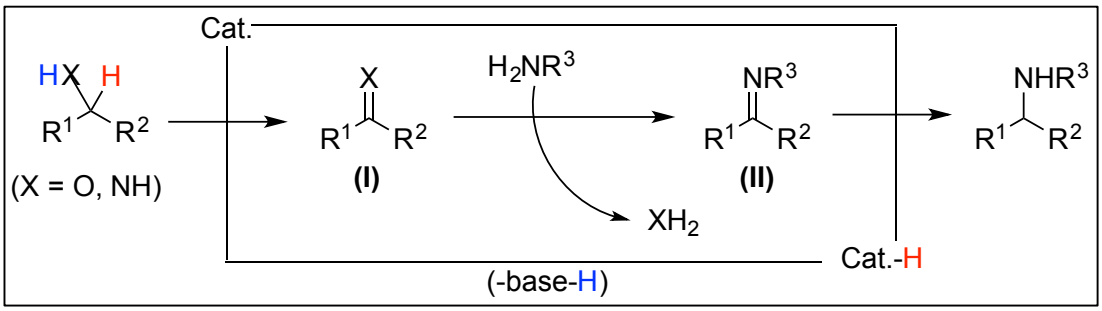

Scheme 48. Mechanistic Pathway of Hydrogen-Autotransfer Process

The use of alcohols or amines as alkylating agents is ideal in this process as they are transformed into species that are at carbon after oxidation. When alcohols are used, alkylation via this process is a thermodynamically driven process with generation of water

as a byproduct. It involves cleavage of C-O and N-H bonds, which is compensated by the generation of C-N and O-H bonds. In the case of using amines serving as the electrophiles, generation of ammonia (often liberated as a gas) is the driving force.

As far as homogenous-based transition metal catalysis goes, this process has been investigated in detail but there are only a few examples where this reaction has been performed in a heterogeneous fashion. Though great selectivity and efficacy can be achieved in homogenous environments, industries generally prefer heterogeneous catalysis due to the ease of separation of the product as well as recycling of the catalyst. Keeping this in mind, we will restrict our discussion to research in the field of heterogeneous alkylation with alcohols and its application in constructing C-N bonds.

4.2.1.1 Nickel Based *N*-Alkylation

Nickel has been extensively used as a catalyst in the *N*-alkylation of amines using alcohols as electrophilic reagents. Nickel particles, obtained via reduction of NiO at 300 °C has shown to alkylate aniline or *p*-toluidine with aliphatic alcohols. Ethylation of aniline has been performed using 2 to 1 ratio of ethanol and aniline at 180 °C with 10% weight of these Ni particles in an autoclave. The ethylaniline was obtained in 30% yield in 12 h.[243]

RANEY®-Nickel, developed by treating nickel-aluminum alloy with concentrated sodium hydroxide to dissolve aluminium out of the alloy, is one of the most frequently used nickel-based catalysts. *N*-alkyl substituted anilines have been afforded using RANEY®-Nickel with 500 mol% of alcohols under reflux conditions. The yields with straight chain primary alcohols ranged around 78-83% and branched alcohols gave 41-49%. On using 1 equivalent of aluminum *tert*-butoxide, the RANEY®-Nickel required in this reaction decreased to 30% and amount of alcohol decreased to 3 to 1 with respect to aniline and 96-98% yields were

afforded. Aniline substituted with electron donating as well as electron withdrawing groups was studied with this set-up with rates favoring the former.

RANEY®-Nickel has also been used in the alkylation of diamines with diols as in the case of 1,6-hexanediamine and 1,4-butanediol (1:1) under reflux conditions using toluene as a solvent. The reaction using toluene as solvent at ambient pressure produced azepane derivative with 15% yield as shown in **Scheme 49**. Intermolecular double hydrogen-autotransfer has been observed with RANEY®-Nickel (Ra-Ni) as in the case of 1-aminopropan-2-ol to generate piperazine along with some aromatized product pyrazine.[244] Different 4-aminobutan-1-ol derivatives under H_2 (80-90 atm) at 195 °C and RANEY®-Nickel (Ra-Ni) (ca. 40 mol%) have been used to synthesize pyrrolidines in moderate yields (50-92%). In situ alkylation of amines has been reported using thioamides that undergoes desulfinylation in the presence of Raney-nickel, H_2 and alcohols under reflux conditions.[245] Hydrazobenzene and azoxybenzene have been synthesized in similar fashion using 500 mol% of RANEY®-Nickel (Ra-Ni) giving 43% and 36% in yield.[246] Though this catalyst has shown great efficacy, most reaction conditions still involve high temperatures and large amounts of nickel; the presence of H_2 in certain cases is also required (**Scheme 49**).

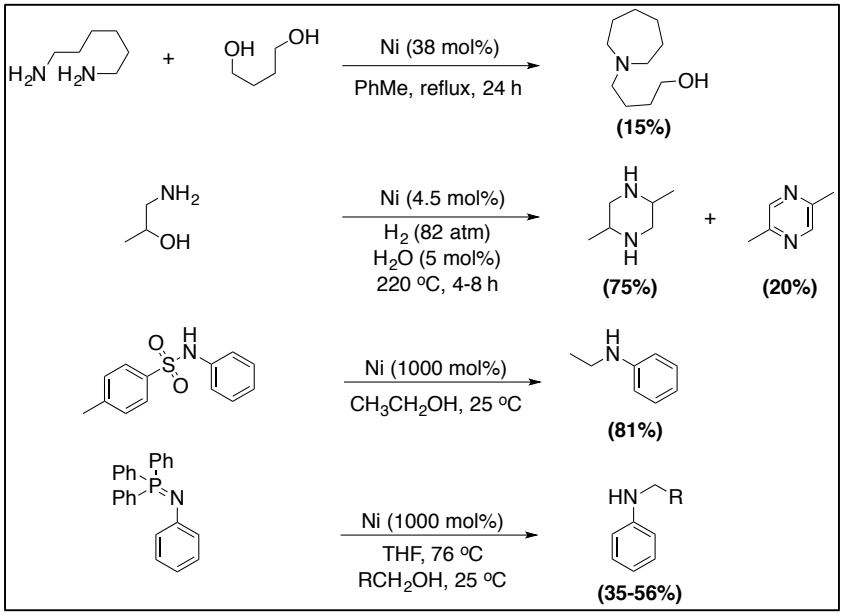

Scheme 49. Ni-Catalyzed *N*-Alkylation

4.2.1.2 Silicon Based *N*-Alkylation

Alkylation of aniline using an excess of aliphatic primary alcohols (100-200 mol%) at high temperature (362-400 °C) has been demonstrated with silica gel via a hydrogen autotransfer process.[247] Moderate conversion of 35% was observed when aniline was reacted with ethanol under these reaction conditions, generating 81% of monoalkylated and 14% of dialkylated. The conversion was further enhanced by wet impregnation of silica with NH_4VO_3 and oxalic acid giving 93% conversion with 20% V_2O_5:SiO_2.[248] The selectivity towards monoalkylated (70%) product was not altered. Though these transformations were run at high temperatures, they were still suggestive of the ability of silicon to exercise hydrogen autotransfer (**Scheme 50**).

4.2.1.3 Aluminum Based *N*-Alkylation

Alumina (Al_2O_3) formed either from aluminum isopropoxide or bought commercially as γ-Al_2O_3 has been shown to alkylate amines via hydrogen-autotransfer. The vaporized mixture of aniline and methanol (15,000 mol%) in a conventional flow reactor at 400 °C showed 32% of monoalkylated and 50% of dialkylated product with Al_2O_3 prepared from aluminum isopropoxide while the commercially available γ-Al_2O_3 under similar reaction conditions produced monoalkylated aniline as the major product, signifying the importance of method of preparation of the catalyst. Other aliphatic and aromatic alcohols such as methanol, 1-pentanol and benzyl alcohol have also been used as alkylating agents.[244,249] This system affords moderate yields but generally requires severe temperatures like 300-400 °C, thus limiting its use (**Scheme 50**).

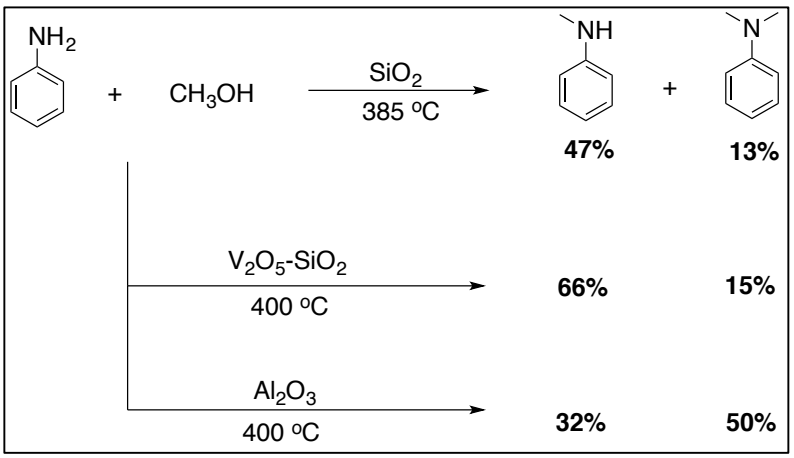

Scheme 50. Examples of Silica and Alumina-Based Alkylations

4.2.1.4 Copper Based *N*-Alkylation

Copper-Chromite catalyst ($CuCr_2O_4$-$BaCr_2O_4$) prepared via ignition of mixture of barium nitrate, copper nitrate, and ammonium chromate at 350-400 °C has been used to catalyze alkylation of amines with alcohols. This reaction, operated in the presence of H_2 at 125 atm

and 180-250 °C uses equimolar amounts of amine and alcohol and produce alkylated amines in moderate yields of 15-67% (**Scheme 51**).[250] Several other complexes of copper such as CuO-γ-Al_2O_3,[251,252] CuO-MgO,[251,252] and CuO-ZrO-γ-Al_2O_3[253] have also been investigated, revealing that copper is distinctly responsible for the dehydrogenation of alcohol as well as the imine reduction while the presence of other elements enhances the metal surface area, hydrogen adsorption and storage, and the acid sites. Another complex of copper, a colloidal system of Cu/Ni/Ba (5:1:1) has been expanded to a commercial setting where it was demonstrated with 5,763 kg of dodecyl alcohol, 1.36 eq. of isopropylamine, 0.29 eq. of H_2 at 210 °C in 4 h to generate tertiary amine (*N*-dodecyl-*N*-isopropyldodecan-1-amine) in 90% yield.[254,255]

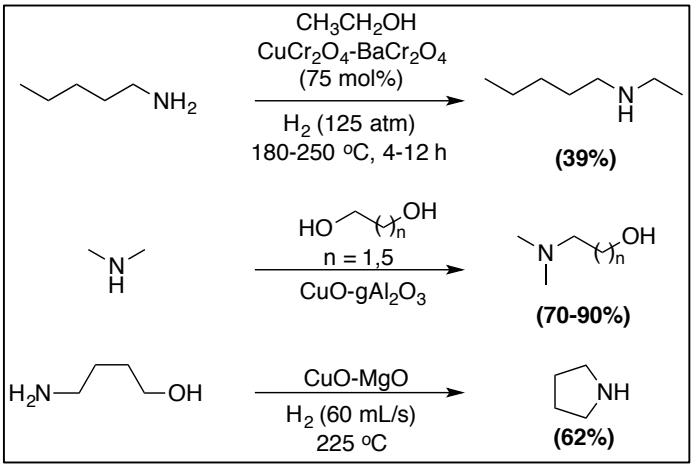

Scheme 51. Examples of Copper-Based Alkylations

4.2.1.5 Pt Group Based *N*-Alkylation

Pt-derived catalysts have been effective in promoting *N*-alkylation in the past. Pt supported on silica (ca. 5 wt%) transformed cyclohexanol and ammonia to cyclohexylamine in a continuous-flow reactor at 267 °C with a moderate yield of 30%.[30] Benzylic amine has been alkylated by electrolysis in alcoholic solutions like methanol and ethanol using a Pt

black-coated anode and coiled Pt cathode. Yields ranging from 27% to 91% have been reported in this work.[241,256]

Pt-TiO_2 (1.4 mol%) has been used to alkylate ammonia via photoirradiation with a 400 W high-pressure mercury lamp at room temperature and yields ranging from 9-60% were observed with alcohols like methanol, ethanol and 1-butanol.[257]

Ruthenium impregnated on magnetite ($Ru(OH)_3$-Fe_3O_4) has been used to perform *N*-monoalkylation of aromatic and heteroaromatic amines, sulfonamides, sulfonamides, and nitroarenes with benzyl alcohol under basic condition. The reactions were conducted in toluene using 1.3 mol% of the catalyst, 130 mol% of potassium hydroxide (KOH) at 130 °C and yields as high as 99% were observed in certain cases.[258]

Synthesis of 2° or 3° amines using allyl alcohol with palladium black (0.2 g) at 110 °C has been reported by Murahashi et al. The reaction between *n*-hexylamine and allyl alcohol gave *N*-propylidenehexylamine in 87% yield in 12 h.[259]

4.3 Experimental

4.3.1 Reaction Procedure

The experiments were carried out in 1-C or 2-C glass cell. The 2-C glass cell was separated with a Dupont® Nafion-117 membrane (**Figure 6**) and 20 mL of 0.01 M phosphate buffer (pH 7 or pH 8.5) were placed in each compartment to serve as the electrolyte for the experiment operated t 60°C and ambient pressure. The cells were placed in an oil bath to operate at the desired temperature. The reactions were carried out under galvanostatic control.

4.3.2 Analysis

An aliquot of 1 ml was taken every 2 h and acidified with concentrated HCl to prepare the quaternary salt solution. The salt solution was then dried under a stream of N_2 to remove H_2O from the samples. D_2O (0.6 ml) was added to the salt and the liquid sample (quaternary salt) was analyzed using an Agilent 500 MHz superconducting NMR spectrometer at 298 K. NMR tubes with an external diameter of 5 mm were used (Wilmad-LabGlass, Buena, NJ). The β-methylene protons in pyrrolidine were used as an internal standard to determine the relative content of the product and %conversions were determined. Spectra were referenced using dimethyl sulfoxide (DMSO) and the yield of the substrates was determined using the qEstimate tool of Agilent VnmrJ 4 employing 0.0485 M solution of triphenyl phosphate in $CDCl_3$.

4.4 Results and Discussion

Pyrrolidine was used as a model compound with methanol serving as the alkylating agent for our preliminary investigation. The conversion of 20 mM of 2˚ amine (pyrrolidine) to 3˚ amine (1-methylpyrrolidine, **64**) would theoretically require only 20 mM of methanol but we observed almost negligible conversion in that case. We investigated the optimum concentration of alcohol required to complete the reaction in a practically viable time. We studied several concentrations: 1% v/v (250 mM), 2% v/v (500 mM), 5% v/v (1,250 mM), 10% v/v (2,500 mM), 20% v/v (5,000 mM), and 30% v/v (7,250 MM) in 0.01 M phosphate buffer pH 7. As the results indicate the rate of reaction increased with the concentration of methanol added till it reached a saturation point at 20% v/v (**Figure 70 (A)**). The relatively high concentration of alcohol needed for the reaction can be attributed to the evaporation of

methanol and its diffusion across the Nafion® membrane, which will be discussed below. We decided to continue with 20% v/v alcohol for further optimization of this reaction.

We then studied the effect of the current density on the rate of the reaction, exploring values ranging from 0.4 mA/cm^2 to 44.4 mA/cm^2. Initially, we hypothesized that the reaction followed the hydrogen-autotransfer process where Ru/ACC would catalyze oxidation of alcohol, followed by the nucleophilic attack of amine to generate imine or iminium species. The iminium species would undergo reduction on the surface of the catalyst making it an electrocatalytic reaction. The required current should only be for the electroactivation of Ru, a level determined earlier to be 2.2 mA/cm^2 in the case of Ru-catalyzed H/D reaction. Here, the reaction rate showed a direct relationship to the current density, reaching a maximum rate at 44.4 mA/cm^2 indicative of a true electrochemical process. As far as the optimization is concerned, we decided to carry forward with 33.3 mA/cm^2 (**Figure 70 (B)**).

The next parameter we studied was temperature. As expected, increasing temperature increased the rate of the reaction. However, even at a temperature as low as 36 ^{o}C, alkylation proceeded at useful rates, demonstrating the reaction's mildness (**Figure 70 (C)**).

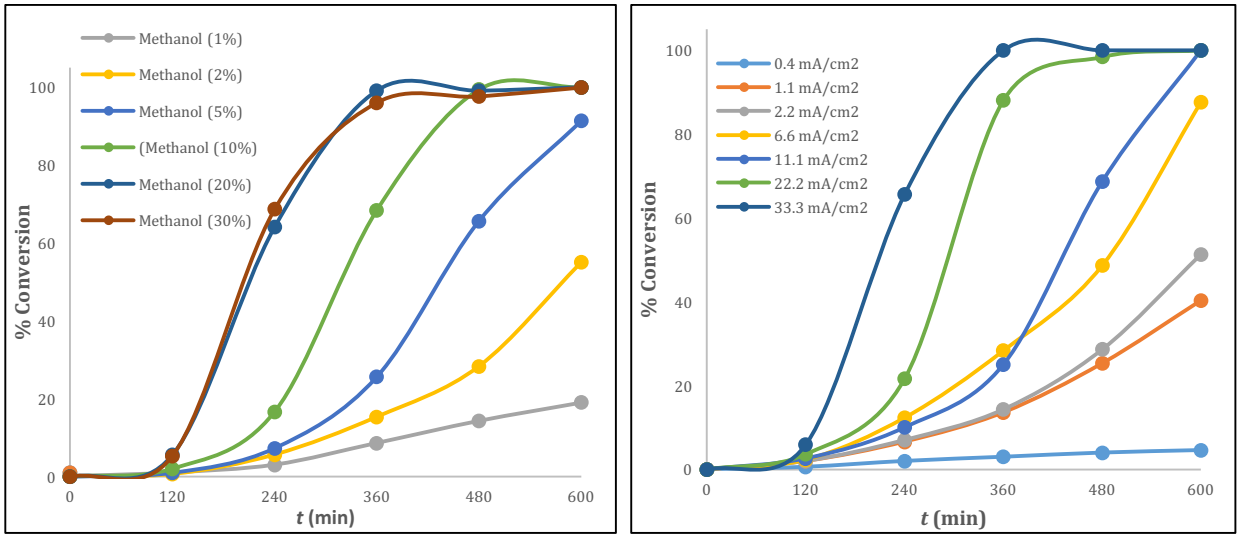

(A) **(B)**

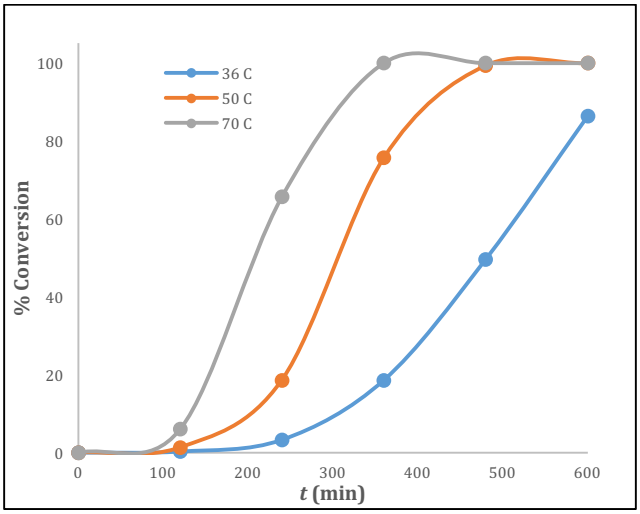

(C)

Figure 74. (A) Effect of Alcohol Concentration; (B) Effect of Current Density and (C) Effect of Temperature. Conditions: Pyrrolidine (20 mM in 20 mL) & alcohol is added to the cathodic chamber.

To better understand the role of the catalyst and the mechanism of the reaction, we conducted a series of control experiments. To verify the importance of current density, an experiment using Ru/ACC (cathode) and Pt (anode) with pyrrolidine and methanol added to

the cathodic chamber was run with no current passed. This yielded no alkylated product, confirming the need for current to enable the reaction. We followed that study with reaction operated where current was passed under similar conditions, but in the absence of methanol, and as expected, no alkylation was observed. We then investigated the role of Ru; and instead of Ru/ACC, we used plain ACC (cathode) and Pt (anode). To our surprise, we observed progress like the results with Ru/ACC indicating that Ru is not an essential component in the reaction. To confirm this observation, we conducted a series of experiments, one involving rinsing the H-cell with aqua regia for 96 h, and one using a completely brand new cell to eliminate the possibility of the presence of even minute amounts of remaining Ru that could catalyze the reaction. Both scenarios yielded the alkylated product.

Our initial hypothesis had envisioned a hydrogen-autotransfer process on the surface of ruthenium. Another contradictory experiment that pointed to an electrochemical reaction over hydrogen auto-transfer was increase in the rate of alkylation if the carbonyl species is added directly to the reaction (isopropyl alcohol *vs*. acetone). Using Ru/ACC as cathode and Pt as an anode at 33.3 mA/cm^2, we observed 92% conversion of pyrrolidine to 1-isopropylpyrrolidine in the presence of 20% v/v acetone in 4 h as compared 62% in the same duration in the case of isopropyl alcohol (**Scheme 52**).

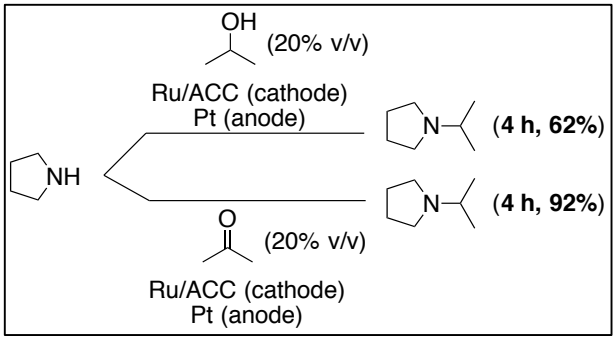

Scheme 52. Control Reactions

We hypothesized that methanol might be permeating through the Nafion®-117 membrane into the anodic chamber where it was being oxidizing to formaldehyde by platinum. Formaldehyde (hydrated) then presumably permeated back to the cathodic chamber where pyrrolidine attacked the sp^2 carbon, yielding iminium followed by its reduction on the ACC. To test this hypothesis, we created a set up with ACC (cathode) and Pt (anode). The amine (pyrrolidine) was added to the cathodic chamber whereas methanol was added to the anodic chamber. If methanol is indeed oxidized by Pt, this transformation should happen either at a faster or comparable rate to the one that involved addition of methanol to the cathodic chamber. Our results showed a faster rate of methylation, supporting this hypothesis (**Figure 75**). During optimization studies of 2-C cell with Ru/ACC (cathode) and Pt (anode), we consistently observed negligible conversion in the first 2 h. We considered two possibilities for this induction period: (a) electroactivation of ruthenium and (b) diffusion of methanol from the cathodic chamber to the anodic chamber and return of formaldehyde after oxidation. Based on these results, we presume it to be the second case as that induction phase is shortened on addition of methanol directly to the anodic chamber (**Figure 75**).

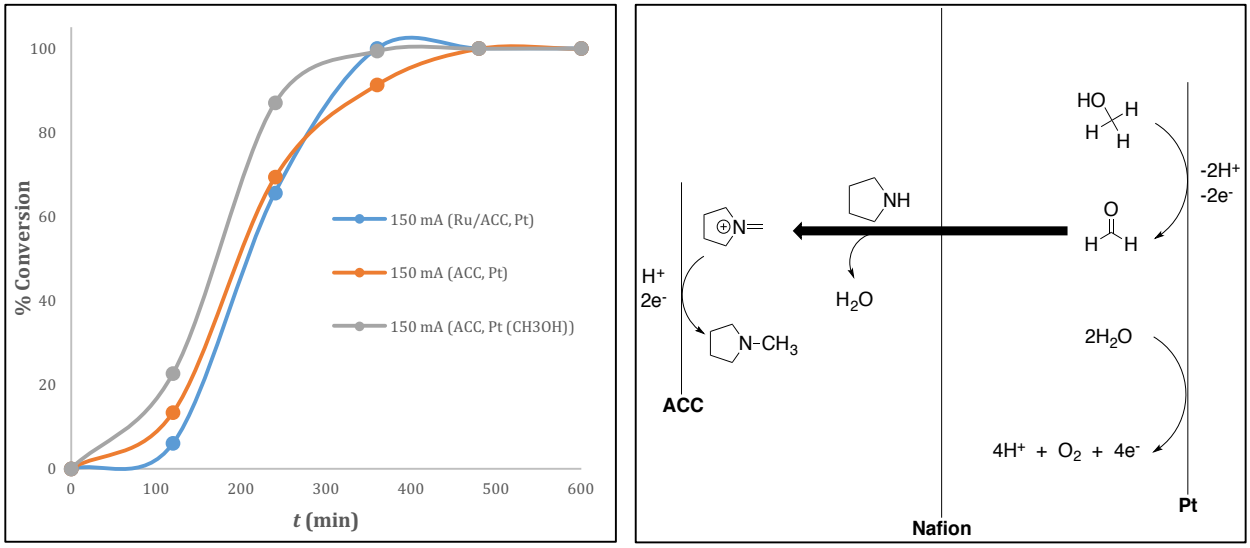

Figure 75. Mechanistic Analysis of Alkylation. Conditions: Pyrrolidine (20 mM in 20 mL) & 70 °C.

These above observations prompted us to look at our H/D exchange process again. Though several control reactions for that methodology had been previously performed. we decided to re-run multiple experiments in the same 2-C cell. We investigated L-alanine and noticed no H/D exchange using ACC as cathode and Pt as an anode. We considered that the presence of $-CO_2H$ group might have interfered with the permeation of L-alanine across the membrane so we next examined 3-pentanol for the control reaction. Again, no H/D exchange was observed indicating that Ru is needed in the H/D exchange reaction. L-alanine and 3-pentanol were studied at 2.2 mA/cm^2 to replicate the exact deuteration conditions previously optimized; we investigated pyrrolidine in the presence of methanol at 2.2 mA/cm^2 using ACC (cathode) and Pt (anode) at 70 ^{o}C. The rates of reaction with ACC or Ru/ACC were relatively similar. Although, the conditions involved in using ACC as cathode and Pt as an anode are relatively harsher with 33.3 mA/cm^2 and 70 °C, we sought to expand our substrate scope by attempting methylation to give 1,4-dimethylpiperazine (**65**), 1-methylmorpholine (**66**), 1-methyldicyclohexylamine (**67**), and 1-methylpiperidine-4-

carboxylic acid (**68**) using methanol. Except for morpholine, we observed relatively low conversion rates in our system, but the results did demonstrate the ability of the 2-C cell to effect alkylation with more diverse substrates (**Figure 76**).

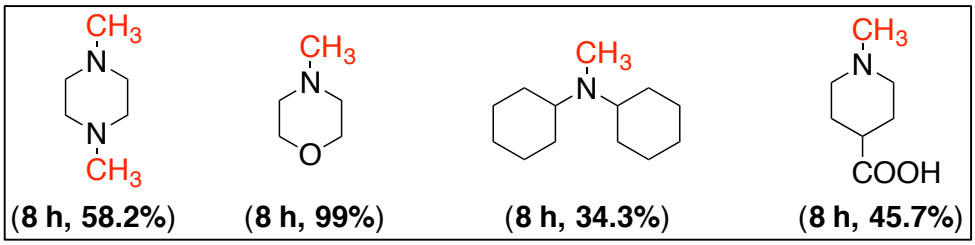

Figure 76. Substrate Scope: ACC/Pt in 2-C Cell. Conditions: Substrate (20 mM in 20 mL), 33.3 mA/cm^2, 70 °C & CH_3OH (20% v/v added to anodic chamber).

Since the above findings indicated that alkylation of pyrrolidine is driven by the oxidation of alcohol at Pt rather than the Ru/ACC, we decided to set up the reaction in a 1-C cell. We investigated different current densities and concentrations of alcohol to optimize conditions for 1-C cell. We used ACC as a cathode and Pt as an anode to run the reaction. The optimum current density (2.2 mA/cm^2), alcohol (5% v/v) and temperature (60 °C) required for the reaction to proceed decreased, when we transitioned to a 1-C cell (**Figure 77**). As compared to H/D exchange reactions where current is only needed to activate the catalyst, alkylation of pyrrolidine with methanol is a stoichiometric process requiring 2e$^-$ per molecule to reduce its iminium species. Using **eqn. 10**, we computed the current efficiency (CE%) for the alkylation reaction in the 1-C cell to be 22%. This value does not consider losses due to adsorption of the organic substrates into the ACC cloth.

$$CE\% = \frac{Conc_{Prod}\,(M) \times F\,(C/mol) \times n_{e^-}}{I\,(A) \times t\,(sec)} \qquad \textbf{Eqn. 10}$$

where $Conc_{Prod}$ = concentration of alkylated product (molarity), F = Faraday's constant, 96,485 C/mol, n_{e^-} = number of electrons per reaction, I = current in amperes and, t *(sec)* = time in seconds.

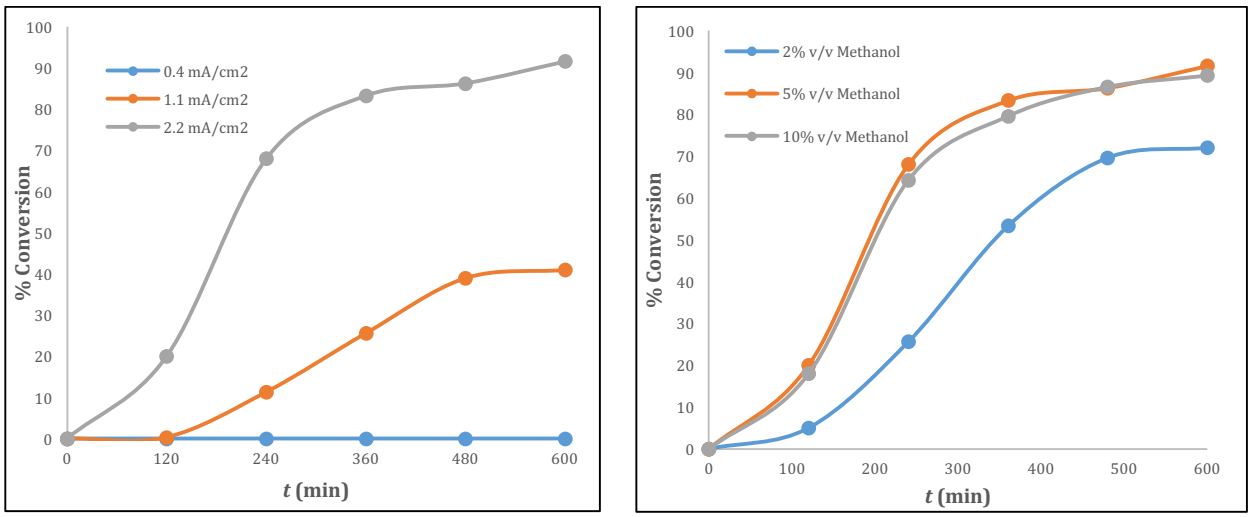

Figure 77. Effect of Current Density and Alcohol Concentration on Alkylation (1-C Cell). Conditions: Pyrrolidine (20 mM in 20 mL), ACC (cathode) & Pt (anode)/1-C Cell & 60 °C.

Using the 1-C cell with ACC (cathode) and Pt (anode), we explored alkylation of pyrrolidine with ethanol and isopropanol and our preliminary data indicated <30% conversion in both the cases. Troy Dolmetch, an undergraduate student funded by MSU's Chemistry REU program over the summer of 2016, explored the possibility of using alternative combinations of catalysts as cathode and anode to drive the reaction to completion. With Pt serving as an effective catalyst for oxidation of alcohol, he investigated the ability of ACC to oxidize alcohols, a study inspired by our finding of its ability to oxidize water in the Ru/ACC-catalyzed H/D exchange reactions. Using pyrrolidine and methanol as our model reactants, he observed no alkylation when he used ACC as both cathode and anode. He explored the use of Ru as an oxidizing agent by using Ru/ACC as the anode with ACC as cathode and observed a relatively better conversion (98.3% *vs*. 83.3% in 6 h) and CE% (30% *vs*. 22%) than in the case of ACC cathode and Pt anode. (*Note: The CE% here doesn't reflect the true comparison between using Pt as an anode vs. Ru/ACC as an anode*

because the amounts of organics adsorbed will be higher in the case of ACC (cathode)/Ru/ACC (anode) vs. ACC(cathode)/Pt(anode) as we are using two cloths in the system and we are not correcting the CE% for adsorption). We hypothesized that using Ru/ACC as a cathode in addition to Ru/ACC as an anode would accelerate the reaction as Ru/ACC can reduce the iminium species better than ACC. He then explored the possibility of using Ru/ACC as a cathode and ACC as anode to investigate the ability of Ru to perform alkylation. As ACC is incapable of performing oxidation, we proposed that the presence of alkylated product in this case would demonstrate the ability of electroactivated Ru to distinctly perform alkylation (**Figure 74**). He observed alkylation in this case, though not at rates comparable to the ACC (cathode)/Ru (anode) combination. Nonetheless the presence of alkylated product did indicate the ability of Ru/ACC to effect hydrogen transfer reaction.

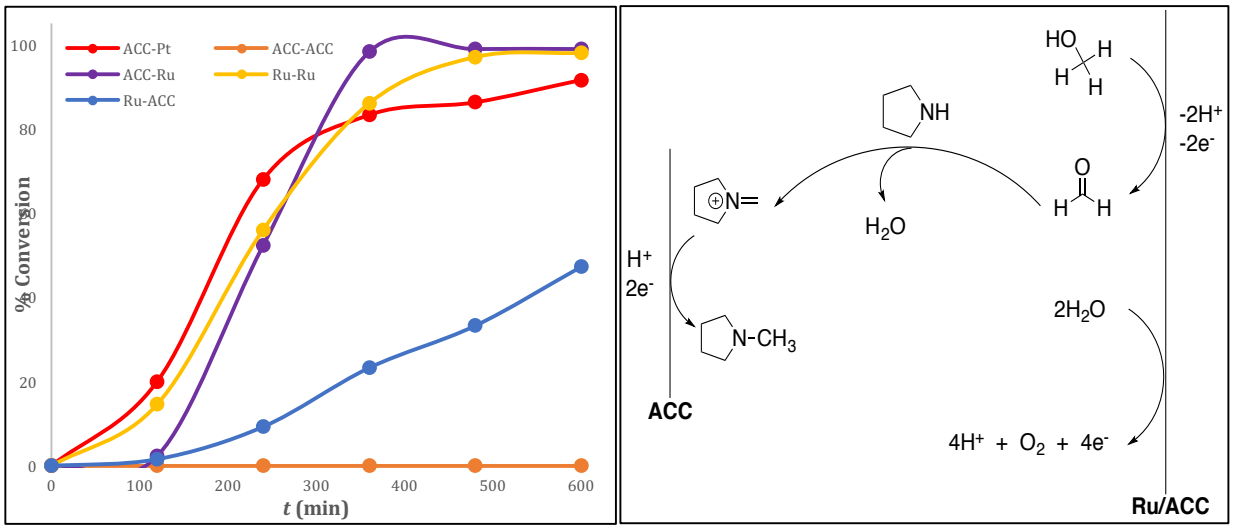

Figure 78. Mechanistic Analysis of Alkylation (1-C). Conditions: Pyrrolidine: (20 mM in 20 mL), 2.2 mA/cm^2, 60 °C and CH_3OH (5% v/v)/1-C Cell.

We confirmed that ACC (cathode) and Ru/ACC (anode) is the most optimized combination for our alkylation reaction and we expanded our substrate scope using this optimized set-up. In addition to methanol, as of now we have explored ethanol, isopropanol and benzyl

alcohol (**Figure 79**) as candidate alkylating alcohols. A more detailed substrate library should be explored using Ru/ACC as cathode and Pt as anode. In the case of amines that are sensitive to anodic oxidation, a 2-C cell with the similar combination of cathode and anode should be explored. The use of Ru/ACC as cathode should also be explored further to understand and confirm the hydrogen-autotransfer process.

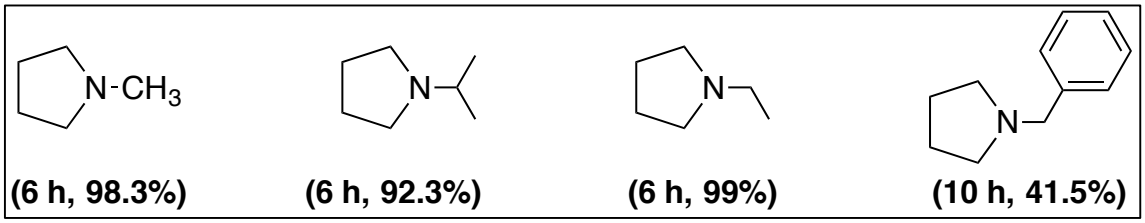

Figure 79. Substrate Scope. Conditions: Substrate (20 mM in 20 mL), 2.2 mA/cm^2, 60 °C & CH_3OH (5% v/v), ACC (cathode) & Ru/ACC (anode)/1-C Cell.

4.5 Summary

In conclusion, we have developed an electrochemical system to drive alkylation of amines using alcohols as alkylating agents. We started our work with the initial hypothesis of Ru-catalyzed hydrogen-autotransfer process and eventually determined that electrochemical process is underway when ACC is used as a cathode and Pt as the anode. We optimized our 2-C and 1-C set-ups and deduced initially that ACC (cathode) and Pt (anode) at 2.2 mA/cm^2, 60 °C and at ambient pressure to be the most optimum conditions. We explored **64** to **68** using these conditions and then explored the possibility of using alternative combination of cathode and anode. Under similar reaction environment but using ACC as cathode and Ru/ACC as the anode demonstrated the fastest reaction rate. Using these condition, a more detailed substrate scope in terms of alcohol, amines is warranted and heterocyclization can also be explored in this set-up.

4.6 Characterization

Optimization of 2-C and 1-C Systems

Reaction #	Cathode	Anode	Cell Type	Amine (Concentration)	Alcohol (Concentration)	Cell Volume (ml)	Current (mA)	Temperature	pH (Initial)	pH (Final)	Stirring	Time (h)	Conversion (%)
SAB 379	Ru/ACC	Pt	2-C	Pyrrolidine (20 mM)	Methanol (20% v/v)	20	150	70	7	12	slow	10	99
SAB 396	Ru/ACC	Pt	2-C	Pyrrolidine (20 mM)	Methanol (20% v/v)	20	0	70	7	7	slow	10	0
SAB 416	Ru/ACC	Pt	Pt	Pyrrolidine (20 mM)	No Alcohol	20	150	70	7	12	slow	10	0
SAB 404	Ru/ACC	Pt	2-C	Pyrrolidine (20 mM)	Methanol (20% v/v)	20	2	70	7	N/A	slow	10	4.3
SAB 378	Ru/ACC	Pt	2-C	Pyrrolidine (20 mM)	Methanol (20% v/v)	20	5	70	7	N/A	slow	10	40.3
SAB 377	Ru/ACC	Pt	2-C	Pyrrolidine (20 mM)	Methanol (20% v/v)	20	10	70	7	12	slow	10	51.3
SAB 379	Ru/ACC	Pt	2-C	Pyrrolidine (20 mM)	Methanol (20% v/v)	20	30	70	7	12	slow	10	87.6
SAB 371	Ru/ACC	Pt	2-C	Pyrrolidine (20 mM)	Methanol (20% v/v)	20	50	70	7	12	slow	10	91.3
SAB 372	Ru/ACC	Pt	2-C	Pyrrolidine (20 mM)	Methanol (20% v/v)	20	100	70	7	12	slow	10	96
SAB 380	Ru/ACC	Pt	2-C	Pyrrolidine (20 mM)	Methanol (20% v/v)	20	200	70	7	12	slow	6	95.6
SAB 387	Ru/ACC	Pt	2-C	Pyrrolidine (20 mM)	Methanol (30% v/v)	20	150	70	7	12	slow	8	97
SAB 383	Ru/ACC	Pt	2-C	Pyrrolidine (20 mM)	Methanol (1% v/v)	20	150	70	7	12	slow	10	19
SAB 384	Ru/ACC	Pt	2-C	Pyrrolidine (20 mM)	Methanol (2% v/v)	20	150	70	7	12	slow	10	55
SAB 385	Ru/ACC	Pt	2-C	Pyrrolidine (20 mM)	Methanol (5% v/v)	20	150	70	7	12	slow	8	91.3
SAB 386	Ru/ACC	Pt	2-C	Pyrrolidine (20 mM)	Methanol (10% v/v)	20	150	70	7	12	slow	10	99
SAB 392	Ru/ACC	Pt	2-C	Pyrrolidine (20 mM)	Methanol (20% v/v)	20	150	36	7	12	slow	10	86.3
SAB 393	Ru/ACC	Pt	2-C	Pyrrolidine (20 mM)	Methanol (20% v/v)	20	150	50	7	12	slow	10	99
SAB 417	ACC	Pt	2-C	Pyrrolidine (20 mM)	Methanol (20% v/v)	20	150	70	7	12	slow	6	91.3
SAB 426	ACC	Pt	2-C	Pyrrolidine (20 mM)	Methanol (20% v/v)/Anolyte	20	150	70	7	12	slow	6	97
SAB 462	ACC	Pt	1-C	Pyrrolidine (20 mM)	Methanol (5% v/v)	20	2	60	7	7	slow	10	0
SAB 463	ACC	Pt	1-C	Pyrrolidine (20 mM)	Methanol (5% v/v)	20	5	60	7	7	slow	10	41.6
SAB 461	ACC	Pt	1-C	Pyrrolidine (20 mM)	Methanol (5% v/v)	20	10	60	7	7	slow	10	86.7
SAB 464	ACC	Pt	1-C	Pyrrolidine (20 mM)	Methanol (10% v/v)	20	10	60	7	7	slow	10	90.6
SAB 544	ACC	ACC	1-C	Pyrrolidine (20 mM)	Methanol (5% v/v)	20	10	60	7	7	slow	10	0
SAB 470	ACC	Pt	1-C	Pyrrolidine (20 mM)	Methanol (2% v/v)	20	10	60	7	7	slow	10	73.3
SAB 596	ACC	Ru/ACC	1-C	Pyrrolidine (20 mM)	Methanol (5% v/v)	20	10	60	7	7	slow	10	98.3
SAB 598	Ru/ACC	Ru/ACC	1-C	Pyrrolidine (20 mM)	Methanol (5% v/v)	20	10	60	7	7	slow	10	98
SAB 597	Ru/ACC	ACC	1-C	Pyrrolidine (20 mM)	Methanol (5% v/v)	20	10	60	7	7	slow	10	47.3

Table 5. Optimization of Pd/ACC-Catalyzed H/D Exchange

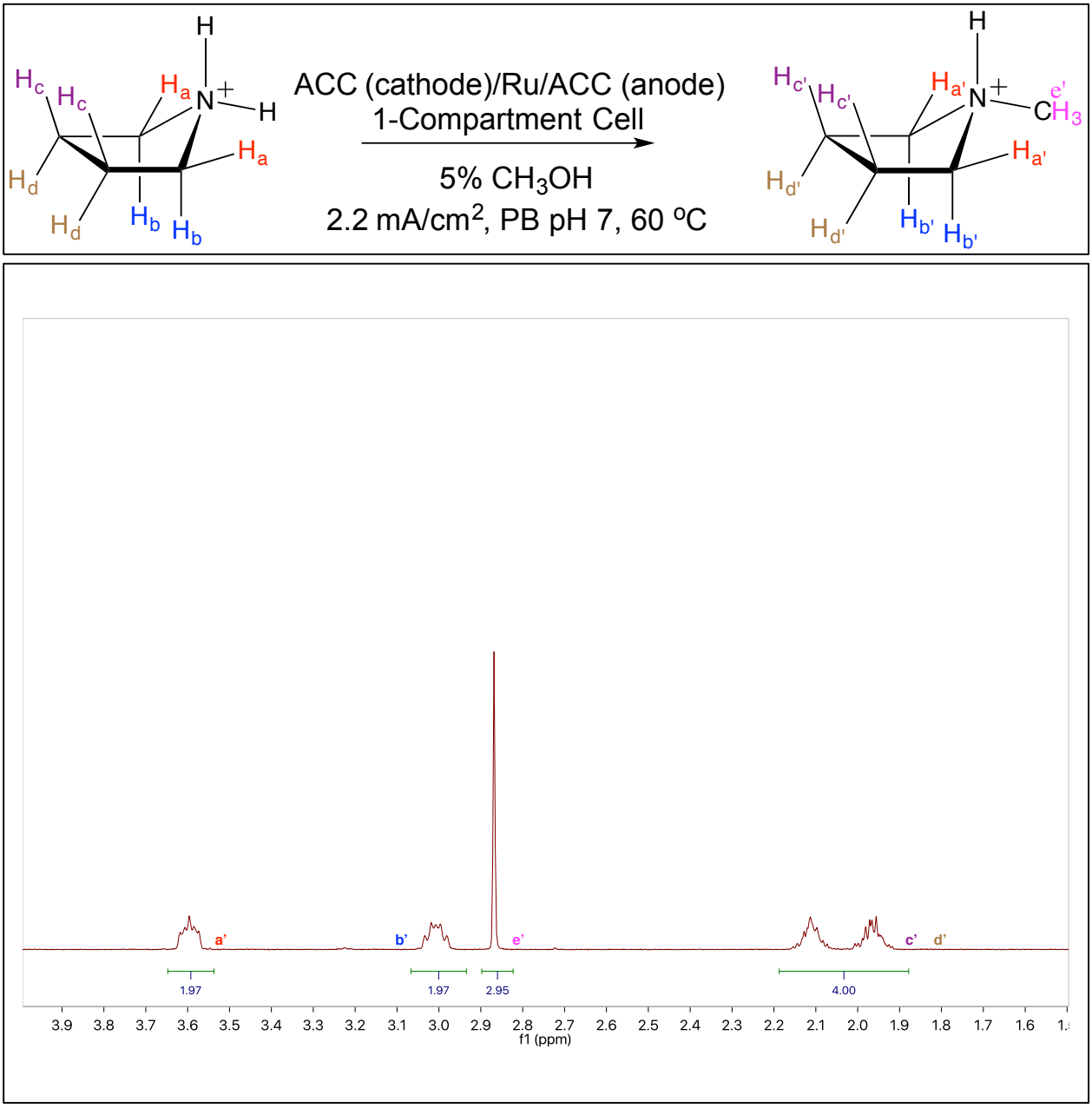

Figure 80. ^{1}H NMR spectrum of 1-methylpyrrolidine (pH 1), 64.

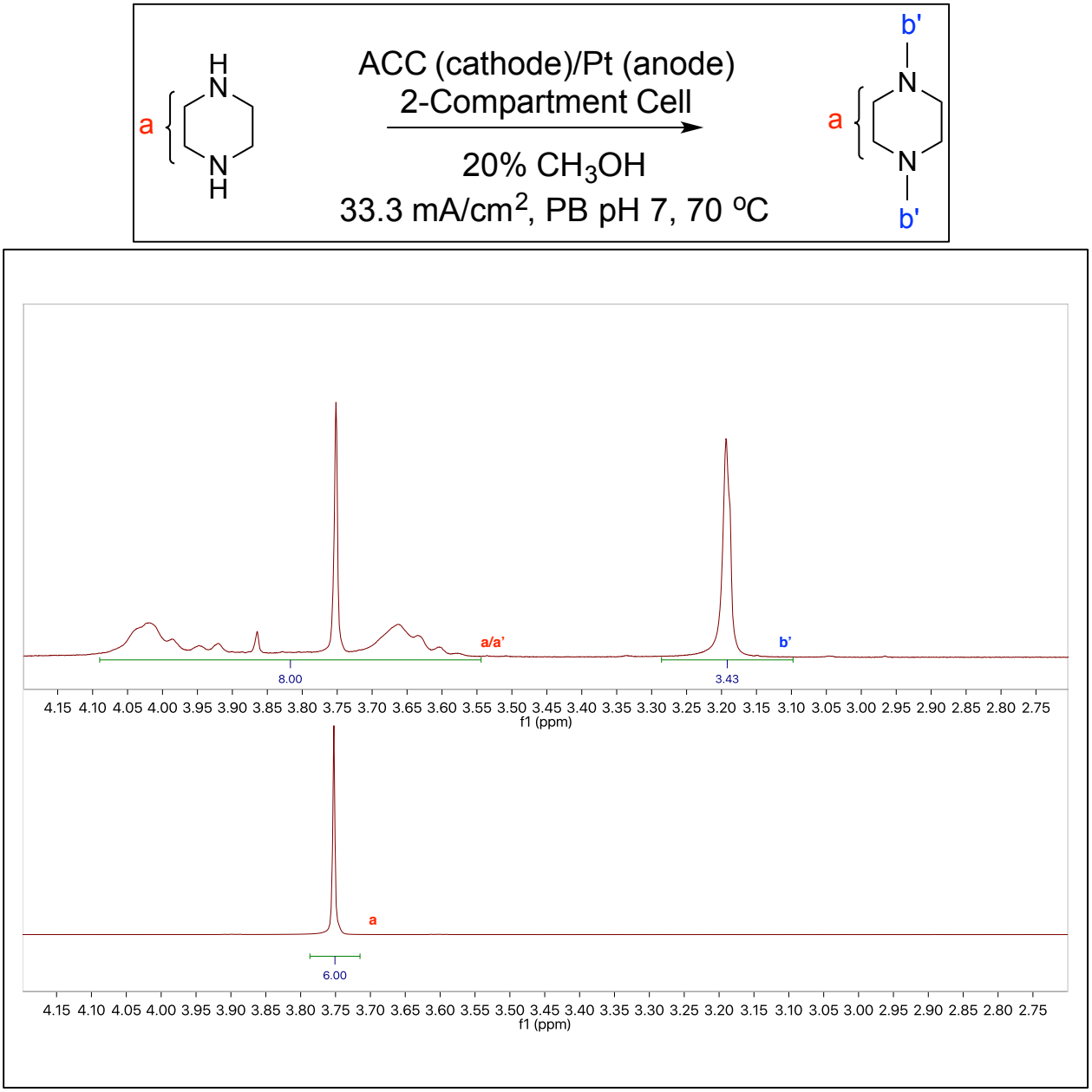

Figure 81. ^{1}H NMR spectrum of 1,4-dimethylpiperazine (pH 1), 65 (Yield 27.5%).

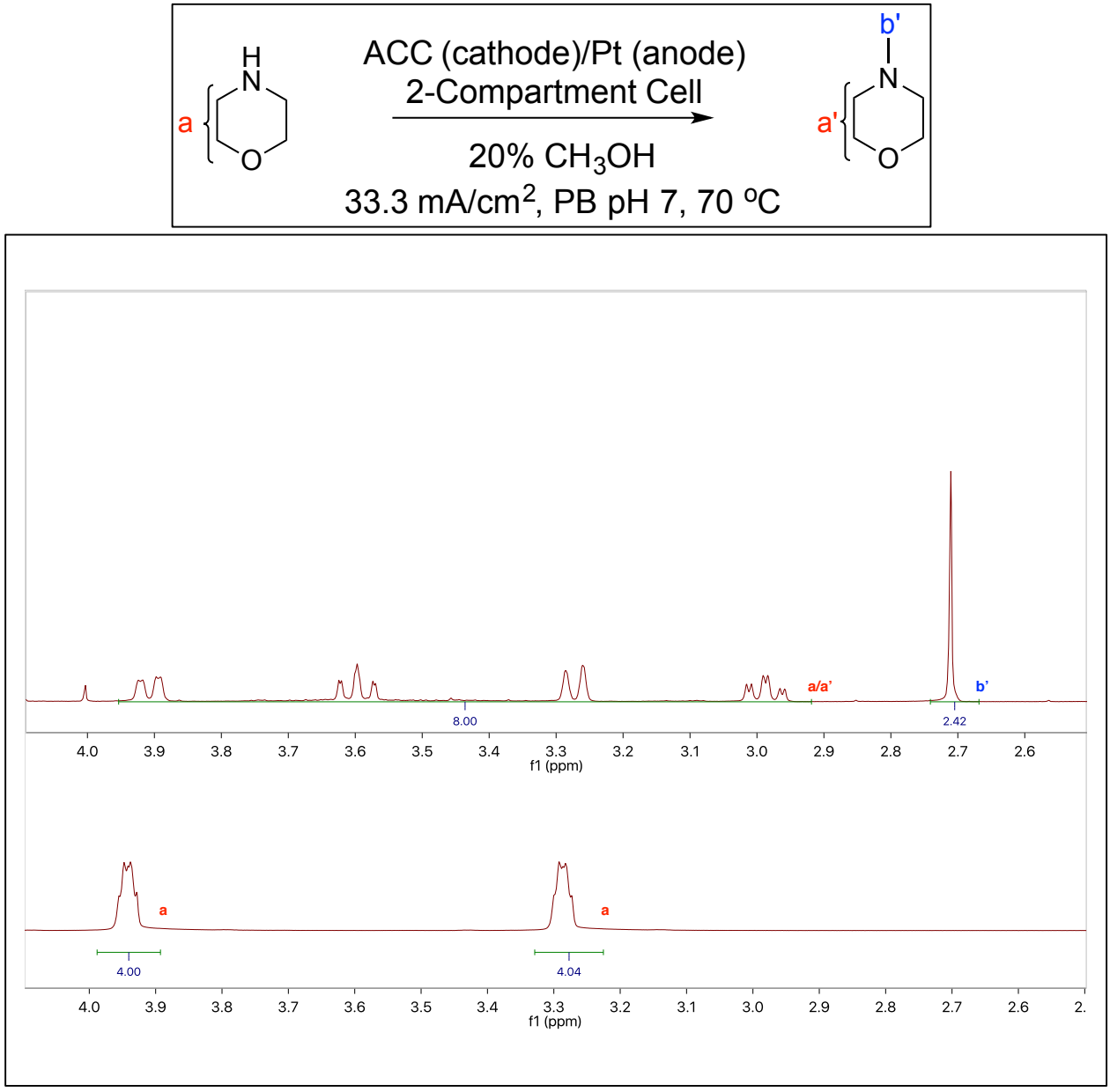

Figure 82. ^{1}H NMR spectrum of 1-methylmorpholine (pH 1), 66 (Yield 43.2%).

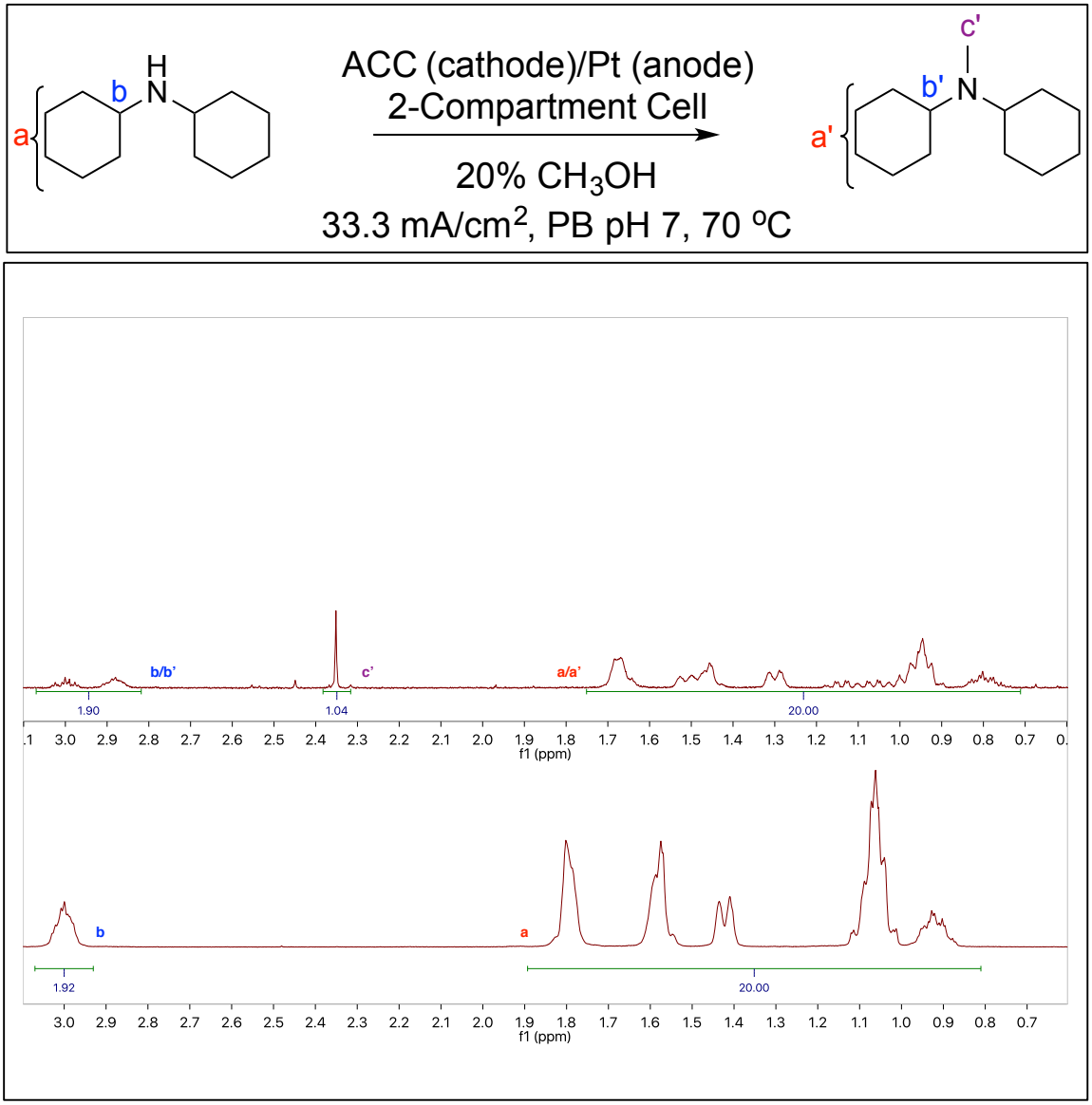

Figure 83. ^{1}H NMR spectrum of 1-methyldicyclohexylamine (pH 1), 67 (Yield 4%).

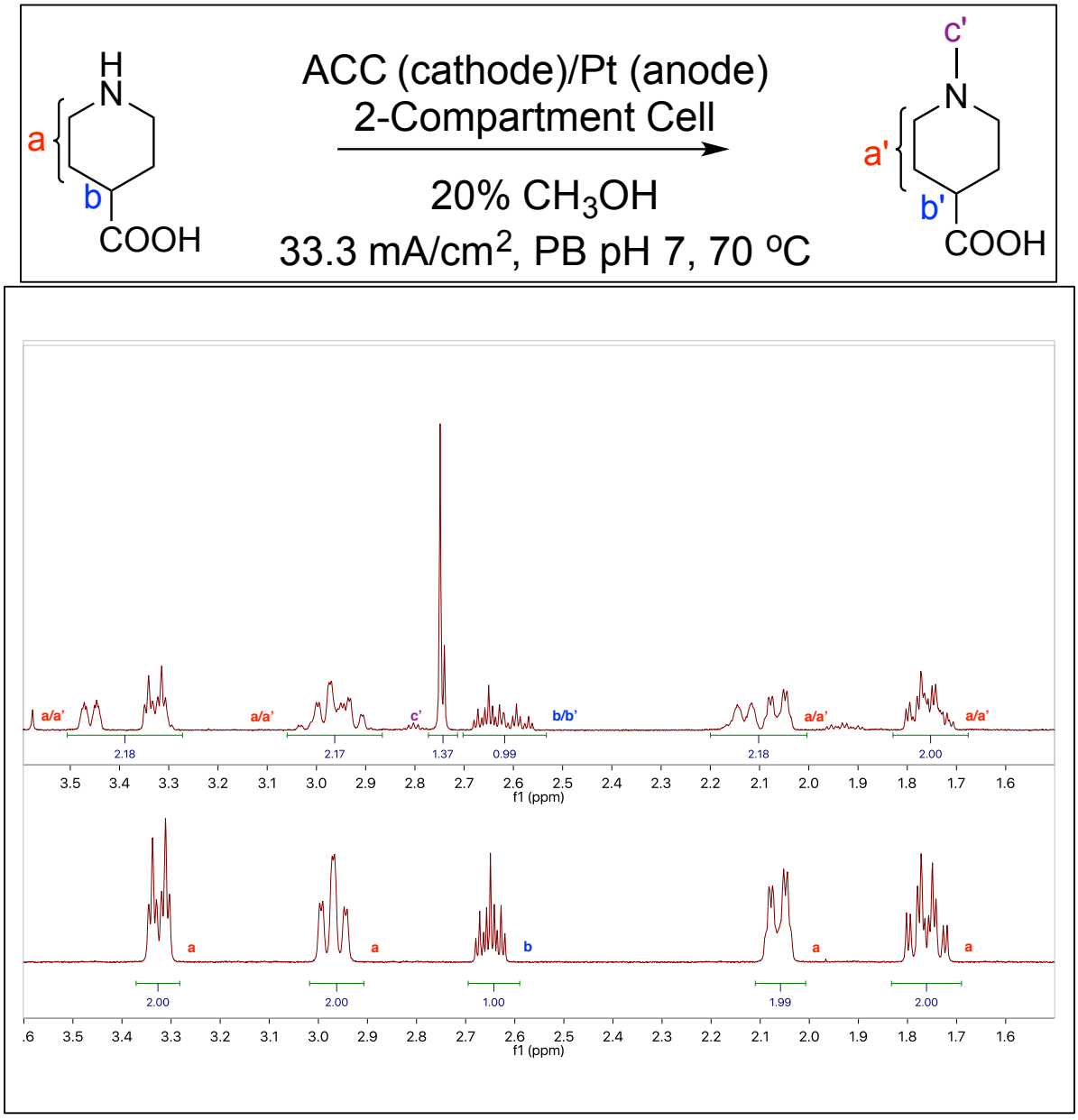

Figure 84. ^{1}H NMR spectrum of 1-methylpiperidine-4-carboxylic acid (pH 1), 68 (Yield 33%).

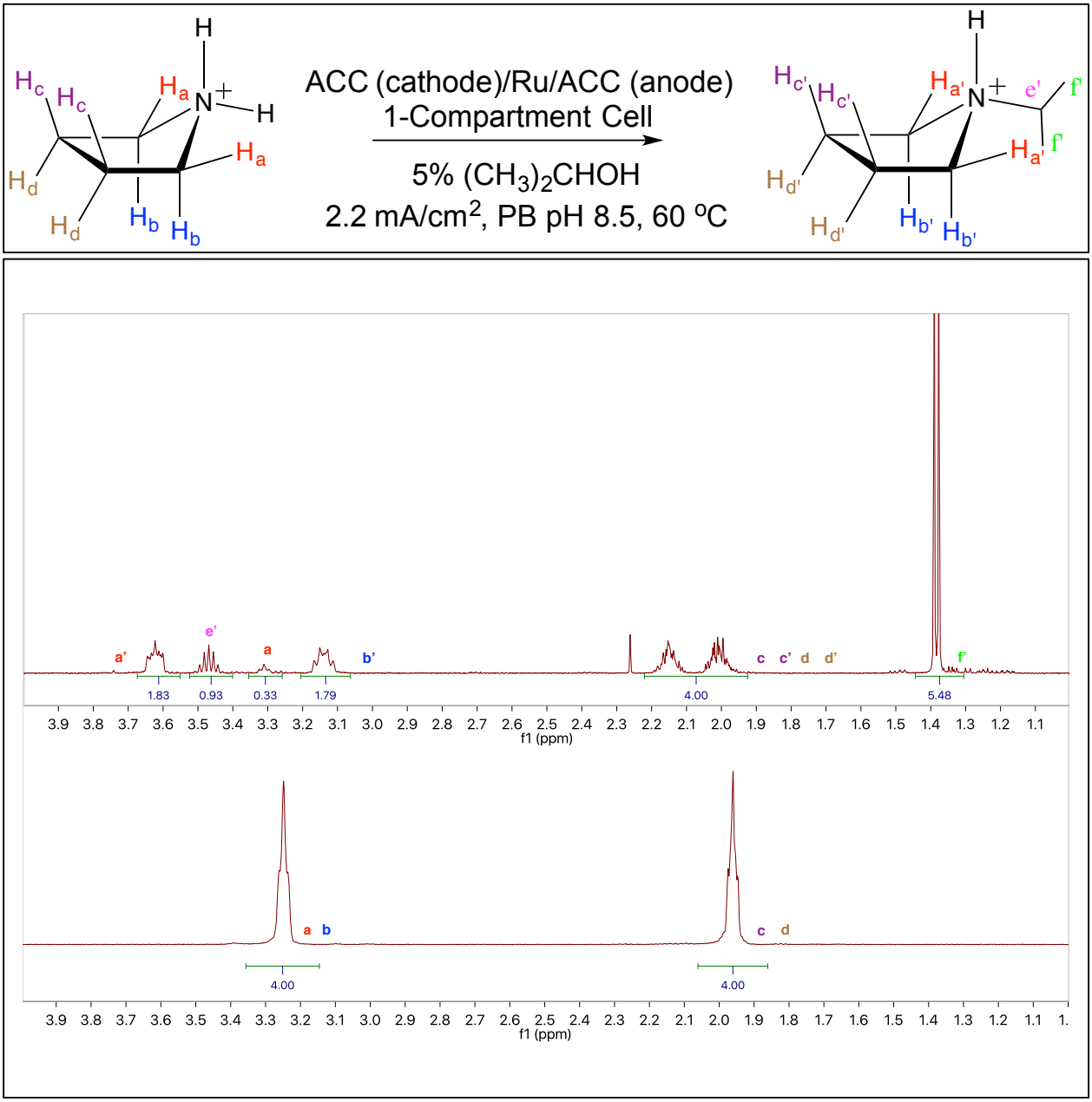

Figure 85. ^{1}H NMR spectrum of 1-isopropylpyrrolidine (pH 1), 69 (Yield 26%).

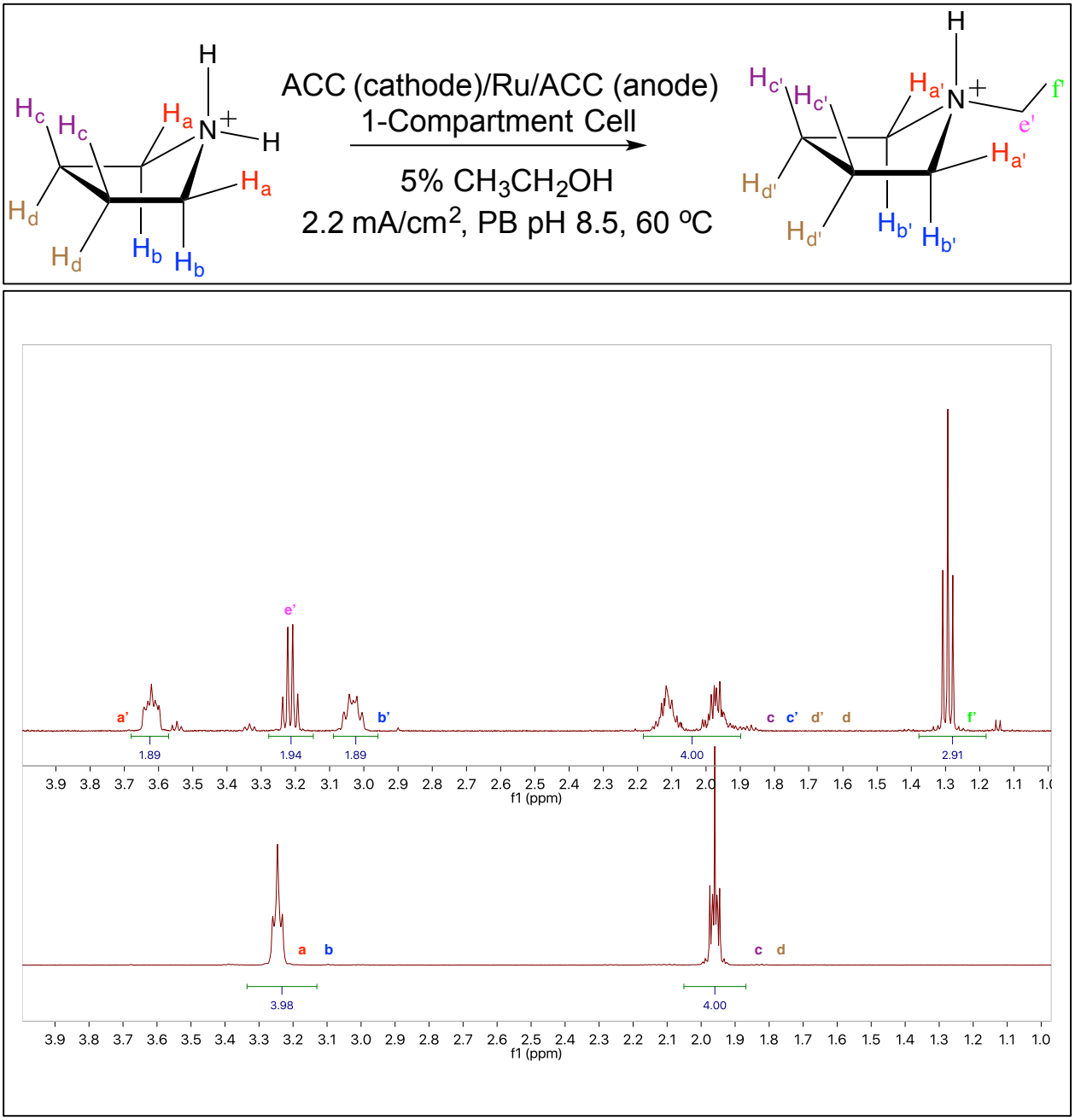

Figure 86. ^{1}H NMR spectrum of 1-ethylpyrrolidine (pH 1), 70 (Yield 44.2%).

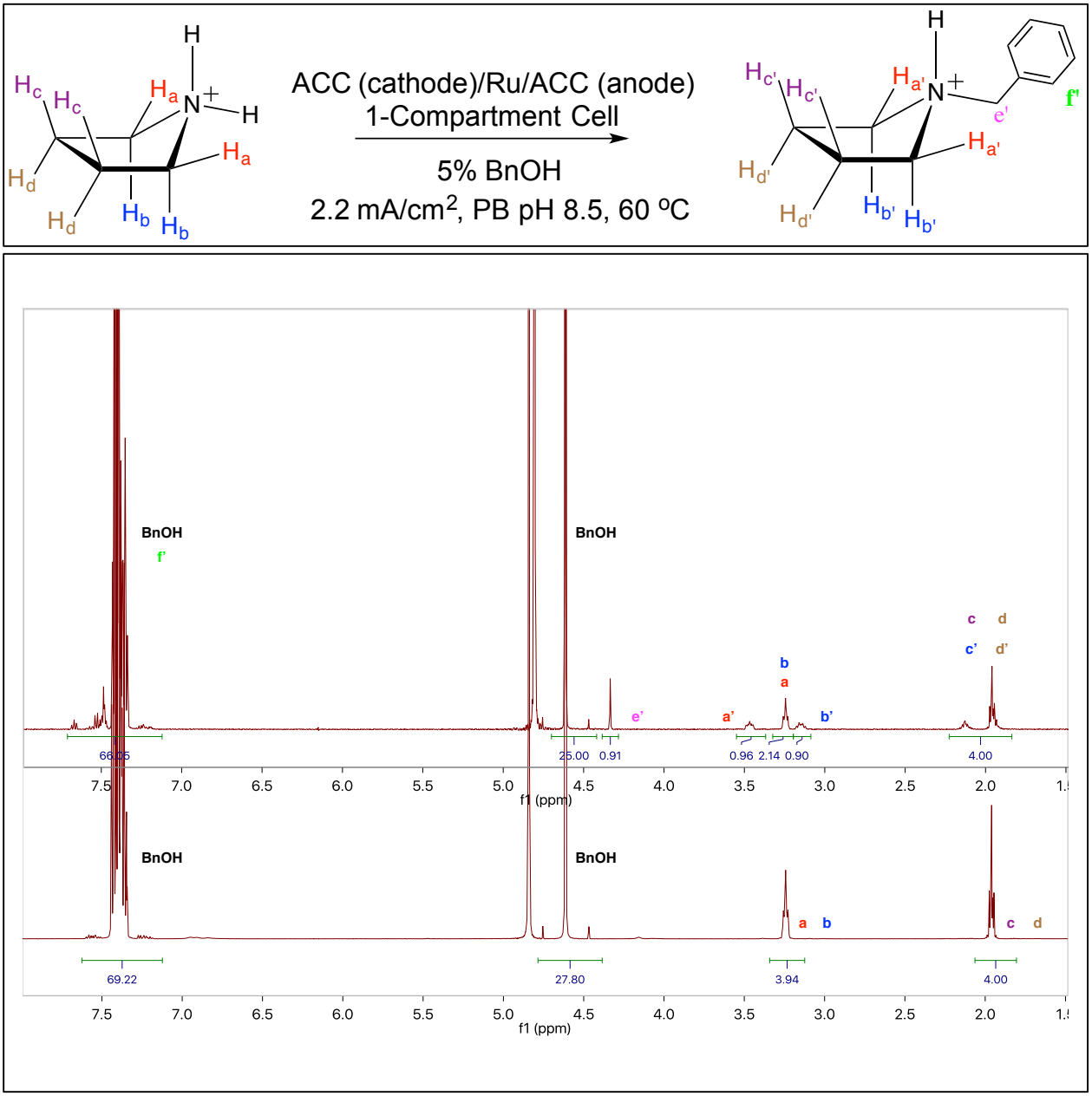

Figure 87. ^{1}H NMR spectrum of 1-benzylpyrrolidine (pH 1), 71 (Yield 8%).

Chapter 5. Conclusion & Future Directions

5.1 Conclusion

In conclusion, we have developed a simple electroactivated system to effect H/D exchange at sites α to amines and alcohols in variety of substrates. In the case of chiral amino acids, stereochemistry was fully retained along with near quantitative deuterium incorporation using D_2O, the lowest cost source of deuterium. It was also noted that the catalyst retains its catalytic ability over multiple runs, and the optimum practical current density to enable the desired reactions while minimizing losses via the competing desorption processes was found to be 1.1 mA/cm^2. The low isolated yield for reactions run under dilute conditions was attributed to adsorption of organic substrates by the activated carbon cloth and using an appropriate organic solvent helped us to extract the organic substrate out of the cloth without losing its catalytic activity. We also developed a method of cathode preparation that avoids the use of H_2 in a high-pressure batch reactor to develop a Ru/ACC catalyst; instead the ruthenium was deposited via electrochemical reduction, giving an electrocatalyst of similar efficacy. The use of ACC as an anode instead of Pt was also successful. The H/D exchange studied herein demonstrates the potential of the electroactivated Ru to effect C-H activation in aliphatic heteroatom-based compounds. In chapter 3, we expanded the range of electroactivated catalysts to deuterate aromatic compounds. Specifically, benzylic sites were selectively activated using Pd/ACC. The Pd/ACC in this system was also electroreductively deposited and the reaction were run at ambient pressure, 60 °C and a current density of 33.3 mA/cm^2. With Pd/ACC, in addition to quantitative deuterium incorporation at benzylic sites, *ortho*-H/D exchange in the presence

of a directing group (amino or hydroxyl) was also observed. The ability of Pd to activate benzylic sites can be imagined via π-benzylic complex formation whereas *ortho*-H/D exchange was attributed to the directing group mediated C-H activation but further mechanistic insight is warranted.

In chapter 4, the ability of the electrocatalytic systems to activate alcohols was applied to alkylate amines. We investigated the use of various cathode-anode set-ups to activate alcohols like ACC-Pt, ACC-Ru/ACC, Ru/ACC-ACC and observed Ru/ACC as anode and ACC as cathode to be the optimal system to alkylate amines electrochemically (i.e. via oxidation at the anode and reduction at the cathode). For single-electrode electrocatalytic activation, the use of Ru/ACC as cathode and ACC as anode was found to be best. These findings call for further study of substrate scope in both electrocatalytic and electrochemical approaches.

5.2 Future Directions

5.2.1 Development of Smaller Scale Reactions Set-up (NMR Tube)

The H/D exchange work described above was conducted in a 2- C cell where 20 ml of electrolyte (phosphate buffer prepared in D_2O) was used as a catholyte and anolyte. Using 40 ml of D_2O for every H/D investigation is economically non-viable for future research. In addition to the use of large volumes of D_2O, transitioning to a smaller scale reaction set-up will decrease the reaction time, thereby enabling study of more substrates in a relatively short time while still giving the required qualitative and quantitative data. We propose use a NMR tube with an external diameter of 5 mm were used (Wilmad-LabGlass, Buena, NJ). An average reaction volume in this tube will be 0.6 ml and the compartment will be separated via a Nafion® sleeve wrapped around pencil carbon. As ACC is used as a carbon support, we

have the flexibility to cut it to our required dimension and ruthenium or palladium will be electrodeposited based on the desired chemistry. The analysis time in the proposed set-up will also decrease as the reaction can be continuously monitored via NMR (**Figure 88**).

The 1-C set-up is also proposed for the alkylation chemistry and although it cannot be monitored like the H/D exchange work (*Note: Alkylation chemistry is performed in H_2O vs. D_2O for H/D exchange*), nonetheless moles of substrates and reaction time can be decreased.

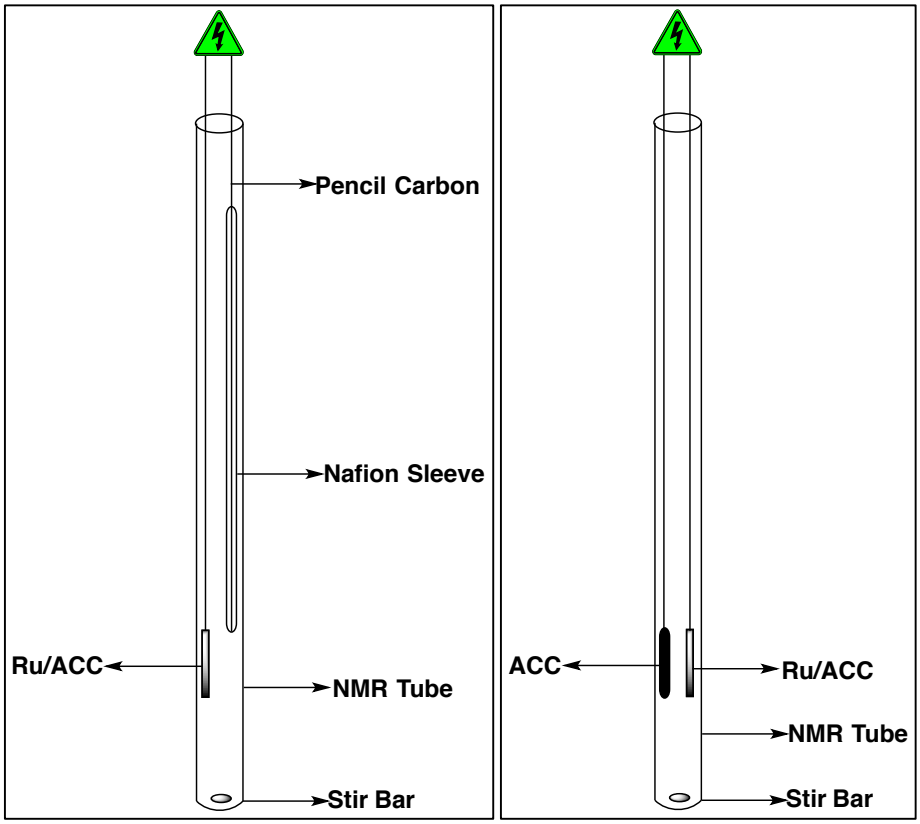

Figure 88. NMR Scale Reaction Set-Up (2-C and 1-C)

5.2.2 Development of Continuous-Flow Reactor (Design proposed by Andrew Henika)

One of the active concern of our work is that it's a batch system. To make it economically more feasible and attractive to industry, a transition to a continuous flow-reaction is desired. The design of the reactor and its working is proposed by Andrew Henika, a graduate student

in Dr. Jackson's lab. Herein, we are proposing to operate our H/D exchange and alkylation chemistry in a continuous-flow reactor.

The proposed flow electrocatalytic reactor would utilize Nafion®-117, a solid polymer electrolyte (SPE), to separate the anode from the cathode in lieu of a salt bridge. A 5 cm x 2 cm x 2 cm block will be cast from two-part epoxy resin and machined to the dimensions shown in **Figure 89** Reactant will flow into the input port at the bottom of the cathode channel and product will flow out of the output port at the top of the cathode channel. The anode assembly will be constructed from a graphite stick sheathed in Nafion®-117, which will then be heat-crimped at one end and glued into a plastic threaded connector at the other end. A short length of the graphite stick will protrude from the opposite side of the threaded connector to act as an electrical contact for the positive terminal on a potentiostat. This assembly will be threaded into the end of the reactor body such that the anode runs centered down the length of the cathode channel. Transition metal coated activated carbon cloth will be rolled and inserted into the cathode channel around the anode. A conductive screw serving as the cathode contact will be threaded into the reactor body opposite the anode assembly to contact the carbon cloth at the end of cathode channel. The outer portion of the metal screw will serve as the electrical contact for the negative terminal on a potentiostat.

The reactor will be positioned vertically during operation to allow generated gases to escape through the output port, and the cathode channel will be filled with reactant solution prior to energizing the reactor. During normal operation, water molecules will be able to diffuse through the SPE membrane to the anode surface where they are oxidized into oxygen, protons, and electrons. The oxygen gas will diffuse back out of the SPE membrane along with the deuterons (H^+ or D^+) generated at the anode surface. These cations can then diffuse to

the surface of the metal particles of the cathode where they will be reduced to be delivered to the substrate. Reactants will be pumped into the input port of the reactor via a peristaltic pump and flow into the cathode channel. As the reactants flow up toward the output port they will diffuse though the cloth serving as the cathode where they can be deuterated. The products, generated gases, and any unreacted reactants will flow out of the reactor body through the output port where they may either be collected or recycled back through the input port again. Several variables will be investigated for the flow-based reactor including operating current & potential, catalyst loading, residence time, and flow rate.

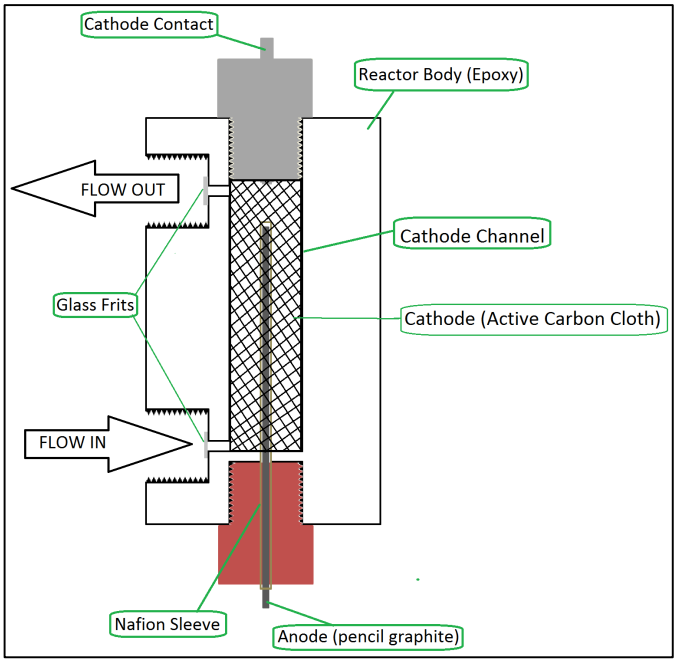

Figure 89. Continuous Flow-Based Electrocatalytic Reactor Cell

APPENDIX

APPENDIX

Computational Data
HF/6-31G(d) and MP2(full)/6-31G(d) geometries and energies from G3 calculations.

Isopropyl alcohol, C_1

HF/6-31G(d), E= -193.11542

C	-1.324475	-0.549566	-0.086789
C	-0.001464	0.047689	0.361359
C	1.195257	-0.776363	-0.100920
O	0.049962	1.352343	-0.169279
H	0.007101	0.100160	1.449702
H	-2.148214	0.069733	0.248928
H	-1.454653	-1.548391	0.317600
H	-1.362428	-0.606390	-1.169703
H	2.128887	-0.320864	0.220633
H	1.160825	-1.780988	0.309161
H	1.209570	-0.844232	-1.183864
H	0.843314	1.781669	0.119869

MP2(full)/6-31G(d), E= -193.70655

C	-1.313275	-0.563514	-0.088979
C	-0.000926	0.036459	0.370128
C	1.200721	-0.764480	-0.104920
O	0.027191	1.363691	-0.167516
H	0.007371	0.082146	1.470506
H	-2.147811	0.054994	0.247675
H	-1.438709	-1.574274	0.308341
H	-1.334005	-0.607253	-1.181009
H	2.136462	-0.299324	0.223163
H	1.177735	-1.784436	0.289968
H	1.202842	-0.807818	-1.197189
H	0.859467	1.775646	0.121305

Isopropyl alcohol cation, C_1

HF/6-31G(d), E= -192.28784

C	1.351539	-0.543416	-0.005895
C	0.004455	0.069402	-0.001483
C	-1.235362	-0.744938	0.004873

O -0.031344 1.325185 -0.003915
H 1.354197 -1.457192 -0.585993
H 2.095174 0.154675 -0.361456
H 1.580182 -0.808134 1.026248
H -1.110766 -1.607909 0.647380
H -2.107032 -0.177075 0.303055
H -1.380943 -1.115250 -1.009118
H -0.903853 1.723115 0.026232

MP2(full)/6-31G(d), E= -192.85460

C 1.341867 -0.547933 -0.005850
C 0.004361 0.059836 0.000181
C -1.232595 -0.741181 0.004985
O -0.019491 1.339580 -0.004083
H 1.356951 -1.429905 -0.651118
H 2.106350 0.172959 -0.293826
H 1.545544 -0.898546 1.016390
H -1.117860 -1.604055 0.666414
H -2.117170 -0.165343 0.283825
H -1.370081 -1.139131 -1.010639
H -0.929601 1.723047 0.025726

Isopropyl alcohol anion, C_s

HF/6-31G(d), E= -192.40519

C 0.368209 0.345147 0.000000
O -1.007494 0.944511 0.000000
C 0.368209 -0.557810 1.231290
C 0.368209 -0.557810 -1.231290
H -0.445966 -1.310325 1.259347
H -0.445966 -1.310325 -1.259347
H 0.275545 0.022701 2.153411
H 0.275545 0.022701 -2.153411
H 1.308192 -1.115230 1.305687
H 1.308192 -1.115230 -1.305687
H -0.843345 1.872464 0.000000

MP2(full)/6-31G(d), E= -193.00276

C 0.377163 0.352913 0.000000
O -1.033712 0.931058 0.000000
C 0.377163 -0.552542 1.217091
C 0.377163 -0.552542 -1.217091
H -0.435899 -1.324907 1.223283

H	-0.435899	-1.324907	-1.223283
H	0.261028	0.020830	2.149341
H	0.261028	0.020830	-2.149341
H	1.330143	-1.101380	1.295815
H	1.330143	-1.101380	-1.295815
H	-0.829773	1.875475	0.000000

Isopropyl alcohol radical, C_1

HF/6-31G(d) E= -192.49389

C	1.355045	-0.550215	0.027874
C	0.006923	0.035505	-0.253809
C	-1.232131	-0.761560	0.038446
O	-0.040314	1.367443	0.074272
H	2.133235	0.077688	-0.390921
H	1.536064	-0.630512	1.100582
H	1.441747	-1.542537	-0.401299
H	-2.114393	-0.294260	-0.393649
H	-1.154833	-1.761032	-0.374208
H	-1.402261	-0.853769	1.112456
H	-0.896065	1.722490	-0.122207

MP2(full)/6-31G(d) E= -193.05987

C	1.346347	-0.556685	0.029514
C	0.007007	0.027365	-0.255538
C	-1.231931	-0.754640	0.038524
O	-0.025822	1.375923	0.068068
H	2.131745	0.080965	-0.382936
H	1.523699	-0.646770	1.111677
H	1.433456	-1.552772	-0.410847
H	-2.117331	-0.279519	-0.399755
H	-1.159066	-1.763553	-0.373823
H	-1.405414	-0.843867	1.122113
H	-0.929048	1.701889	-0.085970

Isopropylamine, C_1

HF/6-31G(d), E= -173.28515

C	1.369261	-0.464609	0.083926
C	-0.001603	0.029748	-0.368985
C	-1.119954	-0.902365	0.108833
N	-0.167512	1.414667	0.058700
H	-0.012079	0.041961	-1.455386

H 2.148499 0.189167 -0.289462
H 1.560008 -1.472560 -0.271284
H 1.434256 -0.479095 1.169817
H -2.090962 -0.549996 -0.228899
H -0.984218 -1.912419 -0.267408
H -1.143179 -0.951607 1.195211
H -1.040933 1.783934 -0.266682
H -0.185035 1.471305 1.060548

MP2(full)/6-31G(d), E= -173.86364

C 1.359317 -0.476018 0.084574
C -0.001722 0.025421 -0.373876
C -1.124104 -0.891160 0.109688
N -0.148085 1.421982 0.054418
H -0.012419 0.038888 -1.470878
H 2.148145 0.184202 -0.281233
H 1.548000 -1.491418 -0.274915
H 1.407229 -0.493157 1.179404
H -2.099563 -0.526376 -0.227789
H -0.998690 -1.913504 -0.261365
H -1.135446 -0.927134 1.204794
H -1.056643 1.775575 -0.246418
H -0.164960 1.449599 1.075151

Isopropylamine cation, C_{2V}

HF/6-31G(d), E= -172.49752

C 0.000000 0.000000 0.065922
N 0.000000 0.000000 1.346048
H 0.000000 0.850714 1.875453
H 0.000000 -0.850714 1.875453
C 0.000000 1.290882 -0.683977
C 0.000000 -1.290882 -0.683977
H 0.000000 2.151679 -0.029785
H 0.000000 -2.151679 -0.029785
H -0.873993 1.325734 -1.325370
H -0.873993 -1.325734 -1.325370
H 0.873993 1.325734 -1.325370
H 0.873993 -1.325734 -1.325370

MP2(full)/6-31G(d), E= -173.052608

C 0.000000 0.000000 0.056759
N 0.000000 0.000000 1.352240

H	0.000000	0.867446	1.888958
H	0.000000	-0.867446	1.888958
C	0.000000	1.286215	-0.683132
C	0.000000	-1.286215	-0.683132
H	0.000000	2.155960	-0.024925
H	0.000000	-2.155960	-0.024925
H	-0.879069	1.323883	-1.334181
H	-0.879069	-1.323883	-1.334181
H	0.879069	1.323883	-1.334181
H	0.879069	-1.323883	-1.334181

Isopropylamine anion, C_s

HF/6-31G(d), E= -172.56439

C	-0.382800	0.333405	0.000000
N	1.026278	0.956478	0.000000
C	-0.382800	-0.577800	1.225219
C	-0.382800	-0.577800	-1.225219
H	0.442905	-1.319454	1.262090
H	0.442905	-1.319454	-1.262090
H	-1.316890	-1.144613	1.289398
H	-1.316890	-1.144613	-1.289398
H	-0.311958	-0.007252	2.159608
H	-0.311958	-0.007252	-2.159608
H	1.039166	1.590230	0.785295
H	1.039166	1.590230	-0.785295

MP2(full)/6-31G(d), E= -173.15016

C	-0.386744	0.340744	0.000000
N	1.037243	0.936345	0.000000
C	-0.386744	-0.569713	1.209221
C	-0.386744	-0.569713	-1.209221
H	0.447483	-1.323941	1.229732
H	0.447483	-1.323941	-1.229732
H	-1.328919	-1.137064	1.271444
H	-1.328919	-1.137064	-1.271444
H	-0.304173	-0.007604	2.156874
H	-0.304173	-0.007604	-2.156874
H	1.035957	1.587450	0.794565
H	1.035957	1.587450	-0.794565

Isopropylamine radical, C_s

HF/6-31G(d), E= -172.66740

C	0.218670	0.110262	0.000000
N	-0.609746	1.255778	0.000000
H	-0.487714	1.824527	0.813818
H	-0.487714	1.824527	-0.813818
C	0.218670	-0.660540	1.289454
C	0.218670	-0.660540	-1.289454
H	0.407771	-0.010121	2.139726
H	0.407771	-0.010121	-2.139726
H	0.986937	-1.426417	1.282775
H	0.986937	-1.426417	-1.282775
H	-0.740915	-1.150758	1.461615
H	-0.740915	-1.150758	-1.461615

MP2(full)/6-31G(d), E= -173.22112

C	0.218098	0.107808	0.000000
N	-0.609152	1.250585	0.000000
H	-0.484443	1.826289	0.828385
H	-0.484443	1.826289	-0.828385
C	0.218098	-0.657318	1.283269
C	0.218098	-0.657318	-1.283269
H	0.405041	-0.000125	2.139973
H	0.405041	-0.000125	-2.139973
H	0.995663	-1.425449	1.275149
H	0.995663	-1.425449	-1.275149
H	-0.747109	-1.157276	1.459278
H	-0.747109	-1.157276	-1.459278

Isopropyl methyl ether, C_1

HF/6-31G(d), E= -232.14161

C	1.572406	-0.935198	-0.007881
C	0.410520	-0.007326	0.311249
C	0.707674	1.434951	-0.091546
O	-0.707964	-0.516078	-0.372048
C	-1.955246	-0.107070	0.092148
H	0.215056	-0.042765	1.383288
H	1.336560	-1.949677	0.292069
H	2.473135	-0.620436	0.509703
H	1.769928	-0.934636	-1.074756
H	-0.113174	2.100266	0.152973
H	1.590633	1.799817	0.424122
H	0.884621	1.494302	-1.160635
H	-2.701262	-0.656359	-0.466219

H -2.077558 -0.329392 1.150758
H -2.126346 0.955360 -0.058738

MP2(full)/6-31G(d), E= -232.86682

C 1.608778 -0.883870 -0.008689
C 0.419790 -0.003740 0.321853
C 0.644379 1.440600 -0.102298
O -0.691672 -0.587495 -0.359631
C -1.947780 -0.111584 0.089252
H 0.227764 -0.039464 1.407495
H 1.411831 -1.913458 0.296806
H 2.509370 -0.528338 0.499420
H 1.785836 -0.871065 -1.087273
H -0.202909 2.079891 0.156424
H 1.532540 1.849826 0.388044
H 0.791603 1.481534 -1.184968
H -2.703585 -0.727773 -0.399474
H -2.047841 -0.216996 1.178522
H -2.122242 0.937368 -0.178651

Isopropyl methyl ether cation, C_s

HF/6-31G(d), E= -231.32455

C -0.698269 1.764613 0.000000
C 0.000000 0.455630 0.000000
C 1.487204 0.369210 0.000000
C -0.724370 -0.558048 0.000000
C -0.248928 -1.937979 0.000000
H -1.769657 1.637268 0.000000
H 1.929913 1.353348 0.000000
H -1.147354 -2.527147 0.000000
H 0.327864 -2.107278 0.894144
H 0.327864 -2.107278 -0.894144
H 1.824229 -0.175189 0.877407
H 1.824229 -0.175189 -0.877407
H -0.381085 2.328499 0.873130
H -0.381085 2.328499 -0.873130

MP2(full)/6-31G(d), E= -232.02567

C -0.693886 1.765440 0.000000
C 0.000000 0.465863 0.000000
C 1.475416 0.360307 0.000000
O -0.754276 -0.559257 0.000000

C	-0.220785	-1.937536	0.000000
H	-1.775697	1.642221	0.000000
H	1.934859	1.347257	0.000000
H	-1.110874	-2.558052	0.000000
H	0.367703	-2.082962	0.903865
H	0.367703	-2.082962	-0.903865
H	1.813707	-0.195589	0.882660
H	1.813707	-0.195589	-0.882660
H	-0.370685	2.337642	0.877995
H	-0.370685	2.337642	-0.877995

Isopropyl methyl ether anion, C_s

HF/6-31G(d), E= -231.43717

C	-0.445393	0.369303	0.000000
O	0.548025	-0.749488	0.000000
C	-0.064636	-1.971232	0.000000
H	0.701010	-2.756623	0.000000
H	-0.700858	-2.129704	0.876077
H	-0.700858	-2.129704	-0.876077
C	-0.064636	1.182114	1.233630
C	-0.064636	1.182114	-1.233630
H	0.985725	1.533701	1.257392
H	0.985725	1.533701	-1.257392
H	-0.216399	0.610867	2.152681
H	-0.216399	0.610867	-2.152681
H	-0.693174	2.074501	1.313395
H	-0.693174	2.074501	-1.313395

MP2(full)/6-31G(d), E= -232.16959

C	-0.448185	0.362186	0.000000
O	0.584332	-0.741592	0.000000
C	-0.074311	-1.968081	0.000000
H	0.686828	-2.769529	0.000000
H	-0.722375	-2.107016	0.882799
H	-0.722375	-2.107016	-0.882799
C	-0.074311	1.176789	1.222818
C	-0.074311	1.176789	-1.222818
H	0.978843	1.559377	1.227162
H	0.978843	1.559377	-1.227162
H	-0.196560	0.596024	2.148821
H	-0.196560	0.596024	-2.148821
H	-0.727293	2.059698	1.311883
H	-0.727293	2.059698	-1.311883

Isopropyl methyl ether radical, C_1

HF/6-31G(d), E= -231.51827

C	-1.688994	-0.814981	-0.034545
C	-0.447724	0.005484	-0.213019
C	-0.508578	1.486511	0.047442
O	0.652854	-0.676963	0.231280
C	1.915438	-0.169997	-0.089951
H	-1.536959	-1.816156	-0.421142
H	-1.955616	-0.904595	1.019326
H	-2.528371	-0.365170	-0.553790
H	0.320766	2.022655	-0.401268
H	-1.423803	1.897532	-0.362819
H	-0.498063	1.698130	1.117977
H	2.634741	-0.932580	0.173909
H	1.999046	0.042428	-1.151535
H	2.144577	0.731360	0.469535

MP2(full)/6-31G(d), E= -232.217810

C	-1.719729	-0.756949	-0.014705
C	-0.458664	0.009646	-0.227545
C	-0.443611	1.480826	0.047985
O	0.627775	-0.745232	0.173293
C	1.909332	-0.172795	-0.061435
H	-1.611288	-1.774163	-0.397848
H	-1.972216	-0.827891	1.053840
H	-2.555917	-0.273737	-0.526085
H	0.404511	1.990379	-0.416220
H	-1.356906	1.935130	-0.342721
H	-0.404399	1.685432	1.129526
H	2.631145	-0.960083	0.155226
H	2.016195	0.142145	-1.104790
H	2.102704	0.680279	0.596924

***N*-methylisopropylamine**, C_1

HF/6-31G(d), E= -212.311398

C	-1.654760	-0.881161	-0.014788
C	-0.437771	-0.010263	-0.319334
C	-0.681913	1.442133	0.111872
N	0.737341	-0.629360	0.277365
C	2.019886	-0.083506	-0.113096

H	-0.276677	-0.021789	-1.394470
H	-1.488627	-1.895087	-0.358677
H	-2.546994	-0.491156	-0.495031
H	-1.845557	-0.916452	1.055575
H	0.156674	2.084319	-0.134672
H	-1.561278	1.849276	-0.378506
H	-0.844291	1.501204	1.185953
H	0.652106	-0.632083	1.275843
H	2.808862	-0.668409	0.346268
H	2.133646	-0.168970	-1.188711
H	2.178092	0.961446	0.156939

MP2(full)/6-31G(d), E= -213.025444

C	-1.673778	-0.845334	-0.010945
C	-0.441258	-0.009249	-0.326355
C	-0.637433	1.441571	0.116953
N	0.724624	-0.674609	0.258819
C	2.007819	-0.086277	-0.105809
H	-0.281434	-0.022626	-1.413094
H	-1.527861	-1.873593	-0.347553
H	-2.565208	-0.433490	-0.492857
H	-1.854828	-0.860782	1.069789
H	0.225101	2.065240	-0.130404
H	-1.516279	1.882510	-0.363652
H	-0.789987	1.484083	1.201454
H	0.625581	-0.663936	1.275029
H	2.808008	-0.680411	0.342784
H	2.120589	-0.141131	-1.192348
H	2.151842	0.962136	0.196053

<u>*N*-methylisopropylamine cation</u>, C_S

HF/6-31G(d), E= -211.532887

C	0.671376	1.803044	0.000000
C	0.000000	0.469035	0.000000
C	-1.496179	0.397502	0.000000
N	0.702792	-0.599830	0.000000
C	0.203159	-1.985412	0.000000
H	1.750389	1.730270	0.000000
H	-1.926115	1.387683	0.000000
H	1.698701	-0.493706	0.000000
H	1.057213	-2.642759	0.000000
H	-1.845110	-0.136866	0.877500

H -1.845110 -0.136866 -0.877500
H -0.387132 -2.165839 0.886357
H -0.387132 -2.165839 -0.886357
H 0.347306 2.358856 0.873960
H 0.347306 2.358856 -0.873960

MP2(full)/6-31G(d), E= -212.22498

C 0.676744 1.801236 0.000000
C 0.000000 0.479685 0.000000
C -1.485731 0.394353 0.000000
N 0.708311 -0.607057 0.000000
C 0.184588 -1.982389 0.000000
H 1.765499 1.724585 0.000000
H -1.927476 1.389618 0.000000
H 1.724029 -0.503002 0.000000
H 1.031693 -2.664358 0.000000
H -1.838520 -0.148896 0.883335
H -1.838520 -0.148896 -0.883335
H -0.417949 -2.146298 0.893957
H -0.417949 -2.146298 -0.893957
H 0.353699 2.367817 0.879534
H 0.353699 2.367817 -0.879534

***N*-methylisopropylamine anion**, C_1

HF/6-31G(d), E= -211.60389

C -0.767973 1.390509 0.052670
C -0.423432 -0.022181 -0.417283
C -1.589035 -0.929841 -0.055512
N 0.738601 -0.521667 0.350149
C 2.010691 -0.094094 -0.164263
H -1.656184 1.779001 -0.454334
H -0.981123 1.480447 1.146507
H 0.033288 2.107224 -0.148754
H -2.507369 -0.631903 -0.572320
H -1.388273 -1.966645 -0.331278
H -1.853465 -0.951384 1.029146
H 0.689500 -0.261624 1.332567
H 2.122656 -0.465592 -1.177994
H 2.159729 0.993702 -0.209764
H 2.829524 -0.497920 0.441509
MP2(full)/6-31G(d), E= -212.32797

C -0.679686 1.383772 0.065475

C	-0.427011	-0.019818	-0.434627
C	-1.621215	-0.855497	-0.055266
N	0.703531	-0.601067	0.302703
C	1.986921	-0.100632	-0.146517
H	-1.571196	1.835565	-0.397831
H	-0.852043	1.433319	1.184454
H	0.154819	2.073483	-0.134802
H	-2.543538	-0.504012	-0.545209
H	-1.481249	-1.910726	-0.327679
H	-1.849000	-0.850866	1.053072
H	0.630402	-0.380791	1.324653
H	2.104806	-0.379496	-1.197937
H	2.125238	0.998184	-0.092776
H	2.802987	-0.554146	0.440744

<u>*N*-methylisopropylamine radical</u>, C_1

HF/6-31G(d), E= -211.69264

C	1.734947	-0.792298	-0.031821
C	0.471087	0.003859	-0.208073
C	0.546088	1.484480	0.048278
N	-0.689523	-0.660284	0.243257
C	-1.988031	-0.106710	-0.084321
H	2.017203	-0.870697	1.019408
H	1.623673	-1.804167	-0.413827
H	2.560594	-0.330413	-0.562435
H	0.543544	1.704093	1.117645
H	1.460505	1.890849	-0.369839
H	-0.282453	2.024671	-0.397533
H	-0.652965	-1.632945	0.019703
H	-2.753900	-0.796720	0.249203
H	-2.144260	0.827293	0.440608
H	-2.129833	0.074039	-1.150108

MP2(full)/6-31G(d), E= -212.38226

C	1.747513	-0.760264	-0.022977
C	0.475451	0.004389	-0.210062
C	0.506168	1.477719	0.045073
N	-0.671394	-0.682063	0.226089
C	-1.979999	-0.116114	-0.073278
H	2.032736	-0.830666	1.038395
H	1.657931	-1.784039	-0.404204
H	2.570393	-0.278053	-0.557161
H	0.494513	1.704913	1.123497

H	1.419294	1.908434	-0.373249
H	-0.341357	1.999583	-0.408279
H	-0.628145	-1.663790	-0.033515
H	-2.745381	-0.832769	0.231450
H	-2.132898	0.796538	0.505483
H	-2.122127	0.119905	-1.137576

***N,N*-methylisopropylamine**, C_1

HF/6-31G(d), E= -251.33665

C	-1.714845	-0.806511	-0.583195
C	-0.660873	0.281402	-0.369001
C	-1.033958	1.179522	0.820413
N	0.682834	-0.293804	-0.316884
C	1.736295	0.648997	-0.617742
H	-0.669854	0.902129	-1.259735
C	0.992996	-1.074958	0.860553
H	-1.433808	-1.443484	-1.413890
H	-2.678104	-0.356353	-0.804060
H	-1.845679	-1.430199	0.295325
H	-0.297934	1.960340	0.982096
H	-1.989816	1.662140	0.639819
H	-1.125130	0.609284	1.739796
H	2.671639	0.114571	-0.746010
H	1.520019	1.162775	-1.547489
H	1.892632	1.403118	0.158320
H	1.920945	-1.611928	0.695598
H	0.222003	-1.811122	1.046404
H	1.115553	-0.475351	1.765854

MP2(full)/6-31G(d), E= -252.18999

C	-1.733145	-0.779350	-0.555764
C	-0.660767	0.289547	-0.377649
C	-0.981494	1.194549	0.815437
N	0.675760	-0.323171	-0.355981
C	1.736448	0.641818	-0.593911
H	-0.669470	0.910505	-1.282997
C	0.962957	-1.096858	0.842165
H	-1.469647	-1.438600	-1.385794
H	-2.699907	-0.312708	-0.767260
H	-1.853915	-1.386063	0.346040
H	-0.218712	1.964643	0.959304
H	-1.939461	1.699405	0.658192
H	-1.060734	0.614556	1.739359

H	2.680591	0.105616	-0.728911
H	1.525918	1.196451	-1.512474
H	1.878239	1.367596	0.225843
H	1.901074	-1.638657	0.690017
H	0.177845	-1.834888	1.015992
H	1.073871	-0.483902	1.752884

***N,N*-dimethylisopropylamine cation**, C_{2V}

HF/6-31G(d), E= -250.56036

C	0.000000	0.000000	-0.675543
N	0.000000	0.000000	0.606112
C	0.000000	1.220586	1.433885
C	0.000000	-1.220586	1.433885
C	0.000000	1.292411	-1.451393
C	0.000000	-1.292411	-1.451393
H	0.000000	1.093973	-2.510861
H	0.000000	-1.093973	-2.510861
H	0.879531	1.880149	-1.214680
H	0.879531	-1.880149	-1.214680
H	-0.879531	1.880149	-1.214680
H	-0.879531	-1.880149	-1.214680
H	0.000000	2.109929	0.832753
H	0.000000	-2.109929	0.832753
H	0.881680	1.208339	2.058876
H	0.881680	-1.208339	2.058876
H	-0.881680	1.208339	2.058876
H	-0.881680	-1.208339	2.058876

MP2(full)/6-31G(d), E=-251.39307

C	0.000000	0.000000	-0.689865
N	0.000000	0.000000	0.612411
C	0.000000	1.225058	1.433785
C	0.000000	-1.225058	1.433785
C	0.000000	1.292378	-1.447496
C	0.000000	-1.292378	-1.447496
H	0.000000	1.097872	-2.517766
H	0.000000	-1.097872	-2.517766
H	0.886082	1.888924	-1.209951
H	0.886082	-1.888924	-1.209951
H	-0.886082	1.888924	-1.209951
H	-0.886082	-1.888924	-1.209951
H	0.000000	2.117014	0.817788
H	0.000000	-2.117014	0.817788

H 0.890664 1.210769 2.064151
H 0.890664 -1.210769 2.064151
H -0.890664 1.210769 2.064151
H -0.890664 -1.210769 2.064151

***N,N*-dimethylisopropylamine anion**, C_S

HF/6-31G(d), E= -250.62297

C 0.467776 0.658114 0.000000
N -0.334404 -0.651164 0.000000
C -0.007356 1.463637 1.214397
C -0.007356 1.463637 -1.214397
C -0.007356 -1.437453 1.161932
C -0.007356 -1.437453 -1.161932
H -1.106696 1.583338 1.300605
H -1.106696 1.583338 -1.300605
H 0.329595 1.060023 2.171975
H 0.329595 1.060023 -2.171975
H 0.408842 2.472079 1.162989
H 0.408842 2.472079 -1.162989
H 1.074497 -1.589890 1.276345
H 1.074497 -1.589890 -1.276345
H -0.364378 -0.960467 2.067491
H -0.364378 -0.960467 -2.067491
H -0.486508 -2.417458 1.110137
H -0.486508 -2.417458 -1.110137

MP2(full)/6-31G(d), E= -251.48789

C 0.460868 0.642772 0.000000
N -0.367982 -0.638122 0.000000
C -0.001293 1.449343 1.203055
C -0.001293 1.449343 -1.203055
C -0.001293 -1.427028 1.160242
C -0.001293 -1.427028 -1.160242
H -1.111845 1.593957 1.272192
H -1.111845 1.593957 -1.272192
H 0.314232 1.035417 2.172583
H 0.314232 1.035417 -2.172583
H 0.439699 2.455829 1.154810
H 0.439699 2.455829 -1.154810
H 1.099942 -1.534897 1.247775
H 1.099942 -1.534897 -1.247775
H -0.361487 -0.953580 2.077748
H -0.361487 -0.953580 -2.077748

H -0.459689 -2.425509 1.103248
H -0.459689 -2.425509 -1.103248

***N,N*-dimethylisopropylamine radical**, C_1

HF/6-31G(d), E= -250.71509

C -1.708848 -0.920151 -0.450884
C -0.687543 0.164112 -0.248114
C -1.091003 1.359485 0.580246
N 0.672208 -0.238687 -0.319596
C 1.632927 0.823619 -0.512111
C 1.102576 -1.201281 0.677650
H -2.636950 -0.500272 -0.827594
H -1.350997 -1.652113 -1.165897
H -1.954953 -1.445724 0.473893
H -0.476192 2.230177 0.380840
H -2.121488 1.631845 0.377542
H -1.017300 1.150889 1.650212
H 2.578580 0.396009 -0.827809
H 1.291292 1.489609 -1.294805
H 1.820644 1.416083 0.386254
H 2.085029 -1.577831 0.414352
H 0.424049 -2.043836 0.705552
H 1.164182 -0.778731 1.683908

MP2(full)/6-31G(d), E= -251.54175

C -1.655874 -0.996528 -0.327673
C -0.695582 0.144958 -0.252292
C -1.144853 1.386685 0.459443
N 0.670777 -0.187710 -0.329933
C 1.602989 0.924028 -0.352380
C 1.141789 -1.273433 0.524379
H -2.638177 -0.637010 -0.648895
H -1.314524 -1.742639 -1.050582
H -1.806449 -1.506620 0.637387
H -0.560956 2.268873 0.186019
H -2.191772 1.596249 0.223087
H -1.076247 1.281718 1.555672
H 2.584082 0.551462 -0.660164
H 1.274192 1.660549 -1.087674
H 1.720418 1.423879 0.623144
H 2.148314 -1.563724 0.209932
H 0.492202 -2.142986 0.423029
H 1.182663 -0.990042 1.589720

REFERENCES

REFERENCES

(1) Westheimer, F. H. *Chem. Rev.* **1960**, *61*, 265.

(2) Hurd, A. D.; Meinart, R. N. *Org. Synth. Coll.* **1943**, *2*, 541.

(3) Eisenbraun, E. J. *Org. Synth. Coll.* **1973**, *4*, 310.

(4) Westheimer, F. H.; Nicolaides, N. *J. Am. Chem. Soc.* **1949**, *71* (1), 25.

(5) Shiner Jr, V. J. *J. Am. Chem. Soc.* **1952**, *74* (21), 5285.

(6) Wolff, M. E. *Chem. Rev.* **1963**, *63* (1), 55.

(7) Löffler, K.; Kober, S. *Ber.* **1990**, *42*, 3431.

(8) Titouani, S. L.; Lavergne, J.-P.; Viallefont, P.; Jacquier, R. *Tetrahedron* **1980**, *36* (20), 2961.

(9) Corey, E. J.; Hertler, W. R. *J. Am. Chem. Soc.* **1960**, *82* (7), 1657.

(10) Houk, K. N.; Lin, Y. T.; Brown, F. K. *J. Am. Chem. Soc.* **1986**, *108* (3), 554.

(11) Smith, M. B.; March, J. *March's Advanced Organic Chemistry*; Wiley-Interscience: New York, 2001.

(12) Hey, A. E.; Elbein, A. D. *J. Bacteriol.* **1968**, *96* (1), 105.

(13) Vijayakumar, P.; Ross, W.; Reese, E. T. *Can. J. Microbiol.* **1978**, *24* (10), 1280.

(14) Hutson, D. H.; Manners, D. J. *Biochem. J.* **1965**, *94* (3), 783.

(15) Alexander, A. G. *Plant Cell Physiol.* **1973**, *14* (1), 157.

(16) Saito, S. *J. Biochem.* **1960**, *48* (1), 101.

(17) Talbot, B. G.; Huber, R. E. *Insect Biochem.* **1975**, *5* (3), 337.

(18) Mitsumasu, K.; Azuma, M.; Niimi, T.; Yamashita, O.; Yaginuma, T. *Insect Mol. Biol.* **2005**, *14* (5), 501.

(19) Sacktor, B. *Proc. Natl. Acad. Sci. U. S. A.* **1968**, *60*, 1007.

(20) Nakano, M.; Sumi, Y.; Miyakawa, M. *J. Biochem.* **1977**, *81* (4), 1041.

(21) Mori, H.; Lee, J. H.; Okuyama, M.; Nishimoto, M.; Ohguchi, M.; Kim, D.; Kimura, A.; Chiba, S. *Biosci. Biotechnol. Biochem.* **2009**, *73* (11), 2466.

(22) Butlerow, A. *C. R. Acad. Sci.* **1861**, *53*, 145.

(23) Breslow, R. *Tetrahedron Lett.* **1959**, *1* (21), 22.

(24) Ricardo, A.; Frye, F.; Carrigan, M. A.; Tipton, J. D.; Powell, D. H.; Benner, S. A. *J. Org. Chem.* **2006**, *71* (25), 9503.

(25) Appayee, C.; Breslow, R. *J. Am. Chem. Soc.* **2014**, *136* (10), 3720.

(26) Elison, C.; Elliott, H. W.; Look, M.; Rapoport, H. *J. Med. Chem.* **1963**, *6* (3), 237.

(27) Elison, C.; Rapoport, H.; Laursen, R.; Elliott, H. W. *Science.* **1961**, *134* (3485), 1078.

(28) Tanabe, M.; Yasuda, D.; LeValley, S.; Mitoma, C. *Life Sci.* **1969**, *8* (19), 1123.

(29) Foye, W. O.; Lemke, T. L.; Williams, D. A. *Foye's principles of medicinal chemistry*, Fifth ed.; Lippincott Williams & Wilkins: Philadelphia, 2008.

(30) Baker, M. T.; Ronnenberg Jr, W. C.; Ruzicka, J. A.; Chiang, C.-K.; Tinker, J. H. *Drug Metab. Dispos.* **1993**, *21*, 1170.

(31) Tung, R. US Patent 7678914 B2 March 16, 2010.

(32) Fukuda, T.; Nishida, Y.; Zhou, Q.; Yamamoto, I.; Kondo, S.; Azuma, J. *Eur. J. Clin. Pharmacol.* **2000**, *56* (2), 175.

(33) Gant, T. G.; Sarshar, S. US Patent 7456317 November 25, 2008.

(34) Mutlib, A. E.; Gerson, R. J.; Meunier, P. C.; Haley, P. J.; Chen, H.; Gan, L. S.; Davies, M. H.; Gemzik, B.; Christ, D. D.; Krahn, D. F.; Markwalder, J. A.; Seitz, S. P.; Robertson, R. T.; Miwa, G. T. *Toxicol. Appl. Pharmacol.* **2000**, *169* (1), 102.

(35) Maltais, F.; Jung, Y. C.; Chen, M.; Tanoury, J.; Perni, R. B.; Mani, N.; Laitinen, L.; Huang, H.; Liao, S.; Gao, H.; Tsao, H.; Block, E.; Ma, C.; Shawgo, R. S.; Town, C.; Brummel, C. L.; Howe, D.; Pazhanisamy, S.; Raybuck, S.; Namchuck, M.; Bennani, Y. L. *J. Med. Chem.* **2009**, *52*, 7993.

(36) Phillips, D. H.; Potter, G. A.; Horton, M. N.; Hewker, A.; Crofton-Sleigh, C.; Jarman, M.; Venitt, S. *Carcinogenesis* **1994**, *15* (8), 1487.

(37) Yero, T.; Rey, J. A. *Pharm. Ther.* **2008**, *33* (12), 690.

(38) Pope, L. E.; Khalil, M. H.; Berg, J. E.; Stiles, M.; Yakatan, G. J.; Sellers, E. M. *J. Clin. Pharmacol.* **2004**, *44* (10), 1132.

(39) Xu, X.; Zhao, X.; Yang, Z.; Wang, H.; Meng, X.; Su, C.; Liu, M.; Fawcett, J. P.; Yang, Y.; Gu, J. *Molecules* **2016**, *21* (6), 704.

(40) Xia, G.; Benmohamed, R.; Morimoto, R. I.; Kirsch, D. R.; Silverman, R. B. *Bioorganic Med. Chem. Lett.* **2014**, *24* (21), 5098.

(41) Xu, G.; Lv, B.; Roberge, J. Y.; Xu, B.; Du, J.; Dong, J.; Chen, Y.; Peng, K.; Zhang, L.; Tang, X.; Feng, Y.; Xu, M.; Fu, W.; Zhang, W.; Zhu, L.; Deng, Z.; Sheng, Z.; Welihinda, A.; Sun, X. *J. Med. Chem.* **2014**, *57* (4), 1236.

(42) Guo, S.; Pang, X.; Peng, L.; Zhan, M.; Fan, L.; Gong, Y.; Kang, F.; Chen, Y. *Bioorg. Med. Chem. Lett.* **2015**, *25* (11), 2425.

(43) Xu, R.; Zhan, M.; Peng, L.; Pang, X.; Yang, J.; Zhang, T.; Jiang, H.; Zhao, L.; Chen, Y. *J. Label. Compd. Radiopharm.* **2015**, *58* (7), 308.

(44) Zhang, Y.; Tortorella, M. D.; Wang, Y.; Liu, J.; Tu, Z.; Liu, X.; Bai, Y.; Wen, D.; Lu, X.; Lu, Y.; Talley, J. J. *ACS Med. Chem. Lett.* **2014**, *5* (10), 1162.

(45) Werstiuk, N. H.; Kadai, T. *J. Chem. Soc. D Chem. Commun.* **1971**, No. 21, 1349.

(46) Werstiuk, N. H.; Kadai, T. *Can. J. Chem.* **1974**, *0* (3), 2169.

(47) Werstiuk, N. H.; Kadai, T. *Can. J. Chem.* **1973**, *51* (9), 1485.

(48) Gaston, M. H.; Skidmore, D. R. *OPPI Briefs* **1985**, *17* (2), 138.

(49) Werstiuk, N. H.; Timmins, G. *Can. J. Chem.* **1989**, *67* (11), 1744.

(50) Werstiuk, N. H.; Timmins, G. *Can. J. Chem.* **1981**, *59* (D), 3218.

(51) Martins, A.; Lautens, M. *Org. Lett.* **2008**, *10* (19), 4351.

(52) Vaidyanathan, S.; Surber, B. W. *Tetrahedron Lett.* **2005**, *46* (31), 5195.

(53) Beak, P.; Monroe, E. M. *J. Org. Chem.* **1969**, *34* (3), 589.

(54) Kawazoe, Y.; Ohnishi, M.; Yoshioka, Y. *Chem. Pharm. Bull. (Tokyo).* **1967**, *15* (8), 1225.

(55) Feldman, D.; Halpern, M.; Rabinovitz, M. *J. Org. Chem.* **1985**, *50* (10), 1746.

(56) Castell, J. V.; Martínez, L. A.; Miranda, M. A.; Tárrega, P. *J. Label. Compd. Radiopharm.* **1994**, *34* (1), 93.

(57) Lygo, B.; Humphreys, L. D. *Tetrahedron Lett.* **2002**, *43* (37), 6677.

(58) Zhan, M.; Xu, R.; Tian, Y.; Jiang, H.; Zhao, L.; Xie, Y.; Chen, Y. *European J. Org. Chem.* **2015**, *2015* (15), 3370.

(59) Chen, T.-S.; Wolinska-Mocydlarz, J.; Leitch, L. C. *J. Labelled Compd.* **1970**, *6* (3), 285.

(60) Wang, D.; Chen, S.; Wang, J.; Astruc, D.; Chen, B. *Tetrahedron* **2016**, doi: 10.1016/j.tet.2016.08.033.

(61) Hu, Y.; Liang, L.; Wei, W. T.; Sun, X.; Zhang, X. J.; Yan, M. *Tetrahedron* **2015**, *71* (9), 1425.

(62) Rockett, B. W.; Harris, T. M.; Hauser, C. R. *J. Am. Chem. Soc.* **1963**, *85* (21), 3491.

(63) Jones, J. R.; Lockley, W. J. S.; Lu, S. Y.; Thompson, S. P. *Tetrahedron Lett.* **2001**, *42* (2), 331.

(64) Giles, R.; Lee, A.; Jung, E.; Kang, A.; Jung, K. W. *Tetrahedron Lett.* **2015**, *56* (5), 747.

(65) Fodor-Csorba, K.; Galli, G.; Holly, S.; Gács-Baitz, E. *Tetrahedron Lett.* **2002**, *43* (21), 3789.

(66) Moozeh, K.; So, S. M.; Chin, J. *Angew. Chemie Int. Ed.* **2015**, *54*, 9381.

(67) Junk, T.; Catallo, W. J. *Tetrahedron Lett.* **1996**, *37* (20), 3445.

(68) Campos, J.; Esqueda, A. C.; Carmona, E. *Chem. - A Eur. J.* **2010**, *16* (2), 419.

(69) Himeda, Y.; Miyazawa, S.; Onozawa-Komatsuzaki, N.; Hirose, T.; Kasuga, K. *Dalt. Trans.* **2009**, No. 32, 6286.

(70) Faller, J. W.; Smart, C. J. *Organometallics* **1989**, *8* (3), 602.

(71) Heys, J. R.; Shu, A. Y. L.; Senderoff, S. G.; Phillips, N. M. *J. Label. Compd. Radiopharm.* **1993**, *33* (5), 431.

(72) Heys, R. *J. Chem. Soc. Chem. Commun.* **1992**, No. 9, 680.

(73) Lukey, C. A.; Long, M. A.; Garnett, J. L. *Aust. J. Chem.* **1995**, *48* (1), 79.

(74) Hesk, D.; Das, P. R.; Evans, B. *J. Label. Compd. Radiopharm.* **1995**, *36* (5), 497.

(75) Chen, W.; Garnes, K. T.; Levinson, S. H.; Saunders, D.; Senderoff, S. G.; Shu, A. Y. L.; Villani, A. J.; Heys, J. R. *J. Label. Compd. Radiopharm* **1997**, *39*, 291.

(76) Klei, S. R.; Golden, J. T.; Tilley, T. D.; Bergman, R. G. *J. Am. Chem. Soc.* **2002**, *124* (10), 2092.

(77) Skaddan, M. B.; Yung, C. M.; Bergman, R. G. *Org. Lett.* **2004**, *6* (1), 11.

(78) Kennedy, A. R.; Kerr, W. J.; Moir, R.; Reid, M. *Org. Biomol. Chem.* **2014**, *12* (40), 7927.

(79) Cochrane, A. R.; Irvine, S.; Kerr, W. J.; Reid, M.; Andersson, S.; Nilsson, G. N. *J. Label. Compd. Radiopharm.* **2013**, *56* (9–10), 451.

(80) Klei, S. R.; Tan, K. L.; Golden, J. T.; Yung, C. M.; Thalji, R. K.; Ahrendt, K. A.; Ellman, J. A.; Tilley, D. T.; Bergman, R. G. In *Activation and Functionalization of C-H bonds*; 2004; pp 46–55.

(81) Rhinehart, J. L.; Manbeck, K. a; Buzak, S. K.; Lippa, G. M.; Brennessel, W. W.; Goldberg, K. I.; Jones, W. D.; York, N. *Organometallics* **2012**, *31*, 1943.

(82) Kallepalli, V. A.; Gore, K. A.; Shi, F.; Sanchez, L.; Chotana, G. A.; Miller, S. L.; Maleczka, R. E.; Smith, M. R. *J. Org. Chem.* **2015**, *80* (15), 8341.

(83) Brown, J. A.; Irvine, S.; Kennedy, A. R.; Kerr, W. J.; Andersson, S.; Nilsson, G. N. *Chem. Commun.* **2008**, No. 9, 1115.

(84) Corberán, R.; Sanaú, M.; Peris, E. *J. Am. Chem. Soc.* **2006**, *128* (12), 3974.

(85) Kerr, W. J.; Mudd, R. J.; Owens, P. K.; Reid, M.; Brown, J. A.; Campos, S. *J. Label. Compd. Radiopharm.* **2016**, doi: 10.1002/jlcr.3427.

(86) Hickey, M. J.; Jones, J. R.; Kingston, L. P.; Lockley, W. J. .; Mather, A. N.; McAuley, B. M.; Wilkinson, D. J. *Tetrahedron Lett.* **2003**, *44* (20), 3959.

(87) Devlin, J.; Kerr, W. J.; Lindsay, D. M.; McCabe, T. J. D.; Reid, M.; Tuttle, T. *Molecules* **2015**, *20* (7), 11676.

(88) Kerr, W. J.; Lindsay, D. M.; Reid, M.; Atzrodt, J.; Derdau, V. *Chem. Commun.* **2016**, *52*, 6669.

(89) Slugovc, C.; Perner, B. *Inorganica Chim. Acta* **2004**, *357* (10), 3104.

(90) Kerr, W. J.; Reid, M.; Tuttle, T. *ACS Catal.* **2015**, *5* (1), 402.

(91) Kerr, W. J.; Mudd, R. J.; Paterson, L. C.; Brown, J. A. *Chem. - A Eur. J.* **2014**, *20* (45), 14604.

(92) Hatano, M.; Nishimura, T.; Yorimitsu, H. *Org. Lett.* **2016**, *18* (15), 3674.

(93) Zhou, J.; Hartwig, J. F. *Angew. Chemie* **2008**, *120* (31), 5867.

(94) Brown, J. A.; Cochrane, A. R.; Irvine, S.; Kerr, W. J.; Mondal, B.; Parkinson, J. A.; Paterson, L. C.; Reid, M.; Tuttle, T.; Andersson, S.; Nilsson, G. N. *Adv. Synth. Catal.* **2014**, *356* (17), 3551.

(95) Yung, C. M.; Skaddan, M. B.; Bergman, R. G. *J. Am. Chem. Soc.* **2004**, *126* (40), 13033.

(96) Ellames, G. J.; Gibson, J. S.; Herbert, J. M.; McNeill, A. H. *Tetrahedron* **2001**, *57* (46), 9487.

(97) Modvig, A.; Andersen, T. L.; Taaning, R. H.; Lindhardt, A. T.; Skrydstrup, T. *J. Org. Chem.* **2014**, *79* (12), 5861.

(98) Atzrodt, J.; Derdau, V.; Kerr, W. J.; Reid, M.; Rojahn, P.; Weck, R. *Tetrahedron* **2015**, *71* (13), 1924.

(99) Golden, J. T.; Andersen, R. A.; Bergman, R. G. *J. Am. Chem. Soc.* **2001**, *123* (24), 5837.

(100) Kingston, L. P.; Lockley, W. J. S.; Mather, A. N.; Spink, E.; Thompson, S. P.; Wilkinson, D. J. *Tetrahedron Lett.* **2000**, *41* (15), 2705.

(101) Shu, A. Y. L.; Chen, W.; Heys, J. R. *J. Organomet. Chem.* **1996**, *524* (1–2), 87.

(102) Iluc, V. M.; Fedorov, A.; Grubbs, R. H. *Organometallics* **2012**, *31* (1), 39.

(103) Ibañez, S.; Poyatos, M.; Peris, E. *Dalt. Trans.* **2016**, *45*, 14154.

(104) Romanenko, I.; Norsic, S.; Veyre, L.; Sayah, R.; D'Agosto, F.; Raynaud, J.; Boisson, C.; Lacôte, E.; Thieuleux, C. *Adv. Synth. Catal.* **2016**, *358*, 2317.

(105) Lehman, M. C.; Gary, J. B.; Boyle, P. D.; Sanford, M. S.; Ison, E. A. *ACS Catal.* **2013**, *3* (10), 2304.

(106) Ellames, G. J.; Gibson, J. S.; Herbert, J. M.; Kerr, W. J.; McNeill, A. H. *Tetrahedron Lett.* **2001**, *42* (36), 6413.

(107) Hesk, D.; Jones, J. R.; Lockley, W. J. S. *J. Label. Compd. Radiopharm.* **1990**, *28* (12), 1427.

(108) Hesk, D.; Jones, J. R.; Lockley, W. J. S. *J. Pharm. Sci.* **1991**, *80* (9), 887.

(109) Lenges, C. P.; White, P. S.; Brookhart, M. *J. Am. Chem. Soc.* **1999**, *121* (18), 4385.

(110) Di Giuseppe, A.; Castarlenas, R.; Perez-Torrente, J. J.; Lahoz, F. J.; Oro, L. A. *Chemistry* **2014**, *20* (27), 8391.

(111) Esqueda, A. C.; Conejero, S.; Maya, C.; Carmona, E. *Organometallics* **2010**, *29* (21), 5481.

(112) Lockley, W. J. S.; Hesk, D. *J. Label. Compd. Radiopharm.* **2010**, *53* (11–12), 704.

(113) Webster-Gardiner, M. S.; Piszel, P. E.; Fu, R.; McKeown, B. A.; Nielsen, R. J.; Goddard, W. A.; Gunnoe, T. B. *J. Mol. Catal. A Chem.* **2016**.

(114) Chen, S.; Song, G.; Li, X. *Tetrahedron Lett.* **2008**, *49* (48), 6929.

(115) Gary, J. B.; Carter, T. J.; Sanford, M. S. *Top. Catal.* **2012**, *55* (7–10), 565.

(116) Hanson, S. K.; Heinekey, D. M.; Goldberg, K. I. *Organometallics* **2008**, *27* (7), 1454.

(117) Weil, T. A.; Friedman, S.; Wender, I. *J. Org. Chem.* **1974**, *39* (1), 48.

(118) Lenges, C. P.; Brookhart, M.; Grant, B. E. *J. Organomet. Chem.* **1997**, *528* (1), 199.

(119) Garnett, J. L.; Hodges, R. J. *J. Am. Chem. Soc.* **1967**, *89* (17), 4546.

(120) Buncel, E.; Clement, O. *J. Chem. Soc. Perkin Trans. 2* **1995**, No. 7, 1333.

(121) Benedetti, M.; Barone, C. R.; Girelli, C. R.; Fanizzi, F. P.; Natile, G.; Maresca, L. *Dalton Trans.* **2014**, *43* (9), 3669.

(122) Kramer, B. P. A.; Masters, C.; Hodges, R. J.; Garnett, J. L.; Tyabin, M. B.; Shteinman, A. A.; Webster, D. E.; Wells, P. B.; Garnett, J. L.; Kenyon, R. S. *J. Chem. Soc. Dalt. Trans.* **1975**, 849.

(123) Kiffen, A. A.; Masters, C.; Raynand, L. *J. Chem. Soc. Dalt. Trans.* **1975**, *11*.

(124) Yamamoto, M.; Oshima, K.; Matsubara, S. *Org. Lett.* **2004**, *6* (26), 5015.

(125) Villalobos, J. M.; Hickman, A. J.; Sanford, M. S. *Organometallics* **2010**, *29* (1), 257.

(126) Ogasawara, M.; Saburi, M. *Organometallics* **1994**, *13* (5), 1911.

(127) Collman, J. P.; Fish, H. T.; Wagenknecht, P. S.; Tyvoll, D. A.; Chng, L.-L.; Eberspacher, T. A.; Brauman, J. I.; Bacon, J. W.; Pignolet, L. H. *Inorg. Chem.* **1996**, *35* (23), 6746.

(128) Erdogan, G.; Grotjahn, D. B. *Top. Catal.* **2010**, *53* (15–18), 1055.

(129) Lee, S. H.; Gorelsky, S. I.; Nikonov, G. I. *Organometallics* **2013**, *32* (21), 6599.

(130) Tse, S. K. S.; Xue, P.; Lin, Z.; Jia, G. *Adv. Synth. Catal.* **2010**, *352* (9), 1512.

(131) Gröll, B.; Schnürch, M.; Mihovilovic, M. D. *J. Org. Chem.* **2012**, *77*, 4432.

(132) Chatterjee, B.; Gunanathan, C. *Chem. Commun.* **2016**, *52* (24), 4509.

(133) Zhan, M.; Jiang, H.; Pang, X.; Zhang, T.; Xu, R.; Zhao, L.; Liu, Y.; Gong, Y.; Chen, Y. *Tetrahedron Lett.* **2014**, *55* (36), 5070.

(134) Khaskin, E.; Milstein, D. *ACS Catal.* **2013**, *3* (3), 448.

(135) Kai, S.; Tse, S.; Xue, P.; Wai, C.; Lau, S.; Sung, H. H. Y.; Williams, I. D.; Jia, G. *Chem. - A Eur. J.* **2011**, *17*, 13918.

(136) Bähn, S.; Imm, S.; Neubert, L.; Zhang, M.; Neumann, H.; Beller, M. *Chemistry* **2011**, *17* (17), 4705.

(137) Bai, W.; Lee, K. H.; Tse, S. K. S.; Chan, K. W.; Lin, Z.; Jia, G. *Organometallics* **2015**, *34* (15), 3686.

(138) Prechtl, M. H. G.; Hölscher, M.; Ben-David, Y.; Theyssen, N.; Milstein, D.; Leitner, W. *Eur. J. Inorg. Chem.* **2008**, No. 22, 3493.

(139) Chatterjee, B.; Gunanathan, C. *Org. Lett.* **2015**, *17* (19), 4794.

(140) Piola, L.; Fernandez-Salas, J. A.; Manzini, S.; Nolan, S. P. *Org. Biomol. Chem.* **2014**, *12* (43), 8683.

(141) Prechtl, M. H. G.; Hölscher, M.; Ben-David, Y.; Theyssen, N.; Loschen, R.; Milstein, D.; Leitner, W. *Angew. Chemie - Int. Ed.* **2007**, *46* (13), 2269.

(142) Alexakis, E.; Hickey, M. J.; Jones, J. R.; Kingston, L. P.; Lockley, W. J. S.; Mather, A. N.; Smith, T.; Wilkinson, D. J. *Tetrahedron Lett.* **2005**, *46* (25), 4291.

(143) Leung, C. W.; Zheng, W.; Wang, D.; Ng, S. M.; Yeung, C. H.; Zhou, Z.; Lin, Z.; Lau, C. P. *Organometallics* **2007**, *26* (8), 1924.

(144) Erdogan, G.; Grotjahn, D. B. *J. Am. Chem. Soc.* **2009**, *131* (30), 10354.

(145) Zhang, L.; Nguyen, D. H.; Raffa, G.; Desset, S.; Paul, S.; Dumeignil, F.; Gauvin, R. M. *Catal. Commun.* **2016**, *84*, 67.

(146) Lee, J. H.; Yoo, K. S.; Park, C. P.; Olsen, J. M.; Sakaguchi, S.; Surya Prakash, G. K.; Mathew, T.; Jung, K. W. *Adv. Synth. Catal.* **2009**, *351* (4), 563.

(147) Giles, R.; Ahn, G.; Jung, K. W. *Tetrahedron Lett.* **2015**, *56* (45), 6231.

(148) Cummings, S. P.; Le, T.-N.; Fernandez, G. E.; Quiambao, L. G.; Stokes, B. J. *J. Am. Chem. Soc.* **2016**, *138* (19), 6107.

(149) Janni, M.; Peruncheralathan, S. *Org. Biomol. Chem.* **2016**, *14* (11), 3091.

(150) Saget, T.; Cramer, N. *Angew. Chemie - Int. Ed.* **2012**, *51* (51), 12842.

(151) Ma, S.; Villa, G.; Thuy-Boun, P. S.; Homs, A.; Yu, J. Q. *Angew. Chemie - Int. Ed.* **2014**, *53* (3), 734.

(152) Wang, L.; Hunter, S. C.; Song, Z.; Steren, C. A.; Chen, T.; Wei, Z.; Cai, H.; Xue, Z. L. *Chem. - A Eur. J.* **2014**, *20* (20), 6033.

(153) Beck, R.; Shoshani, M.; Johnson, S. A. *Angew. Chemie - Int. Ed.* **2012**, *51*, 11753.

(154) Eguillor, B.; Esteruelas, M. A.; García-Raboso, J.; Oliván, M.; Oñate, E. *Organometallics* **2009**, *28* (13), 3700.

(155) Mutsumi, T.; Iwata, H.; Maruhashi, K.; Monguchi, Y.; Sajiki, H. *Tetrahedron* **2011**, *67* (6), 1158.

(156) Perthuisot, C.; Fan, M.; Jones, W. D. *Organometallics* **1992**, *11* (11), 3622.

(157) Qiao-Xia, G.; Bao-Jian, S.; Hai-Qing, G.; Tamotsu, T. *Chinese J. Chem.* **2005**, *23* (3), 341.

(158) Rubottom, G. M.; Evain, E. J. *Tetrahedron* **1990**, *46* (15), 5055.

(159) Alexakis, E.; Jones, J. R.; Lockley, W. J. S. *Tetrahedron Lett.* **2006**, *47* (29), 5025.

(160) Jere, F. T.; Miller, D. J.; Jackson, J. E. *Org. Lett.* **2003**, *5* (4), 527.

(161) Jacobs, J. *PhD Diss. Michigan State Univ.* **2009**.

(162) Maegawa, T.; Fujiwara, Y.; Inagaki, Y.; Monguchi, Y.; Sajiki, H. *Adv. Synth. Catal.* **2008**, *350* (14–15), 2215.

(163) Fujiwara, Y.; Iwata, H.; Sawama, Y.; Monguchi, Y.; Sajiki, H. *Chem. Commun.* **2010**, *46* (27), 4977.

(164) Sawama, Y.; Yabe, Y.; Iwata, H.; Fujiwara, Y.; Monguchi, Y.; Sajiki, H. *Chem. Eur. J.* **2012**, *18* (51), 16436.

(165) Bresó-Femenia, E.; Godard, C.; Claver, C.; Chaudret, B.; Castillón, S. *Chem. Commun.* **2015**, *51*, 16342.

(166) Pieters, G.; Taglang, C.; Bonnefille, E.; Gutmann, T.; Puente, C.; Berthet, J. C.; Dugave, C.; Chaudret, B.; Rousseau, B. *Angew. Chemie - Int. Ed.* **2014**, *53* (1), 230.

(167) Taglang, C.; Martínez-Prieto, L. M.; del Rosal, I.; Maron, L.; Poteau, R.; Philippot, K.; Chaudret, B.; Perato, S.; Sam Lone, A.; Puente, C.; Dugave, C.; Rousseau, B.; Pieters, G. *Angew. Chem. Int. Ed.* **2015**, *54* (36), 10474.

(168) Schrage, K.; Burwell, R. L. *J. Am. Chem. Soc.* **1966**, *88* (20), 4549.

(169) Atkinson, J. G.; Luke, M. O.; Stuart, R. S. *Can. J. Chem.* **1967**, *45* (13), 1511.

(170) Browne, W. R.; O'Connor, C. M.; Killeen, J. S.; Guckian, A. L.; Burke, M.; James, P.; Burke, M.; Vos, J. G. *Inorg. Chem.* **2002**, *41* (16), 4245.

(171) Matsubara, S.; Yokota, Y.; Oshima, K. *Chem. Lett.* **2004**, *33* (3), 294.

(172) Matsubara, S.; Yokota, Y.; Oshima, K. *Org. Lett.* **2004**, *6* (12), 2071.

(173) Azran, J.; Shimoni, M.; Buchman, O. *J. Catal.* **1994**, *148* (2), 648.

(174) Sajiki, H.; Hattori, K.; Aoki, F.; Yasunaga, K.; Hirota, K. *Synlett* **2002**, No. 7, 1149.

(175) Kurita, T.; Hattori, K.; Seki, S.; Mizumoto, T.; Aoki, F.; Yamada, Y.; Ikawa, K.; Maegawa, T.; Monguchi, Y.; Sajiki, H. *Chem. - A Eur. J.* **2008**, *14* (2), 664.

(176) Maegawa, T.; Akashi, A.; Esaki, H.; Aoki, F.; Sajiki, H.; Hirota, K. *Synlett* **2005**, No. 5, 845.

(177) Hardacre, C.; Holbrey, J. D.; McMath, S. E. J. *Chem. Commun.* **2001**, No. 4, 367.

(178) Sajiki, H.; Esaki, H.; Aoki, F.; Maegawa, T.; Hirota, K. *Synlett* **2005**, No. 9, 1385.

(179) Esaki, H.; Ito, N.; Sakai, S.; Maegawa, T.; Monguchi, Y.; Sajiki, H. *Tetrahedron* **2006**, *62* (47), 10954.

(180) Modutlwa, N.; Tada, H.; Sugahara, Y.; Shiraki, K.; Hara, N.; Deyashiki, Y.; Ando, T.; Maegawa, T.; Monguchi, Y.; Sajiki, H. *Nucleic Acids Symp. Ser. (Oxf).* **2009**, No. 53, 105.

(181) Sajiki, H.; Kurita, T.; Esaki, H.; Aoki, F.; Maegawa, T.; Hirota, K. *Org. Lett.* **2004**, *6* (20), 3521.

(182) Esaki, H.; Aoki, F.; Umemura, M.; Kato, M.; Maegawa, T.; Monguchi, Y.; Sajiki, H. *Chem. Eur. J.* **2007**, *13* (14), 4052.

(183) Derdau, V.; Atzrodt, J. *Synlett* **2006**, No. 12, 1918.

(184) Kurita, T.; Aoki, F.; Mizumoto, T.; Maejima, T.; Esaki, H.; Maegawa, T.; Monguchi, Y.; Sajiki, H. *Chemistry* **2008**, *14* (11), 3371.

(185) Esaki, H.; Ohtaki, R.; Maegawa, T.; Monguchi, Y.; Sajiki, H. *J. Org. Chem.* **2007**, *72* (6), 2143.

(186) Yabe, Y.; Sawama, Y.; Monguchi, Y.; Sajiki, H. *Chem. - A Eur. J.* **2013**, *19* (2), 484.

(187) Brown, W. G.; Garnett, J. L. *J. Am. Chem. Soc.* **1958**, *80* (19), 5272.

(188) Garnett, J. L.; Henderson, L. J.; Xii, X. P.; Chem, J. P.; Brown, W. G.; Sollich, W. A.; Chem, A. J.; Wolfgang, R.; Rowland, F. S.; Turton, C. N.; Wilz, K. E. *Tetrahedron Lett.* **1961**, *1013* (15), 516.

(189) Ito, N.; Esaki, H.; Maesawa, T.; Imamiya, E.; Maegawa, T.; Sajiki, H. *Bull. Chem. Soc. Jpn.* **2008**, *81* (2), 278.

(190) Yamada, T.; Park, K.; Yasukawa, N.; Morita, K.; Monguchi, Y.; Sawama, Y.; Sajiki, H. *Adv. Synth. Catal.* **2016**, doi:10.1002/adsc.201600363.

(191) Sawama, Y.; Yamada, T.; Yabe, Y.; Morita, K.; Shibata, K.; Shigetsura, M.; Monguchi, Y.; Sajiki, H. *Adv. Synth. Catal.* **2013**, *355* (8), 1529.

(192) Scott, R. W. J.; Datye, A. K.; Crooks, R. M. *J. Am. Chem. Soc.* **2003**, *125* (13), 3708.

(193) Ito, N.; Watahiki, T.; Maesawa, T.; Maegawa, T.; Sajiki, H. *Adv. Synth. Catal.* **2006**, *348* (9), 1025.

(194) Ito, N.; Watahiki, T.; Maesawa, T.; Maegawa, T.; Sajiki, H. *Synthesis (Stuttg).* **2008**, No. 9, 1467.

(195) Bijani, S.; Jain, V.; Padmanabhan, D.; Pandey, B.; Shah, A. *Tetrahedron Lett.* **2015**, *56* (10), 1211.

(196) Maegawa, T.; Ito, N.; Oono, K.; Monguchi, Y.; Sajiki, H. *Synthesis (Stuttg).* **2009**, No. 16, 2674.

(197) Modutlwa, N.; Maegawa, T.; Monguchi, Y.; Sajiki, H. *J. Label. Compd. Radiopharm.* **2010**, *53* (11–12), 686.

(198) Derdau, V.; Atzrodt, J.; Zimmermann, J.; Kroll, C.; Brückner, F. *Chem. - A Eur. J.* **2009**, *15* (40), 10397.

(199) Maegawa, T.; Fujiwara, Y.; Inagaki, Y.; Esaki, H.; Monguchi, Y.; Sajiki, H. *Angew. Chem. Int. Ed.* **2008**, *47* (29), 5394.

(200) Pathak, T.; Chattopadhyaya, J. *Tetrahedron* **1987**, *43* (18), 4227.

(201) Pojer, P. M. *Tetrahedron Lett.* **1984**, *25* (23), 2507.

(202) Koch, H. J.; Stuart, R. S. *Carbohydr. Res.* **1978**, *67* (2), 341.

(203) Angyal, S. J.; Stevens, J. D.; Odier, L. *Carbohydr. Res.* **1986**, *157*, 83.

(204) Angyal, S. J.; Stevens, J. D.; Odier, L. *Carbohydr. Res.* **1987**, *169*, 151.

(205) Price, N. P. J.; Hartman, T. M.; Vermillion, K. E. *Anal. Chem.* **2015**, *87*, 7282−7290.

(206) Cioffi, E. A.; Bell, R. H.; Le, B. *Tetrahedron: Asymmetry* **2005**, *16* (2), 471.

(207) Mukumoto, M.; Tsuzuki, H.; Mataka, S.; Tashiro, M.; Tsukinoki, T.; Nagano, Y. *Chem. Lett.* **1996**, No. 2, 165.

(208) Hickey, M. J.; Jones, J. R.; Kingston, L. P.; Lockley, W. J. S.; Mather, A. N.; Wilkinson, D. J. *Tetrahedron Lett.* **2004**, *45* (47), 8621.

(209) Zhan, M.; Zhang, T.; Huang, H.; Xie, Y. *J. Label. Compd. Radiopharm.* **2014**, *57*, 533.

(210) Ito, Y.; Yoshimatsu, M. *Org. Chem. Front.* **2015**, *2* (3), 201.

(211) Gunter, G. C.; Miller, D. J.; Jackson, J. E. *J. Catal.* **1994**, *148* (1), 252.

(212) Gunter, G. C.; Langford, R. H.; Jackson, J. E.; Miller, D. J. *Ind. Eng. Chem. Res.* **1995**, *34* (3), 974.

(213) Wadley, D. C.; Tam, M. S.; Kokitkar, P. B.; Jackson, J. E.; Miller, D. J. *J. Catal.* **1997**, *165* (2), 162.

(214) Tam, M. S.; Gunter, G. C.; Craciun, R.; Miller, D. J.; Jackson, J. E. *Ind. Eng. Chem. Res.* **1997**, *36* (9), 3505.

(215) Zhang, Z.; Jackson, J. E.; Miller, D. J. *Ind. Eng. Chem. Res.* **2002**, *41* (5), 691.

(216) Zhang, Z.; Jackson, J. E.; Miller, D. J. *Appl. Catal. A Gen.* **2001**, *219* (1–2), 89.

(217) Jere, F. T.; Jackson, J. E.; Miller, D. J. *Ind. Eng. Chem. Res.* **2004**, *43* (13), 3297.

(218) Dalavoy, T. S.; Jackson, J. E.; Swain, G. M.; Miller, D. J.; Li, J.; Lipkowski, J. *J. Catal.* **2007**, *246* (1), 15.

(219) Li, Z.; Garedew, M.; Lam, C. H.; Jackson, J. E.; Miller, D. J.; Saffron, C. M. *Green Chem.* **2012**, *14* (9), 2540.

(220) Brunauer, S.; Emmett, P. H.; Teller, E. *J. Am. Chem. Soc.* **1938**, *60* (2), 309.

(221) Barrett, E. P.; Joyner, L. G.; Halenda, P. P. *J. Am. Chem. Soc.* **1951**, *73* (1), 373.

(222) Schmidt, M. W.; Baldridge, K. K.; Boatz, J. A.; Elbert, S. T.; Gordon, M. S.; Jensen, J. H.; Koseki, S.; Matsunaga, N.; Nguyen, K. A.; Su, S.; Windus, T. L.; Dupuis, M.; Montgomery, J. A. *J. Comput. Chem.* **1993**, *14* (11), 1347.

(223) Bode, B. M.; Gordon, M. S. *J. Mol. Graph. Model.* **1998**, *16* (3), 133.

(224) Curtiss, L. A.; Raghavach Ari, K.; Redfern, P. C.; Rassolov, V.; Pople, J. A. *J. Chem. Phys.* **1998**, *109* (18), 7764.

(225) 03, G.; C.02, R.; Frisch, M. J.; Trucks, G. W.; Schlegel, H. B.; Scuseria, G. E.; Robb, M. A.; Cheeseman, J. R.; J. A. Montgomery, J.; Vreven, T.; Kudin, K. N.; Burant, J. C.; Millam, J. M.; Iyengar, S. S.; Tomasi, J.; Barone, V.; Mennucci, B.; Cossi, M.; Scalmani, G.; Rega, N.; Petersson, G. A.; Nakatsuji, H.; Hada, M.; Ehara, M.; Toyota, K.; Fukuda, R.; Hasegawa,

J.; Ishida, M.; Nakajima, T.; Honda, Y.; Kitao, O.; Nakai, H.; Klene, M.; Li, X.; Knox, J. E.; Hratchian, H. P.; Cross, J. B.; Bakken, V.; Adamo, C.; Jaramillo, J.; Gomperts, R.; Stratmann, R. E.; Yazyev, O.; Austin, A. J.; Cammi, R.; Pomelli, C.; Ochterski, J. W.; Ayala, P. Y.; Morokuma, K.; Voth, G. A.; Salvador, P.; Dannenberg, J. J.; Zakrzewski, V. G.; Dapprich, S.; Daniels, A. D.; Strain, M. C.; Farkas, O.; Malick, D. K.; Rabuck, A. D.; Raghavachari, K.; Foresman, J. B.; Ortiz, J. V.; Cui, Q.; Baboul, A. G.; Clifford, S.; Cioslowski, J.; Stefanov, B. B.; Liu, G.; Liashenko, A.; Piskorz, P.; Komaromi, I.; Martin, R. L.; Fox, D. J.; Keith, T.; Al-Laham, M. A.; Peng, C. Y.; A. Nanayakkara, M. Challacombe, P. M. W. G.; Johnson, B.; Chen, W.; Wong, M. W.; Gonzalez, C.; Pople, J. A. No. Gaussian, Inc.,.

(226) Subrenat, A.; Baléo, J. N.; Le Cloirec, P.; Blanc, P. E. *Carbon N. Y.* **2001**, *39* (5), 707.

(227) Chen, Y.; Miller, D. J.; Jackson, J. E. *Ind. Eng. Chem. Res.* **2007**, *46* (10), 3334.

(228) Pimparkar, K. P.; Miller, D. J.; Jackson, J. E. *Ind. Eng. Chem. Res.* **2008**, *47* (20), 7648.

(229) Peereboom, L.; Jackson, J. E.; Miller, D. J. *Green Chem.* **2009**, *11* (12), 1979.

(230) Dubey, P. K.; Sinha, A. S. K.; Talapatra, S.; Koratkar, N.; Ajayan, P. M.; Srivastava, O. N. *Int. J. Hydrogen Energy* **2010**, *35* (9), 3945.

(231) W. Gribble, G. *Chem. Soc. Rev.* **1998**, *27* (6), 395.

(232) Olsen, C. A.; Franzyk, H.; Jaroszewski, J. W. *Synthesis (Stuttg).* **2005**, No. 16, 2631.

(233) Schlummer, B.; Scholz, U. *Adv. Synth. Catal.* **2004**, *346* (13–15), 1599.

(234) Hartwig, J. F. *Acc. Chem. Res.* **2008**, *41* (11), 1534.

(235) Surry, D. S.; Buchwald, S. L. *Angew. Chem. Int. Ed. Engl.* **2008**, *47* (34), 6338.

(236) Beller, M.; Tillack, A.; Seayad, J. In *Transition Metals for Organic Synthesis: Building Blocks and Fine Chemicals*; Beller, M., Bolm, C., Eds.; Viley-VCH: Weinheim, Germany, 2004; Vol. 2, pp 403–414.

(237) Hong, S.; Marks, T. J. *Acc. Chem. Res.* **2004**, *37* (9), 673.

(238) Severin, R.; Doye, S. *Chem. Soc. Rev.* **2007**, *36* (9), 1407.

(239) Aillaud, I.; Collin, J.; Hannedouche, J.; Schulz, E. *Dalt. Trans.* **2007**, No. 44, 5105.

(240) Müller, T. E.; Hultzsch, K. C.; Yus, M.; Foubelo, F.; Tada, M. *Chem. Rev.* **2008**, *108* (9), 3795.

(241) Martínez, R.; Brand, G. J.; Ramón, D. J.; Yus, M. *Tetrahedron Lett.* **2005**, *46* (21), 3683.

(242) Martínez, R.; Ramón, D. J.; Yus, M. *Tetrahedron* **2006**, *62* (38), 8982.

(243) Guyot, A.; Fournier, M. *Bull. Soc. Chim. Fr.* **1930**, *47*, 203.

(244) Langdon, W. K.; Levis, W. W.; Jackson, D. R. *Ind. Eng. Chem. Process Des. Dev.* **1962**, *1* (2), 153.

(245) Kornfeld, E. C. *J. Org. Chem.* **1951**, *16* (1), 131.

(246) Mozingo, R.; Spencer, C.; Folkers, K. *J. Am. Chem. Soc.* **1944**, *66* (11), 1859.

(247) Rice, R. G.; Kohn, E. J.; Daasch, L. W. *J. Org. Chem.* **1958**, *23* (9), 1352.

(248) Charles, F. . W.; Adkins, H. *J. Am. Chem. Soc.* **1932**, *54* (1930), 306.

(249) Baiker, A. *Ind. Eng. Chem. Prod. Res. Dev.* **1981**, *20* (4), 615.

(250) Schwoegler, E. J.; Adkins, H. *J. Am. Chem. Soc.* **1939**, *61* (12), 3499.

(251) Hammerschmidt, W.; Baiker, A.; Wokaun, A.; Fluhr, W. *Appl. Catal.* **1986**, *20* (1), 305.

(252) Kijeński, J.; Niedzielski, P. J.; Baiker, A. *Appl. Catal.* **1989**, *53* (1), 107.

(253) Göbölös, S.; Hegedüs, M.; Kolosova, I.; Maciejewski, M.; Margitfalvi, J. . *Appl. Catal. A Gen.* **1998**, *169* (2), 201.

(254) Kimura, H.; Yokota, Y.; Sawamoto, Y. *Catal. Letters* **2005**, *99* (3), 133.

(255) Kimura, H.; Taniguchi, H. *Catal. Letters* **1996**, *40* (1), 123.

(256) Ohtani, B.; Nakagawa, K.; Nishimoto, S.; Kagiya, T. *Chem. Lett.* **1986**, *15* (11), 1917.

(257) Ohtani, B.; Osaki, H.; Nishimoto, S.; Kagiya, T. *Tetrahedron Lett.* **1986**, *27* (18), 2019.

(258) Cano, R.; Ramón, D. J.; Yus, M. *J. Org. Chem.* **2011**, *76* (14), 5547.

(259) Murahashi, S.-I.; Shimamura, T.; Moritani, I. *J. Chem. Soc. Chem. Commun.* **1974**, No. 22, 931.